Energy-Based Modeling and Tracking Control of Rigid Body Systems with Practical Multicopter Applications

DISSERTATION

zur Erlangung des Grades

des Doktors der Ingenieurwissenschaften
(Dr.-Ing.)

der Naturwissenschaftlich-Technischen Fakultät II
– Physik und Mechatronik –
der Universität des Saarlandes

von

MATTHIAS KONZ

Saarbrücken

September 24, 2025

Abstract

Many machines, vehicles and robots may be modeled as rigid body systems, i.e. a number of interconnected, undeformable bodies subject to inertia, gravity, and other forces. Energy-based methods for derivation of their equations of motion, like the Lagrange formalism, are standard in engineering education and well established in the dedicated literature. These algorithms commonly rely on the use of a minimal set of generalized coordinates. This is appropriate for many applications, e.g. machines containing only one-dimensional joints. For systems whose configuration space is nonlinear, e.g. mobile robots whose configiguration space contains the rigid body attitude, the use of minimal coordinates necessarily leads to singularities. From the point of view of differential geometry, this is a well known fact.

This work resolves this problem by the use of (possibly) redundant configuration coordinates and (possibly) nonholonomic velocity coordinates. The second chapter reviews several established formalisms of analytical mechanics and states them in terms of these more general coordinates. The third chapter applies these results to rigid body systems. Though inertia is the crucial part of the dynamics, this work also investigates dissipation and stiffness. Finally, it presents an algorithm for the derivation of global equations of motion of general rigid body systems.

The literature states computed-torque is a standard approach for tracking control of fully actuated mechanical systems. However, this recipe relies on minimal coordinates and consequently suffers from the problems mentioned above. There is no established “standard” approach for the control of underactuated systems.

This work presents three sightly different algorithms for tracking control of general rigid body systems by means of static state feedback. These essentially minimize the distance between the actual realizable acceleration of the model and a desired acceleration computed from a stable prototype system. The prototype system shares the geometry and kinematics of the actual model, but may have different constitutive properties (inertia, damping, stiffness). The resulting control law can be computed globally and explicitly for any rigid body system. The resulting closed loop system (which may differ from the prototype in the underactuated case), is invariant to the chosen coordinates, i.e. its formulation is covariant. However, so far, there is no general proof of stability. The performance of the proposed approaches are discussed on several examples and simulation results.

The last chapter of this work discusses the experimental realization of the control approach to two small UAVs. The performance is demonstrated on tracking control for several aerobatic maneuvers.

Contents

Chapter 1

Introduction

1.1 Context and state of the art

Modeling. As the title suggests this work deals with modeling and control of rigid body systems. The procedure of physical modeling is illustrated in Figure 1.1. It starts by approximating the system under consideration by a mechanical model. The mathematical part requires the choice of coordinates $\boldsymbol{z}$ to capture the state (positions and velocities) of the model. Combining this with principles of mechanics, we may derive a set of ordinary differential equations that capture its motion. This work mainly deals with this second part, i.e. the derivation of *equations of motion*.

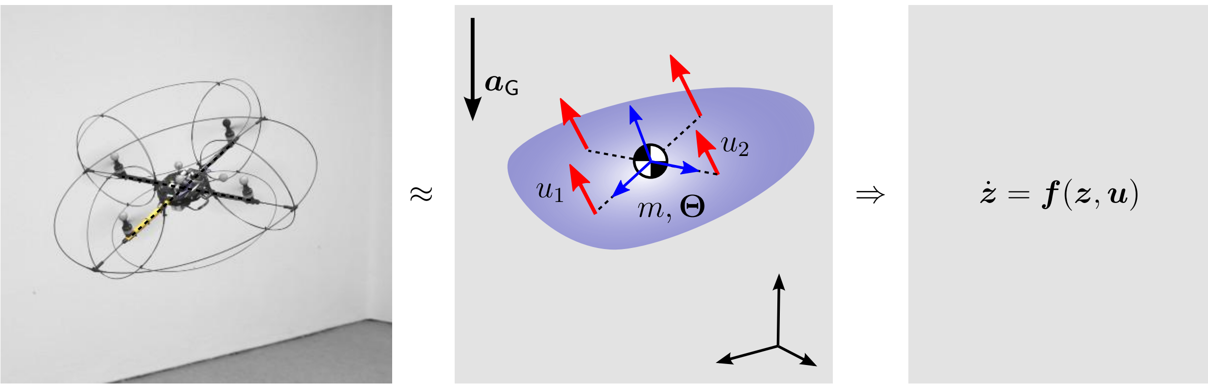

reality | physical model | mathematical model

Figure 1.1: Modeling illustration

A very common approach for deriving equations of motion of finite-demensional, holonomic mechanical systems is the so called *Lagrange formalism*: First, the system is parameterized by so called *generalized coordinates* $\boldsymbol{q}$. Then the kinetic energy $\mathcal{T}$, the potential energy $\mathcal{V}$ and virtual work $\delta\mathcal{W}$ of external forces are formulated in terms of these coordinates and their derivatives $\dot{\boldsymbol{q}} = \mathrm{d}\boldsymbol{q}/\mathrm{d}t$:

$$\mathcal{L}(\boldsymbol{q}, \dot{\boldsymbol{q}}) = \mathcal{T}(\boldsymbol{q}, \dot{\boldsymbol{q}}) - \mathcal{V}(\boldsymbol{q}), \qquad \delta\mathcal{W}^{\mathrm{E}} = (\delta\boldsymbol{q})^{\top} \boldsymbol{f}^{\mathrm{E}}. \tag{1.1}$$

The equations of motion are derived from the Lagrangian $\mathcal{L}$ as

$$\frac{\mathrm{d}}{\mathrm{d}t}\frac{\partial \mathcal{L}}{\partial \dot{\boldsymbol{q}}} - \frac{\partial \mathcal{L}}{\partial \boldsymbol{q}} = \boldsymbol{f}^{\mathrm{E}}. \tag{1.2}$$

The kinetic energy for a time-invariant, mechanical system is always strictly quadratic $\mathcal{T} = \frac{1}{2}\dot{\boldsymbol{q}}^\top \boldsymbol{M}(\boldsymbol{q})\dot{\boldsymbol{q}}$. Furthermore, we assume that the external forces $\boldsymbol{f}^{\mathrm{E}}$ is an affine function of the control inputs $\boldsymbol{u}$. Then the equations of motion take the structure

$$\boldsymbol{M}(\boldsymbol{q})\ddot{\boldsymbol{q}} + \boldsymbol{b}(\boldsymbol{q},\dot{\boldsymbol{q}}) = \boldsymbol{B}(\boldsymbol{q})\boldsymbol{u} \qquad \Leftrightarrow \qquad \tfrac{\mathrm{d}}{\mathrm{d}t}\underbrace{\begin{bmatrix}\boldsymbol{q}\\ \dot{\boldsymbol{q}}\end{bmatrix}}_{\boldsymbol{z}} = \underbrace{\begin{bmatrix}\dot{\boldsymbol{q}}\\ \boldsymbol{M}^{-1}(\boldsymbol{q})(\boldsymbol{B}(\boldsymbol{q})\boldsymbol{u} - \boldsymbol{b}(\boldsymbol{q},\dot{\boldsymbol{q}}))\end{bmatrix}}_{\boldsymbol{f}(\boldsymbol{z},\boldsymbol{u})} \tag{1.3}$$

The right hand side of (1.3) is a standard form for simulation, i.e. numerical solution, or general control design. However, the structure of the left hand side of (1.3) can be exploited for a particular control design.

Feedback Control. From a mathematical point of view, a feedback controller is some map $\boldsymbol{u} = \boldsymbol{g}(\boldsymbol{z},\boldsymbol{r})$ that computes the control input $\boldsymbol{u}$ based on the measured system state $\boldsymbol{z}$ and some reference input $\boldsymbol{r}$. The goal is that the resulting controlled system $\dot{\boldsymbol{z}} = \boldsymbol{f}(\boldsymbol{z},\boldsymbol{g}(\boldsymbol{z},\boldsymbol{r})) = \bar{\boldsymbol{f}}(\boldsymbol{z},\boldsymbol{r})$ has desirable properties.

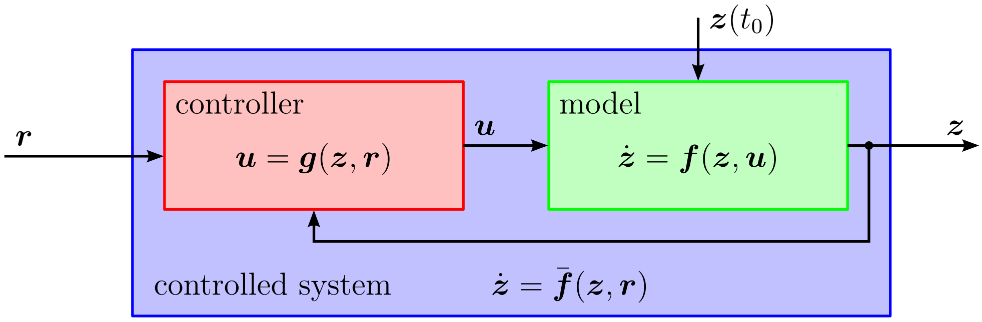

Figure 1.2: Model, controller and controlled system

For a system of the structure (1.3), a typical control objective is, that a given reference trajectory $t \mapsto \boldsymbol{q}_{\mathsf{R}}(t)$ is a stable trajectory of the controlled system. If there are as many control inputs as degrees of freedom $\dim \boldsymbol{u} = \dim \boldsymbol{q} = n$ and the input matrix $\boldsymbol{B}$ is invertible, there is a popular control approach, commonly called *computed torque*: Defining the error dynamics as

$$\ddot{\boldsymbol{e}} + \boldsymbol{\Lambda}_1\dot{\boldsymbol{e}} + \boldsymbol{\Lambda}_0\boldsymbol{e} = \boldsymbol{0}, \quad \boldsymbol{e} = \boldsymbol{q} - \boldsymbol{q}_{\mathsf{R}} \tag{1.4}$$

with the symmetric, positive definite matrices $\boldsymbol{\Lambda}_0, \boldsymbol{\Lambda}_1$ as tuning parameters. Combining this with the model (1.3) yields the control law

$$\boldsymbol{u} = \boldsymbol{B}^{-1}\big(\boldsymbol{M}(\boldsymbol{q})(\ddot{\boldsymbol{q}}_{\mathsf{R}} - \boldsymbol{\Lambda}_1\dot{\boldsymbol{e}} - \boldsymbol{\Lambda}_0\boldsymbol{e}) + \boldsymbol{b}(\boldsymbol{q},\dot{\boldsymbol{q}})\big) = \boldsymbol{g}\big(\underbrace{\boldsymbol{q},\dot{\boldsymbol{q}}}_{\boldsymbol{z}},\underbrace{\boldsymbol{q}_{\mathsf{R}},\dot{\boldsymbol{q}}_{\mathsf{R}},\ddot{\boldsymbol{q}}_{\mathsf{R}}}_{\boldsymbol{r}}\big) \tag{1.5}$$

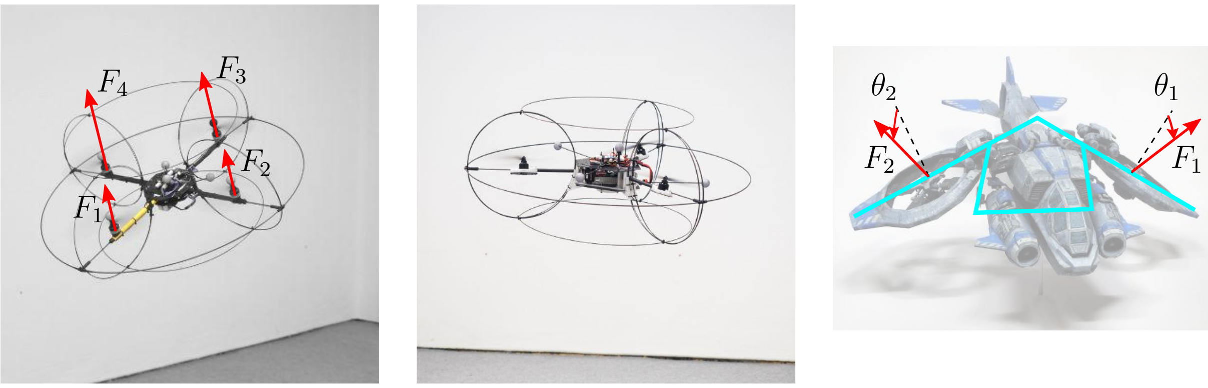

Figure 1.3: lsr-quadcopter (left), lsr-tricopter (middle) and a concept of a bicopter

Multicopters. In contrast to conventional helicopters, multicopters are aerial vehicles that use several rigid (fixed pitch) propellers to generate lift and maneuver. They are usually small and unmanned and are used to carry cameras or other sensors. In particular, the four propeller quadcopter configuration has became quite popular over the last two decades.

The *Chair of Systems Theory and Control Engineering* at Saarland University has developed realizations of a quadcopter and a tricopter with three tiltable propellers (see Figure 1.3). A bicopter with two titlable and inclined propellers has been studied through simulations. In particular the lsr-quadcopter has an excellent thrust to weight ratio and is consequently well suited for aggressive, aerobatic maneuvers, e.g. a looping as shown in Figure 1.4.

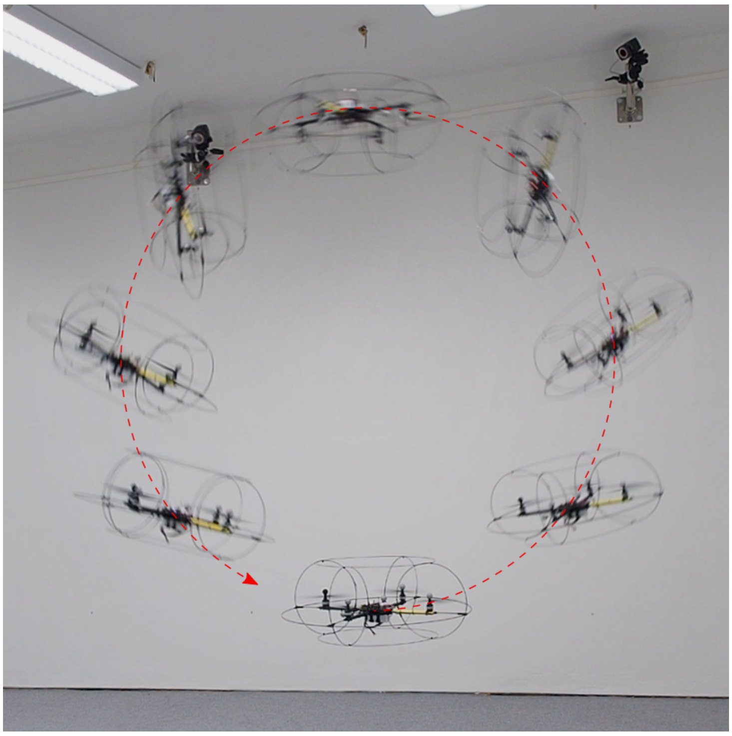

Figure 1.4: Snapshots of the lsr-quadcopter tracking a looping trajectory

From a mechanical point of view, these multicopters may be modelled as a free rigid body moving within Earth's gravity. The difference between them is only the placement of the actuators: the tricopter is fully-actuated, so it poses the easiest control task. The quadcopter only has four actuators for its six degrees of freedom, i.e. it is underactuated. However, its model is well known to be a configuration flat system and corresponding standard control design approaches may be applied. The bicopter is (probably) not a flat system and consequently, poses the toughest control task.

1.2 Motivation example

Consider a free rigid body as illustrated in the middle of Figure 1.1, but fixed at its center of mass, i.e. it may only rotate about this point. For simplicity, we also assume that the chosen frame coincides with its principle axis and there are three independent control torques about these axis. Then the coefficients of inertia are $\boldsymbol{\Theta} = \operatorname{diag}(\Theta_{\mathsf{x}}, \Theta_{\mathsf{y}}, \Theta_{\mathsf{z}})$.

Lagrange's equation. For application of the Lagrange formalism we need to parameterize the system by minimal generalized coordinates. A popular choice for the rigid body orientation are Euler angles in the *roll-pitch-yaw* convention:

$$\boldsymbol{R}(\boldsymbol{q}) = \begin{bmatrix} \mathrm{c}_\varphi \mathrm{c}_\beta & -\mathrm{s}_\varphi \mathrm{c}_\alpha + \mathrm{c}_\varphi \mathrm{s}_\beta \mathrm{s}_\alpha & \mathrm{s}_\varphi \mathrm{s}_\alpha + \mathrm{c}_\varphi \mathrm{s}_\beta \mathrm{c}_\alpha \\ \mathrm{s}_\varphi \mathrm{c}_\beta & \mathrm{c}_\varphi \mathrm{c}_\alpha + \mathrm{s}_\varphi \mathrm{s}_\beta \mathrm{s}_\alpha & -\mathrm{c}_\varphi \mathrm{s}_\alpha + \mathrm{s}_\varphi \mathrm{s}_\beta \mathrm{c}_\alpha \\ -\mathrm{s}_\beta & \mathrm{c}_\beta \mathrm{s}_\alpha & \mathrm{c}_\beta \mathrm{c}_\alpha \end{bmatrix}, \tag{1.6a}$$

$$\boldsymbol{\omega}(\boldsymbol{q}, \dot{\boldsymbol{q}}) = \underbrace{\begin{bmatrix} 1 & 0 & -\mathrm{s}_\beta \\ 0 & \mathrm{c}_\alpha & \mathrm{c}_\beta \mathrm{s}_\alpha \\ 0 & -\mathrm{s}_\alpha & \mathrm{c}_\beta \mathrm{c}_\alpha \end{bmatrix}}_{\boldsymbol{Y}(\boldsymbol{q})} \underbrace{\begin{bmatrix} \dot\alpha \\ \dot\beta \\ \dot\varphi \end{bmatrix}}_{\dot{\boldsymbol{q}}}. \tag{1.6b}$$

The shortcut notation $\mathrm{s}_\varphi := \sin(\varphi)$ and $\mathrm{c}_\varphi := \cos(\varphi)$ used here, will be used throughout this text. With this, we may formulate the kinetic energy $\mathcal{T}(\boldsymbol{q}, \dot{\boldsymbol{q}}) = \frac{1}{2}(\boldsymbol{\omega}(\boldsymbol{q}, \dot{\boldsymbol{q}}))^\top \boldsymbol{\Theta} \boldsymbol{\omega}(\boldsymbol{q}, \dot{\boldsymbol{q}})$ which coincides with the Lagrangian since there is no potential energy. Evaluation of Lagrange's equation (1.2) yields the equations of motion

$$\underbrace{\begin{bmatrix} \Theta_{\mathsf{x}} & 0 & -\Theta_{\mathsf{x}} \mathrm{s}_\beta \\ 0 & \Theta_{\mathsf{y}} \mathrm{c}_\alpha^2 + \Theta_{\mathsf{z}} \mathrm{s}_\alpha^2 & (\Theta_{\mathsf{y}} - \Theta_{\mathsf{z}}) \mathrm{c}_\alpha \mathrm{s}_\alpha \mathrm{c}_\beta \\ -\Theta_{\mathsf{x}} \mathrm{s}_\beta & (\Theta_{\mathsf{y}} - \Theta_{\mathsf{z}}) \mathrm{c}_\alpha \mathrm{s}_\alpha \mathrm{c}_\beta & \Theta_{\mathsf{x}} \mathrm{s}_\beta^2 + (\Theta_{\mathsf{y}} \mathrm{s}_\alpha^2 + \Theta_{\mathsf{z}} \mathrm{c}_\alpha^2) \mathrm{c}_\beta^2 \end{bmatrix}}_{\boldsymbol{M}(\boldsymbol{q})} \underbrace{\begin{bmatrix} \ddot\alpha \\ \ddot\beta \\ \ddot\varphi \end{bmatrix}}_{\ddot{\boldsymbol{q}}}$$
$$+ \underbrace{\begin{bmatrix} (\Theta_{\mathsf{y}} - \Theta_{\mathsf{z}}) \mathrm{c}_\alpha \mathrm{s}_\alpha \dot\beta^2 + \cdots \\ 2(\Theta_{\mathsf{z}} - \Theta_{\mathsf{y}}) \mathrm{s}_\alpha \mathrm{c}_\alpha \dot\beta \dot\alpha + \cdots \\ (2(\Theta_{\mathsf{y}} - \Theta_{\mathsf{z}}) \mathrm{c}_\alpha^2 - \Theta_{\mathsf{x}} - \Theta_{\mathsf{y}} + \Theta_{\mathsf{z}}) \mathrm{c}_\beta \dot\beta \dot\alpha + \cdots \end{bmatrix}}_{\boldsymbol{b}(\boldsymbol{q}, \dot{\boldsymbol{q}})} = \underbrace{\begin{bmatrix} 1 & 0 & 0 \\ 0 & \mathrm{c}_\alpha & -\mathrm{s}_\alpha \\ -\mathrm{s}_\beta & \mathrm{c}_\beta \mathrm{s}_\alpha & \mathrm{c}_\beta \mathrm{c}_\alpha \end{bmatrix}}_{\boldsymbol{Y}^\top(\boldsymbol{q})} \underbrace{\begin{bmatrix} \tau_{\mathsf{x}} \\ \tau_{\mathsf{y}} \\ \tau_{\mathsf{z}} \end{bmatrix}}_{\boldsymbol{u}}. \tag{1.7}$$

The entries in $\boldsymbol{b}$ are not displayed here since they would fill several lines and are actually not of relevance here. What is crucial here is that the model has singularities at $\beta = \pm\frac{\pi}{2}$: $\det \boldsymbol{M} = \Theta_{\mathsf{x}} \Theta_{\mathsf{y}} \Theta_{\mathsf{z}} \mathrm{c}_\beta^2$ and $\det \boldsymbol{Y} = \mathrm{c}_\beta$. For the previous example of aerobatic motions it is should be evident that singularities of this form would be unacceptable for simulation and control design.

Euler's rotation equations. For the particular example of the rigid body orientation one finds another formulation of the equations of motion directly in most textbooks on mechanics, e.g. [Arnold, 1989, p. 143] or [Roberson and Schwertassek, 1988, p. 145]:

$$\frac{\mathrm{d}}{\mathrm{d}t}\underbrace{\begin{bmatrix} R^{\mathsf{x}}_{\mathsf{x}} & R^{\mathsf{x}}_{\mathsf{y}} & R^{\mathsf{x}}_{\mathsf{z}} \\ R^{\mathsf{y}}_{\mathsf{x}} & R^{\mathsf{y}}_{\mathsf{y}} & R^{\mathsf{y}}_{\mathsf{z}} \\ R^{\mathsf{z}}_{\mathsf{x}} & R^{\mathsf{z}}_{\mathsf{y}} & R^{\mathsf{z}}_{\mathsf{z}} \end{bmatrix}}_{\boldsymbol{R}} = \underbrace{\begin{bmatrix} R^{\mathsf{x}}_{\mathsf{x}} & R^{\mathsf{x}}_{\mathsf{y}} & R^{\mathsf{x}}_{\mathsf{z}} \\ R^{\mathsf{y}}_{\mathsf{x}} & R^{\mathsf{y}}_{\mathsf{y}} & R^{\mathsf{y}}_{\mathsf{z}} \\ R^{\mathsf{z}}_{\mathsf{x}} & R^{\mathsf{z}}_{\mathsf{y}} & R^{\mathsf{z}}_{\mathsf{z}} \end{bmatrix}}_{\boldsymbol{R}} \underbrace{\begin{bmatrix} 0 & -\omega_{\mathsf{z}} & \omega_{\mathsf{y}} \\ \omega_{\mathsf{z}} & 0 & -\omega_{\mathsf{x}} \\ -\omega_{\mathsf{y}} & \omega_{\mathsf{x}} & 0 \end{bmatrix}}_{\operatorname{wed}\boldsymbol{\omega}}, \tag{1.8a}$$

$$\underbrace{\begin{bmatrix} \Theta_{\mathsf{x}} & 0 & 0 \\ 0 & \Theta_{\mathsf{y}} & 0 \\ 0 & 0 & \Theta_{\mathsf{z}} \end{bmatrix}}_{\boldsymbol{\Theta}} \underbrace{\begin{bmatrix} \dot\omega_{\mathsf{x}} \\ \dot\omega_{\mathsf{y}} \\ \dot\omega_{\mathsf{z}} \end{bmatrix}}_{\dot{\boldsymbol{\omega}}} + \underbrace{\begin{bmatrix} 0 & -\omega_{\mathsf{z}} & \omega_{\mathsf{y}} \\ \omega_{\mathsf{z}} & 0 & -\omega_{\mathsf{x}} \\ -\omega_{\mathsf{y}} & \omega_{\mathsf{x}} & 0 \end{bmatrix}}_{\operatorname{wed}\boldsymbol{\omega}} \underbrace{\begin{bmatrix} \Theta_{\mathsf{x}} & 0 & 0 \\ 0 & \Theta_{\mathsf{y}} & 0 \\ 0 & 0 & \Theta_{\mathsf{z}} \end{bmatrix}}_{\boldsymbol{\Theta}} \underbrace{\begin{bmatrix} \omega_{\mathsf{x}} \\ \omega_{\mathsf{y}} \\ \omega_{\mathsf{z}} \end{bmatrix}}_{\boldsymbol{\omega}} = \underbrace{\begin{bmatrix} \tau_{\mathsf{x}} \\ \tau_{\mathsf{y}} \\ \tau_{\mathsf{z}} \end{bmatrix}}_{\boldsymbol{u}}. \tag{1.8b}$$

The 9 coefficients of the matrix $\boldsymbol{R}$ have to obey the constraint $\boldsymbol{R}^\top \boldsymbol{R} = \mathbf{I}_3$. However, it can be shown that if this is fulfilled for the initial condition $\boldsymbol{R}(t_0)$, then the kinematic equation (1.8a) ensures that the condition remains fulfilled. This formulation has no singularities and is well suited for global simulation. Moreover, loosely speaking, its mathematical structure reflects the physical symmetries of the model. The obvious draw-back is that due to the lack of generalized coordinates, its unclear how a method like computed torque could be applied.

Discussion. Euler's equations (1.8) and (1.7) describe the same system. In fact one may plug (1.6b) into (1.8b) and multiply it by $\boldsymbol{Y}^\top$ to obtain (1.7).

Each of these formulations has its advantages and draw-backs: Euler's equations are more compact and have a symmetric structure in contrast to (1.7). The downside is that they require 9 coordinates, the coefficients of the rotation matrix $\boldsymbol{R}$, to parameterize the attitude, whereas the Euler-angles $\boldsymbol{q}$ only require 3. The crucial advantage of Lagrange's equation (1.2) is, that it holds for *any* finite dimensional and holonomic mechanical system, whereas Euler's equations only hold for this particular example. However, for this example, the equations (1.7) are quite cumbersome and lack an obvious structure. Probably the worst fact is that the inertia matrix $\boldsymbol{M}(\boldsymbol{q})$ is singular at the point $\beta = \pm\frac{\pi}{2}$ and consequently $\ddot{\boldsymbol{q}}$ is undefined at these points.

It should be stressed that there is no physical reason for the singularity in the Lagrangian version (1.7), it is rather a consequence of an unsuitable parameterization of the system. This is pointed out in [Roberson and Schwertassek, 1988, sec. 1.1.1] as: *[The scientists of the Eighteenth Century] recognized that there was something about rotation [...] which somehow made the analysis of rotation a problem of higher order difficulty. We now know that the problem is in the mathematics, not the physics, but the problem is still with us.*

The set of 3-dimensional rotation matrices $\boldsymbol{R} \in \mathbb{SO}(3)$ captures the actual configuration space of the rigid body orientation well, but it is difficult to work with since the coefficients of the rotation matrix are not independent. Since $\boldsymbol{R} \in \mathbb{SO}(3)$ is compact while $\mathbb{R}^3$ is not, there is no bijection between them, see also [Frankel, 1997, sec. 1.1d]. The chosen set of Euler angles may be regarded as a surjective but not injective function from $\mathbb{R}^3$ to $\boldsymbol{R} \in \mathbb{SO}(3)$ in a similar manner as latitude and longitude serve as coordinates for Earth's surface. The Euler angles fail are unsuited at the so called gimbal lock ($\beta = \pm 90°$) just as longitude fails at Earths poles.

1.3 Goal and outline of this work

The first chapter reviews established methods of analytical mechanics with the addition of allowing redundant coordinates (like the coefficients of a rotation matrix $\boldsymbol{R}$) and non-holonomic velocity coordinates (like the coefficients of the angular velocity $\boldsymbol{\omega}$). It will present a formulation that can derive both of the presented equations of motion for the motivation example, but holds for general finite-dimensional mechanical systems.

The second chapter specializes to rigid body systems, i.e. systems that consist of several interconnected rigid bodies. It presents an algorithm that derives the equations of motion based on chosen coordinates and given constitutive parameters. Furthermore, natural formulations of stiffness, dissipation and inertia for a rigid body are established.

The third chapter proposes tracking control algorithms for rigid body systems. Based on the findings of the second chapter it will present three control algorithms motivated by defining desired stiffness, damping and inertia of the resulting controlled system. Furthermore, these algorithms are extended to tackle underactuated systems. These algorithms are discussed through several examples.

The fourth chapter presents the developed quadcopter and tricopter and their performance for real control of aerobatic maneuvers.

Chapter 2

Some math

This chapter reviews some established mathematical concepts in particular for the context of redundant coordinates.

2.1 Coordinates

The example of the rigid body orientation showed that, though its degree of freedom is $n = 3$, it cannot be *globally* parameterized by 3 coordinates without having singularities. In other words, the configuration space of the rigid body orientation is not isomorphic to $\mathbb{R}^3$ and is called a nonlinear manifold.

If interested in a global parameterization of a n dimensional nonlinear manifold, there are two common approaches:

1. Choose a finite number of overlapping local charts with with *minimal* coordinates $\boldsymbol{q} \in \mathbb{R}^n$, e.g. four distinct sets of Euler angles for the rigid body attitude [Grafarend and Kühnel, 2011]. As this is the common way of defining a smooth manifold, this is always possible.

2. Choose one parameterization with *redundant* coordinates $\boldsymbol{x} \in \mathbb{R}^\nu$, i.e. coordinates that are constrained by smooth equations of the form $\boldsymbol{\phi}(\boldsymbol{x}) = \boldsymbol{0}$. E.g. the coefficients of the rotation matrix as done in (1.8). *Whitney embedding theorem* states that this is always possible with at least $\nu = 2n$ coordinates.

Both approaches have benefits and drawbacks depending on the application, but the first approach and the use of minimal coordinates is far more dominant in the literature. This work utilizes the second approach.

2.1.1 Redundant configuration coordinates

In the notation of this work, we use $\nu > 0$ coordinates $\boldsymbol{x}(t) = [x^1(t), \ldots, x^\nu(t)]^\top \in \mathbb{R}^\nu$ that might be constrained by $c \geq 0$ smooth functions of the form $\boldsymbol{\phi}(\boldsymbol{x}) = [\phi^1(\boldsymbol{x}), \ldots, \phi^c(\boldsymbol{x})]^\top =$

$\mathbf{0}$. For $c > 0$ these coordinates are not independent and are commonly called *redundant*. The set of mutually admissible coordinates is called the configuration space $\mathbb{X}$:

$$\mathbb{X} = \{\boldsymbol{x} \in \mathbb{R}^\nu \,|\, \boldsymbol{\phi}(\boldsymbol{x}) = \mathbf{0}\}. \tag{2.1}$$

Assuming that the rank of $\frac{\partial \boldsymbol{\phi}}{\partial \boldsymbol{x}}$ is constant, the dimension of the configuration space is

$$n = \dim \mathbb{X} = \nu - \operatorname{rank} \frac{\partial \boldsymbol{\phi}}{\partial \boldsymbol{x}}. \tag{2.2}$$

For holonomic systems, n is also called its degree of freedom.

Whitney embedding theorem (see e.g. [Lee, 2003, Theo. 6.14]) states that: *Every smooth manifold of dimension n can be smoothly embedded in the Euclidean space $\mathbb{R}^{2n}$.* The number $2n$ is a worst case bound, i.e. for a particular example a lower dimension for the embedding space $\mathbb{R}^\nu$ might work and a higher dimension is permitted anyway. For this work, it essentially guarantees the existence of a global parameterization by the set $\mathbb{X}$ for any smooth manifold.

2.1.2 Minimal velocity coordinates

For the following it is crucial to note that a geometric constraint is equivalent to its derivative supplemented with a suitable initial condition

$$\phi^\kappa(\boldsymbol{x}) = 0 \tag{2.3a}$$

$$\Leftrightarrow \quad \frac{\partial \phi^\kappa}{\partial x^\alpha}(\boldsymbol{x})\dot{x}^\alpha = 0, \qquad \phi^\kappa(\boldsymbol{x}_0) = 0 \tag{2.3b}$$

$$\Leftrightarrow \quad \frac{\partial \phi^\kappa}{\partial x^\alpha}(\boldsymbol{x})\ddot{x}^\alpha + \frac{\partial^2 \phi^\kappa}{\partial x^\alpha \partial x^\beta}(\boldsymbol{x})\dot{x}^\beta \dot{x}^\alpha = 0, \qquad \phi^\kappa(\boldsymbol{x}_0) = 0,\ \frac{\partial \phi^\kappa}{\partial x^\alpha}(\boldsymbol{x}_0)\dot{x}_0^\alpha = 0 \tag{2.3c}$$

$$\cdots$$

where $\boldsymbol{x}_0 = \boldsymbol{x}(t_0)$. Even though (2.3a) might be nonlinear, its derivative (2.3b) is always *linear* in the velocities $\dot{\boldsymbol{x}}$. So here it is reasonable to choose *minimal velocity coordinates*: Let $\boldsymbol{A}(\boldsymbol{x}) \in \mathbb{R}^{\nu \times n}$ be a matrix with the properties $\frac{\partial \boldsymbol{\phi}}{\partial \boldsymbol{x}}\boldsymbol{A} = \mathbf{0}$ and $\operatorname{rank} \boldsymbol{A} = n$. The first property of $\boldsymbol{A}(\boldsymbol{x})$ is that these columns of $\boldsymbol{A}(\boldsymbol{x})$ are orthogonal to the rows of $\frac{\partial \boldsymbol{\phi}}{\partial \boldsymbol{x}}(\boldsymbol{x})$. The second property implies that the columns of $\boldsymbol{A}(\boldsymbol{x})$ are linearly independent. So the columns of $\boldsymbol{A}(\boldsymbol{x})$ can be interpreted as a *basis vectors* for the tangent space $\mathsf{T}_{\boldsymbol{x}}\mathbb{X}$. We can capture all allowed velocities $\dot{\boldsymbol{x}}(t)$ by the minimal velocity coordinates $\boldsymbol{\xi}(t) \in \mathbb{R}^n$ through

$$\dot{\boldsymbol{x}} = \boldsymbol{A}(\boldsymbol{x})\boldsymbol{\xi} \tag{2.4}$$

This kinematic relation (2.4) ensures that the time derivative (2.3b) of the geometric constraint is fulfilled, and consequently the geometric constraint only has to be imposed on the initial condition $\boldsymbol{\phi}(\boldsymbol{x}(t_0)) = \mathbf{0}$.

Example 1. Consider a single particle constrained to a circle of radius ρ as illustrated in Figure 2.1.

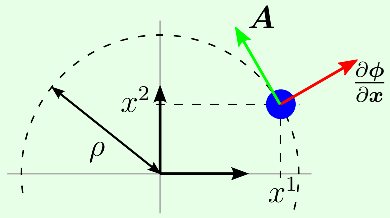

Figure 2.1: Particle on a circle

We use the its Cartesian position $[x^1, x^2]^\top \in \mathbb{R}^2$ constrained by $\phi = (x^1)^2 + (x^2)^2 - \rho^2 = 0$ as configuration coordinates. A reasonable choice for the kinematics matrix $\boldsymbol{A}$ is

$$\underbrace{\begin{bmatrix} 2x^1 & 2x^2 \end{bmatrix}}_{\frac{\partial \phi}{\partial \boldsymbol{x}}} \underbrace{\begin{bmatrix} -x^2 \\ x^1 \end{bmatrix}}_{\boldsymbol{A}} = 0 \tag{2.5}$$

Example 2. Consider the motivation example of the rigid body orientation from section 1.2. Instead of parameterizing the rotation matrix $\boldsymbol{R}$ by minimal coordinates, we take its 9 coefficients $\boldsymbol{x} = [R^{\mathsf{x}}_{\mathsf{x}}, R^{\mathsf{y}}_{\mathsf{x}}, R^{\mathsf{z}}_{\mathsf{x}}, R^{\mathsf{x}}_{\mathsf{y}}, R^{\mathsf{y}}_{\mathsf{y}}, R^{\mathsf{z}}_{\mathsf{y}}, R^{\mathsf{x}}_{\mathsf{z}}, R^{\mathsf{y}}_{\mathsf{z}}, R^{\mathsf{z}}_{\mathsf{z}}]^\top \in \mathbb{R}^9$ as configuration coordinates. The constraints $\boldsymbol{R}^\top \boldsymbol{R} = \mathbf{I}_3$ and $\det \boldsymbol{R} = 1$ read

$$\boldsymbol{\phi}(\boldsymbol{x}) = \begin{bmatrix} (R^{\mathsf{x}}_{\mathsf{x}})^2 + (R^{\mathsf{y}}_{\mathsf{x}})^2 + (R^{\mathsf{z}}_{\mathsf{x}})^2 - 1 \\ (R^{\mathsf{x}}_{\mathsf{y}})^2 + (R^{\mathsf{y}}_{\mathsf{y}})^2 + (R^{\mathsf{z}}_{\mathsf{y}})^2 - 1 \\ (R^{\mathsf{x}}_{\mathsf{z}})^2 + (R^{\mathsf{y}}_{\mathsf{z}})^2 + (R^{\mathsf{z}}_{\mathsf{z}})^2 - 1 \\ R^{\mathsf{x}}_{\mathsf{y}} R^{\mathsf{x}}_{\mathsf{z}} + R^{\mathsf{y}}_{\mathsf{y}} R^{\mathsf{y}}_{\mathsf{z}} + R^{\mathsf{z}}_{\mathsf{y}} R^{\mathsf{z}}_{\mathsf{z}} \\ R^{\mathsf{x}}_{\mathsf{x}} R^{\mathsf{x}}_{\mathsf{z}} + R^{\mathsf{y}}_{\mathsf{x}} R^{\mathsf{y}}_{\mathsf{z}} + R^{\mathsf{z}}_{\mathsf{x}} R^{\mathsf{z}}_{\mathsf{z}} \\ R^{\mathsf{x}}_{\mathsf{x}} R^{\mathsf{x}}_{\mathsf{y}} + R^{\mathsf{y}}_{\mathsf{x}} R^{\mathsf{y}}_{\mathsf{y}} + R^{\mathsf{z}}_{\mathsf{x}} R^{\mathsf{z}}_{\mathsf{y}} \\ R^{\mathsf{x}}_{\mathsf{x}} R^{\mathsf{y}}_{\mathsf{y}} R^{\mathsf{z}}_{\mathsf{z}} + R^{\mathsf{x}}_{\mathsf{y}} R^{\mathsf{y}}_{\mathsf{z}} R^{\mathsf{z}}_{\mathsf{x}} + R^{\mathsf{x}}_{\mathsf{z}} R^{\mathsf{y}}_{\mathsf{x}} R^{\mathsf{z}}_{\mathsf{y}} - R^{\mathsf{x}}_{\mathsf{x}} R^{\mathsf{y}}_{\mathsf{z}} R^{\mathsf{z}}_{\mathsf{y}} - R^{\mathsf{x}}_{\mathsf{y}} R^{\mathsf{y}}_{\mathsf{x}} R^{\mathsf{z}}_{\mathsf{z}} - R^{\mathsf{x}}_{\mathsf{z}} R^{\mathsf{y}}_{\mathsf{y}} R^{\mathsf{z}}_{\mathsf{x}} - 1 \end{bmatrix} = \mathbf{0}. \tag{2.6}$$

The 9 conditions $\boldsymbol{R}^\top \boldsymbol{R} = \mathbf{I}_3$ yields due to symmetry only 6 constraints and already imply $\det \boldsymbol{R} = \pm 1$. Since the determinant is a smooth function, the corresponding manifold must consist of two disjoint components, one with $\det \boldsymbol{R} = +1$ (proper rotations) and one with $\det \boldsymbol{R} = -1$ (rotations with reflection). So the additional constraint $\det \boldsymbol{R} = +1$ does not change the dimension of the configuration space. Formally this means $\operatorname{rank} \frac{\partial \phi}{\partial \boldsymbol{x}} = 6$ and consequently $\dim \mathbb{X} = 9 - 6 = 3$. A kinematics matrix with $\frac{\partial \phi}{\partial \boldsymbol{x}} \boldsymbol{A} = \mathbf{0}$ and $\operatorname{rank} \boldsymbol{A} = 3$

is given by

$$\boldsymbol{A}(\boldsymbol{x}) = \begin{bmatrix} 0 & -R^{\mathsf{x}}_{\mathsf{z}} & R^{\mathsf{x}}_{\mathsf{y}} \\ 0 & -R^{\mathsf{y}}_{\mathsf{z}} & R^{\mathsf{y}}_{\mathsf{y}} \\ 0 & -R^{\mathsf{z}}_{\mathsf{z}} & R^{\mathsf{z}}_{\mathsf{y}} \\ R^{\mathsf{x}}_{\mathsf{z}} & 0 & -R^{\mathsf{x}}_{\mathsf{x}} \\ R^{\mathsf{y}}_{\mathsf{z}} & 0 & -R^{\mathsf{y}}_{\mathsf{x}} \\ R^{\mathsf{z}}_{\mathsf{z}} & 0 & -R^{\mathsf{z}}_{\mathsf{x}} \\ -R^{\mathsf{x}}_{\mathsf{y}} & R^{\mathsf{x}}_{\mathsf{x}} & 0 \\ -R^{\mathsf{y}}_{\mathsf{y}} & R^{\mathsf{y}}_{\mathsf{x}} & 0 \\ -R^{\mathsf{z}}_{\mathsf{y}} & R^{\mathsf{z}}_{\mathsf{x}} & 0 \end{bmatrix}. \tag{2.7}$$

The resulting kinematic equation $\dot{\boldsymbol{x}} = \boldsymbol{A}(\boldsymbol{x})\boldsymbol{\xi}$ can be reordered to the matrix equation $\dot{\boldsymbol{R}} = \boldsymbol{R}\,\mathrm{wed}(\boldsymbol{\xi})$ by introducing the *wedge operator* defined as

$$\mathrm{wed}\begin{bmatrix}\xi^1\\ \xi^2\\ \xi^3\end{bmatrix} = \begin{bmatrix} 0 & -\xi^3 & \xi^2 \\ \xi^3 & 0 & -\xi^1 \\ -\xi^2 & \xi^1 & 0 \end{bmatrix}. \tag{2.8}$$

Pseudoinverse For any matrix $\boldsymbol{S} \in \mathbb{R}^{m\times n}$ there exists a unique *(Moore-Penrose) pseudoinverse* $\boldsymbol{S}^+ \in \mathbb{R}^{n\times m}$ determined by the following conditions [Penrose, 1955, Theo. 1]:

$$\boldsymbol{S}\boldsymbol{S}^+\boldsymbol{S} = \boldsymbol{S}, \tag{2.9a}$$
$$\boldsymbol{S}^+\boldsymbol{S}\boldsymbol{S}^+ = \boldsymbol{S}^+, \tag{2.9b}$$
$$(\boldsymbol{S}\boldsymbol{S}^+)^\top = \boldsymbol{S}\boldsymbol{S}^+, \tag{2.9c}$$
$$(\boldsymbol{S}^+\boldsymbol{S})^\top = \boldsymbol{S}^+\boldsymbol{S}. \tag{2.9d}$$

If the matrix $\boldsymbol{S}$ has linearly independent columns, its pseudoinverse is $\boldsymbol{S}^+ = (\boldsymbol{S}^\top\boldsymbol{S})^{-1}\boldsymbol{S}^\top$. Similarly, if $\boldsymbol{S}$ has linearly independent rows, its pseudoinverse is $\boldsymbol{S}^+ = \boldsymbol{S}^\top(\boldsymbol{S}\boldsymbol{S}^\top)^{-1}$. Consequently, if $\boldsymbol{S}$ is invertible (independent rows and columns) the pseudoinverse coincides with the inverse $\boldsymbol{S}^+ = \boldsymbol{S}^{-1}$.

Some identities involving the pseudo-inverse. Define $\boldsymbol{Y}(\boldsymbol{x}) \in \mathbb{R}^{n\times\nu}$ as $\boldsymbol{Y} = \boldsymbol{A}^+ = (\boldsymbol{A}^\top\boldsymbol{A})^{-1}\boldsymbol{A}^\top$, i.e. the pseudoinverse of the kinematics matrix $\boldsymbol{A}$. Note that this implies $\boldsymbol{Y}\boldsymbol{A} = \mathbf{I}_n$, but $\boldsymbol{A}\boldsymbol{Y} \neq \mathbf{I}_\nu$. We also introduce the matrices $\boldsymbol{\Phi} = \frac{\partial\boldsymbol{\phi}}{\partial\boldsymbol{x}}$ and $\boldsymbol{\Psi} = \boldsymbol{\Phi}^+$. With $\boldsymbol{\Phi}\boldsymbol{A} = \mathbf{0}$ and the Penrose conditions (2.9), we can show[1] that $\boldsymbol{\Psi}^\top\boldsymbol{A} = \mathbf{0}$ and $\boldsymbol{Y}^\top\boldsymbol{\Phi} = \mathbf{0}$. Furthermore, since $\operatorname{rank}\boldsymbol{\Psi} = \operatorname{rank}\boldsymbol{\Phi} = \nu - n$ the columns of $\boldsymbol{\Psi}(\boldsymbol{x})$ span the complementary space $(\mathsf{T}_{\boldsymbol{x}}\mathbb{X})^\perp$ though they might not be a basis since the columns might not be linearly independent.

The matrix $\boldsymbol{P} = \boldsymbol{A}\boldsymbol{Y}$ is an *orthogonal projector*, i.e. $\boldsymbol{P}^2 = \boldsymbol{P}$ and $\boldsymbol{P}^\top = \boldsymbol{P}$ which result directly from the Penrose conditions (2.9). Since $\boldsymbol{\Psi}$ spans the complementary

[1] $\boldsymbol{\Psi}^\top\boldsymbol{A} = (\boldsymbol{\Psi}\boldsymbol{\Phi}\boldsymbol{\Psi})^\top\boldsymbol{A} = \boldsymbol{\Psi}^\top(\boldsymbol{\Psi}\boldsymbol{\Phi})^\top\boldsymbol{A} = \boldsymbol{\Psi}^\top\boldsymbol{\Psi}\boldsymbol{\Phi}\boldsymbol{A} = \mathbf{0}$

space $(\mathsf{T}_{\boldsymbol{x}}\mathbb{X})^{\perp}$, the unique orthogonal projector from $\mathbb{R}^{\nu}$ to $(\mathsf{T}_{\boldsymbol{x}}\mathbb{X})^{\perp}$ can be expressed as $\boldsymbol{P}^{\perp} = \boldsymbol{\Psi\Phi}$. The identity $\boldsymbol{P} + \boldsymbol{P}^{\perp} = \mathbf{I}_{\nu}$ implies

$$\boldsymbol{AY} + \boldsymbol{\Psi\Phi} = \mathbf{I}_{\nu}. \tag{2.10}$$

2.2 Calculus

This section reviews some of the established tools of calculus for the context of redundant coordinates and nonholonomic velocity coordinates as introduced in the previous section.

2.2.1 Directional derivative and Hessian

Consider a function $\mathcal{V} : \mathbb{R}^{\nu} \to \mathbb{R}$ and a curve $\boldsymbol{x} : \mathbb{R} \to \mathbb{X}$. Since $\mathbb{X} \subset \mathbb{R}^{\nu}$, their composition $\mathcal{V} \circ \boldsymbol{x} = f : \mathbb{R} \to \mathbb{R}$ is a scalar function and has the the Taylor expansion

$$\begin{aligned}\underbrace{\mathcal{V}(\boldsymbol{x}(t))}_{f(t)} = \underbrace{\mathcal{V}(\boldsymbol{x}(0))}_{f(0)} &+ t\underbrace{\frac{\partial \mathcal{V}}{\partial x^{\alpha}}(\boldsymbol{x}(0))\dot{x}^{\alpha}(0)}_{\dot{f}(0)} \\ &+ \tfrac{1}{2}t^2 \underbrace{\Big(\frac{\partial^2 \mathcal{V}}{\partial x^{\beta}\partial x^{\alpha}}(\boldsymbol{x}(0))\dot{x}^{\alpha}(0)\dot{x}^{\beta}(0) + \frac{\partial \mathcal{V}}{\partial x^{\alpha}}(\boldsymbol{x}(0))\ddot{x}^{\alpha}(0)\Big)}_{\ddot{f}(0)} + \mathcal{O}(t^3).\end{aligned} \tag{2.11}$$

Now let the curve be parameterized by $\dot{\boldsymbol{x}}(t) = \boldsymbol{A}(\boldsymbol{x}(t))\boldsymbol{\xi}(t)$ and we use the shorthand notations $\bar{\boldsymbol{x}} = \boldsymbol{x}(0)$, $\bar{\boldsymbol{\xi}} = \boldsymbol{\xi}(0)$ and $\bar{\boldsymbol{A}} = \boldsymbol{A}(\boldsymbol{x}(0))$ to write

$$\begin{aligned}\mathcal{V}(\boldsymbol{x}(t)) = \mathcal{V}(\bar{\boldsymbol{x}}) &+ t\frac{\partial \mathcal{V}}{\partial x^{\alpha}}(\bar{\boldsymbol{x}})\bar{A}_i^{\alpha}\bar{\xi}^i \\ &+ \tfrac{1}{2}t^2\Big(\frac{\partial^2 \mathcal{V}}{\partial x^{\beta}\partial x^{\alpha}}(\bar{\boldsymbol{x}})\bar{A}_i^{\alpha}\bar{A}_j^{\beta}\bar{\xi}^i\bar{\xi}^j + \frac{\partial \mathcal{V}}{\partial x^{\alpha}}(\bar{\boldsymbol{x}})\Big(\frac{\partial A_i^{\alpha}}{\partial x^{\beta}}(\bar{\boldsymbol{x}})\bar{A}_j^{\beta}\bar{\xi}^i\bar{\xi}^j + \bar{A}_i^{\alpha}\dot{\bar{\xi}}^i\Big)\Big) + \mathcal{O}(t^3)\end{aligned} \tag{2.12}$$

Introducing the notation

$$\partial_i = A_i^{\alpha}\frac{\partial}{\partial x^{\alpha}},\ \ i = 1, \dots, n \tag{2.13}$$

for the derivative in the direction of the i-th basis vector, we can state the Taylor expansion as

$$\mathcal{V}(\boldsymbol{x}(t)) = \mathcal{V}(\bar{\boldsymbol{x}}) + t\,\partial_i\mathcal{V}(\bar{\boldsymbol{x}})\bar{\xi}^i + \tfrac{1}{2}t^2\big(\partial_i\partial_j\mathcal{V}(\bar{\boldsymbol{x}})\bar{\xi}^i\bar{\xi}^j + \partial_i\mathcal{V}(\bar{\boldsymbol{x}})\dot{\bar{\xi}}^i\big) + \mathcal{O}(t^3). \tag{2.14}$$

There are two more things we can derive from this equation:

- If $\partial_i\mathcal{V}(\bar{\boldsymbol{x}}) = 0, i = 1, \dots, n$ then $\bar{\boldsymbol{x}}$ is called a *critical point* of $\mathcal{V}$. At a critical point the expansion (2.14) reduces to

$$\mathcal{V}(\boldsymbol{x}(t)) = \mathcal{V}(\bar{\boldsymbol{x}}) + \tfrac{1}{2}t^2\underbrace{(\partial_i\partial_j\mathcal{V})(\bar{\boldsymbol{x}})}_{\bar{H}_{ij}}\bar{\xi}^i\bar{\xi}^j + \mathcal{O}(t^3). \tag{2.15}$$

  This relation holds for any sufficiently smooth curve $t \mapsto \boldsymbol{x}(t)$ through $\bar{\boldsymbol{x}}$ and consequently for any velocity vector $\bar{\boldsymbol{\xi}}$ at the critical point. So if the matrix $\bar{\boldsymbol{H}}$ is positive (negative) definite, then $\bar{\boldsymbol{x}}$ is a local minimum (maximum) of $\mathcal{V}$.

- Assume the curve $t \mapsto \boldsymbol{x}(t)$ is a *geodesic*, i.e. $\dot{\xi}^i = -\Gamma^i_{jk}\xi^j\xi^k$ with the connection coefficients Γ^i_{jk} that will be discussed later. Plugging this into (2.14) we find a coordinate form of the *Hessian tensor* $\boldsymbol{\nabla}^2\mathcal{V}$ of the potential:

$$\mathcal{V}(\boldsymbol{x}(t)) = \mathcal{V}(\bar{\boldsymbol{x}}) + t(\partial_i\mathcal{V})(\bar{\boldsymbol{x}})\bar{\xi}^i + \tfrac{1}{2}t^2\underbrace{\big(\partial_i\partial_j\mathcal{V} - \Gamma^k_{ij}\partial_k\mathcal{V}\big)}_{(\boldsymbol{\nabla}^2\mathcal{V})_{ij}}(\bar{\boldsymbol{x}})\bar{\xi}^i\bar{\xi}^j + \mathcal{O}(t^3). \tag{2.16}$$

  At a critical point $\bar{\boldsymbol{x}}$, the Hessian of the potential is independent of the connection coefficients Γ^i_{jk} and consequently of the underlying metric. There it coincides with the matrix $\bar{\boldsymbol{H}}$ defined in (2.15).

2.2.2 Commutation coefficients

For a function $\mathcal{V} : \mathbb{R}^\nu \to \mathbb{R}$ we are used to the fact that partial derivatives commute, i.e. $\partial^2\mathcal{V}/\partial x^\alpha\partial x^\beta = \partial^2\mathcal{V}/\partial x^\beta\partial x^\alpha$. Unfortunately this is (in general) not the case for a directional derivatives like ∂_i defined in (2.13). Consequently we investigate the following commutation relation

$$\begin{aligned}
\partial_i\partial_j\mathcal{V} - \partial_j\partial_i\mathcal{V} &= A^\alpha_i\frac{\partial}{\partial x^\alpha}\left(A^\beta_j\frac{\partial\mathcal{V}}{\partial x^\beta}\right) - A^\beta_j\frac{\partial}{\partial x^\beta}\left(A^\alpha_i\frac{\partial\mathcal{V}}{\partial x^\alpha}\right)\\
&= A^\alpha_i\frac{\partial A^\beta_j}{\partial x^\alpha}\frac{\partial\mathcal{V}}{\partial x^\beta} - A^\beta_j\frac{\partial A^\alpha_i}{\partial x^\beta}\frac{\partial\mathcal{V}}{\partial x^\alpha} + A^\alpha_i A^\beta_j\underbrace{\left(\frac{\partial^2\mathcal{V}}{\partial x^\alpha\partial x^\beta} - \frac{\partial^2\mathcal{V}}{\partial x^\beta\partial x^\alpha}\right)}_{=0}\\
&= \left(A^\beta_i\frac{\partial A^\alpha_j}{\partial x^\beta} - A^\beta_j\frac{\partial A^\alpha_i}{\partial x^\beta}\right)\frac{\partial\mathcal{V}}{\partial x^\alpha}.
\end{aligned} \tag{2.17}$$

Now using the identity (2.10) with $\Phi^\kappa_\alpha = \frac{\partial\phi^\kappa}{\partial x^\alpha}$ and $\Phi^\kappa_\alpha A^\alpha_i = 0 \Rightarrow \Phi^\kappa_\alpha\frac{\partial A^\alpha_i}{\partial x^\beta} = -\frac{\partial\Phi^\kappa_\alpha}{\partial x^\beta}A^\alpha_i$ to shape this expressions a bit further

$$\begin{aligned}
\partial_i\partial_j\mathcal{V} - \partial_j\partial_i\mathcal{V} &= \left(A^\beta_i\frac{\partial A^\alpha_j}{\partial x^\beta} - A^\beta_j\frac{\partial A^\alpha_i}{\partial x^\beta}\right)\overbrace{(A^\sigma_k Y^k_\alpha + \Psi^\sigma_\kappa\Phi^\kappa_\alpha)}^{\delta^\sigma_\alpha}\frac{\partial\mathcal{V}}{\partial x^\sigma}\\
&= \left(A^\beta_i\frac{\partial A^\alpha_j}{\partial x^\beta} - A^\beta_j\frac{\partial A^\alpha_i}{\partial x^\beta}\right)Y^k_\alpha A^\sigma_k\frac{\partial\mathcal{V}}{\partial x^\sigma} - \left(A^\beta_i A^\alpha_j\frac{\partial\Phi^\kappa_\alpha}{\partial x^\beta} - A^\beta_j A^\alpha_i\frac{\partial\Phi^\kappa_\alpha}{\partial x^\beta}\right)\Psi^\sigma_\kappa\frac{\partial\mathcal{V}}{\partial x^\sigma}\\
&= \underbrace{\left(A^\beta_i\frac{\partial A^\alpha_j}{\partial x^\beta} - A^\beta_j\frac{\partial A^\alpha_i}{\partial x^\beta}\right)Y^k_\alpha}_{\gamma^k_{ij}}\underbrace{A^\sigma_k\frac{\partial\mathcal{V}}{\partial x^\sigma}}_{\partial_k\mathcal{V}} - A^\beta_j A^\alpha_i\underbrace{\left(\frac{\partial^2\phi^\kappa}{\partial x^\alpha\partial x^\beta} - \frac{\partial^2\phi^\kappa}{\partial x^\beta\partial x^\alpha}\right)}_{=0}\Psi^\sigma_\kappa\frac{\partial\mathcal{V}}{\partial x^\sigma}.
\end{aligned} \tag{2.18}$$

Since this relation holds for any function $\mathcal{V}$ we can state it in operator form and introduce the *commutation coefficients* γ^k_{ij} as

$$\partial_i\partial_j - \partial_j\partial_i = \gamma^k_{ij}\partial_k, \qquad \gamma^k_{ij} = \big(\partial_i A^\alpha_j - \partial_j A^\alpha_i\big)(A^+)^k_\alpha. \tag{2.19}$$

Note the skew symmetry $\gamma^k_{ij} = -\gamma^k_{ji}$.

Example 3. The commutation coefficients γ_{ij}^k associated with the kinematics matrix $\boldsymbol{A}$ from (2.7) are

$$
\begin{aligned}
\gamma_{23}^1 = \gamma_{31}^2 = \gamma_{12}^3 &= +1, \\
\gamma_{32}^1 = \gamma_{13}^2 = \gamma_{21}^3 &= -1, \\
\gamma_{11}^1 = \gamma_{12}^1 = \gamma_{13}^1 = \gamma_{21}^1 = \gamma_{22}^1 = \gamma_{31}^1 = \gamma_{33}^1 &= 0, \\
\gamma_{11}^2 = \gamma_{12}^2 = \gamma_{21}^2 = \gamma_{22}^2 = \gamma_{23}^2 = \gamma_{32}^2 = \gamma_{33}^2 &= 0, \\
\gamma_{11}^3 = \gamma_{13}^3 = \gamma_{22}^3 = \gamma_{23}^3 = \gamma_{31}^3 = \gamma_{32}^3 = \gamma_{33}^3 &= 0.
\end{aligned}
$$

This coincides with the three dimensional Levi-Civita symbol commonly defined as

$$
\gamma_{ij}^k = \begin{cases} +1, & (i,j,k) \text{ even permutation of } (1,2,3) \\ -1, & (i,j,k) \text{ odd permutation of } (1,2,3) \\ 0, & \text{else} \end{cases} . \tag{2.20}
$$

It is related to the 3 dimensional *cross product* by $\boldsymbol{a}, \boldsymbol{b} \in \mathbb{R}^3 : [\gamma_{ij}^k a^i b^j]_{k=1..3} = \boldsymbol{a} \times \boldsymbol{b}$ and to the previously defined wed operator by $\boldsymbol{a} \in \mathbb{R}^3 : [\gamma_{ij}^k a^i]_{j,k=1..3} = \mathrm{wed}(\boldsymbol{a})$.

The right hand side of (2.19) appears in the context of Lagrange's equation in [Boltzmann, 1902, p. 687] and [Hamel, 1904a, p. 10] for the case of minimal configuration coordinates and consequently with a square matrix $\boldsymbol{A}$. In the contemporary literature on this context, the quantities γ_{ij}^k are sometimes called the *Boltzmann three-index symbols* [Lurie, 2002, sec. 1.8] or *Hamel coefficients* [Bremer, 2008, p. 75]. The left hand side of (2.19) appears in the context of tensor algebra in [Misner et al., 1973, Box 8.4] where γ_{ij}^k are called the *commutation coefficients*. From the way γ_{ij}^k is defined here, this naming seems most fitting and will be used throughout this work.

The case of redundant configuration coordinates and consequently a non-square matrix $\boldsymbol{A}$ as derived above, is not established in the literature to the best of the authors knowledge.

It is worth noting that the commutation coefficients are *invariant* to the choice of configuration coordinates $\boldsymbol{x}$, even though the coordinates appear explicitly in the definition: For a change of configuration coordinates $\boldsymbol{x} = f(\hat{\boldsymbol{x}})$ the commutation symbols transform like $\hat{\gamma}_{ij}^k(\hat{\boldsymbol{x}}) = \gamma_{ij}^k(f(\hat{\boldsymbol{x}}))$. This might be obvious from a geometric point of view, but the explicit calculation of the coordinate transformation is shown in see [sec:TrafoRules]. It will even turn out that for most of our examples the coefficients will be constants.

The commutation coefficients γ_{jk}^i vanish if the corresponding velocity coordinates ξ^i are *integrable*, i.e.

$$
\begin{aligned}
\exists\, \pi^i : \dot{\pi}^i = \xi^i = Y_\alpha^i \dot{x}^\alpha \quad &\Rightarrow \quad Y_\alpha^i = \frac{\partial \pi^i}{\partial x^\beta} \\
&\Rightarrow \quad \frac{\partial Y_\alpha^i}{\partial x^\alpha} = \frac{\partial^2 \pi^i}{\partial x^\beta \partial x^\alpha} = \frac{\partial Y_\beta^i}{\partial x^\alpha}, \quad \Rightarrow \quad \gamma_{jk}^i = 0.
\end{aligned} \tag{2.21}
$$

This is not the case in general. Nevertheless the quantities π are introduced as *nonholonomic coordinates* in [Boltzmann, 1902] or as *quasi coordinates* in [Lurie, 2002, sec. 1.5].

Then we could write $\partial_i(\partial_j f) - \partial_j(\partial_i f) = \partial^2 f/\partial\pi^i\partial\pi^j - \partial^2 f/\partial\pi^j\partial\pi^i \neq 0$ what might lead to the conception that partial derivatives do not commute. The commutativity clearly holds, the issue is rather π are no proper coordinates. To avoid confusion of this kind we do not pick up this notation here. See also [Hamel, 1904b] for an extensive discussion on this topic.

2.2.3 Linearization about a trajectory

Let $\bar{\boldsymbol{x}} : [t_1, t_2] \to \mathbb{X}$ be a smooth curve with the velocity coordinates $\bar{\boldsymbol{\xi}} : [t_1, t_2] \to \mathbb{R}^n : t \mapsto \boldsymbol{A}^+(\bar{\boldsymbol{x}}(t))\dot{\bar{\boldsymbol{x}}}(t)$. For a small deviation $\boldsymbol{x} \approx \bar{\boldsymbol{x}}$ with $\boldsymbol{x} \in \mathbb{X}$ we may approximate the geometric constraint as

$$\boldsymbol{\phi}(\boldsymbol{x}) \approx \underbrace{\boldsymbol{\phi}(\bar{\boldsymbol{x}})}_{=\boldsymbol{0}} + \frac{\partial \boldsymbol{\phi}}{\partial \boldsymbol{x}}(\bar{\boldsymbol{x}})(\boldsymbol{x} - \bar{\boldsymbol{x}}) = \boldsymbol{0}. \tag{2.22}$$

Since this constraint is affine w.r.t. $\boldsymbol{x}$ it is reasonable to use a the basis $\boldsymbol{\varepsilon}(t) \in \mathbb{R}^n$ for the deviated configuration coordinates:

$$\boldsymbol{x} = \bar{\boldsymbol{x}} + \boldsymbol{A}(\bar{\boldsymbol{x}})\boldsymbol{\varepsilon}, \qquad \boldsymbol{\varepsilon} = \boldsymbol{A}^+(\bar{\boldsymbol{x}})(\boldsymbol{x} - \bar{\boldsymbol{x}}), \tag{2.23}$$

For the velocity coordinates $\boldsymbol{\xi}$ of the deviated curve $\boldsymbol{x}$ we use again the first order approximation and $\boldsymbol{Y} = \boldsymbol{A}^+$:

$$\begin{aligned}
\xi^i &= Y^i_\alpha(\boldsymbol{x})\dot{x}^\alpha \\
&\approx Y^i_\alpha(\bar{\boldsymbol{x}} + \boldsymbol{A}(\bar{\boldsymbol{x}})\boldsymbol{\varepsilon})\tfrac{\mathrm{d}}{\mathrm{d}t}\big(\bar{x}^\alpha + A^\alpha_j(\bar{\boldsymbol{x}})\,\varepsilon^j\big) \\
&\approx Y^i_\alpha(\bar{\boldsymbol{x}})\big(\dot{x}^\alpha_{\mathsf{R}} + \tfrac{\partial A^\alpha_j}{\partial x^\beta}(\bar{\boldsymbol{x}})\,\dot{x}^\beta_{\mathsf{R}}\varepsilon^j + A^\alpha_j(\bar{\boldsymbol{x}})\,\dot{\varepsilon}^j\big) + \tfrac{\partial Y^i_\alpha}{\partial x^\beta}(\bar{\boldsymbol{x}})A^\beta_j(\bar{\boldsymbol{x}})\,\varepsilon^j\dot{x}^\alpha_{\mathsf{R}} \\
&= \bar{\xi}^i + \dot{\varepsilon}^i + \gamma^i_{kj}(\bar{\boldsymbol{x}})\bar{\xi}^k\varepsilon^j
\end{aligned} \tag{2.24}$$

Using these results we may formulate an approximation of a general smooth function f along the trajectory $t \mapsto \bar{\boldsymbol{x}}(t)$ as

$$\begin{aligned}
f(\boldsymbol{x}, \boldsymbol{\xi}, \dot{\boldsymbol{\xi}}) &\approx f(\bar{\boldsymbol{x}}, \bar{\boldsymbol{\xi}}, \dot{\bar{\boldsymbol{\xi}}}) + \frac{\partial f}{\partial x^\alpha}(\bar{\boldsymbol{x}}, \bar{\boldsymbol{\xi}}, \dot{\bar{\boldsymbol{\xi}}})(x^\alpha - \bar{x}^\alpha) + \frac{\partial f}{\partial \xi^i}(\bar{\boldsymbol{x}}, \bar{\boldsymbol{\xi}}, \dot{\bar{\boldsymbol{\xi}}})(\xi^i - \bar{\xi}^i) \\
&\quad + \frac{\partial f}{\partial \dot{\xi}^i}(\bar{\boldsymbol{x}}, \bar{\boldsymbol{\xi}}, \dot{\bar{\boldsymbol{\xi}}})(\dot{\xi}^i - \dot{\bar{\xi}}^i) \\
&\approx f(\bar{\boldsymbol{x}}, \bar{\boldsymbol{\xi}}, \dot{\bar{\boldsymbol{\xi}}}) + (\partial_i f)(\bar{\boldsymbol{x}}, \bar{\boldsymbol{\xi}}, \dot{\bar{\boldsymbol{\xi}}})\varepsilon^i + \frac{\partial f}{\partial \xi^i}(\bar{\boldsymbol{x}}, \bar{\boldsymbol{\xi}}, \dot{\bar{\boldsymbol{\xi}}})(\dot{\varepsilon}^i + \gamma^i_{kj}(\bar{\boldsymbol{x}})\bar{\xi}^k\varepsilon^j) \\
&\quad + \frac{\partial f}{\partial \dot{\xi}^i}(\bar{\boldsymbol{x}}, \bar{\boldsymbol{\xi}}, \dot{\bar{\boldsymbol{\xi}}})(\ddot{\varepsilon}^i + \gamma^i_{kj}(\bar{\boldsymbol{x}})\bar{\xi}^k\dot{\varepsilon}^j + \gamma^i_{kj}(\bar{\boldsymbol{x}})\dot{\bar{\xi}}^k\varepsilon^j + \partial_l\gamma^i_{kj}(\bar{\boldsymbol{x}})\bar{\xi}^l\bar{\xi}^k\varepsilon^j) \\
&= \bar{f} + \bar{F}^0_i\varepsilon^i + \bar{F}^1_i\dot{\varepsilon}^i + \bar{F}^2_i\ddot{\varepsilon}^i
\end{aligned} \tag{2.25}$$

where

$$\begin{aligned}
\bar{f} &= f(\bar{\boldsymbol{x}}, \bar{\boldsymbol{\xi}}, \dot{\bar{\boldsymbol{\xi}}}),\\
\bar{F}_i^0 &= (\partial_i f)(\bar{\boldsymbol{x}}, \bar{\boldsymbol{\xi}}, \dot{\bar{\boldsymbol{\xi}}}) + \frac{\partial f}{\partial \xi^j}(\bar{\boldsymbol{x}}, \bar{\boldsymbol{\xi}}, \dot{\bar{\boldsymbol{\xi}}})\gamma_{ki}^j(\bar{\boldsymbol{x}})\bar{\xi}^k + \frac{\partial f}{\partial \dot{\xi}^j}(\bar{\boldsymbol{x}}, \bar{\boldsymbol{\xi}}, \dot{\bar{\boldsymbol{\xi}}})\big(\gamma_{ki}^j(\bar{\boldsymbol{x}})\dot{\bar{\xi}}^k + \partial_l \gamma_{ki}^j(\bar{\boldsymbol{x}})\bar{\xi}^l\bar{\xi}^k\big),\\
\bar{F}_i^1 &= \frac{\partial f}{\partial \xi^i}(\bar{\boldsymbol{x}}, \bar{\boldsymbol{\xi}}, \dot{\bar{\boldsymbol{\xi}}}) + \frac{\partial f}{\partial \dot{\xi}^j}(\bar{\boldsymbol{x}}, \bar{\boldsymbol{\xi}}, \dot{\bar{\boldsymbol{\xi}}})\gamma_{ki}^j(\bar{\boldsymbol{x}})\bar{\xi}^k,\\
\bar{F}_i^2 &= \frac{\partial f}{\partial \dot{\xi}^i}(\bar{\boldsymbol{x}}, \bar{\boldsymbol{\xi}}, \dot{\bar{\boldsymbol{\xi}}}).
\end{aligned}$$

Evidently, the expressions simplify significantly is the velocity coordinates are holonomic, i.e. $\gamma = 0$, or if the approximation is about a static point $\bar{\boldsymbol{x}} = const. \Rightarrow \boldsymbol{\xi} = \mathbf{0}$.

2.2.4 Calculus of variations

The calculus of variations is concerned with the extremals of functionals, i.e. functions of functions. For the particular context of classical mechanics we are interested in the curves $t \mapsto \boldsymbol{x}(t)$ for which the functional

$$\mathcal{J}[\boldsymbol{x}] = \int_{t_1}^{t_2} \mathcal{L}(\boldsymbol{x}(t), \boldsymbol{\xi}(t), t)\,\mathrm{d}t \tag{2.26}$$

for given boundary conditions $\boldsymbol{x}(t_1)$ and $\boldsymbol{x}(t_2)$ is *stationary.* The *Lagrangian* $\mathcal{L}$ is here a function of the configuration coordinates $\boldsymbol{x}$, its derivatives $\dot{\boldsymbol{x}} = \boldsymbol{A}\boldsymbol{\xi}$ parameterized in the velocity coordinates $\boldsymbol{\xi}$ and may depend explicitly on the time t as well.

For the standard case, $\boldsymbol{x} = \boldsymbol{q}$ and $\boldsymbol{\xi} = \dot{\boldsymbol{q}}$, a derivation of may be found in e.g. [Courant and Hilbert, 1924, chap. 4, §3], [Lanczos, 1986, ch. II] or [Arnold, 1989, sec. 12]. For the present case we modify the well known derivation slightly: Suppose that $\boldsymbol{x} : [t_1, t_2] \mapsto \mathbb{X}$ is the solution to the variational problem. With the function $\boldsymbol{\chi}(t) \in \mathbb{R}^\nu$ and the parameter $\varepsilon \in \mathbb{R}$ we define a perturbation to it by

$$\bar{\boldsymbol{x}} = \boldsymbol{x} + \varepsilon\boldsymbol{\chi}. \tag{2.27}$$

We need $\bar{\boldsymbol{x}}(t) \in \mathbb{X}$ and consequently $\boldsymbol{\phi}(\bar{\boldsymbol{x}}) = \mathbf{0}$. Assuming ε to be sufficiently small, we may use the first order approximation analog to subsection 2.2.3: With the *variation coordinates* $\boldsymbol{h} : [t_1, t_2] \to \mathbb{R}^n$ we parameterize $\boldsymbol{\chi} = \boldsymbol{A}(\boldsymbol{x})\boldsymbol{h}$. Using the inverse kinematic relation $\boldsymbol{\xi} = \boldsymbol{Y}(\boldsymbol{x})\dot{\boldsymbol{x}}$ we can write the functional for the varied path as

$$\mathcal{J}[\bar{\boldsymbol{x}}] = \int_{t_1}^{t_2} \mathcal{L}\big(\boldsymbol{x} + \varepsilon\boldsymbol{A}(\boldsymbol{x})\boldsymbol{h}, \boldsymbol{Y}(\boldsymbol{x} + \varepsilon\boldsymbol{A}(\boldsymbol{x})\boldsymbol{h})\tfrac{\mathrm{d}}{\mathrm{d}t}(\boldsymbol{x} + \varepsilon\boldsymbol{A}(\boldsymbol{x})\boldsymbol{h}), t\big)\,\mathrm{d}t =: \mathcal{P}(\varepsilon) \tag{2.28}$$

Now if $\boldsymbol{x}(t)$ is indeed the solution to the variational problem, then $\mathcal{P}(\varepsilon)$ must have a minimum at $\mathcal{P}(0)$ and consequently $\partial\mathcal{P}/\partial\varepsilon(0) = 0$. Evaluation of this "ordinary" differentiation yields

$$\begin{aligned}
0 = \frac{\partial \mathcal{P}}{\partial \varepsilon}\Big|_{\varepsilon=0} &= \int_{t_1}^{t_2} \left(\frac{\partial \mathcal{L}}{\partial x^\alpha}A_i^\alpha h^i + \frac{\partial \mathcal{L}}{\partial \xi^i}\left(\frac{\partial Y_\alpha^i}{\partial x^\beta}A_j^\beta h^j \dot{x}^\alpha + Y_\alpha^i \frac{\partial A_j^\alpha}{\partial x^\beta}h^j \dot{x}^\beta + \dot{h}^i\right)\right)\mathrm{d}t\\
&= \int_{t_1}^{t_2} \left(\partial_i \mathcal{L}\, h^i + \frac{\partial \mathcal{L}}{\partial \xi^i}\big(\gamma_{kj}^i h^j \xi^k + \dot{h}^i\big)\right)\mathrm{d}t
\end{aligned} \tag{2.29}$$

where we have found again the commutation coefficients γ^i_{kj} previously derived in (2.19). Integrating by parts with the boundary conditions $\boldsymbol{h}(t_1) = \boldsymbol{h}(t_2) = \mathbf{0}$ gives

$$\int_{t_1}^{t_2} h^i \left(A_i^\alpha \frac{\partial \mathcal{L}}{\partial x^\alpha} - \frac{\mathrm{d}}{\mathrm{d}t}\frac{\partial \mathcal{L}}{\partial \xi^i} - \gamma^k_{ij}\xi^j \frac{\partial \mathcal{L}}{\partial \xi^k} \right) \mathrm{d}t = 0. \tag{2.30}$$

Since the variation coordinates $h^i, i = 1, \ldots, n$ are independent by definition, the *fundamental lemma of the calculus of variations* (see e.g. [Courant and Hilbert, 1924, p. 166] or [Arnold, 1989, p. 57]) states that, for the integral to vanish, the terms in the brackets have to vanish. Together with the kinematic equation, we have the following necessary conditions for the functional (2.26) to be stationary:

$$\dot{x}^\alpha = A_i^\alpha \xi^i, \qquad \alpha = 1 \ldots \nu, \tag{2.31a}$$

$$\frac{\mathrm{d}}{\mathrm{d}t}\frac{\partial \mathcal{L}}{\partial \xi^i} + \gamma^k_{ij}\xi^j \frac{\partial \mathcal{L}}{\partial \xi^k} - \partial_i \mathcal{L} = 0, \qquad i = 1, \ldots, n. \tag{2.31b}$$

For the special case $\boldsymbol{x}(t) = \boldsymbol{q}(t) \in \mathbb{R}^n$ and $\boldsymbol{\xi}(t) = \dot{\boldsymbol{q}}(t)$ we have $\boldsymbol{A} = \mathbf{I}_n$ and $\gamma = 0$. Then (2.31) coincides with the *Euler-Lagrange equation* (1.2).

Example 4. Consider again the configuration coordinates $\boldsymbol{x} = [\boldsymbol{R}_\mathsf{x}^\top, \boldsymbol{R}_\mathsf{y}^\top, \boldsymbol{R}_\mathsf{z}^\top]^\top$ and the velocity coordinates $\boldsymbol{\xi} = \boldsymbol{\omega}$ related by $\dot{\boldsymbol{R}} = \boldsymbol{R}\,\mathrm{wed}(\boldsymbol{\omega})$ as discussed in the previous example (2.7). The commutation coefficients were derived in (2.20).

For the Lagrangian

$$\mathcal{L} = \tfrac{1}{2}\boldsymbol{\omega}^\top \boldsymbol{\Theta}\boldsymbol{\omega} \tag{2.32}$$

we obain

$$\left[\frac{\mathrm{d}}{\mathrm{d}t}\frac{\partial \mathcal{L}}{\partial \xi^i} + \gamma^k_{ij}\xi^j \frac{\partial \mathcal{L}}{\partial \xi^k} - A_i^\alpha \frac{\partial \mathcal{L}}{\partial x^\alpha}\right]_{i=1,2,3} = \boldsymbol{\Theta}\dot{\boldsymbol{\omega}} + \boldsymbol{\omega} \times \boldsymbol{\Theta}\boldsymbol{\omega}. \tag{2.33}$$

2.2.5 Hamilton's equations

Legendre transformation. Define the *generalized momentum* $\boldsymbol{p}$ as

$$p_i = \frac{\partial \mathcal{L}}{\partial \xi^i}, \quad i = 1, \ldots, n. \tag{2.34}$$

and assume that these relations can be inverted to express the velocity $\boldsymbol{\xi} = \boldsymbol{\zeta}(\boldsymbol{x}, \boldsymbol{p}, t)$ in terms of the momentum. Then define the *Hamiltonian* $\mathcal{H}$ as

$$\mathcal{H}(\boldsymbol{x}, \boldsymbol{p}, t) = \Big[p_i \xi^i - \mathcal{L}(\boldsymbol{x}, \boldsymbol{\xi}, t)\Big]_{\boldsymbol{\xi}=\boldsymbol{\zeta}(\boldsymbol{x},\boldsymbol{p},t)} = p_i \zeta^i(\boldsymbol{x}, \boldsymbol{p}, t) - \mathcal{L}(\boldsymbol{x}, \boldsymbol{\zeta}(\boldsymbol{x}, \boldsymbol{p}, t), t). \tag{2.35}$$

The definitions (2.34) and (2.35) describe the *Legendre transformation* $(\mathcal{L}, \boldsymbol{\xi}) \to (\mathcal{H}, \boldsymbol{p})$, see [Lanczos, 1986, ch. VI.1] or [Arnold, 1989, sec. 14] for some geometric background. Note that the configuration coordinates $\boldsymbol{x}$ and the time t do not participate in the transformation.

Hamilton's canonical equations. Evaluation of the differentials of (2.35), we get the relations

$$\partial_j \mathcal{H} = p_i \partial_j \zeta^i - \partial_j \mathcal{L} - \frac{\partial \mathcal{L}}{\partial \xi^i} \partial_j \zeta^i = -\partial_j \mathcal{L} \tag{2.36a}$$

$$\frac{\partial \mathcal{H}}{\partial p_j} = \zeta^j + p_i \frac{\partial \zeta^i}{\partial p_j} - \frac{\partial \mathcal{L}}{\partial \xi^i} \frac{\partial \zeta^i}{\partial p_j} = \xi^j \tag{2.36b}$$

$$\frac{\partial \mathcal{H}}{\partial t} = p_i \frac{\partial \zeta^i}{\partial t} - \frac{\partial \mathcal{L}}{\partial \xi^i} \frac{\partial \zeta^i}{\partial t} - \frac{\partial \mathcal{L}}{\partial t} = -\frac{\partial \mathcal{L}}{\partial t}, \tag{2.36c}$$

With this we can express the Euler-Lagrange equation (2.31) in terms of the generalized momentum $\boldsymbol{p}$ and the Hamiltonian $\mathcal{H}$ as

$$\dot{x}^\alpha = A_i^\alpha \frac{\partial \mathcal{H}}{\partial p_i}, \qquad \alpha = 1, \ldots, \nu, \tag{2.37a}$$

$$\dot{p}_i + \gamma_{ij}^k \frac{\partial \mathcal{H}}{\partial p_j} p_k + \partial_i \mathcal{H} = 0, \qquad i = 1, \ldots, n. \tag{2.37b}$$

For the special case of minimal configuration coordinates $\boldsymbol{q}$ and velocity coordinates $\boldsymbol{\xi} = \dot{\boldsymbol{q}}$ we have $\boldsymbol{A} = \mathbf{I}_n$ and (2.37) is called *Hamilton's canonical equations.*

Conservation law. The time derivative of the Hamiltonian along the the solutions of (2.37) is

$$\frac{\mathrm{d}\mathcal{H}}{\mathrm{d}t} = \frac{\partial \mathcal{H}}{\partial x^\alpha} \dot{x}^\alpha + \frac{\partial \mathcal{H}}{\partial p_i} \dot{p}_i + \frac{\partial \mathcal{H}}{\partial t} = \underbrace{\frac{\partial \mathcal{H}}{\partial x^\alpha} A_i^\alpha \frac{\partial \mathcal{H}}{\partial p_i} - \frac{\partial \mathcal{H}}{\partial p_i} A_i^\alpha \frac{\partial \mathcal{H}}{\partial x^\alpha}}_{0} - p_k \underbrace{\gamma_{ij}^k \frac{\partial \mathcal{H}}{\partial p_i} \frac{\partial \mathcal{H}}{\partial p_j}}_{0} + \frac{\partial \mathcal{H}}{\partial t} \tag{2.38}$$

and consequently

$$\frac{\mathrm{d}\mathcal{H}}{\mathrm{d}t} = \frac{\partial \mathcal{H}}{\partial t} = -\frac{\partial \mathcal{L}}{\partial t}. \tag{2.39}$$

This is the well known conservation law for the Hamiltonian, see e.g. [Lanczos, 1986, ch. VI.6]. The remarkable aspect of the conservation law (and for the Legendre transformation) is that there is no particular assumption on the structure of the Lagrangian $\mathcal{L}$.

Example 5. Consider a Lagrangian as

$$\mathcal{L}(\boldsymbol{x}, \boldsymbol{\xi}, t) = \tfrac{1}{2} M_{ij}(\boldsymbol{x}, t) \xi^j \xi^i + b_i(\boldsymbol{x}, t) \xi^i + c(\boldsymbol{x}, t). \tag{2.40}$$

The corresponding generalized momentum and Hamiltonian are

$$p_i = \frac{\partial \mathcal{L}}{\partial \xi^i} = M_{ij} \xi^i + b_i \qquad \Leftrightarrow \qquad \xi^i = M^{ij}(p_j - b_j) \tag{2.41}$$

$$\mathcal{H} = \tfrac{1}{2} M^{ij} (p_i - b_i)(p_j - b_j) - c. \tag{2.42}$$

Evaluation of (2.37) yields

$$\dot{x}^\alpha = A_i^\alpha M^{ij}(p_j - b_j), \tag{2.43a}$$

$$\dot{p}_i + \big(\gamma_{il}^k M^{lj} p_k + \tfrac{1}{2}\partial_i M^{kj}(p_k - b_k) - M^{kj}\partial_i b_k\big)(p_j - b_j) + \partial_i c = 0, \tag{2.43b}$$

The Euler-Lagrange equation evaluates to

$$\dot{x}^\alpha = A_i^\alpha \xi^i, \tag{2.44a}$$

$$M_{ij}\dot{\xi}^j + \big(\partial_k M_{ij} + \gamma_{ij}^l M_{lk} - \tfrac{1}{2}\partial_i M_{kj}\big)\xi^j\xi^k + \big(\frac{\partial M_{ij}}{\partial t} + \gamma_{ij}^k b_k\big)\xi^j + \frac{\partial b_i}{\partial t} - \partial_i c \tag{2.44b}$$

Note that the Hamiltonian in terms of Lagrangian coordinates reads

$$\mathcal{H} = \tfrac{1}{2}M_{ij}\xi^i\xi^j - c. \tag{2.45}$$

2.3 Linear algebra

2.3.1 Matrix sets

The following sets of real matrices that are frequently used in the work:

(symmetric)	$\mathbb{SYM}(n) = \{\boldsymbol{A} \in \mathbb{R}^{n\times n} \mid \boldsymbol{A} = \boldsymbol{A}^\top\},$	(2.46a)
(symmetric, pos. def.)	$\mathbb{SYM}^+(n) = \{\boldsymbol{A} \in \mathbb{SYM}(n) \mid \boldsymbol{x}^\top\boldsymbol{A}\boldsymbol{x} > 0 \,\forall\, \boldsymbol{x} \in \mathbb{R}^n\backslash\{\boldsymbol{0}\}\},$	(2.46b)
(sym., pos. semi-def.)	$\mathbb{SYM}_0^+(n) = \{\boldsymbol{A} \in \mathbb{SYM}(n) \mid \boldsymbol{x}^\top\boldsymbol{A}\boldsymbol{x} \geq 0 \,\forall\, \boldsymbol{x} \in \mathbb{R}^n\backslash\{\boldsymbol{0}\}\},$	(2.46c)
(unit sphere)	$\mathbb{S}^n = \{\boldsymbol{a} \in \mathbb{R}^n \mid \boldsymbol{a}^\top\boldsymbol{a} = 1\},$	(2.46d)
(orthogonal)	$\mathbb{O}(n) = \{\boldsymbol{A} \in \mathbb{R}^{n\times n} \mid \boldsymbol{A}^\top\boldsymbol{A} = \mathbf{I}_n\},$	(2.46e)
(special orthogonal)	$\mathbb{SO}(n) = \{\boldsymbol{R} \in \mathbb{O}(n) \mid \det\boldsymbol{R} = +1\},$	(2.46f)

2.3.2 Inner product, norm and metric

Inner product. For matrices $\boldsymbol{A}, \boldsymbol{B} \in \mathbb{R}^{n\times m}$ and a symmetric, positive definite matrix $\boldsymbol{K} \in \mathbb{SYM}^+(n)$, define an *inner product* as

$$\langle \boldsymbol{A}, \boldsymbol{B}\rangle_{\boldsymbol{K}} = \mathrm{tr}(\boldsymbol{A}^\top\boldsymbol{K}\boldsymbol{B}). \tag{2.47}$$

Setting $\boldsymbol{K} = \mathbf{I}_n$ in the definition (2.47) is called the *Frobenius inner product* in [Horn and Johnson, 1985, sec. 5.2] or *Hilbert-Schmidt inner product* in [Hall, 2015, sec. A.6]. Furthermore, for $\boldsymbol{A}, \boldsymbol{B} \in \mathbb{R}^{n\times 1}$ it coincides with the common *dot product*.

Norm. The inner product (2.47) induces the norm

$$\|\boldsymbol{A}\|_{\boldsymbol{K}} = \sqrt{\langle \boldsymbol{A}, \boldsymbol{A} \rangle_{\boldsymbol{K}}}. \tag{2.48}$$

Again for $\boldsymbol{K} = \mathbf{I}_n$ this coincides with the established *Frobenius norm*, e.g. [Golub and Loan, 1996, p 55]. Furthermore, for $\boldsymbol{A}, \boldsymbol{B} \in \mathbb{R}^{n\times 1}$ it coincides with the common *Euclidian norm* or 2-norm.

Metric. The norm (2.48) induces the metric

$$d_{\boldsymbol{K}}(\boldsymbol{A}, \boldsymbol{B}) = \|\boldsymbol{A} - \boldsymbol{B}\|_{\boldsymbol{K}}. \tag{2.49}$$

Again for $\boldsymbol{K} = \mathbf{I}_n$ this coincides with the established *Euclidean metric.*

The introduced inner product, norm and metric may be regarded as weighted versions of their established forms. For $\boldsymbol{K} = \mathbf{I}_n$, this work uses the shorthand notation

$$\langle \cdot, \cdot \rangle \equiv \langle \cdot, \cdot \rangle_{\mathbf{I}_n}, \qquad \| \cdot \| \equiv \| \cdot \|_{\mathbf{I}_n}, \qquad d(\cdot, \cdot) \equiv d_{\mathbf{I}_n}(\cdot, \cdot). \tag{2.50}$$

2.3.3 Vee and wedge

Established definitions. Define the wedge operator as

$$\mathrm{wed} : \mathbb{R}^3 \to \mathbb{R}^{3\times 3} \; : \; \begin{bmatrix} \omega_1 \\ \omega_2 \\ \omega_3 \end{bmatrix} \mapsto \begin{bmatrix} 0 & -\omega_3 & \omega_2 \\ \omega_3 & 0 & -\omega_1 \\ -\omega_2 & \omega_1 & 0 \end{bmatrix} \tag{2.51a}$$

Its inverse is denoted $\mathrm{vee}(\cdot)$, i.e. $\mathrm{vee}(\mathrm{wed}(\boldsymbol{\omega}) = \boldsymbol{\omega}$. The wed and vee operators are well established in the literature, see e.g. [Murray et al., 1994, sec. 2.3.2], and have already been used in previous sections.

New definitions. The following operators are not established in the literature, but will prove quite useful for this work. Define the vee2 operator through: $\boldsymbol{M} \in \mathbb{R}^{3\times 3}$:

$$\mathrm{tr}\left(\boldsymbol{M}(\mathrm{wed}\,\boldsymbol{\omega})^\top\right) = \boldsymbol{\omega}^\top \, \mathrm{vee2}(\boldsymbol{M}), \tag{2.52}$$

this is

$$\mathrm{vee2} : \mathbb{R}^{3\times 3} \to \mathbb{R}^3 \; : \; \boldsymbol{M} \mapsto \mathrm{vee}(\boldsymbol{M} - \boldsymbol{M}^\top) \tag{2.53}$$

Note that we have $\mathrm{vee2}(\mathrm{wed}\,\boldsymbol{\omega}) = 2\,\mathrm{vee}(\mathrm{wed}\,\boldsymbol{\omega}) = 2\boldsymbol{\omega}$, thus giving the motivation for the name.

Define the Vee operator through

$$\mathrm{tr}\left(\mathrm{wed}\,\boldsymbol{\omega}\,\boldsymbol{M}(\mathrm{wed}\,\boldsymbol{\eta})^\top\right) = \boldsymbol{\eta}^\top(\mathrm{Vee}\,\boldsymbol{M})\boldsymbol{\omega}, \tag{2.54}$$

this is

$$\mathrm{Vee} : \mathbb{R}^{3\times 3} \to \mathbb{R}^{3\times 3} \; : \boldsymbol{M} \mapsto \mathrm{tr}(\boldsymbol{M})\mathbf{I}_3 - \boldsymbol{M} \tag{2.55}$$

Noting that $\mathrm{tr}(\mathrm{Vee}(\boldsymbol{M})) = 2\,\mathrm{tr}(\boldsymbol{M})$, we may write the inverse $\mathrm{Wed}(\mathrm{Vee}(\boldsymbol{M})) = \boldsymbol{M}$ as

$$\mathrm{Wed} : \mathbb{R}^{3\times 3} \to \mathbb{R}^{3\times 3} \; : \boldsymbol{M} \mapsto \tfrac{1}{2}\,\mathrm{tr}(\boldsymbol{M})\mathbf{I}_3 - \boldsymbol{M}. \tag{2.56}$$

Identities. For $\boldsymbol{a}, \boldsymbol{b}, \boldsymbol{c} \in \mathbb{R}^3$ and $\boldsymbol{M} \in \mathbb{R}^{3\times 3}$, the following identities may be checked by direct computation:

$$\operatorname{wed}(\boldsymbol{a})^\top = -\operatorname{wed}(\boldsymbol{a}), \tag{2.57a}$$

$$\operatorname{wed}(\boldsymbol{a})\boldsymbol{b} = \operatorname{vee2}(\boldsymbol{b}\boldsymbol{a}^\top), \tag{2.57b}$$

$$\operatorname{wed}(\boldsymbol{a})\operatorname{wed}(\boldsymbol{b}) = \boldsymbol{b}\boldsymbol{a}^\top - (\boldsymbol{b}^\top\boldsymbol{a})\mathbf{I}_3 = -\operatorname{Vee}(\boldsymbol{b}\boldsymbol{a}^\top), \tag{2.57c}$$

$$\operatorname{wed}(\boldsymbol{a})\operatorname{wed}(\boldsymbol{b})\boldsymbol{c} + \operatorname{wed}(\boldsymbol{b})\operatorname{wed}(\boldsymbol{c})\boldsymbol{a} + \operatorname{wed}(\boldsymbol{c})\operatorname{wed}(\boldsymbol{a})\boldsymbol{b} = \mathbf{0}, \tag{2.57d}$$

$$\operatorname{vee2}(\operatorname{wed}(\boldsymbol{b})\boldsymbol{M}) = \operatorname{Vee}(\boldsymbol{M})\boldsymbol{b}. \tag{2.57e}$$

2.3.4 Singular value decomposition

Definition [Golub and Loan, 1996, Theo. 2.5.2]: For any matrix $\boldsymbol{M} \in \mathbb{R}^{n\times m}$ there exist orthonormal matrices $\boldsymbol{X} \in \mathbb{O}(n)$, $\boldsymbol{Y} \in \mathbb{O}(m)$ and a matrix $\boldsymbol{\Sigma} \in \mathbb{R}^{n\times m}$ with $i \neq j : \Sigma_{ij} = 0$, $\Sigma_{ii} = \sigma_i$ with $\sigma_1 \geq \ldots, \geq \sigma_p \geq 0$, $p = \max(n, m)$ such that $\boldsymbol{M} = \boldsymbol{X}\boldsymbol{\Sigma}\boldsymbol{Y}^\top$.

- The columns of $\boldsymbol{X}$ are eigenvectors of $\boldsymbol{M}\boldsymbol{M}^\top = \boldsymbol{X}(\boldsymbol{\Sigma}\boldsymbol{\Sigma}^\top)\boldsymbol{X}^\top$
- The columns of $\boldsymbol{Y}$ are eigenvectors of $\boldsymbol{M}^\top\boldsymbol{M} = \boldsymbol{Y}(\boldsymbol{\Sigma}^\top\boldsymbol{\Sigma})\boldsymbol{Y}^\top$
- The square of the non-zero singular values σ_i^2 coincide with the non-zero eigenvalues of $\boldsymbol{M}\boldsymbol{M}^\top$ and $\boldsymbol{M}^\top\boldsymbol{M}$

Due to the descending order of the singular values, the matrix $\boldsymbol{\Sigma}$ is unique. The matrices $\boldsymbol{X}$ and $\boldsymbol{Y}$ are unique up to orthogonal transformations of the subspaces of each singular value and the kernel and co-kernel of $\boldsymbol{M}$.

2.4 An important function on the special orthogonal group

Motivation. In the context of satellite navigation, the following problem [Wahba, 1965] arose, now commonly called *Wahba's problem*: given $\boldsymbol{u}_k, \boldsymbol{v}_k \in \mathbb{R}^3$, find $\boldsymbol{R} \in \mathbb{SO}(3)$ that minimizes

$$\begin{aligned}\mathcal{V}_1(\boldsymbol{R}) = \sum_k \|\boldsymbol{u}_k - \boldsymbol{R}\boldsymbol{v}_k\|^2 &= \sum_k \big(\|\boldsymbol{u}_k\|^2 + \|\boldsymbol{v}_k\|^2 - \langle \boldsymbol{u}_k, \boldsymbol{R}\boldsymbol{v}_k\rangle\big)\\ &= \underbrace{\sum_k \big(\|\boldsymbol{u}_k\|^2 + \|\boldsymbol{v}_k\|^2\big)}_{const.} - \operatorname{tr}\big(\boldsymbol{R}\underbrace{\sum_k \boldsymbol{v}_k\boldsymbol{u}_k^\top}_{\boldsymbol{P}_1}\big).\end{aligned} \tag{2.58}$$

In [Koditschek, 1989] the following function with parameters $\boldsymbol{K} \in \mathbb{SYM}^+(3)$ and $\boldsymbol{R}_\mathsf{R} \in \mathbb{SO}(3)$ is called a *navigation function on* $\mathbb{SO}(3)$:

$$\mathcal{V}_2(\boldsymbol{R}) = \operatorname{tr}\big(\boldsymbol{K}(\mathbf{I}_3 - \boldsymbol{R}_\mathsf{R}^\top\boldsymbol{R})\big) = \underbrace{\operatorname{tr}\boldsymbol{K}}_{const.} - \operatorname{tr}(\underbrace{\boldsymbol{K}\boldsymbol{R}_\mathsf{R}^\top}_{\boldsymbol{P}_2}\boldsymbol{R}). \tag{2.59}$$

Using the metric from (2.49) with a weight $\boldsymbol{K} \in \mathbb{SYM}^+(3)$ we may ask for the rotation matrix $\boldsymbol{R} \in \mathbb{SO}(3)$ which is closest to a given matrix $\boldsymbol{Q} \in \mathbb{R}^{3\times 3}$, i.e. which minimizes

$$\begin{aligned}\mathcal{V}_3(\boldsymbol{R}) = \tfrac{1}{2} d_{\boldsymbol{K}}^2(\boldsymbol{Q}, \boldsymbol{R}) = \tfrac{1}{2} \operatorname{tr}\left((\boldsymbol{Q} - \boldsymbol{R})^\top \boldsymbol{K}(\boldsymbol{Q} - \boldsymbol{R})\right)& \\ = \underbrace{\tfrac{1}{2} \operatorname{tr}\left(\boldsymbol{Q}^\top \boldsymbol{K}\boldsymbol{Q} + \boldsymbol{K}\right)}_{const.} - \operatorname{tr}\big(\underbrace{\boldsymbol{Q}^\top \boldsymbol{K}}_{\boldsymbol{P}_3} \boldsymbol{R}\big)& \qquad (2.60)\end{aligned}$$

Each of these problems essentially asks for an $\boldsymbol{R} \in \mathbb{SO}(3)$ wich minimizes $\mathcal{V} = -\operatorname{tr}(\boldsymbol{P}\boldsymbol{R})$ for some given $\boldsymbol{P} \in \mathbb{R}^{3\times 3}$.

Solutions to Wahba's problem are given in [Davenport, 1968] using attitude quaternions and in [Kabsch, 1976] using the singular value decomposition. A proof of a unique minimum in [Bullo and Murray, 1999] relies on $\boldsymbol{P}$ having distinct singular values.

In the following we extend theses results in the sense that, we do not impose assumptions on $\boldsymbol{P}$ and are also interested other extrema of $\mathcal{V}$.

Problem definition. Similar problems to the ones above will also appear in this work. So we are interested in the extrema, and their nature, of the of the function

$$\mathcal{V} : \mathbb{SO}(3) \to \mathbb{R} \,:\, \boldsymbol{R} \mapsto -\operatorname{tr}(\boldsymbol{P}\boldsymbol{R}) \qquad (2.61)$$

with the parameter $\boldsymbol{P} \in \mathbb{R}^{3\times 3}$.

Coordinate transformation. Consider a singular value decomposition $\boldsymbol{P} = \boldsymbol{X}\boldsymbol{\Sigma}\boldsymbol{Y}^\top$ with $\boldsymbol{X}, \boldsymbol{Y} \in \mathbb{O}(3)$ and $\boldsymbol{\Sigma} = \operatorname{diag}(\sigma_1, \sigma_2, \sigma_3)$, $\sigma_1 \geq \sigma_2 \geq \sigma_3 \geq 0$. [Kabsch, 1976]: Define

$$\begin{aligned}\bar{\boldsymbol{X}} &= \boldsymbol{X} \operatorname{diag}(1, 1, \det \boldsymbol{X}) \in \mathbb{SO}(3), && (2.62a)\\ \bar{\boldsymbol{Y}} &= \boldsymbol{Y} \operatorname{diag}(1, 1, \det \boldsymbol{Y}) \in \mathbb{SO}(3), && (2.62b)\\ \bar{\boldsymbol{\Sigma}} &= \operatorname{diag}(\sigma_1, \sigma_2, \bar{\sigma}_3),\ \ \bar{\sigma}_3 = \det \boldsymbol{X} \det \boldsymbol{Y} \sigma_3 && (2.62c)\end{aligned}$$

which yields a decomposition $\boldsymbol{P} = \bar{\boldsymbol{X}}\bar{\boldsymbol{\Sigma}}\bar{\boldsymbol{Y}}^\top$ with proper rotations. Using the cyclic permutation property of the trace we get

$$\mathcal{V}(\boldsymbol{R}) = -\operatorname{tr}(\bar{\boldsymbol{X}}\bar{\boldsymbol{\Sigma}}\bar{\boldsymbol{Y}}^\top \boldsymbol{R}) = -\operatorname{tr}(\bar{\boldsymbol{\Sigma}}\underbrace{\bar{\boldsymbol{Y}}^\top \boldsymbol{R}\bar{\boldsymbol{X}}}_{\bar{\boldsymbol{R}}}) =: \bar{\mathcal{V}}(\bar{\boldsymbol{R}}) \qquad (2.63)$$

Since the SVD is not unique in general, the transformed function $\bar{\mathcal{V}}$ is neither. However, since the coordinate transformation $\boldsymbol{R} = \bar{\boldsymbol{Y}}\bar{\boldsymbol{R}}\bar{\boldsymbol{X}}^\top$ is bijective, no information is lost here.

Critical points. Using the operators defined above, we may formulate the differential and Hessian of the transformed function as

$$\begin{aligned}\boldsymbol{\nabla}\bar{\mathcal{V}}(\bar{\boldsymbol{R}}) &= \operatorname{vee2}(\bar{\boldsymbol{\Sigma}}\bar{\boldsymbol{R}}), && (2.64)\\ \boldsymbol{\nabla}^2\bar{\mathcal{V}}(\bar{\boldsymbol{R}}) &= \operatorname{Vee}(\bar{\boldsymbol{\Sigma}}\bar{\boldsymbol{R}})^\top. && (2.65)\end{aligned}$$

For a critical point $\bar{\boldsymbol{R}}_0 : \boldsymbol{\nabla}\bar{\mathcal{V}}(\bar{\boldsymbol{R}}_0) = \mathbf{0}$ we need the matrix $\bar{\boldsymbol{\Sigma}}\bar{\boldsymbol{R}}_0$ to be symmetric. For the following it will be useful to substitute the entries/eigenvalues of $\mathrm{Vee}(\bar{\boldsymbol{\Sigma}}) = \mathrm{diag}(\lambda_1, \lambda_2, \lambda_3) = \boldsymbol{\Lambda}$ as

$$\left.\begin{aligned} \lambda_1 &= \sigma_2 + \bar{\sigma}_3, \\ \lambda_2 &= \bar{\sigma}_3 + \sigma_1, \\ \lambda_3 &= \sigma_1 + \sigma_2 \end{aligned}\right\} \qquad \Leftrightarrow \qquad \left\{\begin{aligned} \sigma_1 &= \tfrac{1}{2}(\lambda_2 + \lambda_3 - \lambda_1), \\ \sigma_2 &= \tfrac{1}{2}(\lambda_3 + \lambda_1 - \lambda_2), \\ \bar{\sigma}_3 &= \tfrac{1}{2}(\lambda_1 + \lambda_2 - \lambda_3) \end{aligned}\right. \tag{2.66}$$

Note that $\sigma_1 \geq \sigma_2 \geq |\bar{\sigma}_3| \geq 0$ implies $\lambda_3 \geq \lambda_2 \geq \lambda_1 \geq 0$. Depending on the constellation of the eigenvalues we have the following critical points:

- Distinct eigenvalues: $\lambda_3 > \lambda_2 > \lambda_1 > 0$: We have the critical points

$$\begin{aligned} &\bar{\boldsymbol{R}}_0 = \mathbf{I}_3 \ : \\ &\quad \mathcal{V}(\bar{\boldsymbol{R}}_0) = -\tfrac{\lambda_1}{2} - \tfrac{\lambda_2}{2} - \tfrac{\lambda_3}{2}, \quad \mathrm{eig}(\boldsymbol{\nabla}^2\bar{\mathcal{V}}(\bar{\boldsymbol{R}}_0)) = \{\lambda_3, \lambda_2, \lambda_1\} \end{aligned} \tag{2.67a}$$

$$\begin{aligned} &\bar{\boldsymbol{R}}_1 = \mathrm{diag}(1, -1, -1) \ : \\ &\quad \mathcal{V}(\bar{\boldsymbol{R}}_1) = \tfrac{3\lambda_1 - \lambda_2 - \lambda_3}{2}, \quad \mathrm{eig}(\boldsymbol{\nabla}^2\bar{\mathcal{V}}(\bar{\boldsymbol{R}}_1)) = \{\lambda_3 - \lambda_1, \lambda_2 - \lambda_1, -\lambda_1\} \end{aligned} \tag{2.67b}$$

$$\begin{aligned} &\bar{\boldsymbol{R}}_2 = \mathrm{diag}(-1, 1, -1) \ : \\ &\quad \mathcal{V}(\bar{\boldsymbol{R}}_2) = \tfrac{3\lambda_2 - \lambda_1 - \lambda_3}{2}, \quad \mathrm{eig}(\boldsymbol{\nabla}^2\bar{\mathcal{V}}(\bar{\boldsymbol{R}}_2)) = \{\lambda_3 - \lambda_2, \lambda_1 - \lambda_2, -\lambda_2\} \end{aligned} \tag{2.67c}$$

$$\begin{aligned} &\bar{\boldsymbol{R}}_3 = \mathrm{diag}(-1, -1, 1) \ : \\ &\quad \mathcal{V}(\bar{\boldsymbol{R}}_3) = \tfrac{3\lambda_3 - \lambda_1 - \lambda_2}{2}, \quad \mathrm{eig}(\boldsymbol{\nabla}^2\bar{\mathcal{V}}(\bar{\boldsymbol{R}}_3)) = \{\lambda_2 - \lambda_3, \lambda_1 - \lambda_3, -\lambda_3\} \end{aligned} \tag{2.67d}$$

  so $\bar{\boldsymbol{R}}_0$ is a minimum, $\bar{\boldsymbol{R}}_1$ and $\bar{\boldsymbol{R}}_2$ are saddle points, and $\bar{\boldsymbol{R}}_3$ is a maximum.

- Double eigenvalue: $\lambda_3 > \lambda_2 = \lambda_1 > 0$: We have a minimum at $\bar{\boldsymbol{R}}_0$, a maximum at $\bar{\boldsymbol{R}}_3$ and a saddle on the circular manifold

$$\bar{\boldsymbol{R}}_4 = \begin{bmatrix} -c & s & 0 \\ s & c & 0 \\ 0 & 0 & -1 \end{bmatrix}, \ c^2 + s^2 = 1 \ :$$

$$\mathcal{V}(\bar{\boldsymbol{R}}_4) = \lambda_1 - \tfrac{\lambda_3}{2}, \quad \mathrm{eig}(\boldsymbol{\nabla}^2\bar{\mathcal{V}}(\bar{\boldsymbol{R}}_4)) = \{\lambda_3 - \lambda_1, 0, -\lambda_1\} \tag{2.67e}$$

  which includes the points $\bar{\boldsymbol{R}}_1$ and $\bar{\boldsymbol{R}}_2$.

- Double eigenvalue: $\lambda_3 = \lambda_2 > \lambda_1 > 0$: Analog to above we have a minimum at $\bar{\boldsymbol{R}}_0$, a saddle at $\bar{\boldsymbol{R}}_1$ and a maximum on the circular manifold

$$\bar{\boldsymbol{R}}_5 = \begin{bmatrix} -1 & 0 & 0 \\ 0 & c & s \\ 0 & s & -c \end{bmatrix}, \ c^2 + s^2 = 1 \ :$$

$$\mathcal{V}(\bar{\boldsymbol{R}}_5) = \lambda_2 - \tfrac{\lambda_1}{2}, \quad \mathrm{eig}(\boldsymbol{\nabla}^2\bar{\mathcal{V}}(\bar{\boldsymbol{R}}_5)) = \{0, \lambda_1 - \lambda_2, -\lambda_2\} \tag{2.67f}$$

  which includes the points $\bar{\boldsymbol{R}}_2$ and $\bar{\boldsymbol{R}}_3$.

- Triple eigenvalue: $\lambda_3 = \lambda_2 = \lambda_1 > 0$: Minimum at $\bar{\boldsymbol{R}}_0$ and a maximum on the spherical manifold

$$\bar{\boldsymbol{R}}_6 = \begin{bmatrix} q_\mathsf{x}^2 - q_\mathsf{y}^2 - q_\mathsf{z}^2 & 2q_\mathsf{x}q_\mathsf{y} & 2q_\mathsf{x}q_\mathsf{z} \\ 2q_\mathsf{x}q_\mathsf{y} & q_\mathsf{y}^2 - q_\mathsf{x}^2 + q_\mathsf{z}^2 & 2q_\mathsf{y}q_\mathsf{z} \\ 2q_\mathsf{x}q_\mathsf{z} & 2q_\mathsf{y}q_\mathsf{z} & q_\mathsf{z}^2 - q_\mathsf{x}^2 - q_\mathsf{y}^2 \end{bmatrix}, \ q_\mathsf{x}^2 + q_\mathsf{y}^2 + q_\mathsf{z}^2 = 1 :$$

$$\mathcal{V}(\bar{\boldsymbol{R}}_6) = \tfrac{\lambda_1}{2}, \quad \mathrm{eig}(\boldsymbol{\nabla}^2\bar{\mathcal{V}}(\bar{\boldsymbol{R}}_6)) = \{0, 0, -\lambda_1\} \tag{2.67g}$$

which includes the points $\bar{\boldsymbol{R}}_1$, $\bar{\boldsymbol{R}}_2$ and $\bar{\boldsymbol{R}}_3$ and the circles $\bar{\boldsymbol{R}}_4$ and $\bar{\boldsymbol{R}}_5$. It corresponds to a 180° rotation about an arbitrary axis $[q_\mathsf{x}, q_\mathsf{y}, q_\mathsf{z}]^\top \in \mathbb{S}^2$.

- One zero eigenvalue: $\lambda_3 > \lambda_2 > \lambda_1 = 0$: We have a minimum on the circular manifold

$$\bar{\boldsymbol{R}}_7 = \begin{bmatrix} 1 & 0 & 0 \\ 0 & c & -s \\ 0 & s & c \end{bmatrix},\ c^2 + s^2 = 1\ :$$
$$\mathcal{V}(\bar{\boldsymbol{R}}_7) = -\tfrac{\lambda_2+\lambda_3}{2}, \qquad \operatorname{eig}(\boldsymbol{\nabla}^2\bar{\mathcal{V}}(\bar{\boldsymbol{R}}_7)) = \{\lambda_3, \lambda_2, 0\} \tag{2.67h}$$

  which includes $\bar{\boldsymbol{R}}_0$ and $\bar{\boldsymbol{R}}_1$. Furthermore we have a saddle point at $\bar{\boldsymbol{R}}_2$ and a maximum at $\bar{\boldsymbol{R}}_3$.

- Double eigenvalue and zero eigenvalue: $\lambda_3 = \lambda_2 > \lambda_1 = 0$: We have a minimum on $\bar{\boldsymbol{R}}_7$ and a maximum on $\bar{\boldsymbol{R}}_5$.

- Two zero eigenvalues: $\lambda_3 > \lambda_2 = \lambda_1 = 0$: We have a minimum on the spherical manifold

$$\bar{\boldsymbol{R}}_8 = \begin{bmatrix} q_\mathsf{w}^2 + q_\mathsf{x}^2 - q_\mathsf{y}^2 & 2q_\mathsf{x}q_\mathsf{y} & 2q_\mathsf{w}q_\mathsf{y} \\ 2q_\mathsf{x}q_\mathsf{y} & q_\mathsf{w}^2 - q_\mathsf{x}^2 + q_\mathsf{y}^2 & -2q_\mathsf{w}q_\mathsf{x} \\ -2q_\mathsf{w}q_\mathsf{x} & 2q_\mathsf{w}q_\mathsf{x} & q_\mathsf{w}^2 - q_\mathsf{x}^2 - q_\mathsf{y}^2 \end{bmatrix},\ q_\mathsf{w}^2 + q_\mathsf{x}^2 + q_\mathsf{y}^2 = 1\ :$$
$$\mathcal{V}(\bar{\boldsymbol{R}}_8) = -\tfrac{\lambda_3}{2}, \qquad \operatorname{eig}(\boldsymbol{\nabla}^2\bar{\mathcal{V}}(\bar{\boldsymbol{R}}_8)) = \{\lambda_3, 0, 0\} \tag{2.67i}$$

  which includes $\bar{\boldsymbol{R}}_0$, $\bar{\boldsymbol{R}}_1$ and $\bar{\boldsymbol{R}}_2$ and corresponds to an arbitrary rotation about an axis $[q_\mathsf{x}, q_\mathsf{y}, 0]^\top$. Furthermore we have a maximum at $\bar{\boldsymbol{R}}_3$.

- All zero Eigenvalues: $\lambda_3 = \lambda_2 = \lambda_1 = 0$: for this we have $\bar{\boldsymbol{\Sigma}} = \boldsymbol{P} = \boldsymbol{0}$ and the function is $\mathcal{V} = 0$.

We may conclude that the function $\bar{\mathcal{V}}$ has a minimum at $\bar{\boldsymbol{R}}_0 = \mathbf{I}_3$ and a maximum at $\bar{\boldsymbol{R}}_3 = \operatorname{diag}(-1, -1, 1)$, though they may not be strict. The minimum is strict if and only if $\lambda_1 > 0$. The maximum is strict if and only if $\lambda_3 > \lambda_2$.

It should also be noted that the results of this paragraph would be much more "symmetric" if we would not have required the descending order of the singular values σ_i. This did however reduce the number of cases to distinguish.

Original coordinates. The original function $\mathcal{V}$ has a minimum at $\boldsymbol{R}_0 = \bar{\boldsymbol{Y}}\bar{\boldsymbol{X}}^\top$. The minimum $\boldsymbol{R}_0$ is strict, if, and only if, $\lambda_i > 0, i = 1, 2, 3$ or equivalently if $\boldsymbol{K} \in \mathbb{SYM}_0^+(3)$ is positive definite:

$$\boldsymbol{K} = \boldsymbol{\nabla}^2\mathcal{V}(\boldsymbol{R}_0) = \operatorname{Vee}(\boldsymbol{P}\boldsymbol{R}_0) = \operatorname{Vee}(\bar{\boldsymbol{X}}\bar{\boldsymbol{\Sigma}}\bar{\boldsymbol{Y}}^\top\bar{\boldsymbol{Y}}\bar{\boldsymbol{X}}^\top) = \bar{\boldsymbol{X}}\operatorname{Vee}(\bar{\boldsymbol{\Sigma}})\bar{\boldsymbol{X}}^\top = \bar{\boldsymbol{X}}\boldsymbol{\Lambda}\bar{\boldsymbol{X}}^\top. \tag{2.68}$$

Special polar decomposition. From the results of this section we may also conclude the following: For any matrix $\boldsymbol{M} \in \mathbb{R}^{3\times3}$ there is a matrix $\boldsymbol{R} \in \mathbb{SO}(3)$ and a unique matrix $\boldsymbol{K} \in \mathbb{SYM}_0^+(3)$, such that $\boldsymbol{M} = \boldsymbol{R}\operatorname{Wed}(\boldsymbol{K})$. The matrix $\boldsymbol{R}$ is unique if, and only if, the matrix $\boldsymbol{K}$ is positive definite. Within this work, this will be called the *special polar decomposition*.

Chapter 3

Analytical mechanics of particle systems

Goal. Established approaches of analytical mechanics commonly rely on the parameterization of the system in terms of *minimal* generalized coordinates $\boldsymbol{q}$ and their derivatives $\dot{\boldsymbol{q}}$. In this section we like to generalize this to handle redundant configuration coordinates $\boldsymbol{x}(t) \in \mathbb{X}$ and nonholonomic velocity coordinates $\boldsymbol{\xi}(t) \in \mathbb{R}^n$ as introduced in the previous section. The resulting formulations might become more cumbersome, but with some examples we like to show that it is worth it.

3.1 A single free particle

[Landau and Lifshitz, 1960, §1]: *One of the fundamental concepts of mechanics is that of a particle, also called material point.* This abstracts a body whose dimensions may be neglected and all its mass $\mathfrak{m}$ is located at a point with the Cartesian coordinates $\mathfrak{r}(t) \in \mathbb{R}^3$ at time t. Its motion obeys Newton's second law [Newton, 1687, p. 13, lex II], english translation [Newton, 1846, p. 83]: *The alternation of motion is ever proportional to the motive force impressed; and is made in the direction of the right line in which that force is impressed.* The contemporary version reads (e.g. [Lurie, 2002, eq. 6.1.1] or [Goldstein, 1951, eq. 1.3])

$$\mathfrak{m}\ddot{\mathfrak{r}} = \boldsymbol{\mathfrak{F}}^{\mathsf{A}}. \tag{3.1}$$

where $\ddot{\mathfrak{r}} \equiv \mathrm{d}^2\mathfrak{r}/\mathrm{d}t^2$ is Newton's notation of differentiation and the applied force $\boldsymbol{\mathfrak{F}}^{\mathsf{A}}$ collects all other (non inertial) influences on the particle. In this work we will investigate three sources of applied forces: gravity, linear springs and viscous friction.

Gravity. For far most engineering applications we are dealing with systems that move close to the surface of the Earth and where Galilei's gravitation principle [Galilei, 1638, Day 3] holds. In a contemporary formulation it states that a particle with mass $\mathfrak{m}_p$ is subject to the gravitational force

$$\boldsymbol{\mathfrak{F}}^{\mathsf{G}} = \mathfrak{m}\boldsymbol{a}_{\mathsf{G}} \tag{3.2}$$

where $\boldsymbol{a}_\mathsf{G}$ are the coefficients of the gravitational acceleration of the earth w.r.t. the chosen reference frame. Commonly the reference frame is chosen such that the $\boldsymbol{e}_\mathsf{z}$ axis is opposing gravity and we have $\boldsymbol{a}_\mathsf{G} = [0, 0, -g]^\top$ with the *gravity of earth* $g = 9.8\,\frac{\mathrm{m}}{\mathrm{s}^2}$.

Linear spring. Let the particle be connected with a spring to a point $\mathfrak{r}_0$. The simplest model of a spring is that of Hooke's law [Hooke, 1678]: The force $\mathfrak{F}^\mathsf{K}$ on the particle is opposite and proportional by a factor $\mathfrak{k} \in \mathbb{R}^+$ to the spring displacement $\mathfrak{r} - \mathfrak{r}_0$, i.e.

$$\mathfrak{F}^\mathsf{K} = -\mathfrak{k}(\mathfrak{r} - \mathfrak{r}_0). \tag{3.3}$$

Viscous friction. [Rayleigh, 1877, §81]: *There is another group of forces whose existence is often advantageous to recognize specially, namely those arising from friction or viscosity. [..] we suppose that each particle is retarded by forces proportional to its component velocities.* We may think of the particle to be immersed in a viscous fluid which, at the particle position, has the velocity $\mathfrak{v}_0$. The force on the particle is

$$\mathfrak{F}^\mathsf{D} = -\mathfrak{d}(\dot{\mathfrak{r}} - \mathfrak{v}_0) \tag{3.4}$$

with the damping parameter $\mathfrak{d} \in \mathbb{R}^+$.

Equation of motion. A single free particle that is subject to all the aforementioned forces and a general, not further specified external force $\mathfrak{F}^\mathsf{E}$, i.e. $\mathfrak{F}^\mathsf{A} = \mathfrak{F}^\mathsf{G} + \mathfrak{F}^\mathsf{K} + \mathfrak{F}^\mathsf{D} + \mathfrak{F}^\mathsf{E}$, has the equation of motion

$$\mathfrak{m}(\ddot{\mathfrak{r}} - \boldsymbol{a}_\mathsf{G}) + \mathfrak{d}(\dot{\mathfrak{r}} - \mathfrak{v}_0) + \mathfrak{k}(\mathfrak{r} - \mathfrak{r}_0) = \mathfrak{F}^\mathsf{E}. \tag{3.5}$$

Control engineering. From a control engineering perspective the structure of this system is already nice enough to consider it as a desired closed loop dynamics: If we want the particle to track a sufficiently smooth reference trajectory $t \mapsto \mathfrak{r}_\mathsf{R}(t)$ a reasonable desired closed loop dynamics is

$$\mathfrak{r}_\mathrm{E} = \mathfrak{r} - \mathfrak{r}_0, \qquad \mathfrak{m}\ddot{\mathfrak{r}}_\mathrm{E} + \bar{\mathfrak{d}}\dot{\mathfrak{r}}_\mathrm{E} + \bar{\mathfrak{k}}\mathfrak{r}_\mathrm{E} = \mathbf{0}. \tag{3.6}$$

This is essentially the same as above (3.5), but we replaced the spring origin $\mathfrak{r}_0$ with the reference position $\mathfrak{r}_\mathsf{R}$, the fluid velocity $\mathfrak{v}_0$ with the reference velocity $\dot{\mathfrak{r}}_\mathsf{R}$ and the free-fall acceleration $\boldsymbol{a}_\mathsf{G}$ with the reference acceleration $\ddot{\mathfrak{r}}_\mathsf{R}$. Furthermore, we replaced the spring stiffness $\mathfrak{k}$ and viscosity $\mathfrak{d}$ by analog tuning parameters $\bar{\mathfrak{k}}, \bar{\mathfrak{d}} \in \mathbb{R}^+$. Plugging the desired dynamics (3.6) into the plant dynamics (3.5) yields the required control law

$$\mathfrak{F}^\mathsf{E} = \mathfrak{m}(\ddot{\mathfrak{r}}_\mathsf{R} - \boldsymbol{a}_\mathsf{G}) + \mathfrak{d}(\dot{\mathfrak{r}} - \mathfrak{v}_0) + \mathfrak{k}(\mathfrak{r} - \mathfrak{r}_0) - \bar{\mathfrak{d}}(\dot{\mathfrak{r}} - \dot{\mathfrak{r}}_\mathsf{R}) - \bar{\mathfrak{k}}(\mathfrak{r} - \mathfrak{r}_\mathsf{R}) - \mathfrak{m}\boldsymbol{a}_\mathsf{G}. \tag{3.7}$$

As this control approach is so closely related to basic mechanics, it could be more intuitive for an engineer than other generic mathematical approaches.

3.2 Systems of constrained particles

System under consideration. For this section we consider a system of $\mathfrak{N}$ particles under geometric constraints: The *position* of a particle with respect to a given inertial frame at a given time t is $\mathfrak{r}_p(t) \in \mathbb{R}^3, p = 1, \ldots, \mathfrak{N}$ and the collection of all particle positions is $\mathfrak{x} = [\mathfrak{r}_1^\top, \ldots, \mathfrak{r}_\mathfrak{N}^\top]^\top \in \mathbb{R}^{3\mathfrak{N}}$. *Geometric constraints* on the particles are captured in $\mathfrak{H} \geq 0$ smooth functions of the form $\mathfrak{c}(\mathfrak{x}) = [\mathfrak{c}^1(\mathfrak{x}), \ldots, \mathfrak{c}^\mathfrak{H}(\mathfrak{x})]^\top = \mathbf{0}$. The set of all mutually admissible particle positions

$$\mathfrak{X} = \{\mathfrak{x} \in \mathbb{R}^{3\mathfrak{N}} \mid \mathfrak{c}(\mathfrak{x}) = \mathbf{0}\} \tag{3.8}$$

is called the *configuration space*. We require $\frac{\partial \mathfrak{c}}{\partial \mathfrak{x}}(\mathfrak{x})$ to have a constant, though not necessarily full rank.

3.2.1 First principles

Principle of constraint release. The principle of constraint release (see e.g. [Hamel, 1949, sec. 32] or [Lurie, 2002, sec. 6.1]) states that the motion of system of geometrically constrained particles is governed by

$$\mathfrak{c}(\mathfrak{x}) = \mathbf{0}, \quad \mathfrak{m}_p \ddot{\mathfrak{r}}_p = \mathfrak{F}_p^\mathsf{A} + \lambda_\kappa \frac{\partial \mathfrak{c}^\kappa}{\partial \mathfrak{r}_p}, \quad p = 1, \ldots, \mathfrak{N}. \tag{3.9}$$

Lagrange-d'Alembert principle. For a system of geometrically constrained particles states (e.g. [Goldstein, 1951, sec. 1.4] or [Lurie, 2002, sec. 6.3]):

$$\sum_{p=1}^{\mathfrak{N}} \langle \delta \mathfrak{r}_p, \mathfrak{F}_p^\mathsf{A} - \mathfrak{m}_p \ddot{\mathfrak{r}}_p \rangle = 0 \qquad \forall \quad \frac{\partial \mathfrak{c}}{\partial \mathfrak{x}} \delta \mathfrak{x} = \mathbf{0}. \tag{3.10}$$

The *virtual displacements* $\delta \mathfrak{r}_p$ are tangents to possible motions: For particle positions constrained by $\mathfrak{c}(\mathfrak{x}) = \mathbf{0}$ the displacements have to fulfill $\frac{\partial \mathfrak{c}}{\partial \mathfrak{x}} \delta \mathfrak{x} = \mathbf{0}$.

Gauß principle. Gauss's principle of least constraint was originally described in [Gauß, 1829] in words rather than equations. Maybe because of this, one finds somewhat different mathematical formulations in more contemporary sources, e.g. [Päsler, 1968, sec. 7], [Lanczos, 1986, sec. IV.8], [Bremer, 2008, sec. 2.2].

For the system given above, Gauss' principle states that the particle accelerations $\ddot{\mathfrak{r}}_p, p = 1, \ldots, \mathfrak{N}$ minimize the so-called Gaussian constrain $\mathcal{G}$:

$$\begin{aligned} \min_{\ddot{\mathfrak{x}} \in \mathbb{R}^{3\mathfrak{N}}} \quad & \mathcal{G} = \tfrac{1}{2} \sum_{p=1}^{\mathfrak{N}} \mathfrak{m}_p \|\ddot{\mathfrak{r}}_p - \ddot{\mathfrak{r}}_p^\mathsf{f}\|^2 \\ \text{s. t.} \quad & \ddot{\mathfrak{c}}(\mathfrak{x}, \dot{\mathfrak{x}}, \ddot{\mathfrak{x}}) = \mathbf{0} \end{aligned} \tag{3.11}$$

where $\ddot{\mathfrak{r}}_p^\mathsf{f}$ are the *unconstrained* particle accelerations, i.e. Newtons's second law $\ddot{\mathfrak{r}}_p^\mathsf{f} = \frac{\mathfrak{F}_p^\mathsf{A}}{\mathfrak{m}_p}$. Its crucial to note that the constraint equations $\ddot{\mathfrak{c}}(\mathfrak{x}, \dot{\mathfrak{x}}, \ddot{\mathfrak{x}}) = \mathbf{0}$ are *linear* in the accelerations $\ddot{\mathfrak{x}}$. Consequently, as stressed in [Gauß, 1829], the principle (3.11) is a (static) quadratic optimization problem with linear constraints.

Hamilton's principle. [Lanczos, 1986, p. 113]: *Hamilton's principle states that the motion of a mechanical system occurs in such a way that the action $\mathcal{A} = \int_{t_0}^{t_1} \mathcal{L}\,\mathrm{d}t$ becomes stationary for arbitrary possible variations of the configuration of the system, provided the initial and final conditions are prescribed. The Lagrangian $\mathcal{L} = \mathcal{T} - \mathcal{V}$ is the excess of kinetic energy $\mathcal{T}$ over potential energy $\mathcal{V}$.* For the system considered here, the kinetic energy is $\mathcal{T} = \frac{1}{2}\sum_{p=1}^{\mathfrak{N}} \mathfrak{m}_p \|\dot{\mathfrak{r}}_p\|^2$. The potential energy may have various origins, some of them will be discussed later.

The remarkable quality of the principle of stationary action is that it is used interdisciplinary: With appropriate formulation of the Lagrangian $\mathcal{L}$ it has applications in all branches of physics e.g. general relativity [Einstein, 1916], electromagnetic field theory [Landau and Lifshitz, 1971, ch. 4] or optics, the original context of Hamilton [Klein, 1926, p. 192]. Apart form physics, there is optimal control that builds up on essentially the same idea e.g. [Bryson, 1975].

For the context of this work, the statement above is actually not that useful since it does not allow for generic impressed forces $\mathfrak{F}_p^{\mathsf{A}}$. To mend this one finds a similar statement in e.g. [Lurie, 2002, eq. 12.2.14] or [Szabó, 1956, sec. I.3]:

$$\delta'\mathcal{A} = \int_{t_1}^{t_2} \big(\delta\mathcal{T} - \delta'\mathcal{W}\big)\mathrm{d}t = 0, \qquad \mathcal{T} = \tfrac{1}{2}\sum\nolimits_p \mathfrak{m}_p\|\dot{\mathfrak{r}}_p\|^2,\ \delta'\mathcal{W} = \langle \delta\mathfrak{r}_p, \mathfrak{F}_p^{\mathsf{A}}\rangle. \tag{3.12}$$

Here $\delta'\mathcal{W}$ is an variational quantity, but in general, there is no $\mathcal{W}$ that it is the variation of, unless the impressed forces $\mathfrak{F}_p^{\mathsf{A}}$ may be derived from a potential. Consequently, there is generally no quantity $\mathcal{A}$ which becomes stationary, thus the naming is not suitable here.

3.2.2 Coordinates

Generalized coordinates. In most cases we are not really interested in the motion of the individual particles but rather in the system as a whole. Using the constraint equations it is possible to capture the configuration of the system by $\dim\mathfrak{X} = 3\mathfrak{N} - \operatorname{rank}\frac{\partial\mathfrak{c}}{\partial\mathfrak{r}} = n$ coordinates, commonly called *generalized coordinates* and commonly denoted by $\boldsymbol{q}$. Its components, in contrast to the Cartesian particle coordinates, may be lengths, angles or some completely generic quantity stressed by the term “generalized“. What is more crucial but usually implicit, is that they have to be independent from another to parameterize the n dimensional configuration space with its n components. Whenever used in this work, these coordinates are referred to as *minimal* generalized coordinates $\boldsymbol{q} \in \mathbb{R}^n$.

Redundant configuration coordinates and velocity coordinates. As motivated in section 2.1, in some cases it can be beneficial to use use a slightly larger number of *redundant* generalized coordinates $\boldsymbol{x}(t) \in \mathbb{X} = \{\boldsymbol{x} \in \mathbb{R}^\nu \,|\, \boldsymbol{\phi}(\boldsymbol{x}) = \mathbf{0}\}$ and *minimal* velocity coordinates $\boldsymbol{\xi}(t) \in \mathbb{R}^n$ related by $\dot{\boldsymbol{x}} = \boldsymbol{A}\boldsymbol{\xi}$. Of course this includes common minimal parameterization $\boldsymbol{x} = \boldsymbol{q} \in \mathbb{R}^n$ and $\boldsymbol{\xi} = \dot{\boldsymbol{q}} \in \mathbb{R}^n$ as the special case $\mathbb{X} = \mathbb{R}^n$ and $\boldsymbol{A} = \mathbf{I}_n$.

Particle parameterization. Let the admissible particle positions $\mathfrak{r} \in \mathfrak{X}$ be parameterized $\mathfrak{r}_p = \mathfrak{r}_p(\boldsymbol{x}, t)$ by possibly redundant coordinates $\boldsymbol{x} \in \mathbb{X}$. This means $\boldsymbol{\phi}(\boldsymbol{x}) =$

$\mathbf{0} \Rightarrow \mathfrak{c}(\mathfrak{x}(\boldsymbol{x},t)) = \mathbf{0}$ and consequently $\boldsymbol{x} \in \mathbb{X} \Rightarrow \mathfrak{x}(\boldsymbol{x}) \in \mathfrak{X}$. The particle velocities and accelerations in terms of the coordinates we have

$$\dot{\mathfrak{r}}_p = \partial_i \mathfrak{r}_p \xi^i + \frac{\partial \mathfrak{r}_p}{\partial t} \tag{3.13a}$$

$$\ddot{\mathfrak{r}}_p = \partial_i \mathfrak{r}_p \dot{\xi}^i + \partial_j \partial_i \mathfrak{r}_p \xi^i \xi^j + \underbrace{\Big(\partial_i \frac{\partial \mathfrak{r}_p}{\partial t} + \frac{\partial}{\partial t} \partial_i \mathfrak{r}_p\Big)\xi^i + \frac{\partial^2 \mathfrak{r}_p}{\partial t^2}}_{\mathfrak{a}_p^{\mathsf{E}}}. \tag{3.13b}$$

The following relations will be useful for the next steps of this section:

- From (3.13) it is evident that

$$\partial_i \mathfrak{r}_p = \frac{\partial \dot{\mathfrak{r}}_p}{\partial \xi^i} = \frac{\partial \ddot{\mathfrak{r}}_p}{\partial \dot{\xi}^i}. \qquad i = 1, \dots, n. \tag{3.14}$$

- From $\frac{\mathrm{d}}{\mathrm{d}t}\partial_i \mathfrak{r}_p = \partial_j \partial_i \mathfrak{r}_p \xi^j + \frac{\partial}{\partial t}\partial_i \mathfrak{r}_p = (\partial_i \partial_j - \gamma_{ij}^k \partial_k)\mathfrak{r}_p \xi^j + \partial_i \frac{\partial \mathfrak{r}_p}{\partial t} = \partial_i \dot{\mathfrak{r}}_p - \gamma_{ij}^k \partial_k \mathfrak{r}_p \xi^j$ with the commutation coefficients γ_{ij}^k established in subsection 2.2.2, we obtain the commutation relation

$$\partial_i \dot{\mathfrak{r}}_p - \frac{\mathrm{d}}{\mathrm{d}t}\partial_i \mathfrak{r}_p = \gamma_{ij}^k \partial_k \mathfrak{r}_p \xi^j, \qquad i = 1, \dots, n. \tag{3.15}$$

- As $\frac{\mathrm{d}}{\mathrm{d}t}\mathfrak{c}^\kappa = \sum_p \frac{\partial \mathfrak{c}^\kappa}{\partial \mathfrak{r}_p}\dot{\mathfrak{r}}_p = \sum_p \frac{\partial \mathfrak{c}^\kappa}{\partial \mathfrak{r}_p}\big(\partial_i \mathfrak{r}_p \xi^i + \frac{\partial \mathfrak{r}_p}{\partial t}\big) = 0$ has to hold for any $\boldsymbol{\xi}$ we have

$$\sum\nolimits_p \frac{\partial \mathfrak{c}^\kappa}{\partial \mathfrak{r}_p}\partial_i \mathfrak{r}_p = 0, \qquad \kappa = 1, \dots, \mathfrak{H},\ i = 1, \dots, n \tag{3.16a}$$

$$\sum\nolimits_p \frac{\partial \mathfrak{c}^\kappa}{\partial \mathfrak{r}_p}\frac{\partial \mathfrak{r}_p}{\partial t} = 0, \qquad \kappa = 1, \dots, \mathfrak{H}. \tag{3.16b}$$

Application to the principle of constraint release. Summing up the projections of (3.9) on $\partial_i \mathfrak{r}_p$ eliminates the constraint forces $\boldsymbol{\lambda}$ due to (3.16a):

$$\underbrace{\sum\nolimits_p \langle \partial_i \mathfrak{r}_p, \mathfrak{m}_p \ddot{\mathfrak{r}}_p \rangle}_{f_i^{\mathrm{M}}} = \underbrace{\sum\nolimits_p \langle \partial_i \mathfrak{r}_p, \mathfrak{F}_p^{\mathsf{A}} \rangle}_{f_i^{\mathrm{A}}} + \lambda_\kappa \underbrace{\sum\nolimits_p \langle \partial_i \mathfrak{r}_p, \frac{\partial \mathfrak{c}^\kappa}{\partial \mathfrak{r}_p} \rangle}_{0}, \quad i = 1, \dots, n. \tag{3.17}$$

We call $\boldsymbol{f}^{\mathrm{M}}$ the generalized inertia force and $\boldsymbol{f}^{\mathrm{A}}$ the generalized applied force.

Parameterizing the particle accelerations $\ddot{\mathfrak{r}}_p$ in terms of the chosen coordinates (3.13b) yields

$$\begin{aligned} &\sum\nolimits_p \mathfrak{m}_p \langle \partial_i \mathfrak{r}_p, \overbrace{\partial_j \mathfrak{r}_p \dot{\xi}^j + \partial_k \partial_j \mathfrak{r}_p \xi^k \xi^j + \mathfrak{a}_p^{\mathsf{E}}}^{\ddot{\mathfrak{r}}_p} \rangle = \sum\nolimits_p \langle \partial_i \mathfrak{r}_p, \mathfrak{F}_p^{\mathsf{A}} \rangle, \quad i = 1, \dots, n \\ \Leftrightarrow \quad &\underbrace{\sum\nolimits_p \mathfrak{m}_p \langle \partial_i \mathfrak{r}_p, \partial_j \mathfrak{r}_p \rangle}_{M_{ij}} \dot{\xi}^j = \underbrace{\sum\nolimits_p \langle \partial_i \mathfrak{r}_p, \mathfrak{F}_p^{\mathsf{A}} - \mathfrak{m}_p\big(\partial_k \partial_j \mathfrak{r}_p \xi^k \xi^j + \mathfrak{a}_p^{\mathsf{E}}\big) \rangle}_{b_i}, \quad i = 1, \dots, n. \end{aligned} \tag{3.18}$$

Mathematically, the matrix $\boldsymbol{M}$ is symmetric and (assuming $\mathfrak{m}_p \geq 0$) is positive semidefinite. Physically, we may assume that $\boldsymbol{M}$ is actually positive definite, otherwise there is a degree of freedom with no inertia attached which would rather be an error in modeling. For this work we will assume that $\boldsymbol{M}$ is symmetric positive definite and consequently invertible. Then the acceleration coordinates can be expressed as

$$\dot{\boldsymbol{\xi}} = \boldsymbol{M}^{-1}\boldsymbol{b}. \tag{3.19}$$

Application to the Lagrange-d'Alembert principle. Analog to the velocity, we may parameterize virtual displacements as $\delta\mathfrak{r}_p = \partial_i \mathfrak{r}_p h^i, p = 1, \ldots, \mathfrak{N}$ in terms of *minimal* displacements coordinates $\boldsymbol{h} \in \mathbb{R}^n$. Plugging this into (3.10) we get

$$h^i \sum\nolimits_p \langle \partial_i \mathfrak{r}_p, \mathfrak{F}_p^{\mathsf{A}} - \mathfrak{m}_p \ddot{\mathfrak{r}}_p \rangle = 0 \qquad \forall \quad \boldsymbol{h} \in \mathbb{R}^n. \tag{3.20}$$

Since this has to hold for any $\boldsymbol{h}$, we have the identical result as above (3.17).

Application to the Gauß principle. Parameterizing the particle accelerations $\ddot{\mathfrak{r}}_p = \ddot{\mathfrak{r}}_p(\boldsymbol{x}, \boldsymbol{\xi}, \dot{\boldsymbol{\xi}})$ in terms of the chosen coordinates (3.13b) in Gauß' principle (3.11) eliminates the constraints. So it essentially transforms it to an *unconstrained* minimization problem. The Gaussian constraint now reads

$$\begin{aligned}
\mathcal{G} &= \tfrac{1}{2} \sum\nolimits_p \mathfrak{m}_p \| \overbrace{\partial_j \mathfrak{r}_p \dot{\xi}^j + \partial_k \partial_j \mathfrak{r}_p \xi^k \xi^j + \mathfrak{a}_p^{\mathsf{E}}}^{\ddot{\mathfrak{r}}_p} - \tfrac{\mathfrak{F}_p^{\mathsf{A}}}{\mathfrak{m}_p} \|^2 \\
&= \underbrace{\tfrac{1}{2} \sum\nolimits_p \mathfrak{m}_p \langle \partial_i \mathfrak{r}_p, \partial_j \mathfrak{r}_p \rangle}_{M_{ij}} \dot{\xi}^i \dot{\xi}^j - \underbrace{\sum\nolimits_p \langle \partial_i \mathfrak{r}_p, \mathfrak{F}_p^{\mathsf{A}} - \mathfrak{m}_p (\partial_k \partial_j \mathfrak{r}_p \xi^k \xi^j + \mathfrak{a}_p^{\mathsf{E}}) \rangle}_{b_i} \dot{\xi}^i \\
&\qquad + \underbrace{\tfrac{1}{2} \sum\nolimits_p \tfrac{1}{\mathfrak{m}_p} \| \mathfrak{F}_p^{\mathsf{A}} - \mathfrak{m}_p (\partial_k \partial_j \mathfrak{r}_p \xi^k \xi^j + \mathfrak{a}_p^{\mathsf{E}}) \|^2}_{\mathcal{G}_0} \\
&= \tfrac{1}{2} \dot{\boldsymbol{\xi}}^\top \boldsymbol{M} \dot{\boldsymbol{\xi}} - \dot{\boldsymbol{\xi}}^\top \boldsymbol{b} + \mathcal{G}_0.
\end{aligned} \tag{3.21}$$

The necessary condition for a critical point is

$$\frac{\partial \mathcal{G}}{\partial \dot{\boldsymbol{\xi}}} = \mathbf{0} \qquad \Leftrightarrow \qquad \boldsymbol{M}\dot{\boldsymbol{\xi}} = \boldsymbol{b}. \tag{3.22}$$

Which is, again, the same result as above. Since $\partial^2 \mathcal{G} / \partial \dot{\boldsymbol{\xi}} \partial \dot{\boldsymbol{\xi}} = \boldsymbol{M}$ is positive definite, the solution $\dot{\boldsymbol{\xi}} = \boldsymbol{M}^{-1}\boldsymbol{b}$ is a minimum of the Gaussian constraint $\mathcal{G}$.

Application to Hamilton's principle. As discussed above, Hamilton's principle of stationary action is not applicable for generic forces as assumed here. However, it might still be instructive to apply it to our system when setting $\boldsymbol{f}^{\mathrm{A}} = \mathbf{0}$ and $\mathcal{L} = \mathcal{T}$.

The kinetic energy $\mathcal{T}$ in terms of the chosen coordinates is

$$\mathcal{T}(\boldsymbol{x}, \boldsymbol{\xi}, t) = \tfrac{1}{2} \sum\nolimits_p \mathfrak{m}_p \| \dot{\mathfrak{r}}_p(\boldsymbol{x}, \boldsymbol{\xi}, t) \|^2, \qquad \dot{\mathfrak{r}}_p(\boldsymbol{x}, \boldsymbol{\xi}, t) = \partial_i \mathfrak{r}_p(\boldsymbol{x}) \xi^i + \frac{\partial \mathfrak{r}_p}{\partial t}(\boldsymbol{x}, t) \tag{3.23}$$

As this is the structure assumed in (2.26) we may use the result (2.31) from the calculus of variations to obtain

$$f_i^{\mathrm{M}} = \frac{\mathrm{d}}{\mathrm{d}t}\frac{\partial \mathcal{T}}{\partial \xi^i} + \gamma_{ij}^k \xi^j \frac{\partial \mathcal{T}}{\partial \xi^k} - \partial_i \mathcal{T} = 0 \quad i = 1, \dots, n. \tag{3.24}$$

Evaluation and some rearrangement using the identities (3.14) and (3.15) yields

$$\begin{aligned} f_i^{\mathrm{M}} &= \sum\nolimits_p \mathfrak{m}_p \Big(\frac{\mathrm{d}}{\mathrm{d}t} \langle \frac{\partial \dot{\mathfrak{r}}_p}{\partial \xi^i}, \dot{\mathfrak{r}}_p \rangle + \gamma_{ij}^k \xi^j \langle \frac{\partial \dot{\mathfrak{r}}_p}{\partial \xi^k}, \dot{\mathfrak{r}}_p \rangle - \langle \partial_i \dot{\mathfrak{r}}_p, \dot{\mathfrak{r}}_p \rangle \Big) \\ &= \sum\nolimits_p \mathfrak{m}_p \Big(\langle \partial_i \mathfrak{r}_p, \ddot{\mathfrak{r}}_p \rangle + \langle \underbrace{\frac{\mathrm{d}}{\mathrm{d}t} \partial_i \mathfrak{r}_p + \gamma_{ij}^k \xi^j \partial_k \mathfrak{r}_p - \partial_i \dot{\mathfrak{r}}_p}_{0}, \dot{\mathfrak{r}}_p \rangle \Big) \end{aligned} \tag{3.25}$$

Which matches the generalized inertial force derived above (3.17).

3.2.3 Inertia

In (3.17) we have introduced the generalized inertia force $\boldsymbol{f}^{\mathrm{M}} = \sum_p \langle \partial_i \mathfrak{r}_p, \mathfrak{F}_p^{\mathsf{M}} \rangle$ as the projection of the particle inertia forces $\mathfrak{F}_p^{\mathsf{M}} = \mathfrak{m}_p \ddot{\mathfrak{r}}_p$. With this we will review some established formalisms and extend them for the use of redundant configuration coordinates.

Gibbs-Appell formulation. Using the identity of the differentials (3.14) we may formulate

$$f_i^{\mathrm{M}} = \sum\nolimits_p \langle \frac{\partial \ddot{\mathfrak{r}}_p}{\partial \dot{\xi}^i}, -\mathfrak{m}_p \ddot{\mathfrak{r}}_p \rangle = -\frac{\partial}{\partial \dot{\xi}^i} \underbrace{\Big(\tfrac{1}{2} \sum\nolimits_p \mathfrak{m}_p \| \ddot{\mathfrak{r}}_p \|^2 \Big)}_{\mathcal{S}}, \qquad i = 1, \dots, n. \tag{3.26}$$

So the generalized inertia force $\boldsymbol{f}^{\mathrm{M}}$ may be derived from the function $\mathcal{S} = \mathcal{S}(\boldsymbol{x}, \boldsymbol{\xi}, \dot{\boldsymbol{\xi}}, t)$ which is commonly called the *acceleration energy* though its dimension is *not* that of energy.

This formulation was first proposed by [Gibbs, 1879] for Cartesian, minimal coordinates and by [Appell, 1900] also using nonholonomic velocity coordinates. Some historic overview is given in [Lewis, 1996, sec. 1].

Euler-Lagrange formulation. Using the identity of the differentials (3.14), the commutation relation (3.15) and the product rule of differentiation we may formulate

$$\begin{aligned} f_i^{\mathrm{M}} &= \sum\nolimits_p \langle \frac{\partial \dot{\mathfrak{r}}_p}{\partial \xi^i}, \frac{\mathrm{d}}{\mathrm{d}t} (\mathfrak{m}_p \dot{\mathfrak{r}}_p) \rangle \\ &= \sum\nolimits_p \mathfrak{m}_p \Big(\frac{\mathrm{d}}{\mathrm{d}t} \langle \frac{\partial \dot{\mathfrak{r}}_p}{\partial \xi^i}, \dot{\mathfrak{r}}_p \rangle - \langle \frac{\mathrm{d}}{\mathrm{d}t} \frac{\partial \dot{\mathfrak{r}}_p}{\partial \xi^i}, \dot{\mathfrak{r}}_p \rangle \Big) \\ &= \sum\nolimits_p \mathfrak{m}_p \Big(\frac{\mathrm{d}}{\mathrm{d}t} \langle \frac{\partial \dot{\mathfrak{r}}_p}{\partial \xi^i}, \dot{\mathfrak{r}}_p \rangle - \langle \partial_i \dot{\mathfrak{r}}_p - \gamma_{ij}^k \frac{\partial \dot{\mathfrak{r}}_p}{\partial \xi^k} \xi^j, \dot{\mathfrak{r}}_p \rangle \Big) \\ &= \Big(\frac{\mathrm{d}}{\mathrm{d}t} \frac{\partial}{\partial \xi^i} + \gamma_{ij}^k \xi^j \frac{\partial}{\partial \xi^k} - \partial_i \Big) \underbrace{\Big(\tfrac{1}{2} \sum\nolimits_p \mathfrak{m}_p \| \dot{\mathfrak{r}}_p \|^2 \Big)}_{\mathcal{T}}, \qquad i = 1, \dots, n. \end{aligned} \tag{3.27}$$

So the generalized inertia force $\boldsymbol{f}^{\mathrm{M}}$ may be derived from the *kinetic energy* $\mathcal{T} = \mathcal{T}(\boldsymbol{x}, \boldsymbol{\xi}, t)$ formulated in terms of the chosen coordinates. This has already been shown in (3.24) and the computation is essentially (3.25) backwards.

For the special case of minimal configuration coordinates $\boldsymbol{x} = \boldsymbol{q}$ and the holonomic velocity coordinates $\boldsymbol{\xi} = \dot{\boldsymbol{q}}$, which implies $\gamma = 0$, this formulation and its derivation may be found in any graduate textbook on mechanics and is commonly called the *Euler-Lagrange equation*. A nearly identical form as (3.27) can be found in [Hamel, 1904a, p. 17]. The difference is that, in contrast to this work, the directional derivative ∂_i and the commutation coefficients γ_{ij}^k are therein restricted to minimal configuration coordinates.

It is worth noting that the quatitiy $2\mathcal{T}$ which appeared in this context, was called *vis viva* in older publications and translated to *living force* or *lebendige Kraft* [Hamel, 1904a]. The contemporary term *kinetic energy* seems to have established in the early 20th century.

Levi-Civita formulation. Formulation of the particle accelerations $\ddot{\mathfrak{r}}_p$ explicitly in terms of the chosen coordinates (3.13b) yields

$$\begin{aligned} f_i^{\mathrm{M}} &= \sum\nolimits_p \langle \partial_i \mathfrak{r}_p, \mathfrak{m}_p \overbrace{\left(\partial_j \mathfrak{r}_p \dot{\xi}^j + \partial_k \partial_j \mathfrak{r}_p \xi^k \xi^j + \mathfrak{a}_p^{\mathsf{E}}\right)}^{\ddot{\mathfrak{r}}_p} \rangle \qquad (3.28) \\ &= \underbrace{\sum\nolimits_p \mathfrak{m}_p \langle \partial_i \mathfrak{r}_p, \partial_j \mathfrak{r}_p \rangle}_{M_{ij}} \dot{\xi}^j + \underbrace{\sum\nolimits_p \mathfrak{m}_p \langle \partial_i \mathfrak{r}_p, \partial_k \partial_j \mathfrak{r}_p \rangle}_{\Gamma_{ijk}} \xi^k \xi^j + \sum\nolimits_p \mathfrak{m}_p \langle \partial_i \mathfrak{r}_p, \mathfrak{a}_p^{\mathsf{E}} \rangle, \ i = 1, \ldots, n. \end{aligned}$$

The inertia matrix $\boldsymbol{M}$ was already discussed above. Here we are interested in the terms denoted by Γ_{ijk}. Based on their definition in (3.28) one may validate the following identities

$$\partial_k M_{ij} = \Gamma_{ijk} + \Gamma_{jik}, \qquad (3.29a)$$

$$\gamma_{ij}^s M_{sk} = \Gamma_{kji} - \Gamma_{kij}. \qquad (3.29b)$$

Plugging these together while permuting the indices, we find

$$\begin{aligned} \Gamma_{ijk} &= \partial_k M_{ij} - \Gamma_{jik} \\ &= \partial_k M_{ij} + \gamma_{ik}^s M_{sj} - \Gamma_{jki} \\ &= \partial_k M_{ij} + \gamma_{ik}^s M_{sj} - \partial_i M_{kj} + \Gamma_{kji} \\ &= \partial_k M_{ij} + \gamma_{ik}^s M_{sj} - \partial_i M_{kj} + \gamma_{ij}^s M_{sk} + \Gamma_{kij} \\ &= \partial_k M_{ij} + \gamma_{ik}^s M_{sj} - \partial_i M_{kj} + \gamma_{ij}^s M_{sk} + \partial_j M_{ik} - \Gamma_{ikj} \\ &= \partial_k M_{ij} + \gamma_{ik}^s M_{sj} - \partial_i M_{kj} + \gamma_{ij}^s M_{sk} + \partial_j M_{ik} - \gamma_{kj}^s M_{si} - \Gamma_{ijk} \qquad (3.30) \\ \Leftrightarrow \quad \Gamma_{ijk} &= \tfrac{1}{2}\left(\partial_k M_{ij} + \partial_j M_{ik} - \partial_i M_{jk} + \gamma_{ij}^s M_{sk} + \gamma_{ik}^s M_{sj} - \gamma_{jk}^s M_{si}\right). \qquad (3.31) \end{aligned}$$

This means the coefficients Γ_{ijk} are completely determined by the inertia matrix $\boldsymbol{M}$ and the geometric matrix $\boldsymbol{A}$ which determines the directional derivative ∂_i and the commutation coefficients $\boldsymbol{\gamma}$.

A similar, coordinate free derivation can be found in [Abraham and Marsden, 1978, proof of Theorem 2.7.6] for the proof of the fundamental theorem of Riemannian geometry, i.e. the existence and uniqueness of the *Levi-Civita connection*. However, all coordinate versions therein are restricted to minimal holonomic coordinates. For this *special case*, i.e. $\boldsymbol{x} = \boldsymbol{q}$, $\boldsymbol{\xi} = \dot{\boldsymbol{q}}$, $\boldsymbol{A} = \mathbf{I}_n$ and consequently $\gamma = 0$, (3.31) simplifies to the familiar definition of the *Christoffel symbols* $\mathit{\Gamma}_{ijk} = \frac{1}{2}\big(\frac{\partial M_{ij}}{\partial q^k} + \frac{\partial M_{ik}}{\partial q^j} - \frac{\partial M_{jk}}{\partial q^i}\big)$, see e.g. [Abraham and Marsden, 1978, p. 145] or [Spivak, 1999, Vol. 2, p. 221]. In [Frankel, 1997, sec. 9.2] it is pointed out that the name Christoffel symbols is exclusive for the holonomic case, whereas in general $\mathit{\Gamma}_{ijk}$ are referred to as the *(Levi-Civita) connection coefficients*. To the best of the authors knowledge, the only popular source that states the coordinate version (3.31) explicitly is [Misner et al., 1973, eq. 8.24], though restricted to minimal coordinates and in a rather different context of relativistic point masses. Since the directional derivative ∂_i and the commutation coefficients γ_{ij}^s are defined in a setting supporting redundant coordinates, so does (3.31) as definition of the connection coefficients.

3.2.4 Gravitation

Earth's gravity acts on a system of particles just as on a single particle (3.2), i.e. with a force $\mathfrak{F}_p^{\mathsf{G}} = \mathfrak{m}_p \boldsymbol{a}_{\mathsf{G}}$ on each particle. The resulting generalized force on the system is

$$f_i^{\mathrm{G}} = \sum\nolimits_p \langle \partial_i \mathfrak{r}_p, \mathfrak{F}_p^{\mathsf{G}} \rangle = \sum\nolimits_p \mathfrak{m}_p \langle \partial_i \mathfrak{r}_p, \boldsymbol{a}_{\mathsf{G}} \rangle = \partial_i \underbrace{\sum\nolimits_p \mathfrak{m}_p \langle \mathfrak{r}_p, -\boldsymbol{a}_{\mathsf{G}} \rangle}_{\mathcal{V}^{\mathrm{G}}} . \tag{3.32}$$

The force may also be derived from the *gravitational potential* $\mathcal{V}^{\mathrm{G}}$ of the system which is simply the sum of the potentials of the individual particles.

The *gravitational mass* $\mathfrak{m}_p$ in (3.32) takes the same value as the *inertial mass* from the previous section. This is sometimes referred to as the *(Galilean) equivalence principle* and is crucial topic for general relativity, see e.g., [Misner et al., 1973, chap. 16]. In this context, there is no *absolute* acceleration $\ddot{\mathfrak{r}}_p$, instead, we are interested in the deviation from the free fall acceleration $\boldsymbol{a}_{\mathsf{G}}$. This motivates the following formulation for the sum of generalized inertial and gravitational force

$$\begin{aligned} f_i^{\mathrm{M}} + f_i^{\mathrm{G}} &= \sum\nolimits_p \mathfrak{m}_p \langle \partial_i \mathfrak{r}_p, \ddot{\mathfrak{r}}_p - \boldsymbol{a}_{\mathsf{G}} \rangle = \sum\nolimits_p \mathfrak{m}_p \langle \frac{\partial \ddot{\mathfrak{r}}_p}{\partial \dot{\xi}^i}, \ddot{\mathfrak{r}}_p - \boldsymbol{a}_{\mathsf{G}} \rangle \\ &= \frac{\partial}{\partial \dot{\xi}^i} \underbrace{\Big(\tfrac{1}{2} \sum\nolimits_p \mathfrak{m}_p \| \ddot{\mathfrak{r}}_p - \boldsymbol{a}_{\mathsf{G}} \|^2 \Big)}_{\mathcal{S}^{\mathrm{G}}}, \qquad i = 1, \ldots, n. \end{aligned} \tag{3.33}$$

The quantity $\mathcal{S}^{\mathrm{G}}$ may be regarded as a metric for the deviation of the system to its natural acceleration, the free fall.

Taking this one step further, we may consider the free fall velocities $\mathfrak{v}_{p\mathsf{G}}(t) = \boldsymbol{a}_{\mathsf{G}} t + \mathfrak{v}_{p0}$

with arbitrary initial velocities $\mathfrak{v}_{p0} \in \mathbb{R}^3, p = 1, \ldots, \mathfrak{N}$ and compute analog to (3.27):

$$\begin{aligned} f_i^{\mathrm{M}} + f_i^{\mathrm{G}} &= \sum\nolimits_p \mathfrak{m}_p \langle \frac{\partial \dot{\mathfrak{r}}_p}{\partial \xi^i}, \frac{\mathrm{d}}{\mathrm{d}t}(\dot{\mathfrak{r}}_p - \mathfrak{v}_{p\mathsf{G}}) \rangle \\ &= \sum\nolimits_p \mathfrak{m}_p \Big(\frac{\mathrm{d}}{\mathrm{d}t} \langle \frac{\partial \dot{\mathfrak{r}}_p}{\partial \xi^i}, \dot{\mathfrak{r}}_p - \mathfrak{v}_{p\mathsf{G}} \rangle - \langle \frac{\mathrm{d}}{\mathrm{d}t} \frac{\partial \dot{\mathfrak{r}}_p}{\partial \xi^i}, \dot{\mathfrak{r}}_p - \mathfrak{v}_{p\mathsf{G}} \rangle \Big) \\ &= \sum\nolimits_p \mathfrak{m}_p \Big(\frac{\mathrm{d}}{\mathrm{d}t} \langle \frac{\partial \dot{\mathfrak{r}}_p}{\partial \xi^i}, \dot{\mathfrak{r}}_p - \mathfrak{v}_{p\mathsf{G}} \rangle - \langle \partial_i \dot{\mathfrak{r}}_p - \gamma_{ij}^k \frac{\partial \dot{\mathfrak{r}}_p}{\partial \xi^k} \xi^j, \dot{\mathfrak{r}}_p - \mathfrak{v}_{p\mathsf{G}} \rangle \Big) \\ &= \Big(\frac{\mathrm{d}}{\mathrm{d}t} \frac{\partial}{\partial \xi^i} + \gamma_{ij}^k \xi^j \frac{\partial}{\partial \xi^k} - \partial_i \Big) \underbrace{\Big(\tfrac{1}{2} \sum\nolimits_p \mathfrak{m}_p \| \dot{\mathfrak{r}}_p - \mathfrak{v}_{p\mathsf{G}} \|^2 \Big)}_{\mathcal{T}^{\mathrm{G}}}, \qquad i = 1, \ldots, n. \end{aligned} \tag{3.34}$$

3.2.5 Stiffness

Consider that *one* particle $\mathfrak{r}_p$ of the system is connected by a linear spring with stiffness $\mathfrak{k}_p$ to a position $\mathfrak{p}_p$. The force on this one particle, as proposed in (3.3), is $\mathfrak{F}_p^{\mathsf{K}} = \mathfrak{k}_p(\mathfrak{p}_p - \mathfrak{r}_p)$. The generalized force on the system is

$$f_i^{\mathrm{K}} = \langle \partial_i \mathfrak{r}_p, \mathfrak{F}_p^{\mathsf{K}} \rangle = \mathfrak{k}_p \langle \partial_i \mathfrak{r}_p, \mathfrak{p}_p - \mathfrak{r}_p \rangle = -\partial_i \underbrace{\left(\tfrac{1}{2} \mathfrak{k}_p \| \mathfrak{r}_p - \mathfrak{p}_p \|^2 \right)}_{\mathcal{V}_p^{\mathrm{K}}}. \tag{3.35}$$

We may also consider a spring with stiffness $\mathfrak{k}_{pq}$ between two particles of the system: Then we have the force $\mathfrak{F}_p^{\mathsf{K}} = \mathfrak{k}_{pq}(\mathfrak{r}_q - \mathfrak{r}_p)$ on particle $\mathfrak{r}_p$ and the opposite force $\mathfrak{F}_q^{\mathsf{K}} = \mathfrak{k}_{pq}(\mathfrak{r}_p - \mathfrak{r}_q)$ on particle $\mathfrak{r}_q$. The generalized force on the system is

$$f_i^{\mathrm{K}} = \langle \partial_i \mathfrak{r}_p, \mathfrak{F}_p^{\mathsf{K}} \rangle + \langle \partial_i \mathfrak{r}_q, \mathfrak{F}_q^{\mathsf{K}} \rangle = -\mathfrak{k}_{pq} \langle \partial_i (\mathfrak{r}_p - \mathfrak{r}_q), \mathfrak{r}_p - \mathfrak{r}_q \rangle = -\partial_i \underbrace{\left(\tfrac{1}{2} \mathfrak{k}_{pq} \| \mathfrak{r}_p - \mathfrak{r}_q \|^2 \right)}_{\mathcal{V}_{pq}^{\mathrm{K}}}. \tag{3.36}$$

In both cases the generalized force can be derived from a potential $\mathcal{V}^{\mathrm{K}}$.

For a system with an arbitrary number of linear springs, one may simply sum up the individual potentials to obtain the stiffness potential $\mathcal{V}^{\mathrm{K}}$ and derive the corresponding generalized force $\boldsymbol{f}^{\mathrm{K}} = \boldsymbol{\nabla} \mathcal{V}^{\mathrm{K}}$. Note that non-negativity of the spring constants $\mathfrak{k} \geq 0$ implies non-negativity of the potential $\mathcal{V}^{\mathrm{K}} \geq 0$.

3.2.6 Dissipation

Let the system of particles move within a viscous fluid with velocities $\mathfrak{v}_p^{\mathsf{D}}$ at the positions $\mathfrak{r}_p$ of the particles. Then, as proposed in (3.4), each particle is subject to a friction force $\mathfrak{F}_p^{\mathsf{D}} = -\mathfrak{d}_p(\dot{\mathfrak{r}}_p - \mathfrak{v}_p^{\mathsf{D}})$. The generalized force on the the system is

$$f_i^{\mathsf{D}} = \sum\nolimits_p \langle \partial_i \mathfrak{r}_p, \mathfrak{F}_p^{\mathsf{D}} \rangle = -\sum\nolimits_p \mathfrak{d}_p \langle \frac{\partial \dot{\mathfrak{r}}_p}{\partial \xi^i}, \dot{\mathfrak{r}}_p - \mathfrak{v}_p^{\mathsf{D}} \rangle = -\frac{\partial}{\partial \xi^i} \underbrace{\left(\tfrac{1}{2} \sum\nolimits_p \mathfrak{d}_p \| \dot{\mathfrak{r}}_p - \mathfrak{v}_p^{\mathsf{D}} \|^2 \right)}_{\mathcal{R}}. \tag{3.37}$$

This dissipative force may be derived from $\mathcal{R}$, which is commonly called *Rayleigh dissipation function*, e.g. [Goldstein, 1951, p. 24]. Its dimension is that of power, i.e. watts. Note that non-negativity of the damping parameters $\mathfrak{k} \geq 0$ implies non-negativity of the dissipation function $\mathcal{V}^{\mathrm{K}} \geq 0$.

3.2.7 Energy

Total energy. The time derivative of the kinetic energy may be formulated as

$$\dot{\mathcal{T}} = \sum\nolimits_p \mathfrak{m}_p \langle \dot{\mathfrak{r}}_p, \ddot{\mathfrak{r}}_p \rangle = \xi^i \underbrace{\sum\nolimits_p \mathfrak{m}_p \langle \partial_i \mathfrak{r}_p, \ddot{\mathfrak{r}}_p \rangle}_{f_i^{\mathrm{M}}} + \sum\nolimits_p \mathfrak{m}_p \langle \frac{\partial \mathfrak{r}_p}{\partial t}, \ddot{\mathfrak{r}}_p \rangle. \tag{3.38}$$

In subsection 3.2.4 and subsection 3.2.4 we have seen potentials of the form $\mathcal{V}(\boldsymbol{x}, t)$ and their associated generalized force $f_i^{\mathrm{V}} = \partial_i \mathcal{V}$. The time derivative of this potential is

$$\dot{\mathcal{V}} = \xi^i \underbrace{\partial_i \mathcal{V}}_{f_i^{\mathrm{V}}} + \frac{\partial \mathcal{V}}{\partial t}. \tag{3.39}$$

The sum $\mathcal{W} = \mathcal{T} + \mathcal{V}$ is commonly called the *total energy*. Its time derivative is

$$\dot{\mathcal{W}} = \boldsymbol{\xi}^\top \big(\boldsymbol{f}^{\mathrm{M}} + \boldsymbol{f}^{\mathrm{V}} \big) + \sum\nolimits_p \mathfrak{m}_p \langle \frac{\partial \mathfrak{r}_p}{\partial t}, \ddot{\mathfrak{r}}_p \rangle + \frac{\partial \mathcal{V}}{\partial t}. \tag{3.40}$$

Note that the equation of motion implies $\boldsymbol{f}^{\mathrm{M}} + \boldsymbol{f}^{\mathrm{V}} = \boldsymbol{f}^{\mathrm{E}} - \boldsymbol{f}^{\mathrm{D}}$.

A mechanical system is called skleronomic (otherwise rheonomic) if it does not contain explicit time dependency. For this important case the change of total energy may be exressed by the external and dissipative forces alone

$$\dot{\mathcal{W}} = \boldsymbol{\xi}^\top \big(\boldsymbol{f}^{\mathrm{E}} - \boldsymbol{f}^{\mathrm{D}} \big). \tag{3.41}$$

Lagrangian and Hamiltonian. Define the *Lagrangian* as $\mathcal{L} = \mathcal{T} - \mathcal{V}$ which according to subsection 2.2.5 implies the generalized momentum and *Hamiltonian* as

$$p_i = \frac{\partial \mathcal{L}}{\partial \xi^i} = \sum\nolimits_p \mathfrak{m}_p \langle \partial_i \mathfrak{r}_p, \dot{\mathfrak{r}}_p \rangle, \quad i = 1, \ldots, n, \tag{3.42}$$

$$\mathcal{H} = p_i \xi^i - \mathcal{L} = \underbrace{\tfrac{1}{2} \sum\nolimits_p \mathfrak{m}_p \| \dot{\mathfrak{r}}_p \|^2 + \mathcal{V}}_{\mathcal{W}} - \sum\nolimits_p \mathfrak{m}_p \langle \frac{\partial \mathfrak{r}_p}{\partial t}, \dot{\mathfrak{r}}_p \rangle. \tag{3.43}$$

Extending the derivation from subsection 2.2.5 with the nonconservative forces $\boldsymbol{f}^{\mathrm{D}}$ and $\boldsymbol{f}^{\mathrm{E}}$ we find the change of the Hamiltonian along the solutions of the equations of motion as

$$\dot{\mathcal{H}} = \boldsymbol{\xi}^\top \big(\boldsymbol{f}^{\mathrm{E}} - \boldsymbol{f}^{\mathrm{D}} \big) - \frac{\partial \mathcal{L}}{\partial t} = \boldsymbol{\xi}^\top \big(\boldsymbol{f}^{\mathrm{E}} - \boldsymbol{f}^{\mathrm{D}} \big) - \sum\nolimits_p \mathfrak{m}_p \langle \frac{\partial \dot{\mathfrak{r}}_p}{\partial t}, \dot{\mathfrak{r}}_p \rangle + \frac{\partial \mathcal{V}}{\partial t} \tag{3.44}$$

Note that for a skleronomic system, the Hamiltonian $\mathcal{H}$ coincides with the total energy $\mathcal{W}$.

3.3 A single free rigid body

Established textbooks on physics (e.g. [Goldstein, 1951, chap. 4], [Landau and Lifshitz, 1960, §31] or [Boltzmann, 1897, §44]) define a *rigid body* as a a system of a *finite* number $\mathfrak{N}$ particles such that the distances $d_{pq} = \|\mathfrak{r}_p - \mathfrak{r}_q\|$ between their positions $\mathfrak{r}_p$ are constant. Textbooks that are more focused on engineering like [Hamel, 1949, sec. 8, § 1], [Bremer, 2008, sec. 4.1] or [Roberson and Schwertassek, 1988, sec. 6.1.1] rather define a rigid body as a rigid volume over which mass is continuously distributed. Both modeling assumptions eventually lead to the same equations of motion when using the same generalized coordinates. They differ in the computation of the inertial parameters of total mass, center of mass and moment of inertia: The physics perspective uses a finite sum over the particles, whereas the engineering point of view requires an integral over the body volume. This work will consider a finite number of particles.

In contrast to the sources mentioned above, this section will investigate apart from inertia and gravitation, also stiffness and damping for a rigid body. In particular for the latter two parts, the model of concentrated particles is more intuitive in the authors humble opinion.

3.3.1 Coordinates

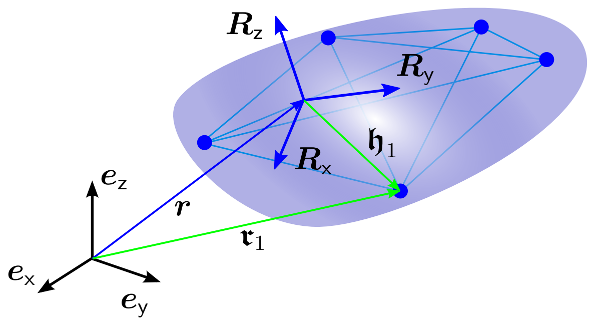

Figure 3.1: body fixed frame and particle positions

Body fixed frame. A common approach for modeling the rigid body (used in all sources above) is the use of a *body fixed frame*. This is the choice of a position $\boldsymbol{r} \in \mathbb{R}^3$ and a triple of orthonormal, right handed vectors $[\boldsymbol{R}_\mathrm{x}, \boldsymbol{R}_\mathrm{y}, \boldsymbol{R}_\mathrm{z}] = \boldsymbol{R} \in \mathbb{SO}(3)$ which are rigidly attached to the body, i.e. move with it, see Figure 3.1. With this, the position of any particle of the body may then be written as

$$\mathfrak{r}_p = \boldsymbol{r} + \boldsymbol{R}\mathfrak{h}_p, \quad p = 1, \dots, \mathfrak{N} \tag{3.45}$$

where the relative particle positions $\mathfrak{h}_p \in \mathbb{R}^3$ to the body fixed frame are *constant*. Consequently, the motion of the rigid body is completely captured by the position $\boldsymbol{r}(t) \in \mathbb{R}^3$ and orientation $\boldsymbol{R}(t) \in \mathbb{SO}(3)$ of the body fixed frame.

Usefulness of these particular coordinates. This is an example par excellence for the use of redundant parameters as discussed in the previous chapter: The system of particles has $\mathfrak{N}$ has $\nu = 3\mathfrak{N}$ coordinates, the coefficients of the particle positions $\mathfrak{r}_p, p = 1, \ldots, \mathfrak{N}$, and $c = \frac{1}{2}\mathfrak{N}(\mathfrak{N}-1)$ fixing their distances to each other. Actually, just fixing the distances between the particles still allows a mirroring of the rigid body, which from a physical perspective is not permitted. To resolve this there should be additional constraints on the "handedness" of the particles. Even without the "handedness" constraints, the number of distance constraints c surpasses the number of coordinates ν for larger number of particles. Consequently, the distance constraints cannot be independent. All these issues discourage us from working with the particle positions as configuration parameters.

On the other hand, since the configuration space of the rigid body $\mathbb{X} \cong \mathbb{R}^3 \times \mathbb{SO}(3)$ contains $\mathbb{SO}(3)$, any set of $n = \dim \mathbb{X} = 6$ minimal generalized coordinates will lead to singularities as discussed in section 1.2.

This particular choice of coordinates $(\boldsymbol{r}, \boldsymbol{R})$ may be regarded as a trade-off between these two extremes: It uses a fixed number of $\nu = 12$ coordinates and constraints and respects the topology of the configuration space. Furthermore, the interpretation of $\boldsymbol{r}$ and the columns of $\boldsymbol{R}$ as a body fixed frame are quite intuitive for practical applications.

Velocity. For parameterization of the velocity of the rigid body, we will use the body fixed velocity $\boldsymbol{v}(t) \in \mathbb{R}^3$ and the angular velocity $\boldsymbol{\omega}(t) \in \mathbb{R}^3$ which are related to the configuration by

$$\dot{\boldsymbol{r}} = \boldsymbol{R}\boldsymbol{v}, \qquad \dot{\boldsymbol{R}} = \boldsymbol{R}\,\mathrm{wed}(\boldsymbol{\omega}). \tag{3.46}$$

With this we may express the velocity and accelerations of the body particles as

$$\dot{\mathfrak{r}}_p = \boldsymbol{R}\big(\boldsymbol{v} - \mathrm{wed}(\boldsymbol{\mathfrak{h}}_p)\boldsymbol{\omega}\big), \tag{3.47a}$$

$$\ddot{\mathfrak{r}}_p = \boldsymbol{R}\big(\dot{\boldsymbol{v}} - \mathrm{wed}(\boldsymbol{\mathfrak{h}}_p)\dot{\boldsymbol{\omega}} + \mathrm{wed}(\boldsymbol{\omega})(\boldsymbol{v} - \mathrm{wed}(\boldsymbol{\mathfrak{h}}_p)\boldsymbol{\omega})\big), \quad p = 1, \ldots, \mathfrak{N} \tag{3.47b}$$

Compliance with the framework. In order to comply to the framework from the previous chapter we may group the configuration coordinates as $\boldsymbol{x} = [\boldsymbol{r}^\top, \boldsymbol{R}_\mathsf{x}^\top, \boldsymbol{R}_\mathsf{y}^\top, \boldsymbol{R}_\mathsf{z}^\top]^\top \in \mathbb{X} \subset \mathbb{R}^{12}$ and their geometric constraint as $\boldsymbol{\phi}(\boldsymbol{x}) = \boldsymbol{0}$ are the constraints of $\mathbb{SO}(3)$ as given in (2.6). The vector form of the kinematic relation (3.46) is

$$\underbrace{\begin{bmatrix} \dot{\boldsymbol{r}} \\ \dot{\boldsymbol{R}}_\mathsf{x} \\ \dot{\boldsymbol{R}}_\mathsf{y} \\ \dot{\boldsymbol{R}}_\mathsf{z} \end{bmatrix}}_{\dot{\boldsymbol{x}}} = \underbrace{\begin{bmatrix} \boldsymbol{R}_\mathsf{x} & \boldsymbol{R}_\mathsf{y} & \boldsymbol{R}_\mathsf{z} & \boldsymbol{0} & \boldsymbol{0} & \boldsymbol{0} \\ \boldsymbol{0} & \boldsymbol{0} & \boldsymbol{0} & \boldsymbol{0} & -\boldsymbol{R}_\mathsf{z} & \boldsymbol{R}_\mathsf{y} \\ \boldsymbol{0} & \boldsymbol{0} & \boldsymbol{0} & \boldsymbol{R}_\mathsf{z} & \boldsymbol{0} & -\boldsymbol{R}_\mathsf{x} \\ \boldsymbol{0} & \boldsymbol{0} & \boldsymbol{0} & -\boldsymbol{R}_\mathsf{y} & \boldsymbol{R}_\mathsf{x} & \boldsymbol{0} \end{bmatrix}}_{\boldsymbol{A}} \underbrace{\begin{bmatrix} v_\mathsf{x} \\ v_\mathsf{y} \\ v_\mathsf{z} \\ \omega_\mathsf{x} \\ \omega_\mathsf{y} \\ \omega_\mathsf{z} \end{bmatrix}}_{\boldsymbol{\xi}}. \tag{3.48}$$

Commutation coefficients. Plugging the kinematic matrix $\boldsymbol{A}$ from (3.48) into the definition (2.19) of the commutation symbols $\boldsymbol{\gamma}$ yields

$$\begin{aligned} \gamma^1_{26} = \gamma^1_{53} = \gamma^2_{34} = \gamma^2_{61} = \gamma^3_{15} = \gamma^3_{42} = \gamma^4_{56} = \gamma^5_{64} = \gamma^6_{45} = 1\ , \\ \gamma^1_{62} = \gamma^1_{35} = \gamma^2_{43} = \gamma^2_{16} = \gamma^3_{51} = \gamma^3_{24} = \gamma^4_{65} = \gamma^5_{46} = \gamma^6_{54} = -1 \end{aligned} \tag{3.49}$$

and the remaining coefficients vanish. With this we have

$$\left[\gamma_{ij}^k \xi^j\right]_{i=1\ldots6}^{k=1\ldots6} = \begin{bmatrix} \operatorname{wed}(\boldsymbol{\omega}) & 0 \\ \operatorname{wed}(\boldsymbol{v}) & \operatorname{wed}(\boldsymbol{\omega}) \end{bmatrix} = -\operatorname{ad}_{\boldsymbol{\xi}}^\top \tag{3.50}$$

whose naming will be discussed later.

3.3.2 Inertia

The previous section derived several formulations for the generalized inertial force $\boldsymbol{f}^{\mathsf{M}}$. These will now be applied to the the rigid body and the chosen coordinates.

Kinetic energy. With the particle velocities $\dot{\mathfrak{r}}_p$ in terms of the chosen coordinates (3.47a) we obtain the kinetic energy $\mathcal{T}$ of a free rigid body as

$$\begin{aligned} \mathcal{T} &= \tfrac{1}{2}\sum_p \mathfrak{m}_p \| \overbrace{\boldsymbol{R}\big(\boldsymbol{v} - \operatorname{wed}(\mathfrak{h}_p)\boldsymbol{\omega}\big)}^{\dot{\mathfrak{r}}_p} \|^2 \\ &= \tfrac{1}{2}\underbrace{\sum_p \mathfrak{m}_p}_{m} \|\boldsymbol{v}\|^2 - \boldsymbol{v}^\top \underbrace{\sum_p \mathfrak{m}_p \operatorname{wed}(\mathfrak{h}_p)}_{m\operatorname{wed}(\boldsymbol{s})}\boldsymbol{\omega} + \tfrac{1}{2}\boldsymbol{\omega}^\top \underbrace{\sum_p \mathfrak{m}_p \operatorname{wed}(\mathfrak{h}_p)^\top \operatorname{wed}(\mathfrak{h}_p)}_{\boldsymbol{\Theta}}\boldsymbol{\omega} \\ &= \tfrac{1}{2}\underbrace{\begin{bmatrix}\boldsymbol{v}^\top & \boldsymbol{\omega}^\top\end{bmatrix}}_{\boldsymbol{\xi}^\top} \underbrace{\begin{bmatrix} m\mathbf{I}_3 & m\operatorname{wed}(\boldsymbol{s})^\top \\ m\operatorname{wed}(\boldsymbol{s}) & \boldsymbol{\Theta}\end{bmatrix}}_{\mathsf{M}} \underbrace{\begin{bmatrix}\boldsymbol{v} \\ \boldsymbol{\omega}\end{bmatrix}}_{\boldsymbol{\xi}}. \end{aligned} \tag{3.51}$$

Here we have substituted some well established inertia parameters: the total mass m, the center of mass $\boldsymbol{s} = m^{-1}\sum_p \mathfrak{m}_p \mathfrak{h}_p$ and the moment of inertia $\boldsymbol{\Theta} = \boldsymbol{\Theta}^\top$. Assuming that the particle masses are positive $\mathfrak{m}_p > 0, p = 1, \ldots, \mathfrak{N}$ implies that the total mass is positive $m > 0$. Furthermore, if the rigid body has at least three particles that do not lie on a line, the inertia matrix is positive definite $\boldsymbol{\Theta} > 0$. It is important to notice that the inertia matrix M for the chosen coordinates is *constant*[1].

Plugging the the kinetic energy (3.51) into the corresponding formulation (3.27) of the generalized inertia force and using the commutation symbols from (3.50) yields

$$\boldsymbol{f}^{\mathrm{M}} = \underbrace{\begin{bmatrix} m\mathbf{I}_3 & m\operatorname{wed}(\boldsymbol{s})^\top \\ m\operatorname{wed}(\boldsymbol{s}) & \boldsymbol{\Theta}\end{bmatrix}}_{\mathsf{M}} \underbrace{\begin{bmatrix}\dot{\boldsymbol{v}} \\ \dot{\boldsymbol{\omega}}\end{bmatrix}}_{\dot{\boldsymbol{\xi}}} + \underbrace{\begin{bmatrix} \operatorname{wed}(\boldsymbol{\omega}) & 0 \\ \operatorname{wed}(\boldsymbol{v}) & \operatorname{wed}(\boldsymbol{\omega}) \end{bmatrix}}_{-\operatorname{ad}_{\boldsymbol{\xi}}^\top} \underbrace{\begin{bmatrix} m\mathbf{I}_3 & m\operatorname{wed}(\boldsymbol{s})^\top \\ m\operatorname{wed}(\boldsymbol{s}) & \boldsymbol{\Theta}\end{bmatrix}}_{\mathsf{M}} \underbrace{\begin{bmatrix}\boldsymbol{v} \\ \boldsymbol{\omega}\end{bmatrix}}_{\boldsymbol{\xi}} \tag{3.52}$$

[1] One reason for the choice of $\boldsymbol{v}$ as velocity coordinates it the fact that the inertia matrix M is *constant*. If we choose instead $\dot{\boldsymbol{r}}$ as velocity coordinates we have

$$\mathcal{T} = \tfrac{1}{2}[\dot{\boldsymbol{r}}^\top, \boldsymbol{\omega}^\top] \begin{bmatrix} m\mathbf{I}_3 & m\boldsymbol{R}\operatorname{wed}(\boldsymbol{s})^\top \\ m\operatorname{wed}(\boldsymbol{s})\boldsymbol{R}^\top & \boldsymbol{\Theta}\end{bmatrix} \begin{bmatrix}\dot{\boldsymbol{r}} \\ \boldsymbol{\omega}\end{bmatrix}.$$

Obviously the body inertia matrix depends on the orientation $\boldsymbol{R}$ of the body and is not constant unless the reference position $\boldsymbol{r}$ coincides with the *center of mass*, i.e. $\boldsymbol{s} = 0$. Actually many textbooks, e.g. [Murray et al., 1994, p. 167] or [Shabana, 2005, p. 153], restrict to this case for their expressions of the kinetic energy. In the next section on rigid body systems we will see that it can be quite useful to use *geometrically* meaningful body fixed frames rather than restricting to the center of mass.

Acceleration energy. With the particle accelerations $\ddot{\mathfrak{r}}_p$ in terms of the coordinates (3.47b) and using the Jacobi identity (2.57d) we find the acceleration energy $\mathcal{S}$ for the free rigid body as

$$\begin{aligned}
\mathcal{S} &= \tfrac{1}{2}\sum\nolimits_p \mathfrak{m}_p \| \overbrace{\boldsymbol{R}\big(\dot{\boldsymbol{v}} - \operatorname{wed}(\mathfrak{h}_p)\dot{\boldsymbol{\omega}} + \operatorname{wed}(\boldsymbol{\omega})(\boldsymbol{v} - \operatorname{wed}(\mathfrak{h}_p)\boldsymbol{\omega})\big)}^{\ddot{\mathfrak{r}}_p} \|^2 \\
&= \tfrac{1}{2}\underbrace{\sum\nolimits_p \mathfrak{m}_p}_{m} \|\dot{\boldsymbol{v}}\|^2 - \dot{\boldsymbol{v}}^\top \underbrace{\sum\nolimits_p \mathfrak{m}_p \operatorname{wed}(\mathfrak{h}_p)}_{m \operatorname{wed}(\boldsymbol{s})} \dot{\boldsymbol{\omega}} + \tfrac{1}{2}\dot{\boldsymbol{\omega}}^\top \underbrace{\sum\nolimits_p \mathfrak{m}_p \operatorname{wed}(\mathfrak{h}_p)^\top \operatorname{wed}(\mathfrak{h}_p)}_{\boldsymbol{\Theta}} \dot{\boldsymbol{\omega}} \\
&\quad + \dot{\boldsymbol{v}}^\top \operatorname{wed}(\boldsymbol{\omega})\Big(\underbrace{\sum\nolimits_p \mathfrak{m}_p}_{m} \boldsymbol{v} - \underbrace{\sum\nolimits_p \mathfrak{m}_p \operatorname{wed}(\mathfrak{h}_p)}_{m \operatorname{wed}(\boldsymbol{s})} \boldsymbol{\omega}\Big) \\
&\quad + \dot{\boldsymbol{\omega}}^\top \Big(\underbrace{\sum\nolimits_p \mathfrak{m}_p \operatorname{wed}(\mathfrak{h}_p)}_{m \operatorname{wed}(\boldsymbol{s})} \operatorname{wed}(\boldsymbol{\omega})\boldsymbol{v} + \operatorname{wed}(\boldsymbol{\omega}) \underbrace{\sum\nolimits_p \mathfrak{m}_p \operatorname{wed}(\mathfrak{h}_p)^\top \operatorname{wed}(\mathfrak{h}_p)}_{\boldsymbol{\Theta}} \boldsymbol{\omega}\Big) \\
&\quad + \tfrac{1}{2}\underbrace{\sum\nolimits_p \mathfrak{m}_p}_{m} \|\operatorname{wed}(\boldsymbol{\omega})\boldsymbol{v}\|^2 + \boldsymbol{v}^\top \operatorname{wed}(\boldsymbol{\omega})^2 \underbrace{\sum\nolimits_p \mathfrak{m}_p \operatorname{wed}(\mathfrak{h}_p)}_{m \operatorname{wed}(\boldsymbol{s})} \boldsymbol{\omega} \\
&\quad + \tfrac{1}{2}\operatorname{tr}\Big(\underbrace{\sum\nolimits_p \mathfrak{m}_p \mathfrak{h}_p \mathfrak{h}_p^\top}_{\boldsymbol{\Theta}' = \frac{1}{2}\operatorname{tr}(\boldsymbol{\Theta})\mathbf{I}_3 - \boldsymbol{\Theta}'} \operatorname{wed}(\boldsymbol{\omega})^4\Big)
\end{aligned} \tag{3.53}$$

Not at all surprisingly, we found the same inertia parameters m, $\boldsymbol{s}$ and $\boldsymbol{\Theta}$ as for the kinetic energy $\mathcal{T}$ in (3.51). Collecting these further in the inertia matrix M we have

$$\begin{aligned}
\mathcal{S} = \tfrac{1}{2} &\underbrace{\begin{bmatrix}\dot{\boldsymbol{v}}^\top & \dot{\boldsymbol{\omega}}^\top\end{bmatrix}}_{\dot{\boldsymbol{\xi}}^\top} \underbrace{\begin{bmatrix} m\mathbf{I}_3 & m\operatorname{wed}(\boldsymbol{s})^\top \\ m\operatorname{wed}(\boldsymbol{s}) & \boldsymbol{\Theta}\end{bmatrix}}_{\mathsf{M}} \underbrace{\begin{bmatrix}\dot{\boldsymbol{v}} \\ \dot{\boldsymbol{\omega}}\end{bmatrix}}_{\dot{\boldsymbol{\xi}}} \\
&+ \underbrace{\begin{bmatrix}\dot{\boldsymbol{v}}^\top & \dot{\boldsymbol{\omega}}^\top\end{bmatrix}}_{\dot{\boldsymbol{\xi}}^\top} \underbrace{\begin{bmatrix}\operatorname{wed}(\boldsymbol{\omega}) & \mathbf{0} \\ \operatorname{wed}(\boldsymbol{v}) & \operatorname{wed}(\boldsymbol{\omega})\end{bmatrix}}_{-\operatorname{ad}_{\boldsymbol{\xi}}^\top} \underbrace{\begin{bmatrix} m\mathbf{I}_3 & m\operatorname{wed}(\boldsymbol{s})^\top \\ m\operatorname{wed}(\boldsymbol{s}) & \boldsymbol{\Theta}\end{bmatrix}}_{\mathsf{M}} \underbrace{\begin{bmatrix}\boldsymbol{v} \\ \boldsymbol{\omega}\end{bmatrix}}_{\boldsymbol{\xi}} \\
&+ \underbrace{\tfrac{1}{2}m\|\operatorname{wed}(\boldsymbol{\omega})\boldsymbol{v}\|^2 + \boldsymbol{v}^\top \operatorname{wed}(\boldsymbol{\omega})^2 m \operatorname{wed}(\boldsymbol{s})\boldsymbol{\omega} + \tfrac{1}{2}\operatorname{tr}\big(\boldsymbol{\Theta}' \operatorname{wed}(\boldsymbol{\omega})^4\big)}_{\mathcal{S}_0}.
\end{aligned} \tag{3.54}$$

Plugging this into the corresponding formulation (3.26) of the generalized inertia force, i.e. $\boldsymbol{f}^{\mathsf{M}} = \partial\mathcal{S}/\partial\dot{\boldsymbol{\xi}}$, we obviously find the same expression as above (3.52). Note that $\mathcal{S}_0$ is independent of the generalized acceleration $\dot{\boldsymbol{\xi}}$ and consequently does not contribute to the inertia force.

Inertia matrix and connection coefficients. We can compute the Jacobian of the particle positions from

$$\boldsymbol{\nabla}\mathfrak{r}_p = \Big[\partial_i \mathfrak{r}_p\Big]_{i=1,\dots,6} = \Big[\frac{\partial \dot{\mathfrak{r}}_p}{\partial \xi^i}\Big]_{i=1,\dots,6} = \begin{bmatrix}\frac{\partial}{\partial \boldsymbol{v}} \\ \frac{\partial}{\partial \boldsymbol{\omega}}\end{bmatrix}^\top \overbrace{\boldsymbol{R}\big(\boldsymbol{v} - \operatorname{wed}(\mathfrak{h}_p)\boldsymbol{\omega}\big)}^{\dot{\mathfrak{r}}_p} = \boldsymbol{R}\begin{bmatrix}\mathbf{I}_3 & \operatorname{wed}(\mathfrak{h}_p)^\top\end{bmatrix}. \tag{3.55}$$

With this, the rigid body inertia matrix may be written as

$$\begin{aligned}\boldsymbol{M} &= \Big[\sum\nolimits_p \mathfrak{m}_p \langle \partial_i \mathfrak{r}_p, \partial_j \mathfrak{r}_p \rangle\Big]_{i,j=1,\ldots,6} = \sum\nolimits_p \mathfrak{m}_p (\boldsymbol{\nabla}\mathfrak{r}_p)^\top \boldsymbol{\nabla}\mathfrak{r}_p \\ &= \sum\nolimits_p \mathfrak{m}_p \begin{bmatrix} \mathbf{I}_3 & \mathrm{wed}(\mathfrak{h}_p)^\top \\ \mathrm{wed}(\mathfrak{h}_p) & \mathrm{wed}(\mathfrak{h}_p)\,\mathrm{wed}(\mathfrak{h}_p)^\top \end{bmatrix} = \begin{bmatrix} m\mathbf{I}_3 & m\,\mathrm{wed}(\boldsymbol{s})^\top \\ m\,\mathrm{wed}(\boldsymbol{s}) & \boldsymbol{\Theta} \end{bmatrix}\end{aligned} \tag{3.56}$$

which obviously coincides with what we found from the kinetic energy (3.51) and from the acceleration energy (3.54).

As already pointed out above, for the chosen velocity coordinates $\boldsymbol{\xi} = (\boldsymbol{v}, \boldsymbol{\omega})$, the coefficients of the rigid body inertia matrix M_{ij} are constant. Consequently, since $\partial_k M_{ij} \equiv 0$, the corresponding connection coefficients Γ_{ijk} only consist of the terms with the commutation coefficients γ:

$$\Gamma_{ijk} = \tfrac{1}{2}\big(\gamma_{ij}^{s} \mathsf{M}_{sk} + \gamma_{ik}^{s} \mathsf{M}_{sj} - \gamma_{jk}^{s} \mathsf{M}_{si}\big) = -\Gamma_{jik}. \tag{3.57}$$

Using the commutation coefficients γ given in (3.49) and taking into account the skew symmetry above, the non-zero connection coefficients are

$$\begin{aligned}
\Gamma_{324} = \Gamma_{135} = \Gamma_{216} &= m, && (3.58a)\\
\Gamma_{254} = \Gamma_{364} = \Gamma_{515} = \Gamma_{616} &= ms_{\mathsf{x}}, && (3.58b)\\
\Gamma_{424} = \Gamma_{145} = \Gamma_{365} = \Gamma_{626} &= ms_{\mathsf{y}}, && (3.58c)\\
\Gamma_{434} = \Gamma_{535} = \Gamma_{146} = \Gamma_{256} &= ms_{\mathsf{z}}, && (3.58d)\\
\Gamma_{654} &= \Theta'_{\mathsf{xx}} = \tfrac{1}{2}\big(\Theta_{\mathsf{yy}} + \Theta_{\mathsf{zz}} - \Theta_{\mathsf{xx}}\big), && (3.58e)\\
\Gamma_{465} &= \Theta'_{\mathsf{yy}} = \tfrac{1}{2}\big(\Theta_{\mathsf{xx}} + \Theta_{\mathsf{zz}} - \Theta_{\mathsf{yy}}\big), && (3.58f)\\
\Gamma_{546} &= \Theta'_{\mathsf{zz}} = \tfrac{1}{2}\big(\Theta_{\mathsf{xx}} + \Theta_{\mathsf{yy}} - \Theta_{\mathsf{zz}}\big), && (3.58g)\\
\Gamma_{464} = \Gamma_{655} &= \Theta'_{\mathsf{xy}} = -\Theta_{\mathsf{xy}}, && (3.58h)\\
\Gamma_{544} = \Gamma_{656} &= \Theta'_{\mathsf{xz}} = -\Theta_{\mathsf{xz}}, && (3.58i)\\
\Gamma_{545} = \Gamma_{466} &= \Theta'_{\mathsf{yz}} = -\Theta_{\mathsf{yz}}. && (3.58j)
\end{aligned}$$

Note that the quantity $\boldsymbol{\Theta}' = \frac{1}{2}\,\mathrm{tr}(\boldsymbol{\Theta})\mathbf{I}_3 - \boldsymbol{\Theta}$ also appeared above in the formulation of the acceleration energy (3.53).

Finally, assembling the terms $f_i^{\mathrm{M}} = M_{ij}\dot{\xi}^j + \mathit{\Gamma}_{ijk}\xi^j\xi^k$ we may check that this is indeed identical to (3.52).

3.3.3 Gravitation

The potential energy $\mathcal{V}^{\mathrm{G}}$ of a rigid body due to a gravitational acceleration $\boldsymbol{a}_{\mathsf{G}}$ according to (3.32) in terms of the chosen coordinates is

$$\mathcal{V}^{\mathrm{G}} = \sum\nolimits_p \langle \overbrace{\boldsymbol{r} + \boldsymbol{R}\mathfrak{h}_p}^{\mathfrak{r}_p}, -\mathfrak{m}_p \boldsymbol{a}_{\mathsf{G}} \rangle = -\langle \underbrace{\sum\nolimits_p \mathfrak{m}_p}_{m} \boldsymbol{r} + \boldsymbol{R} \underbrace{\sum\nolimits_p \mathfrak{m}_p \mathfrak{h}_p}_{m\boldsymbol{s}}, \boldsymbol{a}_{\mathsf{G}} \rangle = -m\langle \boldsymbol{r} + \boldsymbol{R}\boldsymbol{s}, \boldsymbol{a}_{\mathsf{G}} \rangle. \tag{3.59}$$

Note that the parameters of total mass m and center of mass $\boldsymbol{s}$ are the same as found above for the inertia matrix. The resulting generalized force is

$$\boldsymbol{f}^{\mathsf{G}} = \boldsymbol{\nabla}\mathcal{V}^{\mathrm{G}} = -m \begin{bmatrix} \boldsymbol{R}^\top \boldsymbol{a}_{\mathsf{G}} \\ \mathrm{wed}(\boldsymbol{s})\boldsymbol{R}^\top \boldsymbol{a}_{\mathsf{G}} \end{bmatrix}. \tag{3.60}$$

3.3.4 Stiffness

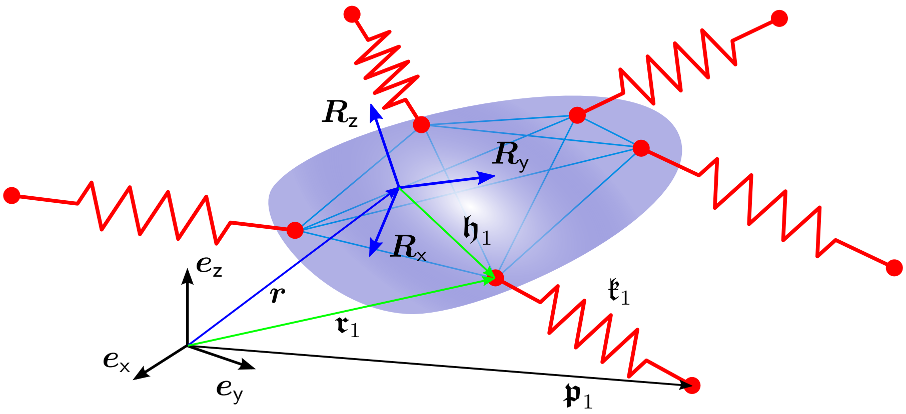

Figure 3.2: springs attached to a rigid body

Assume that every particle of the rigid body with position $\mathfrak{r}_p$ is connected to a position $\mathfrak{p}_p \in \mathbb{R}^3$ by a linear spring with stiffness $\mathfrak{k}_p \in \mathbb{R}^{(+)}$, see Figure 3.2. The resulting potential energy in terms of the rigid body coordinates $\boldsymbol{x} \cong (\boldsymbol{r}, \boldsymbol{R})$ is

$$\mathcal{V}^{\mathrm{K}}(\boldsymbol{x}) = \tfrac{1}{2}\sum\nolimits_p \mathfrak{k}_p \|\boldsymbol{r} + \boldsymbol{R}\mathfrak{h}_p - \mathfrak{p}_p\|^2. \tag{3.61}$$

Stiffness parameters. Using the identities above we may rearrange (3.61) to

$$\begin{aligned}
\mathcal{V}^{\mathrm{K}}(\boldsymbol{x}) &= \tfrac{1}{2}\sum\nolimits_p \mathfrak{k}_p \|\boldsymbol{r} + \boldsymbol{R}\mathfrak{h}_p - \mathfrak{p}_p\|^2 \\
&= \tfrac{1}{2}\sum\nolimits_p \mathfrak{k}_p \big(\|\boldsymbol{r}\|^2 + \underbrace{\|\boldsymbol{R}\mathfrak{h}_p\|^2}_{const.} + \underbrace{\|\mathfrak{p}_p\|^2}_{const.} + 2\langle \boldsymbol{r}, \boldsymbol{R}\mathfrak{h}_p\rangle - 2\langle \boldsymbol{r}, \mathfrak{p}_p\rangle - 2\langle \boldsymbol{R}\mathfrak{h}_p, \mathfrak{p}_p\rangle\big) \\
&= \tfrac{1}{2}k\|\boldsymbol{r}\|^2 + k\langle \boldsymbol{r}, \boldsymbol{R}\boldsymbol{h}\rangle - k\langle \boldsymbol{r}, \boldsymbol{p}\rangle - \mathrm{tr}(\boldsymbol{P}\boldsymbol{R}) + \underbrace{\tfrac{1}{2}\sum\nolimits_p \mathfrak{k}_p\big(\|\mathfrak{h}_p\|^2 + \|\mathfrak{p}_p\|^2\big)}_{\mathcal{V}^{\mathrm{K}}_c = const.}
\end{aligned} \tag{3.62}$$

with substitution of the constant parameters

$$k = \sum\nolimits_p \mathfrak{k}_p, \quad \boldsymbol{h} = k^{-1}\sum\nolimits_p \mathfrak{k}_p\mathfrak{h}_p, \quad \boldsymbol{p} = k^{-1}\sum\nolimits_p \mathfrak{k}_p\mathfrak{p}_p, \quad \boldsymbol{P} = \sum\nolimits_p \mathfrak{k}_p\mathfrak{h}_p\mathfrak{p}_p^\top. \tag{3.63}$$

Note that there was no specific assumption for the particle and spring distribution, i.e. on the values of $\mathfrak{h}_p$, $\mathfrak{p}_p$ and $\mathfrak{k}_p$. Consequently, any constellation may be captured by the $1+3+3+9+1 = 17$ parameters within $(k, \boldsymbol{h}, \boldsymbol{p}, \boldsymbol{P}, \mathcal{V}^{\mathrm{K}}_c)$.

Critical points. The time derivatives of the potential may be written as

$$\begin{aligned}\tfrac{\mathrm{d}}{\mathrm{d}t}\mathcal{V}^{\mathrm{K}} &= k\langle \boldsymbol{r}, \boldsymbol{R}\boldsymbol{v}\rangle + k\langle \boldsymbol{R}\boldsymbol{v}, \boldsymbol{R}\boldsymbol{h}\rangle + k\langle \boldsymbol{r}, \boldsymbol{R}\,\mathrm{wed}(\boldsymbol{\omega})\boldsymbol{h}\rangle - k\langle \boldsymbol{R}\boldsymbol{v}, \boldsymbol{p}\rangle - \mathrm{tr}(\boldsymbol{P}\boldsymbol{R}\,\mathrm{wed}(\boldsymbol{\omega}))\\ &= \boldsymbol{\xi}^\top \underbrace{\begin{bmatrix} k(\boldsymbol{R}^\top(\boldsymbol{r}-\boldsymbol{p})+\boldsymbol{h}) \\ k\,\mathrm{wed}(\boldsymbol{h})\boldsymbol{R}^\top\boldsymbol{r} + \mathrm{vee2}(\boldsymbol{P}\boldsymbol{R})\end{bmatrix}}_{\boldsymbol{\nabla}\mathcal{V}^{\mathrm{K}}}\end{aligned} \tag{3.64}$$

$$\tfrac{\mathrm{d}^2}{\mathrm{d}t^2}\mathcal{V}^{\mathrm{K}} = \dot{\boldsymbol{\xi}}^\top\boldsymbol{\nabla}\mathcal{V}^{\mathrm{K}} + \boldsymbol{\xi}^\top \underbrace{\begin{bmatrix} k\mathbf{I}_3 & k\,\mathrm{wed}\left(\boldsymbol{R}^\top(\boldsymbol{r}-\boldsymbol{p})\right) \\ k\,\mathrm{wed}(\boldsymbol{h}) & k\,\mathrm{wed}(\boldsymbol{h})\,\mathrm{wed}(\boldsymbol{R}^\top\boldsymbol{r}) + \mathrm{tr}(\boldsymbol{P}\boldsymbol{R})\mathbf{I}_3 - (\boldsymbol{P}\boldsymbol{R})^\top\end{bmatrix}}_{\boldsymbol{\nabla}^2\mathcal{V}^{\mathrm{K}}}\boldsymbol{\xi} \tag{3.65}$$

We are interested in configurations $\boldsymbol{x}_{\mathsf{R}} \cong (\boldsymbol{r}_{\mathsf{R}}, \boldsymbol{R}_{\mathsf{R}})$ at which the potential is stationary $\boldsymbol{\nabla}\mathcal{V}^{\mathrm{K}}(\boldsymbol{x}_{\mathsf{R}}) = \mathbf{0}$: From the upper part of (3.64) we get the condition

$$\boldsymbol{r}_{\mathsf{R}} = \boldsymbol{p} - \boldsymbol{R}_{\mathsf{R}}\boldsymbol{h}. \tag{3.66}$$

Plugging this into the lower part of (3.64) we obtain

$$k\,\mathrm{wed}(\boldsymbol{h})\boldsymbol{R}_{\mathsf{R}}^\top(\boldsymbol{p} - \boldsymbol{R}_{\mathsf{R}}\boldsymbol{h}) + \mathrm{vee2}(\boldsymbol{P}\boldsymbol{R}_{\mathsf{R}}) = \mathrm{vee2}(\underbrace{(\boldsymbol{P} - k\boldsymbol{h}\boldsymbol{p}^\top)}_{\boldsymbol{P}_s}\boldsymbol{R}_{\mathsf{R}}) = \mathbf{0}. \tag{3.67}$$

The solution to this subproblem $\mathrm{vee2}(\boldsymbol{P}_s\boldsymbol{R}_{\mathsf{R}}) = \mathbf{0}, \boldsymbol{R}_{\mathsf{R}} \in \mathbb{SO}(3)$ is discussed in great detail in section 2.4: Let $\boldsymbol{P}_s^\top = \boldsymbol{X}\,\mathrm{Wed}(\boldsymbol{\Pi}_{\mathsf{s}})$ with $\boldsymbol{X} \in \mathbb{SO}(3)$, $\boldsymbol{\Pi}_{\mathsf{s}} \in \mathbb{SYM}_0^+(3)$ be a *special polar decomposition*. Then $\boldsymbol{R}_{\mathsf{R}} = \boldsymbol{X}$ is clearly a critical point. Plugging $\boldsymbol{P} = \mathrm{Wed}(\boldsymbol{\Pi}_{\mathsf{s}})\boldsymbol{R}_{\mathsf{R}}^\top + k\boldsymbol{h}\boldsymbol{p}^\top$ into the Hessian matrix, we have

$$\begin{aligned}\boldsymbol{\nabla}^2\mathcal{V}^{\mathrm{K}}(\boldsymbol{x}_{\mathsf{R}}) &= \begin{bmatrix} k\mathbf{I}_3 & k\,\mathrm{wed}(\boldsymbol{h})^\top \\ k\,\mathrm{wed}(\boldsymbol{h}) & \boldsymbol{\Pi}_{\mathsf{s}} - k\,\mathrm{wed}(\boldsymbol{h})^2\end{bmatrix}\\ &= \begin{bmatrix} \mathbf{I}_3 & \mathbf{0} \\ \mathrm{wed}(\boldsymbol{h}) & \mathbf{I}_3\end{bmatrix}\begin{bmatrix} k\mathbf{I}_3 & \mathbf{0} \\ \mathbf{0} & \boldsymbol{\Pi}_{\mathsf{s}}\end{bmatrix}\begin{bmatrix} \mathbf{I}_3 & \mathrm{wed}(\boldsymbol{h})^\top \\ \mathbf{0} & \mathbf{I}_3\end{bmatrix}\end{aligned} \tag{3.68}$$

By Sylvester's law of inertia, the definiteness of $\boldsymbol{\nabla}^2\mathcal{V}^{\mathrm{K}}(\boldsymbol{x}_{\mathsf{R}})$ coincides with the definiteness of $k \geq 0$ and $\boldsymbol{\Pi}_{\mathsf{s}} \geq 0$. Using the results from section 2.4 we may conclude that $\boldsymbol{x}_{\mathsf{R}}$ is a minimum, and it is strict and global, if, and only if, $k > 0$ and $\boldsymbol{\Pi}_{\mathsf{s}} > 0$.

Stiffness parameters cont'd. We may express the parameters $\boldsymbol{p}$ and $\boldsymbol{P}$ in terms of the minimum configuration $(\boldsymbol{r}_{\mathsf{R}}, \boldsymbol{R}_{\mathsf{R}})$ and the matrix $\boldsymbol{\Pi}_{\mathsf{s}}$ as

$$\boldsymbol{p} = \boldsymbol{r}_{\mathsf{R}} + \boldsymbol{R}_{\mathsf{R}}\boldsymbol{h}, \qquad \boldsymbol{P} = \mathrm{Wed}(\boldsymbol{\Pi}_{\mathsf{s}})\boldsymbol{R}_{\mathsf{R}}^\top + k\boldsymbol{h}(\boldsymbol{r}_{\mathsf{R}} + \boldsymbol{R}_{\mathsf{R}}\boldsymbol{h})^\top \tag{3.69}$$

Plugging this into (3.62) we may reformulate the potential energy as

$$\begin{aligned}\mathcal{V}^{\mathrm{K}}(\boldsymbol{x}) &= \tfrac{1}{2}k\|\boldsymbol{r}\|^2 + k\langle \boldsymbol{r}, \boldsymbol{R}\boldsymbol{h}\rangle - k\langle \boldsymbol{r}, \boldsymbol{r}_{\mathsf{R}} + \boldsymbol{R}_{\mathsf{R}}\boldsymbol{h}\rangle - k\langle \boldsymbol{r}_{\mathsf{R}} + \boldsymbol{R}_{\mathsf{R}}\boldsymbol{h}, \boldsymbol{R}\boldsymbol{h}\rangle\\ &\qquad - \mathrm{tr}(\mathrm{Wed}(\boldsymbol{\Pi}_{\mathsf{s}})\boldsymbol{R}_{\mathsf{R}}^\top\boldsymbol{R}) + \tfrac{1}{2}\textstyle\sum_p \mathfrak{k}_p\left(\|\mathfrak{h}_p\|^2 + \|\mathfrak{p}_p\|^2\right)\\ &= \tfrac{1}{2}k\|\boldsymbol{r} + \boldsymbol{R}\boldsymbol{h} - (\boldsymbol{r}_{\mathsf{R}} + \boldsymbol{R}_{\mathsf{R}}\boldsymbol{h})\|^2 + \mathrm{tr}\left(\mathrm{Wed}(\boldsymbol{\Pi}_{\mathsf{s}})(\mathbf{I}_3 - \boldsymbol{R}_{\mathsf{R}}^\top\boldsymbol{R})\right)\\ &\qquad \underbrace{-\tfrac{1}{2}k\|\boldsymbol{r}_{\mathsf{R}} + \boldsymbol{R}_{\mathsf{R}}\boldsymbol{h}\|^2 - \tfrac{1}{2}k\|\boldsymbol{h}\|^2 - \mathrm{tr}\left(\mathrm{Wed}(\boldsymbol{\Pi}_{\mathsf{s}})\right) + \tfrac{1}{2}\textstyle\sum_p \mathfrak{k}_p\left(\|\mathfrak{h}_p\|^2 + \|\mathfrak{p}_p\|^2\right)}_{\mathcal{V}_0^{\mathrm{K}} = \mathcal{V}^{\mathrm{K}}(\boldsymbol{x}_{\mathsf{R}})}\\ &= \tfrac{1}{2}k\|\boldsymbol{r} - \boldsymbol{r}_{\mathsf{R}}\|^2 + k\langle \boldsymbol{r} - \boldsymbol{r}_{\mathsf{R}}, (\boldsymbol{R} - \boldsymbol{R}_{\mathsf{R}})\boldsymbol{h}\rangle + \mathrm{tr}\left(\mathrm{Wed}(\boldsymbol{\Pi})(\mathbf{I}_3 - \boldsymbol{R}_{\mathsf{R}}^\top\boldsymbol{R})\right) + \mathcal{V}_0^{\mathrm{K}}\end{aligned} \tag{3.70}$$

where $\boldsymbol{\mathit{\Pi}} = \boldsymbol{\mathit{\Pi}}_\mathsf{s} + k\,\mathrm{wed}(\boldsymbol{h})\,\mathrm{wed}(\boldsymbol{h})^\top$ and $\mathcal{V}_0^\mathrm{K}$ is the minimal potential, i.e. the potential of the residual displacement of the springs at the minimum $\boldsymbol{x}_\mathsf{R}$. The differential may be written as

$$\boldsymbol{\nabla}\mathcal{V}^\mathrm{K}(\boldsymbol{x}) = \begin{bmatrix} k\boldsymbol{R}^\top(\boldsymbol{r}-\boldsymbol{r}_\mathsf{R}) + (\mathbf{I}_3 - \boldsymbol{R}^\top\boldsymbol{R}_\mathsf{R})k\boldsymbol{h} \\ k\,\mathrm{wed}(\boldsymbol{h})\boldsymbol{R}^\top(\boldsymbol{r}-\boldsymbol{r}_\mathsf{R}) + \mathrm{vee2}\left(\mathrm{Wed}(\boldsymbol{\mathit{\Pi}})\boldsymbol{R}_\mathsf{R}^\top\boldsymbol{R}\right) \end{bmatrix}. \tag{3.71}$$

The Hessian at the minimum is

$$\boldsymbol{\nabla}^2\mathcal{V}^\mathrm{K}(\boldsymbol{x}_\mathsf{R}) = \begin{bmatrix} k\mathbf{I}_3 & k\,\mathrm{wed}(\boldsymbol{h})^\top \\ k\,\mathrm{wed}(\boldsymbol{h}) & \boldsymbol{\mathit{\Pi}} \end{bmatrix} \geq 0 \tag{3.72}$$

Conclusion. The conclusion of this subsection is that any constellation of linear springs attached to a rigid body may be captured by the potential $\mathcal{V}^\mathrm{K}$ from (3.70) and the resulting force $\boldsymbol{f}^\mathrm{K} = \boldsymbol{\nabla}\mathcal{V}^\mathrm{K}$ from (3.71). It is parameterized by 6 parameters within $(\boldsymbol{r}_\mathsf{R}, \boldsymbol{R}_\mathsf{R}) \in \mathbb{R}^3 \times \mathbb{SO}(3)$ which describe the configuration at the minimum, the $1+3+6 = 10$ parameters within $k, \in \mathbb{R}_0^+$, $\boldsymbol{h} \in \mathbb{R}^3$ and $\boldsymbol{\mathit{\Pi}} \in \mathbb{SYM}_0^+(3)$, and the minimum $\mathcal{V}_0^\mathrm{K}$: $\mathcal{V}^\mathrm{K}(\boldsymbol{x}) \geq \mathcal{V}_0^\mathrm{K} \geq 0$. The minimum is strict and global if, and only if, $k > 0$ and $\boldsymbol{\mathit{\Pi}}_\mathsf{s} = \boldsymbol{\mathit{\Pi}} - k\,\mathrm{wed}(\boldsymbol{h})\,\mathrm{wed}(\boldsymbol{h})^\top > 0$.

The rigid body stiffness matrix $\mathbf{K} = \boldsymbol{\nabla}^2\mathcal{V}^\mathrm{K}(\boldsymbol{x}_\mathsf{R})$ has the same structure as the inertia matrix $\mathbf{M} = \partial^2\mathcal{T}/\partial\boldsymbol{\xi}\partial\boldsymbol{\xi}$ for the chosen coordinates. Due to these analogies to the established inertia parameters, we refer to the rigid body stiffness parameters in the following as: total stiffness k, center of stiffness $\boldsymbol{h}$, moment of stiffness $\boldsymbol{\mathit{\Pi}}$, and moment of stiffness at the center of stiffness $\boldsymbol{\mathit{\Pi}}_\mathsf{s}$.

3.3.5 Dissipation

As motivated in the previous section we may motivate damping as particles moving within a viscous fluid which produce a drag force proportional to the particles velocity $\dot{\mathfrak{r}}_p$. Different volumes of the particles may motivate different drag coefficients $\mathfrak{d}_p$, see Figure 3.3.

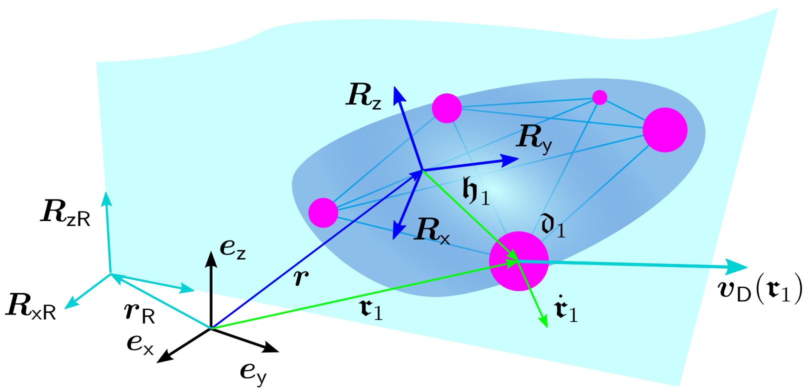

Figure 3.3: rigid body within viscous fluid

General fluid motion. Let the fluid at the position of p-th particle position have the velocity $\boldsymbol{v}_{\mathsf{D}p}(t) \in \mathbb{R}^3$ and let its drag coefficient be $\mathfrak{d}_p \in \mathbb{R}_0^+$. Overall, the dissipation function is

$$\begin{aligned}\mathcal{R} &= \tfrac{1}{2}\sum\nolimits_p \mathfrak{d}_p \| \overbrace{\boldsymbol{R}(\boldsymbol{v} - \mathrm{wed}(\mathfrak{h}_p)\boldsymbol{\omega})}^{\dot{\mathfrak{r}}_p} - \boldsymbol{v}_{\mathsf{D}p})\|^2 \\ &= \tfrac{1}{2}\underbrace{\sum\nolimits_p \mathfrak{d}_p}_{d} \|\boldsymbol{v}\|^2 - \boldsymbol{v}^\top \underbrace{\sum\nolimits_p \mathfrak{d}_p \,\mathrm{wed}(\mathfrak{h}_p)}_{d\,\mathrm{wed}(\boldsymbol{l})}\,\boldsymbol{\omega} + \tfrac{1}{2}\boldsymbol{\omega}^\top \underbrace{\sum\nolimits_p \mathfrak{d}_p \,\mathrm{wed}(\mathfrak{h}_p)^\top \mathrm{wed}(\mathfrak{h}_p)}_{\boldsymbol{\Upsilon}}\,\boldsymbol{\omega} \\ &\quad - \boldsymbol{v}^\top \sum\nolimits_p \mathfrak{d}_p \boldsymbol{R}^\top \boldsymbol{v}_{\mathsf{D}p} + \boldsymbol{\omega}^\top \sum\nolimits_p \mathfrak{d}_p \,\mathrm{wed}(\mathfrak{h}_p)\boldsymbol{R}^\top \boldsymbol{v}_{\mathsf{D}p} + \tfrac{1}{2}\sum\nolimits_p \mathfrak{d}_p \|\boldsymbol{v}_{\mathsf{D}p}\|^2 \end{aligned} \tag{3.73}$$

The resulting generalized force is

$$\boldsymbol{f}^{\mathsf{D}} = \frac{\partial \mathcal{R}}{\partial \boldsymbol{\xi}} = \underbrace{\begin{bmatrix} d\mathbf{I}_3 & d\,\mathrm{wed}(\boldsymbol{l})^\top \\ d\,\mathrm{wed}(\boldsymbol{l}) & \boldsymbol{\Upsilon} \end{bmatrix}}_{\mathsf{D}} \underbrace{\begin{bmatrix} \boldsymbol{v} \\ \boldsymbol{\omega} \end{bmatrix}}_{\boldsymbol{\xi}} + \sum\nolimits_p \mathfrak{d}_p \begin{bmatrix} -\mathbf{I}_3 \\ \mathrm{wed}(\mathfrak{h}_p) \end{bmatrix} \boldsymbol{R}^\top \boldsymbol{v}_{\mathsf{D}p}. \tag{3.74}$$

Again we found parameters similar to the established inertia parameters. In analogy to them we call $d \in \mathbb{R}_0^+$ the total damping, $\boldsymbol{l} \in \mathbb{R}^3$ the center of damping, and $\boldsymbol{\Upsilon} \in \mathbb{SYM}_0^+(3)$ the moment of damping.

Rigid fluid motion. Let us consider a special case in which the fluid velocity also obeys a rigid body motion parameterized by $(\boldsymbol{r}_{\mathsf{R}}, \boldsymbol{R}_{\mathsf{R}})$ and the velocity $(\boldsymbol{v}_{\mathsf{R}}, \boldsymbol{\omega}_{\mathsf{R}})$, see Figure 3.3. The absolute fluid velocity at the particle position is then $\boldsymbol{v}_{\mathsf{D}p} = \boldsymbol{R}_{\mathsf{R}}(\boldsymbol{v}_{\mathsf{R}} + \mathrm{wed}(\boldsymbol{\omega}_{\mathsf{R}})\boldsymbol{R}_{\mathsf{R}}^\top(\mathfrak{r}_p - \boldsymbol{r}_{\mathsf{R}}))$. The we have the dissipation function

$$\begin{aligned}\mathcal{R} &= \tfrac{1}{2}\sum\nolimits_p \mathfrak{d}_p \| \overbrace{\boldsymbol{R}(\boldsymbol{v} - \mathrm{wed}(\mathfrak{h}_p)\boldsymbol{\omega})}^{\dot{\mathfrak{r}}_p} - \overbrace{\boldsymbol{R}_{\mathsf{R}}(\boldsymbol{v}_{\mathsf{R}} + \mathrm{wed}(\boldsymbol{\omega}_{\mathsf{R}})\boldsymbol{R}_{\mathsf{R}}^\top(\boldsymbol{r} + \boldsymbol{R}\mathfrak{h}_p - \boldsymbol{r}_{\mathsf{R}}))}^{\boldsymbol{v}_{\mathsf{D}p}} \|^2 \\ &= \tfrac{1}{2}\sum\nolimits_p \mathfrak{d}_p \| \underbrace{\boldsymbol{v} - \boldsymbol{R}^\top(\boldsymbol{R}_{\mathsf{R}}\boldsymbol{v}_{\mathsf{R}} - \mathrm{wed}(\boldsymbol{r} - \boldsymbol{r}_{\mathsf{R}})\boldsymbol{R}_{\mathsf{R}}\boldsymbol{\omega}_{\mathsf{R}})}_{\boldsymbol{v}_{\mathrm{E}}} - \mathrm{wed}(\mathfrak{h}_p)\underbrace{(\boldsymbol{\omega} - \boldsymbol{R}^\top \boldsymbol{R}_{\mathsf{R}}\boldsymbol{\omega}_{\mathsf{R}})}_{\boldsymbol{\omega}_{\mathrm{E}}} \|^2 \\ &= \tfrac{1}{2}\underbrace{[\boldsymbol{v}_{\mathrm{E}}^\top, \boldsymbol{\omega}_{\mathrm{E}}^\top]}_{\boldsymbol{\xi}_{\mathrm{E}}^\top} \underbrace{\begin{bmatrix} d\mathbf{I}_3 & d\,\mathrm{wed}(\boldsymbol{l})^\top \\ d\,\mathrm{wed}(\boldsymbol{l}) & \boldsymbol{\Upsilon} \end{bmatrix}}_{\mathsf{D}} \underbrace{\begin{bmatrix} \boldsymbol{v}_{\mathrm{E}} \\ \boldsymbol{\omega}_{\mathrm{E}} \end{bmatrix}}_{\boldsymbol{\xi}_{\mathrm{E}}} \end{aligned} \tag{3.75}$$

The resulting generalized force is

$$\boldsymbol{f}^{\mathsf{D}} = \frac{\partial \mathcal{R}}{\partial \boldsymbol{\xi}} = \frac{\partial \mathcal{R}}{\partial \boldsymbol{\xi}_{\mathrm{E}}} = \mathsf{D}\boldsymbol{\xi}_{\mathrm{E}} \tag{3.76}$$

3.3.6 Summary and the special Euclidean group

Special Euclidean group. Instead of collecting the configuration coordinates in a tuple $\boldsymbol{x} = [\boldsymbol{r}^\top, \boldsymbol{R}_{\mathsf{x}}^\top, \boldsymbol{R}_{\mathsf{y}}^\top, \boldsymbol{R}_{\mathsf{z}}^\top]^\top \in \mathbb{X}$ as proposed in the previous chapter, it can also be useful to arrange them within a matrix:

$$\mathsf{G} = \begin{bmatrix} \boldsymbol{R} & \boldsymbol{r} \\ \mathbf{0} & 1 \end{bmatrix} \in \mathbb{SE}(3) = \left\{ \begin{bmatrix} \boldsymbol{R} & \boldsymbol{r} \\ \mathbf{0} & 1 \end{bmatrix} \,\middle|\, \boldsymbol{r} \in \mathbb{R}^3, \boldsymbol{R} \in \mathbb{SO}(3) \right\} \tag{3.77}$$

which is commonly referred to as the *homogeneous representation*, e.g. [Murray et al., 1994, sec. 2.3.1]. The set $\mathbb{SE}(3)$ combined with matrix multiplication forms a Lie group which is called the *special Euclidean group*. Euclidean denotes to the fact that its transformations preserve the Euclidean distance, while special denotes to the fact that it does not permit reflections (analog to the special orthogonal group $\mathbb{SO}(3)$).

Operators. This section already used the wed on $\mathbb{R}^3$ quite extensively. On $\mathbb{R}^6$ we define it as

$$\text{wed} : \mathbb{R}^3 \to \mathfrak{so}(3) \; : \; \begin{bmatrix} \omega_1 \\ \omega_2 \\ \omega_3 \end{bmatrix} \mapsto \begin{bmatrix} 0 & -\omega_3 & \omega_2 \\ \omega_3 & 0 & -\omega_1 \\ -\omega_2 & \omega_1 & 0 \end{bmatrix} \tag{3.78a}$$

$$\text{wed} : \mathbb{R}^6 \to \mathfrak{se}(3) \; : \; \begin{bmatrix} \boldsymbol{v} \\ \boldsymbol{\omega} \end{bmatrix} \mapsto \begin{bmatrix} \text{wed}\,\boldsymbol{\omega} & \boldsymbol{v} \\ \mathbf{0} & 0 \end{bmatrix} \tag{3.78b}$$

Its inverse is denoted $\text{vee}(\cdot)$, i.e. $\text{vee}(\text{wed}(\boldsymbol{\xi})) = \boldsymbol{\xi}$. The wed and vee operators are well established in the literature, see e.g. [Murray et al., 1994, sec. 2.3.2].

Using the wed operator may rewrite the rigid body kinematics from (3.46) in matrix form as:

$$\underbrace{\begin{bmatrix} \dot{\boldsymbol{R}} & \dot{\boldsymbol{r}} \\ \mathbf{0} & 0 \end{bmatrix}}_{\dot{\mathbf{G}}} = \underbrace{\begin{bmatrix} \boldsymbol{R} & \boldsymbol{r} \\ \mathbf{0} & 1 \end{bmatrix}}_{\mathbf{G}} \underbrace{\begin{bmatrix} \text{wed}(\boldsymbol{\omega}) & \boldsymbol{v} \\ \mathbf{0} & 0 \end{bmatrix}}_{\text{wed}(\boldsymbol{\xi})} \tag{3.79}$$

More operators. The following operators are not established in the literature, but will prove quite useful for this work. Define the vee2 operator through

$$\operatorname{tr}\left(\boldsymbol{A}(\text{wed}\,\boldsymbol{\xi})^\top\right) = \boldsymbol{\xi}^\top \,\text{vee2}(\boldsymbol{A}), \tag{3.80}$$

this is

$$\text{vee2} : \mathbb{R}^{3\times3} \to \mathbb{R}^3 \; : \; \boldsymbol{A} \mapsto \text{vee}(\boldsymbol{A} - \boldsymbol{A}^\top) \tag{3.81a}$$

$$\text{vee2} : \mathbb{R}^{4\times4} \to \mathbb{R}^6 \; : \; \begin{bmatrix} \boldsymbol{A} & \boldsymbol{b} \\ * & * \end{bmatrix} \mapsto \begin{bmatrix} \boldsymbol{b} \\ \text{vee2}\,\boldsymbol{A} \end{bmatrix}. \tag{3.81b}$$

Note that for $\boldsymbol{\Omega} \in \mathfrak{so}(3) \subset \mathbb{R}^{3\times3}$ we have $\text{vee2}(\boldsymbol{\Omega}) = 2\,\text{vee}(\boldsymbol{\Omega})$, thus giving the motivation for the name. Define the Vee operator through

$$\operatorname{tr}\left(\text{wed}\,\boldsymbol{\xi}\,\boldsymbol{A}(\text{wed}\,\boldsymbol{\eta})^\top\right) = \boldsymbol{\eta}^\top(\text{Vee}\,\boldsymbol{A})\boldsymbol{\xi}, \tag{3.82}$$

this is

$$\text{Vee} : \mathbb{R}^{3\times3} \to \mathbb{R}^{3\times3} \; : \boldsymbol{A} \mapsto \operatorname{tr}(\boldsymbol{A})\mathbf{I}_3 - \boldsymbol{A} \tag{3.83a}$$

$$\text{Vee} : \mathbb{R}^{4\times4} \to \mathbb{R}^{6\times6} \; : \begin{bmatrix} \boldsymbol{A} & \boldsymbol{b} \\ \boldsymbol{c}^\top & d \end{bmatrix} \mapsto \begin{bmatrix} d\mathbf{I}_3 & (\text{wed}\,\boldsymbol{b})^\top \\ \text{wed}\,\boldsymbol{c} & \text{Vee}\,\boldsymbol{A} \end{bmatrix}. \tag{3.83b}$$

Let $\text{Wed}(\cdot)$ denote its inverse. Combining the definitions (3.82) and (3.80) also yields

$$\text{vee2}\left(\text{wed}\,\boldsymbol{\xi}\,\boldsymbol{A}\right) = \text{Vee}(\boldsymbol{A})\boldsymbol{\xi} \tag{3.84}$$

Adjoint representation. Define

$$\mathbf{G} = \begin{bmatrix} \boldsymbol{R} & \boldsymbol{r} \\ \mathbf{0} & 1 \end{bmatrix} : \qquad \mathrm{Ad}_{\mathbf{G}} = \begin{bmatrix} \boldsymbol{R} & \mathrm{wed}(\boldsymbol{r})\boldsymbol{R} \\ \mathbf{0} & \boldsymbol{R} \end{bmatrix} \tag{3.85a}$$

$$\boldsymbol{\xi} = \begin{bmatrix} \boldsymbol{v} \\ \boldsymbol{\omega} \end{bmatrix} : \qquad \mathrm{ad}_{\boldsymbol{\xi}} = \begin{bmatrix} \mathrm{wed}(\boldsymbol{\omega}) & \mathrm{wed}(\boldsymbol{v}) \\ \mathbf{0} & \mathrm{wed}(\boldsymbol{\omega}) \end{bmatrix} \tag{3.85b}$$

The notation is due to the established notation for the *adjoint representation* for Lie groups and their associated Lie algebras, see e.g. [Hall, 2015, Def. 3.32 & 3.7]. Using this background we have the obvious relations:

$$\mathrm{Ad}_{\mathbf{G}_1\mathbf{G}_2} = \mathrm{Ad}_{\mathbf{G}_1}\mathrm{Ad}_{\mathbf{G}_1}, \qquad \mathrm{Ad}_{\mathbf{G}}^{-1} = \mathrm{Ad}_{\mathbf{G}^{-1}}, \qquad \mathrm{Ad}_{\mathbf{I}_4} = \mathbf{I}_6, \tag{3.86a}$$

$$\mathrm{ad}_{\boldsymbol{\xi}_1}\boldsymbol{\xi}_2 = -\mathrm{ad}_{\boldsymbol{\xi}_2}\boldsymbol{\xi}_1, \qquad \mathrm{ad}_{\boldsymbol{\xi}}\boldsymbol{\xi} = \mathbf{0}. \tag{3.86b}$$

Furthermore, for $\frac{\mathrm{d}}{\mathrm{d}t}\mathbf{G} = \mathbf{G}\,\mathrm{wed}(\boldsymbol{\xi})$ we have

$$\tfrac{\mathrm{d}}{\mathrm{d}t}\mathrm{Ad}_{\mathbf{G}} = \mathrm{Ad}_{\mathbf{G}}\mathrm{ad}_{\boldsymbol{\xi}}. \tag{3.87}$$

Though the Lie group theory can be extremely useful for rigid body mechanics, for this work it is sufficient to regard $\mathrm{Ad}_{(\cdot)}$ and $\mathrm{ad}_{(\cdot)}$ as simple algebraic operators with the identities (3.86).

Rigid body energies. Notice that for $\mathbf{x}, \mathfrak{h}_p \in \mathbb{R}^n$, $\mathbf{X} \in \mathbb{R}^{n\times n}$ we have

$$\begin{aligned}
\sum\nolimits_p \mathfrak{m}_p \|\mathbf{x} + \mathbf{X}\mathfrak{h}_p\|^2 &= \sum\nolimits_p \mathfrak{m}_p \operatorname{tr}\left((\mathbf{x} + \mathbf{X}\mathfrak{h}_p)(\mathbf{x} + \mathbf{X}\mathfrak{h}_p)^\top\right) \\
&= \sum\nolimits_p \mathfrak{m}_p \operatorname{tr}\left(\left(\begin{bmatrix} \mathbf{X} & \mathbf{x} \\ \mathbf{0} & 0 \end{bmatrix}\begin{bmatrix} \mathfrak{h}_p \\ 1 \end{bmatrix}\right)\left(\begin{bmatrix} \mathbf{X} & \mathbf{x} \\ \mathbf{0} & 0 \end{bmatrix}\begin{bmatrix} \mathfrak{h}_p \\ 1 \end{bmatrix}\right)^\top\right) \\
&= \operatorname{tr}\left(\underbrace{\begin{bmatrix} \mathbf{X} & \mathbf{x} \\ \mathbf{0} & 0 \end{bmatrix}}_{\boldsymbol{\Xi}}\underbrace{\left(\sum\nolimits_p \mathfrak{m}_p \begin{bmatrix} \mathfrak{h}_p\mathfrak{h}_p^\top & \mathfrak{h}_p^\top \\ \mathfrak{h}_p & 1 \end{bmatrix}\right)}_{\mathbf{M}'}\underbrace{\begin{bmatrix} \mathbf{X}^\top & \mathbf{0} \\ \mathbf{x}^\top & 0 \end{bmatrix}}_{\boldsymbol{\Xi}^\top}\right) \\
&= \|\boldsymbol{\Xi}^\top\|_{\mathbf{M}'}^2
\end{aligned} \tag{3.88}$$

with the weighted Frobenius norm motivated in (2.48). Furthermore, for the special case $\boldsymbol{\Xi} = \mathrm{wed}\,\boldsymbol{\xi}$ we have due to (3.82):

$$\|\mathrm{wed}(\boldsymbol{\xi})^\top\|_{\mathbf{M}'}^2 = \|\boldsymbol{\xi}\|_{\mathrm{Vee}\,\mathbf{M}'}^2, \tag{3.89}$$

Using this, we may rewrite the kinetic energy $\mathcal{T}$ of a free rigid body (3.51), the acceleration energy $\mathcal{S}$ from (3.53), the dissipation function $\mathcal{R}$ in (3.75), the potential energy $\mathcal{V}$ due to linear springs (3.70) and the potential energy $\mathcal{V}^{\mathrm{G}}$ due to earth's gravitation from (3.59) as

$$\mathcal{T} = \tfrac{1}{2}\sum\nolimits_p \mathfrak{m}_p \| \overbrace{\dot{\boldsymbol{r}} + \dot{\boldsymbol{R}}\mathfrak{h}_p}^{\dot{\mathfrak{r}}_p} \|^2 = \tfrac{1}{2}\|\dot{\mathbf{G}}^\top\|^2_{\mathbf{M}'} = \tfrac{1}{2}\|\boldsymbol{\xi}\|^2_{\mathbf{M}} \tag{3.90a}$$

$$\mathcal{T}^{\mathrm{G}} = \tfrac{1}{2}\sum\nolimits_p \mathfrak{m}_p \| \overbrace{\dot{\boldsymbol{r}} + \dot{\boldsymbol{R}}\mathfrak{h}_p}^{\dot{\mathfrak{r}}_p} - \boldsymbol{a}_{\mathsf{G}} t\|^2 = \tfrac{1}{2}\|(\dot{\mathbf{G}} - \mathrm{wed}(\boldsymbol{\alpha}_{\mathsf{G}} t))^\top\|^2_{\mathbf{M}'} \qquad \boldsymbol{\alpha}_{\mathsf{G}} = \begin{bmatrix} \boldsymbol{a}_{\mathsf{G}} \\ \mathbf{0}_{3\times 1} \end{bmatrix} \tag{3.90b}$$

$$\mathcal{S} = \tfrac{1}{2}\sum\nolimits_p \mathfrak{m}_p \| \overbrace{\ddot{\boldsymbol{r}} + \ddot{\boldsymbol{R}}\mathfrak{h}_p}^{\ddot{\mathfrak{r}}_p} \|^2 = \tfrac{1}{2}\|\ddot{\mathbf{G}}^\top\|^2_{\mathbf{M}'} \tag{3.90c}$$

$$\mathcal{S}^{\mathrm{G}} = \tfrac{1}{2}\sum\nolimits_p \mathfrak{m}_p \| \overbrace{\ddot{\boldsymbol{r}} + \ddot{\boldsymbol{R}}\mathfrak{h}_p}^{\ddot{\mathfrak{r}}_p} - \boldsymbol{a}_{\mathsf{G}}\|^2 = \tfrac{1}{2}\|(\ddot{\mathbf{G}} - \mathrm{wed}(\boldsymbol{\alpha}_{\mathsf{G}}))^\top\|^2_{\mathbf{M}'} \tag{3.90d}$$

$$\mathcal{R} = \tfrac{1}{2}\sum\nolimits_p \mathfrak{d}_p \| \overbrace{\dot{\boldsymbol{r}} + \dot{\boldsymbol{R}}\mathfrak{h}_p}^{\dot{\mathfrak{r}}_p} \|^2 = \tfrac{1}{2}\|\dot{\mathbf{G}}^\top\|^2_{\mathbf{D}'} = \tfrac{1}{2}\|\boldsymbol{\xi}\|^2_{\mathbf{D}} \tag{3.90e}$$

$$\mathcal{V}^{\mathrm{K}} = \tfrac{1}{2}\sum\nolimits_p \mathfrak{k}_p \| \overbrace{\boldsymbol{r} + \boldsymbol{R}\mathfrak{h}_p}^{\mathfrak{r}_p} - \overbrace{(\boldsymbol{r}_{\mathsf{R}} + \boldsymbol{R}_{\mathsf{R}}\mathfrak{h}_p)}^{\mathfrak{r}_{p\mathsf{R}}} \|^2 = \tfrac{1}{2}\|(\mathbf{G} - \mathbf{G}_{\mathsf{R}})^\top\|^2_{\mathbf{K}'} \tag{3.90f}$$

$$\mathcal{V}^{\mathrm{G}} = \sum\nolimits_p \langle \overbrace{\boldsymbol{r} + \boldsymbol{R}\mathfrak{h}_p}^{\mathfrak{r}_p}, -\mathfrak{m}_p \boldsymbol{a}_{\mathsf{G}} \rangle = \langle \mathbf{G}^\top, \mathrm{wed}(-\boldsymbol{\alpha}_{\mathsf{G}})^\top \rangle_{\mathbf{M}'}, \tag{3.90g}$$

where

$$\mathbf{M}' = \sum\nolimits_p \mathfrak{m}_p \begin{bmatrix} \mathfrak{h}_p\mathfrak{h}_p^\top & \mathfrak{h}_p^\top \\ \mathfrak{h}_p & 1 \end{bmatrix} = \begin{bmatrix} \boldsymbol{\Theta}' & m\boldsymbol{s} \\ m\boldsymbol{s}^\top & m \end{bmatrix} = \mathrm{Wed}(\mathbf{M}) \tag{3.91a}$$

$$\mathbf{D}' = \sum\nolimits_p \mathfrak{d}_p \begin{bmatrix} \mathfrak{h}_p\mathfrak{h}_p^\top & \mathfrak{h}_p^\top \\ \mathfrak{h}_p & 1 \end{bmatrix} = \begin{bmatrix} \boldsymbol{\Upsilon}' & d\boldsymbol{l} \\ d\boldsymbol{l}^\top & d \end{bmatrix} = \mathrm{Wed}(\mathbf{D}) \tag{3.91b}$$

$$\mathbf{K}' = \sum\nolimits_p \mathfrak{k}_p \begin{bmatrix} \mathfrak{h}_p\mathfrak{h}_p^\top & \mathfrak{h}_p^\top \\ \mathfrak{h}_p & 1 \end{bmatrix} = \begin{bmatrix} \boldsymbol{\Pi}' & k\boldsymbol{h} \\ k\boldsymbol{h}^\top & k \end{bmatrix} = \mathrm{Wed}(\mathbf{K}) \tag{3.91c}$$

Note that m, $m\boldsymbol{s}$ and $\boldsymbol{\Theta}'$ correspond to the zeroth, first and second *mathematical moments* of the distribution $\mathfrak{m}_p\mathfrak{h}_p, p = 1,\ldots,\mathfrak{N}$. Their collection in the matrix $\mathbf{M}' \in \mathbb{SYM}(4)$ is bijective to the previously encountered inertia matrix $\mathbf{M}' = \mathrm{Wed}(\mathbf{M}) \Leftrightarrow \mathbf{M} = \mathrm{Vee}(\mathbf{M}')$. Obviously, the same holds for the damping $\mathbf{K}'$ and stiffness matrix $\mathbf{D}'$.

Rigid body forces. The corresponding forces forces which were already derived in the previous subsections can be written in a more compact form:

$$\boldsymbol{f}^{\mathrm{M}} = \frac{\partial \mathcal{S}}{\partial \dot{\boldsymbol{\xi}}} = \mathrm{vee2}\left((\mathrm{wed}(\dot{\boldsymbol{\xi}}) + \mathrm{wed}(\boldsymbol{\xi})^2)\mathbf{M}'\right) = \mathbf{M}\dot{\boldsymbol{\xi}} - \mathrm{ad}^\top_{\boldsymbol{\xi}}\mathbf{M}\boldsymbol{\xi} \tag{3.92a}$$

$$\boldsymbol{f}^{\mathrm{D}} = \frac{\partial \mathcal{R}}{\partial \boldsymbol{\xi}} = \mathrm{vee2}\left(\mathrm{wed}(\boldsymbol{\xi})\mathbf{D}'\right) = \mathbf{D}\boldsymbol{\xi} \tag{3.92b}$$

$$\boldsymbol{f}^{\mathrm{K}} = \boldsymbol{\nabla}\mathcal{V}^{\mathrm{K}} = \mathrm{vee2}\left((\mathbf{I}_4 - \mathbf{G}^{-1}\mathbf{G}_{\mathsf{R}})\mathbf{K}'\right) \tag{3.92c}$$

$$\boldsymbol{f}^{\mathrm{G}} = \boldsymbol{\nabla}\mathcal{V}^{\mathrm{G}} = \mathrm{vee2}\left(\mathbf{G}^\top\mathrm{wed}(-\boldsymbol{\alpha}_{\mathsf{G}})\mathbf{M}'\right) = -\mathbf{M}\mathrm{Ad}^{-1}_{\mathbf{G}}\boldsymbol{\alpha}_{\mathsf{G}}. \tag{3.92d}$$

Equation of motion. Combining the results above, the equations of motion of a free rigid body subject to inertia, gravity, viscous friction, linear springs and a generalized force $\boldsymbol{f}^{\mathrm{E}}$ may be written as

$$\dot{\mathbf{G}} = \mathbf{G}\,\mathrm{wed}(\boldsymbol{\xi}), \tag{3.93a}$$
$$\dot{\boldsymbol{\xi}} = \mathrm{Ad}_{\mathbf{G}}^{-1}\boldsymbol{\alpha}_{\mathsf{G}} + \mathbf{M}^{-1}\big(\boldsymbol{f}^{\mathrm{E}} + (\mathrm{ad}_{\boldsymbol{\xi}}^{\top}\mathbf{M} - \mathbf{D})\boldsymbol{\xi} - \mathrm{vee2}\left((\mathbf{I}_4 - \mathbf{G}^{-1}\mathbf{G}_{\mathsf{R}})\mathbf{K}'\right)\big). \tag{3.93b}$$

Thee are three sets of ingredients:

- The chosen coordinates are collected within $\mathbf{G}(t) \in \mathbb{SE}(3)$ and $\boldsymbol{\xi}(t) \in \mathbb{R}^6$.
- The matrices $\mathbf{M}', \mathbf{D}', \mathbf{K}' \in \mathbb{SYM}(4)$ capture the distribution of mass, damping and stiffness.
- External influences are collected within the gravity wrench $\boldsymbol{\alpha}_{\mathsf{G}}^{\top} = [\boldsymbol{a}_{\mathsf{G}}^{\top}, \mathbf{0}_{1\times 3}]$, the equilibrium configuration of the springs $\mathbf{G}_{\mathsf{R}}(t) \in \mathbb{SE}(3)$ and the generalized external force $\boldsymbol{f}^{\mathrm{E}}(t) \in \mathbb{R}^6$.

3.4 Rigid body systems

A rigid body system is a system of $N \geq 1$ rigid bodies which may be constrained to each other and/or to the surrounding space. As before, this section restricts to geometric constraints.

There are many established textbooks on this subject e.g. [Roberson and Schwertassek, 1988], [Murray et al., 1994], [Kane and Levinson, 1985]. However, all these excellent texts restrict to *minimal* generalized coordinates or are even more restrictive by requiring Denavit-Hartenberg parameters [Denavit and Hartenberg, 1955]. While this is just fine when dealing only with one-dimensional joints, it may be too restrictive when dealing with multidimensional joints as e.g. mobile robots. Furthermore, the texts mentioned above mostly focus on inertia but not dissipation and stiffness.

This section deals with the derivation of equations of motion for rigid body systems subject to inertia, gravity, linear springs and viscous friction. It allows for a quite general parameterization as motivated in the previous sections.

3.4.1 Parameterization

Configuration coordinates. As motivated for the single rigid body, let there be a body fixed frame for each body of the system as illustrated in Figure 3.4. The components of the position of the b-th body w.r.t. the inertial frame are ${}^0_b\boldsymbol{r} \in \mathbb{R}^3$ and the components of its attitude are ${}^0_b\boldsymbol{R} = [{}^0_b\boldsymbol{R}_{\mathsf{x}}, {}^0_b\boldsymbol{R}_{\mathsf{y}}, {}^0_b\boldsymbol{R}_{\mathsf{z}}] \in \mathbb{SO}(3)$.

The configuration can also be expressed w.r.t. any other body: ${}^a_b\boldsymbol{r}$ is the position of the b-th frame w.r.t. the frame of the a-th body and analog of the attitude ${}^a_b\boldsymbol{R}$. The left side indices are used for readability but also to emphasize their different nature compared

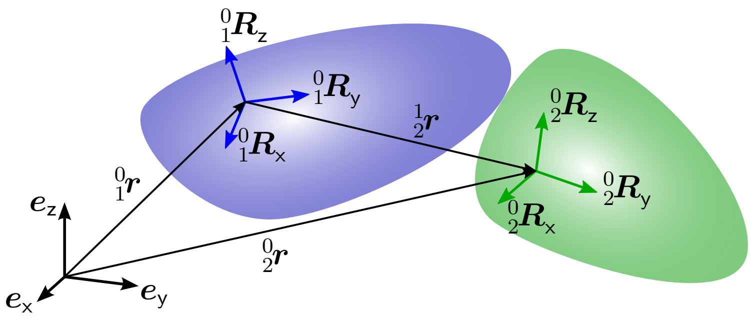

Figure 3.4: reference frame and body fixed frames

to the right side indices. The sum convention does not apply to these indices. For the positions and attitudes we have the following relations

$$
\begin{aligned}
{}^{a}_{c}\boldsymbol{r} &= {}^{a}_{b}\boldsymbol{r} + {}^{a}_{b}\boldsymbol{R}\,{}^{b}_{c}\boldsymbol{r}, & {}^{a}_{c}\boldsymbol{R} &= {}^{a}_{b}\boldsymbol{R}\,{}^{b}_{c}\boldsymbol{R}, & & \quad (3.94a)\\
{}^{b}_{a}\boldsymbol{r} &= -{}^{a}_{b}\boldsymbol{R}^\top\,{}^{a}_{b}\boldsymbol{r}, & {}^{b}_{a}\boldsymbol{R} &= {}^{a}_{b}\boldsymbol{R}^\top, & & \quad (3.94b)\\
{}^{a}_{a}\boldsymbol{r} &= \mathbf{0}, & {}^{a}_{a}\boldsymbol{R} &= \mathbf{I}_3, & a, b, c &= 0, \dots, N. \quad (3.94c)
\end{aligned}
$$

As motivated in the previous section, it will be convenient to merge position ${}^{0}_{b}\boldsymbol{r} \in \mathbb{R}^3$ and rotation matrix ${}^{0}_{b}\boldsymbol{R} \in \mathbb{SO}(3)$ into the (rigid body) configuration matrix

$$
{}^{a}_{b}\mathsf{G} = \begin{bmatrix} {}^{a}_{b}\boldsymbol{R} & {}^{a}_{b}\boldsymbol{r} \\ 0 & 1 \end{bmatrix} \in \mathbb{SE}(3). \tag{3.95}
$$

Then (3.94) is equivalent to

$$
\begin{aligned}
{}^{a}_{c}\mathsf{G} &= {}^{a}_{b}\mathsf{G}\,{}^{b}_{c}\mathsf{G}, & & \quad (3.96a)\\
{}^{b}_{a}\mathsf{G} &= {}^{a}_{b}\mathsf{G}^{-1}, & & \quad (3.96b)\\
{}^{a}_{a}\mathsf{G} &= \mathbf{I}_4, & a, b, c &= 0, \dots, N. \quad (3.96c)
\end{aligned}
$$

For a system of N body fixed frames and a reference frame there are $(N+1)^2$ transformations, but due to the rules (3.96), only N of them can be independent. So, a RBS can have at most $6N$ degrees of freedom, which is only the case if there are no constraints (like joints) between the bodies. Constraints of a joint between body a and b can be captured inside the corresponding transformation ${}^{a}_{b}\mathsf{G}$. We will discuss this in the following example.

Example 6. Tricopter with suspended load: configuration. Consider the Tricopter with a suspended load as shown in Figure 3.5. The top part of the figure shows the body fixed frames which are attached to geometrically meaningful points. The numbering of the bodies is rather arbitrary.

The Tricopter flies freely in space, i.e. there are no constraints between the reference frame and any body of the system. So we chose to describe the configuration of the central body w.r.t. the reference frame as

$$
{}^{0}_{1}\mathsf{G} = \begin{bmatrix} {}^{0}_{1}R^\mathsf{x}_\mathsf{x} & {}^{0}_{1}R^\mathsf{x}_\mathsf{y} & {}^{0}_{1}R^\mathsf{x}_\mathsf{z} & {}^{0}_{1}r^\mathsf{x} \\ {}^{0}_{1}R^\mathsf{y}_\mathsf{x} & {}^{0}_{1}R^\mathsf{y}_\mathsf{y} & {}^{0}_{1}R^\mathsf{y}_\mathsf{z} & {}^{0}_{1}r^\mathsf{y} \\ {}^{0}_{1}R^\mathsf{z}_\mathsf{x} & {}^{0}_{1}R^\mathsf{z}_\mathsf{y} & {}^{0}_{1}R^\mathsf{z}_\mathsf{z} & {}^{0}_{1}r^\mathsf{z} \\ 0 & 0 & 0 & 1 \end{bmatrix}. \tag{3.97a}
$$

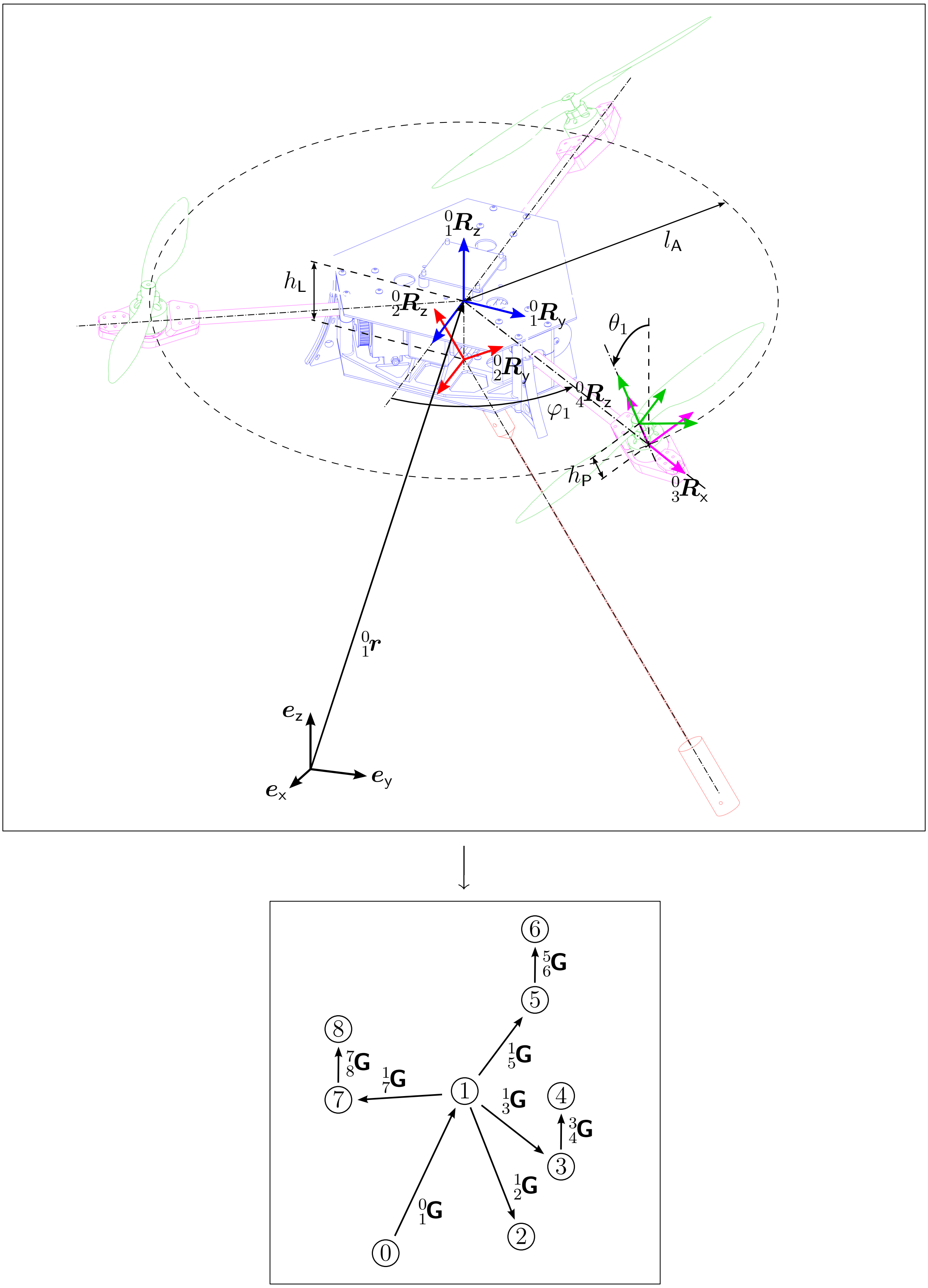

Figure 3.5: Frames attached to the Tricopter bodies (top) and the configuration graph (bottom)

The suspended load is a rigid body that is attached by a spherical joint to the central body. The body fixed frame of the load is placed in the center of this spherical joint. As a consequence, the position of the load (the position of its body fixed frame not the position of its center of mass) w.r.t. the central body is constant. This is reflected by the configuration

$$ {}^{1}_{2}\mathsf{G} = \begin{bmatrix} {}^{1}_{2}R^{\mathsf{x}}_{\mathsf{x}} & {}^{1}_{2}R^{\mathsf{x}}_{\mathsf{y}} & {}^{1}_{2}R^{\mathsf{x}}_{\mathsf{z}} & 0 \\ {}^{1}_{2}R^{\mathsf{y}}_{\mathsf{x}} & {}^{1}_{2}R^{\mathsf{y}}_{\mathsf{y}} & {}^{1}_{2}R^{\mathsf{y}}_{\mathsf{z}} & 0 \\ {}^{1}_{2}R^{\mathsf{z}}_{\mathsf{x}} & {}^{1}_{2}R^{\mathsf{z}}_{\mathsf{z}} & {}^{1}_{2}R^{\mathsf{z}}_{\mathsf{z}} & h_{\mathsf{L}} \\ 0 & 0 & 0 & 1 \end{bmatrix}. \tag{3.97b} $$

The three arms are connected to the central body each by revolute joints with tilt angles θ_k, $k = 1, 2, 3$. The joint axis lie in the plane spanned by ${}^{0}_{1}\boldsymbol{R}_{\mathsf{x}}$ and ${}^{0}_{1}\boldsymbol{R}_{\mathsf{y}}$ and their angles to ${}^{0}_{1}\boldsymbol{R}_{\mathsf{x}}$ are $\varphi_1 = \frac{\pi}{3}, \varphi_2 = \pi, \varphi_3 = -\frac{\pi}{3}$. The body fixed axes are placed such that ${}_{2k+1}^{0}\boldsymbol{R}_{\mathsf{x}}$ coincide with the tilt axis and ${}_{2k+1}^{0}\boldsymbol{R}_{\mathsf{z}}$, $k = 1, 2, 3$ coincide with the propeller spinning axis. The configuration of the k-th arm w.r.t. the central body is

$$ {}_{2k+1}^{1}\mathsf{G} = \begin{bmatrix} \cos\varphi_k & -\sin\varphi_k\cos\theta_k & \sin\varphi_k\sin\theta_k & l_{\mathsf{A}}\cos\varphi_k \\ \sin\varphi_k & \cos\varphi_k\cos\theta_k & -\cos\varphi_k\sin\theta_k & l_{\mathsf{A}}\sin\varphi_k \\ 0 & \sin\theta_k & \cos\theta_k & 0 \\ 0 & 0 & 0 & 1 \end{bmatrix}, \quad k = 1, \ldots, 3. \tag{3.97c} $$

The propellers are connected by revolute joints to the arms. The body fixed frame is attached to the geometric center of the propeller (which will be an important point for its aerodynamic model). The configuration w.r.t. the corresponding arm is

$$ {}_{2k+2}^{2k+1}\mathsf{G} = \begin{bmatrix} \mathrm{c}_k & -\mathrm{s}_k & 0 & 0 \\ \mathrm{s}_k & \mathrm{c}_k & 0 & 0 \\ 0 & 0 & 1 & h_{\mathsf{P}} \\ 0 & 0 & 0 & 1 \end{bmatrix}, \qquad k = 1, \ldots, 3. \tag{3.97d} $$

The set of configurations $\mathcal{G}_0 = \{{}^{0}_{1}\mathsf{G}, {}^{1}_{2}\mathsf{G}, {}^{1}_{3}\mathsf{G}, {}^{3}_{4}\mathsf{G}, {}^{1}_{5}\mathsf{G}, {}^{5}_{6}\mathsf{G}, {}^{1}_{7}\mathsf{G}, {}^{7}_{8}\mathsf{G}\}$ form a directed graph as shown at the bottom of Figure 3.5. With them and the rules from (3.96) we can compute the configuration ${}^{a}_{b}\mathsf{G}$ of any body w.r.t. any other body or the reference frame.

The configurations can be seen as functions ${}^{a}_{b}\mathsf{G}(\boldsymbol{x})$ of the system coordinates

$$ \boldsymbol{x} = \left[{}^{0}_{1}r^{\mathsf{x}}, {}^{0}_{1}r^{\mathsf{y}}, {}^{0}_{1}r^{\mathsf{z}}, {}^{0}_{1}R^{\mathsf{x}}_{\mathsf{x}}, \ldots, {}^{0}_{1}R^{\mathsf{z}}_{\mathsf{z}}, {}^{1}_{2}R^{\mathsf{x}}_{\mathsf{x}}, \ldots, {}^{1}_{2}R^{\mathsf{z}}_{\mathsf{z}}, \theta_1, \theta_2, \theta_3, \mathrm{c}_1, \mathrm{s}_1, \mathrm{c}_2, \mathrm{s}_2, \mathrm{c}_3, \mathrm{s}_3\right]^{\top} \in \mathbb{R}^{30} \tag{3.98} $$

and the constant parameters $h_{\mathsf{L}}, l_{\mathsf{A}}, \varphi_1, \varphi_2, \varphi_3, h_{\mathsf{P}}$. From the rules (3.96) emerge the geometric constraints

$$ \boldsymbol{\phi}(\boldsymbol{x}) = \mathbf{0} \qquad \cong \qquad \begin{cases} {}^{0}_{1}\boldsymbol{R}^{\top}\,{}^{0}_{1}\boldsymbol{R} = \mathbf{I}_3,\ \det {}^{0}_{1}\boldsymbol{R} = +1, \\ {}^{1}_{2}\boldsymbol{R}^{\top}\,{}^{1}_{2}\boldsymbol{R} = \mathbf{I}_3,\ \det {}^{1}_{2}\boldsymbol{R} = +1, \\ (\mathrm{c}_k)^2 + (\mathrm{s}_k)^2 = 1,\ k = 1, 2, 3 \end{cases} \tag{3.99} $$

The configuration space of the rigid body system is

$$ \mathbb{X} = \{\boldsymbol{x} \in \mathbb{R}^{30} \,|\, \boldsymbol{\phi}(\boldsymbol{x}) = 0\} \ \cong\ \mathbb{SE}(3) \times \mathbb{SO}(3) \times \mathbb{R}^3 \times (\mathbb{S}^1)^3. \tag{3.100} $$

This example was mainly chosen as the Tricopter will be discussed in the following chapters. However, it is also an example of a system that is complex enough that one probably does not want to derive the equations of motion without a formalism. It also covers the most common manifolds encountered in rigid body mechanics. Even though the revolute joints for the propeller tilt and the propeller spinning axes both imply a $\mathbb{S}^1$ manifold, the local parameterization by the angle $\theta_k, k = 1, 2, 3$ is chosen. This has a practical motivation: The tilt mechanism also twists the cables to the propeller motor and so $\theta_k = 0$ and $\theta_k = 2\pi$ are really different situations in practice. On the other hand it should also show that the following algorithm handles minimal coordinates just as fine.

A generalization of the example states: A rigid body system can be parameterized by a set of ν (possibly redundant) coordinates $\boldsymbol{x}$ which again parameterize a set of configurations ${}^a_b\mathbf{G}(\boldsymbol{x})$ which form a *connected* graph. The property connected is essential: it ensures that, with the rules (3.96), all remaining configurations of the graph can be computed i.e. the corresponding *complete* graph. Loops in the graph and the property ${}^a_b\mathbf{G} \in \mathbb{SE}(3)$ may imply geometric constraints.

The use of graph theory in the context of algorithms for rigid body systems is quite common, see e.g. [Roberson and Schwertassek, 1988, sec. 8.2] or [Wittenburg, 2008, sec. 5.3]. However, we will not go any deeper into this. All we need for the following is that any configuration ${}^a_b\mathbf{G}(\boldsymbol{x}), a, b = 0 \dots N$ can be expressed in terms of the configuration coordinates $\boldsymbol{x}$.

Body velocity. The previous section motivated particular velocity coordinates $\boldsymbol{\xi} = [\boldsymbol{v}^\top, \boldsymbol{\omega}^\top]^\top$ for the free rigid body, which did lead to a convenient mathematical expressions. In the context of rigid body systems we may associate a *body velocity* ${}^a_b\boldsymbol{\xi} = [{}^a_b\boldsymbol{v}^\top, {}^a_b\boldsymbol{\omega}^\top]^\top$ with any configuration ${}^a_b\mathbf{G}, a, b = 0, \dots, N$ defined by

$$ {}^a_b\boldsymbol{\xi} = \operatorname{vee}\left({}^b_a\mathbf{G}\,{}^a_b\dot{\mathbf{G}}\right), \quad a, b = 0, \dots, N. \tag{3.101} $$

From the rules (3.96) for the configurations we can conclude similar rules for their velocities: For the composition ${}^a_c\mathbf{G} = {}^a_b\mathbf{G}\,{}^b_c\mathbf{G}$ we get

$$ {}^a_c\boldsymbol{\xi} = \operatorname{vee}\left({}^c_b\mathbf{G}\,{}^b_a\mathbf{G}({}^a_b\dot{\mathbf{G}}\,{}^b_c\mathbf{G} + {}^a_b\mathbf{G}\,{}^b_c\dot{\mathbf{G}})\right) = \operatorname{vee}\left({}^c_b\mathbf{G}\operatorname{wed}({}^a_b\boldsymbol{\xi})\,{}^b_c\mathbf{G}\right) + {}^b_c\boldsymbol{\xi} = \operatorname{Ad}_{{}^c_b\mathbf{G}}\,{}^a_b\boldsymbol{\xi} + {}^b_c\boldsymbol{\xi} \tag{3.102a} $$

with the adjoint representation introduced in (3.85a). Differentiation of ${}^a_b\mathbf{G}\,{}^b_a\mathbf{G} = \mathbf{I}$ yields

$$ \tfrac{\mathrm{d}}{\mathrm{d}t}\left({}^a_b\mathbf{G}\,{}^b_a\mathbf{G}\right) = {}^a_b\dot{\mathbf{G}}\,{}^b_a\mathbf{G} + {}^a_b\mathbf{G}\,{}^b_a\dot{\mathbf{G}} = {}^a_b\mathbf{G}\operatorname{wed}({}^a_b\boldsymbol{\xi})\,{}^b_a\mathbf{G} + \operatorname{wed}({}^b_a\boldsymbol{\xi}) = \mathbf{0} \quad \Leftrightarrow \quad {}^b_a\boldsymbol{\xi} = -\operatorname{Ad}_{{}^a_b\mathbf{G}}\,{}^a_b\boldsymbol{\xi} \tag{3.102b} $$

and obviously

$$ {}^a_a\boldsymbol{\xi} = \mathbf{0}. \tag{3.102c} $$

System velocity and body Jacobians. Based on their definition (3.101), the body velocities ${}^a_b\boldsymbol{\xi}$ can be seen as a function of the system coordinates $\boldsymbol{x}$ and their derivatives

$\dot{\boldsymbol{x}} = \boldsymbol{A}(\boldsymbol{x})\boldsymbol{\xi}$. Crucially the velocity is linear in $\dot{\boldsymbol{x}}$ and consequently linear in the system velocity $\boldsymbol{\xi}$ and we can write

$$ {}^{a}_{b}\boldsymbol{\xi}(\boldsymbol{x},\boldsymbol{\xi}) = {}^{a}_{b}\boldsymbol{J}(\boldsymbol{x})\boldsymbol{\xi}, \qquad {}^{a}_{b}\boldsymbol{J}(\boldsymbol{x}) = \frac{\partial\, {}^{a}_{b}\boldsymbol{\xi}}{\partial \boldsymbol{\xi}}(\boldsymbol{x}) = \frac{\partial}{\partial \dot{\boldsymbol{x}}}\operatorname{vee}\left({}^{b}_{a}\mathbf{G}(\boldsymbol{x})\frac{\mathrm{d}}{\mathrm{d}t}\big({}^{a}_{b}\mathbf{G}(\boldsymbol{x})\big)\right)\boldsymbol{A}. \tag{3.103}$$

The matrix ${}^{a}_{b}\boldsymbol{J}(\boldsymbol{x}) \in \mathbb{R}^{6\times n}$ that maps the system velocity $\boldsymbol{\xi}$ to the body velocity ${}^{a}_{b}\boldsymbol{\xi}$ is commonly called the *body Jacobian*. An alternative formula for the body Jacobian, which might give additional geometric insight, is given in [eq:AppendixDefBodyJac]. The following rules emerge directly from (3.102):

$$ {}^{a}_{c}\boldsymbol{J} = \mathrm{Ad}_{{}^{c}_{b}\mathbf{G}}\,{}^{a}_{b}\boldsymbol{J} + {}^{b}_{c}\boldsymbol{J}, \qquad {}^{b}_{a}\boldsymbol{J} = -\mathrm{Ad}_{{}^{a}_{b}\mathbf{G}}\,{}^{a}_{b}\boldsymbol{J}, \qquad {}^{a}_{a}\boldsymbol{J} = \mathbf{0}. \tag{3.104}$$

Example 7. Tricopter with suspended load: kinematics. For the tricopter with load from Example 6 we chose the following velocity coordinates: The components of the body velocity ${}^{0}_{1}\boldsymbol{\xi}$ of the central body w.r.t. the inertial frame, the components of the angular velocity ${}^{0}_{2}\boldsymbol{\omega}$ of the load w.r.t. the inertial frame, the angular velocities $\dot{\theta}_k, k = 1,2,3$ of the arm tilt mechanism and the angular velocities $\varpi_k, k = 1,2,3$ of the propellers w.r.t. the arms. These velocity coordinates $\boldsymbol{\xi} = [{}^{0}_{1}\boldsymbol{\xi}^\top, {}^{0}_{2}\boldsymbol{\omega}^\top, \dot{\theta}_1, \dot{\theta}_2, \dot{\theta}_3, \varpi_1, \varpi_2, \varpi_3]^\top$ are related to the configuration coordinates $\boldsymbol{\xi}$ by the kinematic equation

$$\dot{\boldsymbol{x}} = \boldsymbol{A}\boldsymbol{\xi} \qquad \cong \qquad \begin{cases} {}^{0}_{1}\dot{\mathbf{G}} = {}^{0}_{1}\mathbf{G}\operatorname{wed}({}^{0}_{1}\boldsymbol{\xi}), \\ {}^{1}_{2}\dot{\boldsymbol{R}} = {}^{1}_{2}\boldsymbol{R}\operatorname{wed}({}^{0}_{2}\boldsymbol{\omega}) - \operatorname{wed}({}^{0}_{1}\boldsymbol{\omega}){}^{1}_{2}\boldsymbol{R}, \\ \dot{\theta}_k = \dot{\theta}_k, \;\; k = 1,2,3 \\ \dot{\mathrm{c}}_k = -\mathrm{s}_k\varpi_k, \;\; k = 1,2,3 \\ \dot{\mathrm{s}}_k = \mathrm{c}_k\varpi_k, \;\; k = 1,2,3 \end{cases}. \tag{3.105}$$

The relative velocity ${}^{1}_{2}\boldsymbol{\omega} = \operatorname{vee}({}^{1}_{2}\boldsymbol{R}^\top\,{}^{1}_{2}\dot{\boldsymbol{R}})$ of the load would be another possible and probably more obvious choice. The absolute velocity ${}^{0}_{2}\boldsymbol{\omega}$ is mainly chosen to demonstrate the flexibility of the presented approach but the use of absolute velocities also leads to less cumbersome terms in the system inertia matrix.

The body velocities associated with the configuration matrices from (3.97) are

$$ {}^{0}_{1}\boldsymbol{\xi} = \begin{bmatrix} {}^{0}_{1}v^{\mathsf{x}} \\ {}^{0}_{1}v^{\mathsf{y}} \\ {}^{0}_{1}v^{\mathsf{z}} \\ {}^{0}_{1}\omega^{\mathsf{x}} \\ {}^{0}_{1}\omega^{\mathsf{y}} \\ {}^{0}_{1}\omega^{\mathsf{z}} \end{bmatrix}, \qquad {}^{1}_{2}\boldsymbol{\xi} = \begin{bmatrix} 0 \\ 0 \\ 0 \\ {}^{0}_{2}\omega^{\mathsf{x}} - {}^{1}_{2}R^{\mathsf{x}}_{\mathsf{x}}\,{}^{0}_{2}\omega^{\mathsf{x}} - {}^{1}_{2}R^{\mathsf{y}}_{\mathsf{x}}\,{}^{0}_{2}\omega^{\mathsf{y}} - {}^{1}_{2}R^{\mathsf{z}}_{\mathsf{x}}\,{}^{0}_{2}\omega^{\mathsf{z}} \\ {}^{0}_{2}\omega^{\mathsf{y}} - {}^{1}_{2}R^{\mathsf{x}}_{\mathsf{y}}\,{}^{0}_{2}\omega^{\mathsf{x}} - {}^{1}_{2}R^{\mathsf{y}}_{\mathsf{y}}\,{}^{0}_{2}\omega^{\mathsf{y}} - {}^{1}_{2}R^{\mathsf{z}}_{\mathsf{y}}\,{}^{0}_{2}\omega^{\mathsf{z}} \\ {}^{0}_{2}\omega^{\mathsf{z}} - {}^{1}_{2}R^{\mathsf{x}}_{\mathsf{z}}\,{}^{0}_{2}\omega^{\mathsf{x}} - {}^{1}_{2}R^{\mathsf{y}}_{\mathsf{z}}\,{}^{0}_{2}\omega^{\mathsf{y}} - {}^{1}_{2}R^{\mathsf{z}}_{\mathsf{z}}\,{}^{0}_{2}\omega^{\mathsf{z}} \end{bmatrix}, \tag{3.106a}$$

$$ {}^{\;\;\;\;1}_{2k+1}\boldsymbol{\xi} = \begin{bmatrix} 0 \\ 0 \\ 0 \\ \dot{\theta}_k \\ 0 \\ 0 \end{bmatrix}, \qquad {}^{2k+1}_{2k+2}\boldsymbol{\xi} = \begin{bmatrix} 0 \\ 0 \\ 0 \\ 0 \\ 0 \\ \varpi_k \end{bmatrix}, \qquad k = 1,2,3. \tag{3.106b}$$

From this it should clear how the corresponding body Jacobians look like, e.g. ${}^{0}_{1}\boldsymbol{J} = [\mathbf{I}_6\ 0]$.

For the formulation of the kinetic energy in the following subsection we will need the body Jacobians ${}^{0}_{b}\boldsymbol{J}, b = 1, \dots, N$. From the graph structure and the rules (3.104) we can compute them iteratively as

$$
\begin{aligned}
{}^{0}_{2}\boldsymbol{J} &= \mathrm{Ad}_{{}^{2}_{1}\mathsf{G}}\ {}^{0}_{1}\boldsymbol{J} + {}^{1}_{2}\boldsymbol{J}, && (3.107a)\\
{}^{\ \ \ \ 0}_{2k+1}\boldsymbol{J} &= \mathrm{Ad}_{{}^{2k+1}_{1}\mathsf{G}}\ {}^{0}_{1}\boldsymbol{J} + {}^{\ \ \ \ 1}_{2k+1}\boldsymbol{J}, && (3.107b)\\
{}^{\ \ \ \ 0}_{2k+2}\boldsymbol{J} &= \mathrm{Ad}_{{}^{2k+2}_{2k+1}\mathsf{G}}\ {}^{\ \ \ \ 0}_{2k+1}\boldsymbol{J} + {}^{2k+1}_{2k+2}\boldsymbol{J}. && (3.107c)
\end{aligned}
$$

These terms are significantly more cumbersome, so they are not displayed explicitly.

3.4.2 Inertia

Kinetic energy and inertia matrix. The kinetic energy $\mathcal{T}$ of a rigid body system is simply the sum of the kinetic energies of its bodies. Combining this with the kinetic energy (3.51) of a single free rigid body and the formulation of the absolute body velocities ${}^{0}_{b}\boldsymbol{\xi}$ in terms of the chosen coordinates using the body Jacobian ${}^{0}_{b}\boldsymbol{J}$ from (3.103), yields

$$
\mathcal{T} = \sum\nolimits_b \tfrac{1}{2}\,{}^{0}_{b}\boldsymbol{\xi}^\top\,{}^{0}_{b}\mathbf{M}\,{}^{0}_{b}\boldsymbol{\xi} = \tfrac{1}{2}\boldsymbol{\xi}^\top \underbrace{\sum\nolimits_b {}^{0}_{b}\boldsymbol{J}^\top\,{}^{0}_{b}\mathbf{M}\,{}^{0}_{b}\boldsymbol{J}}_{\boldsymbol{M}}\,\boldsymbol{\xi}. \tag{3.108}
$$

Recall from the previous section, that the constant *body* inertia matrix ${}^{0}_{b}\mathbf{M} \in \mathbb{R}^{6\times 6}$ collects the inertia parameters of the rigid body with index b and w.r.t. its body fixed frame. The matrix $\boldsymbol{M}(\boldsymbol{x}) \in \mathbb{R}^{n\times n}$ is called the *system* inertia matrix.

Connection coefficients. With a rather cumbersome computation (see [eq: ??]), it can be shown that the connection coefficients $\mathit{\Gamma}_{ijk}$ associated to the system inertia matrix $\boldsymbol{M}$ from (3.108) can be expressed in terms of the body Jacobians ${}^{0}_{b}\boldsymbol{J}$, the body inertia matrices ${}^{0}_{b}\mathbf{M}$ and the body connection coefficients ${}^{0}_{b}\mathsf{\Gamma}_{pqr}$ from (3.58) or the body commutation coefficients Υ^{h}_{pq} from (3.49) as

$$
\mathit{\Gamma}_{ijk} = \sum\nolimits_b {}^{0}_{b}J^{p}_{i}\Big({}^{0}_{b}\mathsf{M}_{pq}\partial_k\,{}^{0}_{b}J^{q}_{j} + \underbrace{\tfrac{1}{2}\big(\Upsilon^{h}_{pq}\,{}^{0}_{b}\mathsf{M}_{hr} + \Upsilon^{h}_{pr}\,{}^{0}_{b}\mathsf{M}_{hq} - \Upsilon^{h}_{qr}\,{}^{0}_{b}\mathsf{M}_{hp}\big)}_{{}^{0}_{b}\mathsf{\Gamma}_{pqr}}\,{}^{0}_{b}J^{q}_{j}\,{}^{0}_{b}J^{r}_{k}\Big) \tag{3.109}
$$

Acceleration energy. As with the kinetic energy, the acceleration energy of a rigid body system is simply the sum of the acceleration energies of its bodies. Summing up the body acceleration energies from (3.90c) and plugging in the body velocities ${}^{0}_{b}\boldsymbol{\xi} = {}^{0}_{b}\boldsymbol{J}\boldsymbol{\xi}$

yields

$$\begin{aligned}
\mathcal{S} &= \sum\nolimits_b \tfrac{1}{2}\|({}^0_b\ddot{\mathbf{G}})^\top\|^2_{{}^0_b\mathbf{M}'} \\
&= \sum\nolimits_b \tfrac{1}{2}\|(\mathrm{wed}({}^0_b\boldsymbol{J}\dot{\boldsymbol{\xi}} + {}^0_b\dot{\boldsymbol{J}}\boldsymbol{\xi}) + \mathrm{wed}({}^0_b\boldsymbol{J}\boldsymbol{\xi})^2)^\top\|^2_{{}^0_b\mathbf{M}'} \\
&= \sum\nolimits_b \tfrac{1}{2}\|(\mathrm{wed}({}^0_b\boldsymbol{J}\dot{\boldsymbol{\xi}}))^\top\|^2_{{}^0_b\mathbf{M}'} + \sum\nolimits_b \mathrm{tr}\left(\mathrm{wed}({}^0_b\boldsymbol{J}\dot{\boldsymbol{\xi}}){}^0_b\mathbf{M}'(\mathrm{wed}({}^0_b\dot{\boldsymbol{J}}\boldsymbol{\xi}) + \mathrm{wed}({}^0_b\boldsymbol{J}\boldsymbol{\xi})^2)^\top\right) \\
&\quad + \underbrace{\sum\nolimits_b \tfrac{1}{2}\|(\mathrm{wed}({}^0_b\dot{\boldsymbol{J}}\boldsymbol{\xi}) + \mathrm{wed}({}^0_b\boldsymbol{J}\boldsymbol{\xi})^2)^\top\|^2_{{}^0_b\mathbf{M}'}}_{\mathcal{S}_0} \\
&= \tfrac{1}{2}\dot{\boldsymbol{\xi}}^\top \underbrace{\sum\nolimits_b {}^0_b\boldsymbol{J}^\top {}^0_b\mathbf{M}\, {}^0_b\boldsymbol{J}}_{\boldsymbol{M}}\, \dot{\boldsymbol{\xi}} + \dot{\boldsymbol{\xi}}^\top \underbrace{\sum\nolimits_b {}^0_b\boldsymbol{J}^\top \big({}^0_b\mathbf{M}\, {}^0_b\dot{\boldsymbol{J}} - \mathrm{ad}^\top_{{}^0_b\boldsymbol{J}\boldsymbol{\xi}}\, {}^0_b\mathbf{M}\, {}^0_b\boldsymbol{J}\big)\boldsymbol{\xi}}_{\boldsymbol{c}} + \mathcal{S}_0.
\end{aligned} \tag{3.110}$$

Obviously, we found again the system inertia matrix $\boldsymbol{M}$ and one may check that indeed $c_i = \Gamma_{ijk}\xi^j\xi^k$ with the connection coefficients Γ_{ijk} from (3.109). Note that $\mathcal{S}_0$ is independent of $\dot{\boldsymbol{\xi}}$, so it does not contribute to the generalized inertia force.

Inertia force. As before, there are several equivalent ways for computing the inertia force $\boldsymbol{f}^{\mathrm{M}}$ of a rigid body system: We may use the Lagrange operator on the kinetic energy from (3.108), use the inertia matrix and connection coefficients from (3.109), or taking the differential of the acceleration energy from (3.110). Each of these approaches will yield

$$\boldsymbol{f}^{\mathrm{M}} = \underbrace{\sum\nolimits_b {}^0_b\boldsymbol{J}^\top {}^0_b\mathbf{M}\, {}^0_b\boldsymbol{J}}_{\boldsymbol{M}}\, \dot{\boldsymbol{\xi}} + \underbrace{\sum\nolimits_b {}^0_b\boldsymbol{J}^\top \big({}^0_b\mathbf{M}\, {}^0_b\dot{\boldsymbol{J}} - \mathrm{ad}^\top_{{}^0_b\boldsymbol{J}\boldsymbol{\xi}}\, {}^0_b\mathbf{M}\, {}^0_b\boldsymbol{J}\big)\boldsymbol{\xi}}_{\boldsymbol{c}}\,. \tag{3.111}$$

Similar results are called *the projection equation* in [Bremer, 2008, sec. 4.2.5] and *the Kane equations* [Kane and Levinson, 1985, chap. 6]. There is some controversy (starting in [Desloge, 1987]) about the naming, since the equations result rather directly (as shown above) from the Gibbs-Appell formulation. See [Lesser, 1992] or [Papastavridis, 2002, p. 714] for an overview.

In contrast to the sources above, the derivation here does allow for redundant configuration coordinates $\boldsymbol{x}$ and general velocity coordinates $\boldsymbol{\xi}$. This im mostly due to the more general formulation (3.103) of the body jacobian ${}^0_b\boldsymbol{J}$, wheras the formulation of the inertia matrix $\boldsymbol{M}$ and gyroscopic terms $\boldsymbol{c}$ should look familiar.

3.4.3 Gravitation

The potential energy of gravitation of a rigid body system is the sum of the potentials of the individual bodies (3.90g). This is

$$\mathcal{V}^{\mathrm{G}} = \sum\nolimits_b \langle ({}^0_b\mathbf{G})^\top, \mathrm{wed}(\boldsymbol{\alpha}_{\mathsf{G}})^\top\rangle_{{}^0_b\mathbf{M}'}, \qquad \boldsymbol{\alpha}_{\mathsf{G}}^\top = [\boldsymbol{a}_{\mathsf{G}}^\top, \mathbf{0}_{1\times 3}], \tag{3.112}$$

where ${}^0_b\mathbf{M}' = \mathrm{Vee}({}^0_b\mathbf{M})$ is the body inertia matrix and $\boldsymbol{\alpha}_{\mathsf{G}}$ is Earth's gravity wrench.

Finally, the generalized force of gravity on a rigid body system may be formulated as

$$\begin{aligned}\boldsymbol{f}^{\mathrm{G}} = \boldsymbol{\nabla}\mathcal{V}^{\mathrm{G}} = \frac{\partial \dot{\mathcal{V}}^{\mathrm{G}}}{\partial \boldsymbol{\xi}} &= \frac{\partial}{\partial \boldsymbol{\xi}} \sum\nolimits_b \operatorname{tr}\left({}^0_b\mathbf{G}\,\operatorname{wed}({}^0_b\boldsymbol{\xi})\,{}^0_b\mathbf{M}'\,\operatorname{wed}(\boldsymbol{\alpha}_{\mathsf{G}})^\top\right) \\ &= \sum\nolimits_b \left(\frac{\partial {}^0_b\boldsymbol{\xi}}{\partial \boldsymbol{\xi}}\right)^\top \operatorname{vee2}\left({}^0_b\mathbf{G}^\top \operatorname{wed}(\boldsymbol{\alpha}_{\mathsf{G}})\,{}^0_b\mathbf{M}'\right) = \sum\nolimits_b {}^0_b\boldsymbol{J}^\top\,{}^0_b\mathbf{M}\,\operatorname{Ad}^{-1}_{{}^0_b\mathbf{G}}\boldsymbol{\alpha}_{\mathsf{G}}. \end{aligned} \tag{3.113}$$

3.4.4 Stiffness

In subsection 3.3.4 we considered linear springs between arbitrary points of the body and the inertial frame. For a system of rigid bodies we may consider the same for each body, but additionally we may also consider springs connecting the bodies to each other, see Figure 3.6.

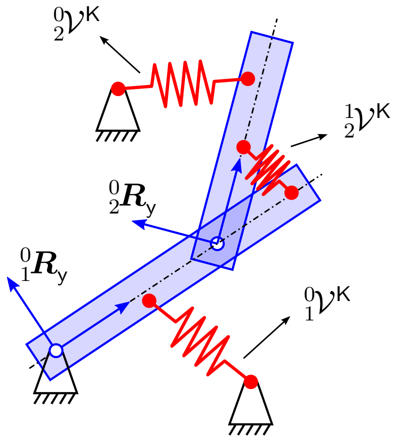

Figure 3.6: MultibodyStiffnessIllustration

The total potential energy $\mathcal{V}^{\mathrm{K}}$ is the sum of the potentials of the individual springs. Here it will make sense to group them differently: Let ${}^a_b\mathcal{V}^{\mathsf{K}}$ with $0 \leq a < b \leq N$ denote the combined potential of all springs connecting body a and b. The total energy is

$$\mathcal{V}^{\mathrm{K}} = \sum_{a=0}^{N-1} \sum_{b=a+1}^{N} {}^a_b\mathcal{V}^{\mathsf{K}} \tag{3.114}$$

Using the results from subsection 3.3.4 it may be shown that each potential can be formulated as

$${}^a_b\mathcal{V}^{\mathsf{K}} = \tfrac{1}{2}\|({}^a_b\mathbf{G} - {}^a_b\mathbf{G}_{\mathsf{R}})^\top\|^2_{{}^a_b\mathbf{K}'} = \tfrac{1}{2}\|({}^a_b\mathbf{G}_{\mathsf{R}}^{-1}\,{}^a_b\mathbf{G} - \mathbf{I}_4)^\top\|^2_{{}^a_b\mathbf{K}'} \tag{3.115}$$

with the constant parameters ${}^a_b\mathbf{K}' \in \mathbb{SYM}(4)$ and ${}^a_b\mathbf{G}_{\mathsf{R}} \in \mathbb{SE}(3)$ resulting from the particular spring distribution between body a and b.

Finally, the generalized force due to an arbitrary constellation of linear springs on a rigid body system may be formulated as

$$
\begin{aligned}
\boldsymbol{f}^{\mathrm{K}} = \boldsymbol{\nabla}\mathcal{V}^{\mathrm{K}} = \frac{\partial \dot{\mathcal{V}}^{\mathrm{K}}}{\partial \boldsymbol{\xi}} = \frac{\partial}{\partial \boldsymbol{\xi}} \sum\nolimits_{a,b} \operatorname{tr}\left(({}^{a}_{b}\mathbf{G} - {}^{a}_{b}\mathbf{G}_{\mathsf{R}}) {}^{a}_{b}\mathbf{K}' ({}^{a}_{b}\mathbf{G} \operatorname{wed}({}^{a}_{b}\boldsymbol{\xi}))^{\top} \right) \\
= \sum\nolimits_{a,b} \left(\frac{\partial {}^{a}_{b}\boldsymbol{\xi}}{\partial \boldsymbol{\xi}} \right)^{\top} \operatorname{vee2}\left({}^{a}_{b}\mathbf{G}^{\top} ({}^{a}_{b}\mathbf{G} - {}^{a}_{b}\mathbf{G}_{\mathsf{R}}) {}^{a}_{b}\mathbf{K}' \right) \\
= \sum\nolimits_{a,b} {}^{a}_{b}\boldsymbol{J}^{\top} \operatorname{vee2}\left((\mathbf{I}_4 - {}^{a}_{b}\mathbf{G}^{-1} {}^{a}_{b}\mathbf{G}_{\mathsf{R}}) {}^{a}_{b}\mathbf{K}' \right)
\end{aligned} \tag{3.116}
$$

3.4.5 Dissipation

Similar to the previous subsection we may consider viscous friction of the bodies to each other and to the inertial frame. Let the body with index b move through a viscous fluid that is attached to the body with index a. The corresponding dissipation function ${}^{a}_{b}\mathcal{R}$ was derived in (3.75):

$$
{}^{a}_{b}\mathcal{R} = \tfrac{1}{2} {}^{a}_{b}\boldsymbol{\xi}^{\top} {}^{a}_{b}\mathbf{D} \, {}^{a}_{b}\boldsymbol{\xi} \tag{3.117}
$$

with the body dissipation matrix ${}^{a}_{b}\mathbf{D}$. Notice that in contrast to stiffness, the dissipation is, in general, not symmetric in the sense ${}^{a}_{b}\mathcal{R} \neq {}^{b}_{a}\mathcal{R}$. But due to ${}^{a}_{a}\boldsymbol{\xi} = \mathbf{0}$ we have ${}^{a}_{a}\mathcal{R} = 0$. For system of rigid bodies we have the dissipation function

$$
\mathcal{R} = \sum_{a=0}^{N} \sum_{b=0, b\neq a}^{N} {}^{a}_{b}\mathcal{R} = \tfrac{1}{2}\boldsymbol{\xi}^{\top} \underbrace{\sum_{a=0}^{N} \sum_{b=0, b\neq a}^{N} {}^{a}_{b}\boldsymbol{J}^{\top} {}^{a}_{b}\mathbf{D} \, {}^{a}_{b}\boldsymbol{J}}_{\boldsymbol{D}} \, \boldsymbol{\xi} \tag{3.118}
$$

where $\boldsymbol{D}$ is called the system dissipation matrix.

Finally, the generalized force due to viscous friction on a rigid body system may be formulated as

$$
\boldsymbol{f}^{\mathrm{D}} = \frac{\partial \mathcal{R}}{\partial \boldsymbol{\xi}} = \boldsymbol{D}\boldsymbol{\xi} \tag{3.119}
$$

3.4.6 Summary

Given a rigid body system subject to inertia, gravity, dissipation and linear springs as discussed in this section, the equation of motion may be derived as follows. The description of the system consists of:

1. the chosen parameterization in the configuration coordinates $\boldsymbol{x}$, the velocity coordinates $\boldsymbol{\xi}$ and their relation captured by the kinematics matrix $\boldsymbol{A}$.
2. a set of transformation matrices ${}^{a}_{b}\mathbf{G}(\boldsymbol{x})$ that maps the coordinates to the chosen rigid body frames. They must form a connected graph including all body frames and the reference frame.

3. the constitutive parameters merged into the inertia matrices ${}^{0}_{b}\mathsf{M}'$, dissipation matrices ${}^{a}_{b}\mathsf{D}'$, stiffness matrices ${}^{a}_{b}\mathsf{K}'$, their corresponding minimum ${}^{a}_{b}\mathsf{G}_{\mathsf{R}}$ and the gravity vector $\boldsymbol{a}_{\mathsf{G}}$. It should be stressed that these only depend on the body frames, but are independent of the chosen coordinates.

Given these inputs, there is an algorithm

$$\big(\boldsymbol{x}, \boldsymbol{\xi}, \boldsymbol{A}, {}^{a}_{b}\mathsf{G}, {}^{0}_{b}\mathsf{M}', {}^{a}_{b}\mathsf{D}', {}^{a}_{b}\mathsf{K}', {}^{a}_{b}\mathsf{G}_{\mathsf{R}}, \boldsymbol{a}_{\mathsf{G}}\big) \;\mapsto\; \big(\boldsymbol{M}, \boldsymbol{c}, \boldsymbol{f}^{\mathrm{D}}, \boldsymbol{f}^{\mathrm{K}}, \boldsymbol{f}^{\mathrm{G}}\big) \tag{3.120}$$

that computes the relevant parts of the equation of motion. It may be summarized as

1. compute the body Jacobians for the given configurations:

$${}^{a}_{b}\boldsymbol{J}(\boldsymbol{x}) = \frac{\partial}{\partial \dot{\boldsymbol{x}}} \operatorname{vee}\Big({}^{b}_{a}\mathsf{G}(\boldsymbol{x}) \frac{\mathrm{d}}{\mathrm{d}t}\big({}^{a}_{b}\mathsf{G}(\boldsymbol{x})\big)\Big) \boldsymbol{A}(\boldsymbol{x}) \tag{3.121}$$

2. use the group rules to compute the missing configurations and Jacobians

$$\begin{aligned}
{}^{a}_{c}\mathsf{G} &= {}^{a}_{b}\mathsf{G}\,{}^{b}_{c}\mathsf{G}, & {}^{b}_{a}\mathsf{G} &= {}^{a}_{b}\mathsf{G}^{-1}, && \text{(3.122a)}\\
{}^{a}_{c}\boldsymbol{J} &= \mathrm{Ad}_{{}^{c}_{b}\mathsf{G}}\,{}^{a}_{b}\boldsymbol{J} + {}^{b}_{c}\boldsymbol{J}, & {}^{b}_{a}\boldsymbol{J} &= -\mathrm{Ad}_{{}^{a}_{b}\mathsf{G}}\,{}^{a}_{b}\boldsymbol{J}, && \text{(3.122b)}\\
{}^{a}_{c}\dot{\boldsymbol{J}} &= \mathrm{Ad}_{{}^{c}_{b}\mathsf{G}}\big({}^{a}_{b}\dot{\boldsymbol{J}} + \mathrm{ad}_{{}^{c}_{b}\boldsymbol{J}\boldsymbol{\xi}}\,{}^{a}_{b}\boldsymbol{J}\big) + {}^{b}_{c}\dot{\boldsymbol{J}}, & {}^{b}_{a}\dot{\boldsymbol{J}} &= -\mathrm{Ad}_{{}^{a}_{b}\mathsf{G}}\big({}^{a}_{b}\dot{\boldsymbol{J}} + \mathrm{ad}_{{}^{a}_{b}\boldsymbol{J}\boldsymbol{\xi}}\,{}^{a}_{b}\boldsymbol{J}\big), && \text{(3.122c)}
\end{aligned}$$

3. assemble the system matrices

$$\begin{aligned}
\boldsymbol{M} &= \sum\nolimits_{b} {}^{0}_{b}\boldsymbol{J}^{\top} \operatorname{Vee}({}^{0}_{b}\mathsf{M}')\,{}^{0}_{b}\boldsymbol{J}, && \text{(3.123a)}\\
\boldsymbol{c} &= \sum\nolimits_{b} {}^{0}_{b}\boldsymbol{J}^{\top} \operatorname{vee2}\big(\big(\operatorname{wed}({}^{0}_{b}\dot{\boldsymbol{J}}\boldsymbol{\xi}) + \operatorname{wed}({}^{0}_{b}\boldsymbol{J}\boldsymbol{\xi})^{2}\big)\,{}^{0}_{b}\mathsf{M}'\big) && \text{(3.123b)}\\
\boldsymbol{D} &= \sum\nolimits_{a,b} {}^{a}_{b}\boldsymbol{J}^{\top} \operatorname{Vee}({}^{a}_{b}\mathsf{D}')\,{}^{a}_{b}\boldsymbol{J} && \text{(3.123c)}\\
\boldsymbol{f}^{\mathrm{K}} &= \sum\nolimits_{a,b} {}^{a}_{b}\boldsymbol{J}^{\top} \operatorname{vee2}\big((\mathbf{I}_4 - {}^{b}_{a}\mathsf{G}\,{}^{a}_{b}\mathsf{G}_{\mathsf{R}})\,{}^{a}_{b}\mathsf{K}'\big) && \text{(3.123d)}\\
\boldsymbol{f}^{\mathrm{G}} &= \sum\nolimits_{b} {}^{0}_{b}\boldsymbol{J}^{\top} \operatorname{vee2}\big({}^{0}_{b}\mathsf{G}^{\top} \operatorname{wed}(-\boldsymbol{\alpha}_{\mathsf{G}})\,{}^{0}_{b}\mathsf{M}'\big), \qquad \boldsymbol{\alpha}_{\mathsf{G}} = [\boldsymbol{a}_{\mathsf{G}}^{\top}, \mathbf{0}_{1\times 3}]^{\top} && \text{(3.123e)}
\end{aligned}$$

The explicit equations of motion reads

$$\begin{aligned}
\dot{\boldsymbol{x}} &= \boldsymbol{A}\boldsymbol{\xi}, && \text{(3.124a)}\\
\dot{\boldsymbol{\xi}} &= \boldsymbol{M}^{-1}(\boldsymbol{f}^{\mathrm{E}} - \boldsymbol{c} - \boldsymbol{D}\boldsymbol{\xi} - \boldsymbol{f}^{\mathrm{K}} - \boldsymbol{f}^{\mathrm{G}}). && \text{(3.124b)}
\end{aligned}$$

The first step (3.121) requires differentiation, so must be performed symbolically. The remaining steps only require basic linear algebra, so can be preformed numerically. For small systems it might be still reasonable to compute $\boldsymbol{M}(\boldsymbol{x})$ symbolically, but for larger systems the explicit expressions can be overwhelming even for contemporary computers.

Chapter 4

Tracking control of rigid body systems

This chapter motivates and discusses several approaches for a model based design of a tracking controller for a rigid body system by static feedback.

System model. The previous chapter discussed the equations of motion of rigid body systems: For chosen configuration coordinates $\boldsymbol{x}(t) \in \mathbb{X}$, velocity coordinates $\boldsymbol{\xi}(t) \in \mathbb{R}^n$ and the control inputs $\boldsymbol{u}(t) \in \mathbb{R}^p$ these have the form

$$\dot{\boldsymbol{x}} = \boldsymbol{A}(\boldsymbol{x})\boldsymbol{\xi}, \qquad \overbrace{\boldsymbol{M}(\boldsymbol{x})\dot{\boldsymbol{\xi}} + \boldsymbol{c}(\boldsymbol{x},\boldsymbol{\xi})}^{\boldsymbol{f}^{\mathrm{M}}(\boldsymbol{x},\boldsymbol{\xi},\dot{\boldsymbol{\xi}})} + \overbrace{\boldsymbol{D}(\boldsymbol{x})\boldsymbol{\xi}}^{\boldsymbol{f}^{\mathrm{D}}(\boldsymbol{x},\boldsymbol{\xi})} + \overbrace{\boldsymbol{\nabla}\mathcal{V}(\boldsymbol{x})}^{\boldsymbol{f}^{\mathrm{K}}(\boldsymbol{x})} = \boldsymbol{B}(\boldsymbol{x})\boldsymbol{u}. \tag{4.1}$$

The forces $\boldsymbol{f}^{\mathrm{M}}, \boldsymbol{f}^{\mathrm{D}}, \boldsymbol{f}^{\mathrm{K}}$ may be computed from the rigid body configurations ${}^a_b\mathsf{G}(\boldsymbol{x})$ and the constitutive parameters ${}^0_b\mathsf{M}$, ${}^a_b\mathsf{D}$, ${}^a_b\mathsf{K}$. This structure will be the main inspiration for the design of the controlled system.

However, mathematically, the control approach does not rely on the model having this structure. We may assume any model of the form

$$\dot{\boldsymbol{x}} = \boldsymbol{A}(\boldsymbol{x})\boldsymbol{\xi}, \qquad \boldsymbol{M}(\boldsymbol{x})\dot{\boldsymbol{\xi}} + \boldsymbol{b}(\boldsymbol{x},\boldsymbol{\xi}) = \boldsymbol{B}(\boldsymbol{x})\boldsymbol{u} \tag{4.2}$$

where $\boldsymbol{A}(\boldsymbol{x}) \in \mathbb{R}^{\nu\times n}$ and $\boldsymbol{B}(\boldsymbol{x}) \in \mathbb{R}^{n\times p}$ are full rank, the system inertia matrix $\boldsymbol{M}(\boldsymbol{x}) \in \mathbb{SYM}^+(n)$ is symmetric, positive definite, and $\boldsymbol{b}(\boldsymbol{x},\boldsymbol{\xi}) \in \mathbb{R}^n$ collects the remaining terms of the kinetic equation. The system is called *fully-actuated* for $p = n$ and *underactuated* for $0 < p < n$. Firstly we will restrict to fully-actuated systems and later try to expand the approach to underactuated systems.

Reference trajectory and tracking controller. Let there be a *reference trajectory* $t \mapsto \boldsymbol{x}_{\mathsf{R}}(t)$ which is compatible with the model (4.2): It must be feasible, i.e. $\boldsymbol{x}_{\mathsf{R}}(t) \in \mathbb{X}$, and sufficiently smooth, so we can define the reference velocity $\boldsymbol{\xi}_{\mathsf{R}} = \boldsymbol{A}^+(\boldsymbol{x}_{\mathsf{R}})\dot{\boldsymbol{x}}_{\mathsf{R}}$ and acceleration $\dot{\boldsymbol{\xi}}_{\mathsf{R}}$. For the underactuated case we also require the kinetic equation $\boldsymbol{M}(\boldsymbol{x}_{\mathsf{R}})\dot{\boldsymbol{\xi}}_{\mathsf{R}} + \boldsymbol{b}(\boldsymbol{x}_{\mathsf{R}},\boldsymbol{\xi}_{\mathsf{R}}) = \boldsymbol{B}(\boldsymbol{x}_{\mathsf{R}})\boldsymbol{u}_{\mathsf{R}}$ to have a solution for $\boldsymbol{u}_{\mathsf{R}}$.

The design task for a *tracking controller* is: Find a function $\boldsymbol{u} = \boldsymbol{u}(\boldsymbol{x},\boldsymbol{\xi},\boldsymbol{x}_{\mathsf{R}},\boldsymbol{\xi}_{\mathsf{R}},\dot{\boldsymbol{\xi}}_{\mathsf{R}})$ (the controller) such that $t \mapsto \boldsymbol{x}_{\mathsf{R}}(t)$ is a stable and attractive trajectory of the closed loop which is the combination of model (4.2) and controller.

State of the art. This is a pretty general task and may be tackled by various standard approaches from control theory, see e.g. [Spong et al., 2006, chap. 7-10] for some overview. For fully actuated systems a popular approach is *computed torque*, see e.g. [Murray et al., 1994, sec. 4.5.2], also called *inverse dynamics* in [Spong et al., 2006, sec. 8.3]. It can be regarded as a particularly simple case of feedback linearization utilizing the fact that any set of minimal generalized coordinates $\boldsymbol{q}(t) \in \mathbb{R}^n$ is a *flat output* of a fully actuated mechanical system [Martin et al., 1997, sec. 7.1].

For underactuated systems there is no standard textbook approach. Examples for the flatness-based approach can be found in e.g. [Rathinam and Murray, 1998], [Murray et al., 1995] or [Martin et al., 1997, sec. 7.1]. General Lyapunov designs can be found in [Olfati-Saber, 2001] and a approach called *controlled Lagrangians* is proposed in [Bloch et al., 2000].

Outline for this chapter. With the computed torque method one might consider the topic to be solved for fully actuated systems. However, for system whose configuration space is not isomorph to $\mathbb{R}^n$ it is only local due to the requirement of minimal coordinates $\boldsymbol{q}(t) \in \mathbb{R}^n$. Furthermore, applying linear dynamics in these coordinates may result in intrinsic singularities for the closed loop. Recalling the satellite example from section 1.2, it should be clear that linear dynamics for the Euler angles would probably not be a good choice, also see [Konz and Rudolph, 2016] for further examples.

If linear dynamics are not a general choice, what *is* a good choice for the closed loop dynamics? This chapter motivates three approaches for designing a closed loop for fully actuated systems which rely on the underlying rigid body structure. In addition, the result will be extended to underactuated systems. Finally the approach will be applied to several example systems including the tricopter (fully-actuated), the quadcopter (underactuated but flat) and the bicopter (underactuated and probably not flat).

4.1 Approach 1: Inspired by particle distribution

4.1.1 Particle system

The basic idea. Consider a system of *free* particles with the equations of motion $\mathfrak{m}_p \ddot{\mathfrak{r}}_p = \mathfrak{F}_p^{\mathsf{A}}, p = 1, \ldots, \mathfrak{N}$ and the control inputs $\mathfrak{F}_p^{\mathsf{A}}$. We want the system to track a smooth reference trajectory $t \mapsto (\mathfrak{r}_{1\mathsf{R}}, \ldots, \mathfrak{r}_{\mathfrak{N}\mathsf{R}})(t)$. Probably the simplest solution is the control law $\mathfrak{F}_p^{\mathsf{A}} = \mathfrak{m}_p \ddot{\mathfrak{r}}_{p\mathsf{R}} - \bar{\mathfrak{d}}_p \dot{\mathfrak{r}}_{p\mathrm{E}} - \bar{\mathfrak{k}}_p \mathfrak{r}_{p\mathrm{E}}$ with the position error $\mathfrak{r}_{p\mathrm{E}} = \mathfrak{r}_p - \mathfrak{r}_{p\mathsf{R}}$ and the design parameters $\bar{\mathfrak{k}}_p, \bar{\mathfrak{d}}_p \in \mathbb{R} > 0$. The resulting closed loop is

$$\mathfrak{m}_p \ddot{\mathfrak{r}}_{p\mathrm{E}} + \bar{\mathfrak{d}}_p \dot{\mathfrak{r}}_{p\mathrm{E}} + \bar{\mathfrak{k}}_p \mathfrak{r}_{p\mathrm{E}} = \mathbf{0}, \qquad p = 1 \ldots \mathfrak{N}. \tag{4.3}$$

It is clearly exponentially stable and the *desired stiffness* $\bar{\mathfrak{k}}_p$ and *desired damping* $\bar{\mathfrak{d}}_p$ are intuitive tuning parameters.

For a system of particles with geometric constraints $\mathfrak{c}(\mathfrak{r}_1, \ldots, \mathfrak{r}_{\mathfrak{N}}) = \mathbf{0}$ we cannot achieve (4.3) in general. As the next best thing we can get as close as possible by formulation of the following constrained optimization problem

$$\begin{array}{rl} \underset{\ddot{\mathfrak{r}} \in \mathbb{R}^{3\mathfrak{N}}}{\text{minimize}} & \bar{\mathcal{G}} = \frac{1}{2} \sum_p \frac{1}{\bar{\mathfrak{m}}_p} \|\bar{\mathfrak{m}}_p \ddot{\mathfrak{r}}_{p\mathrm{E}} + \bar{\mathfrak{d}}_p \dot{\mathfrak{r}}_{p\mathrm{E}} + \bar{\mathfrak{k}}_p \mathfrak{r}_{p\mathrm{E}}\|^2 \\ \text{subject to} & \mathfrak{c}(\mathfrak{r}_1, \ldots, \mathfrak{r}_{\mathfrak{N}}) = \mathbf{0} \end{array} . \tag{4.4}$$

Note that we also replaced the particle masses $\mathfrak{m}_p$ by *desired masses* $\bar{\mathfrak{m}}_p$ as a additional design parameters. This will turn out crucial for control of underactuated systems.

The controlled system. The constrained problem (4.4) can be transformed to an unconstrained one by formulating the particle accelerations $\ddot{\mathfrak{r}}_p = \ddot{\mathfrak{r}}_p(\boldsymbol{x}, \boldsymbol{\xi}, \dot{\boldsymbol{\xi}})$, $p = 1 \ldots \mathfrak{N}$ in terms of minimal acceleration coordinates $\dot{\boldsymbol{\xi}}$. Analogous, let the reference particle positions be formulated in terms of the reference coordinates $\boldsymbol{x}_\mathsf{R}, \boldsymbol{\xi}_\mathsf{R}, \dot{\boldsymbol{\xi}}_\mathsf{R}$, i.e. $\mathfrak{r}_{p\mathsf{R}} = \mathfrak{r}_p(\boldsymbol{x}_\mathsf{R})$, $\dot{\mathfrak{r}}_{p\mathsf{R}} = \dot{\mathfrak{r}}_p(\boldsymbol{x}_\mathsf{R}, \boldsymbol{\xi}_\mathsf{R})$, $\ddot{\mathfrak{r}}_{p\mathsf{R}} = \ddot{\mathfrak{r}}_p(\boldsymbol{x}_\mathsf{R}, \boldsymbol{\xi}_\mathsf{R}, \dot{\boldsymbol{\xi}}_\mathsf{R})$, and the position error $\mathfrak{r}_{p\mathrm{E}} = \mathfrak{r}_{p\mathrm{E}}(\boldsymbol{x}, \boldsymbol{x}_\mathsf{R}) = \mathfrak{r}_p(\boldsymbol{x}) - \mathfrak{r}_p(\boldsymbol{x}_\mathsf{R})$, etc.. With this, the solution of (4.4) can be computed from

$$\begin{aligned} \frac{\partial \bar{\mathcal{G}}}{\partial \dot{\xi}^i} &= \sum_p \langle \bar{\mathfrak{m}}_p \ddot{\mathfrak{r}}_{p\mathrm{E}} + \bar{\mathfrak{d}}_p \dot{\mathfrak{r}}_{p\mathrm{E}} + \bar{\mathfrak{k}}_p \mathfrak{r}_{p\mathrm{E}}, \frac{\partial \ddot{\mathfrak{r}}_p}{\partial \dot{\xi}^i} \rangle \\ &= \sum_p \bar{\mathfrak{m}}_p \langle \ddot{\mathfrak{r}}_{p\mathrm{E}}, \frac{\partial \ddot{\mathfrak{r}}_p}{\partial \dot{\xi}^i} \rangle + \sum_p \bar{\mathfrak{d}}_p \langle \dot{\mathfrak{r}}_{p\mathrm{E}}, \frac{\partial \dot{\mathfrak{r}}_p}{\partial \xi^i} \rangle + \sum_p \bar{\mathfrak{k}}_p \langle \mathfrak{r}_{p\mathrm{E}}, \partial_i \mathfrak{r}_p \rangle \\ &= \underbrace{\frac{\partial}{\partial \dot{\xi}^i} \underbrace{\sum_p \tfrac{1}{2} \bar{\mathfrak{m}}_p \|\ddot{\mathfrak{r}}_{p\mathrm{E}}\|^2}_{\bar{\mathcal{S}}}}_{\bar{f}_i^\mathsf{M}} + \underbrace{\frac{\partial}{\partial \xi^i} \underbrace{\sum_p \tfrac{1}{2} \bar{\mathfrak{d}}_p \|\dot{\mathfrak{r}}_{p\mathrm{E}}\|^2}_{\bar{\mathcal{R}}}}_{\bar{f}_i^\mathsf{D}} + \underbrace{\partial_i \underbrace{\sum_p \tfrac{1}{2} \bar{\mathfrak{k}}_p \|\mathfrak{r}_{p\mathrm{E}}\|^2}_{\bar{\mathcal{V}}}}_{\bar{f}_i^\mathsf{K}} = 0, \; i = 1, \ldots, n. \end{aligned} \tag{4.5}$$

Here we introduced formulations for the *controlled acceleration energy* $\bar{\mathcal{S}}(\boldsymbol{x}, \boldsymbol{\xi}, \dot{\boldsymbol{\xi}}, \boldsymbol{x}_\mathsf{R}, \boldsymbol{\xi}_\mathsf{R}, \dot{\boldsymbol{\xi}}_\mathsf{R})$, the *controlled dissipation function* $\bar{\mathcal{R}}(\boldsymbol{x}, \boldsymbol{\xi}, \boldsymbol{x}_\mathsf{R}, \boldsymbol{\xi}_\mathsf{R})$ and the *controlled potential energy* $\bar{\mathcal{V}}(\boldsymbol{x}, \boldsymbol{x}_\mathsf{R})$. It is worth noting that the inertia force $\bar{\boldsymbol{f}}^\mathsf{M}$ could also be derived from the *controlled kinetic energy* $\bar{\mathcal{T}}(\boldsymbol{x}, \boldsymbol{\xi}, \boldsymbol{x}_\mathsf{R}, \boldsymbol{\xi}_\mathsf{R})$ as

$$\bar{f}_i^\mathsf{M} = \frac{\mathrm{d}}{\mathrm{d}t} \frac{\partial \bar{\mathcal{T}}}{\partial \xi^i} + \gamma_{ij}^k \xi^j \frac{\partial \bar{\mathcal{T}}}{\partial \xi^k} - \partial_i \bar{\mathcal{T}}, \qquad \bar{\mathcal{T}} = \tfrac{1}{2} \sum_p \bar{\mathfrak{m}}_p \|\dot{\mathfrak{r}}_{p\mathrm{E}}\|^2. \tag{4.6}$$

Also note that all the defined "energies" are symmetric in the sense that $\mathcal{V}(\boldsymbol{x}, \boldsymbol{x}_\mathsf{R}) = \bar{\mathcal{V}}(\boldsymbol{x}_\mathsf{R}, \boldsymbol{x})$, etc..

The corresponding forces expressed more explicitly are

$$\begin{aligned} \bar{f}_i^\mathsf{M} = \frac{\partial \bar{\mathcal{S}}}{\partial \dot{\xi}^i} &= \underbrace{\sum_p \bar{\mathfrak{m}}_p \langle \partial_i \mathfrak{r}_p(\boldsymbol{x}), \partial_j \mathfrak{r}_p(\boldsymbol{x}) \rangle}_{\bar{M}_{ij}(\boldsymbol{x})} \dot{\xi}^j + \underbrace{\sum_p \bar{\mathfrak{m}}_p \langle \partial_i \mathfrak{r}_p(\boldsymbol{x}), \partial_k \partial_j \mathfrak{r}_p(\boldsymbol{x}) \rangle}_{\bar{\Gamma}_{ijk}(\boldsymbol{x})} \xi^j \xi^k \\ &\quad - \underbrace{\sum_p \bar{\mathfrak{m}}_p \langle \partial_i \mathfrak{r}_p(\boldsymbol{x}), \partial_j \mathfrak{r}_p(\boldsymbol{x}_\mathsf{R}) \rangle}_{\bar{M}'_{ij}(\boldsymbol{x}, \boldsymbol{x}_\mathsf{R})} \dot{\xi}_\mathsf{R}^j - \underbrace{\sum_p \bar{\mathfrak{m}}_p \langle \partial_i \mathfrak{r}_p(\boldsymbol{x}), \partial_k \partial_j \mathfrak{r}_p(\boldsymbol{x}_\mathsf{R}) \rangle}_{\bar{\Gamma}'_{ijk}(\boldsymbol{x}, \boldsymbol{x}_\mathsf{R})} \xi_\mathsf{R}^j \xi_\mathsf{R}^k, \end{aligned} \tag{4.7a}$$

$$\bar{f}_i^\mathsf{D} = \frac{\partial \bar{\mathcal{R}}}{\partial \xi^i} = \underbrace{\sum_p \bar{\mathfrak{d}}_p \langle \partial_i \mathfrak{r}_p(\boldsymbol{x}), \partial_j \mathfrak{r}_p(\boldsymbol{x}) \rangle}_{\bar{D}_{ij}(\boldsymbol{x})} \xi^j - \underbrace{\sum_p \bar{\mathfrak{d}}_p \langle \partial_i \mathfrak{r}_p(\boldsymbol{x}), \partial_j \mathfrak{r}_p(\boldsymbol{x}_\mathsf{R}) \rangle}_{\bar{D}'_{ij}(\boldsymbol{x}, \boldsymbol{x}_\mathsf{R})} \xi_\mathsf{R}^j, \tag{4.7b}$$

$$\bar{f}_i^\mathsf{K} = \partial_i \bar{\mathcal{V}} = \sum_p \bar{\mathfrak{k}}_p \langle \partial_i \mathfrak{r}_p(\boldsymbol{x}), \mathfrak{r}_p(\boldsymbol{x}) - \mathfrak{r}_p(\boldsymbol{x}_\mathsf{R}) \rangle. \tag{4.7c}$$

So we can rewrite (4.5) as

$$\begin{aligned}\bar{M}_{ij}(\boldsymbol{x})\dot{\xi}^j - \bar{M}'_{ij}(\boldsymbol{x},\boldsymbol{x}_\mathsf{R})\dot{\xi}^j_\mathsf{R} + \bar{\varGamma}_{ijk}(\boldsymbol{x})\xi^j\xi^k - \bar{\varGamma}'_{ijk}(\boldsymbol{x},\boldsymbol{x}_\mathsf{R})\xi^j_\mathsf{R}\xi^k_\mathsf{R}&\\ + \bar{D}_{ij}(\boldsymbol{x})\xi^j - \bar{D}'_{ij}(\boldsymbol{x},\boldsymbol{x}_\mathsf{R})\xi^j_\mathsf{R} + \partial_i\bar{\mathcal{V}}(\boldsymbol{x},\boldsymbol{x}_\mathsf{R}) = 0, \quad i = 1,\dots,n.& \quad (4.8)\end{aligned}$$

Total energy. Having a definition for a kinetic energy $\bar{\mathcal{T}}$ and a potential energy $\bar{\mathcal{V}}$ it is worth investigating the total energy $\bar{\mathcal{W}} = \bar{\mathcal{T}} + \bar{\mathcal{V}}$ and its change along the solutions of closed loop (4.8). Using the substitutions defined in (4.7) and $\boldsymbol{\varPsi}(\boldsymbol{x},\boldsymbol{x}_\mathsf{R}) \in \mathbb{R}^{n\times n}$ defined through $\bar{M}'_{ij}(\boldsymbol{x},\boldsymbol{x}_\mathsf{R}) = \varPsi^s_i(\boldsymbol{x},\boldsymbol{x}_\mathsf{R})\bar{M}_{sj}(\boldsymbol{x})$ we have

$$\bar{\mathcal{W}} = \overbrace{\tfrac{1}{2}\bar{M}_{ij}(\boldsymbol{x})\xi^i\xi^j - \bar{M}'_{ij}(\boldsymbol{x},\boldsymbol{x}_\mathsf{R})\xi^i\xi^j_\mathsf{R} + \tfrac{1}{2}\bar{M}_{ij}(\boldsymbol{x}_\mathsf{R})\xi^i_\mathsf{R}\xi^j_\mathsf{R}}^{\bar{\mathcal{T}}(\boldsymbol{x},\boldsymbol{\xi},\boldsymbol{x}_\mathsf{R},\boldsymbol{\xi}_\mathsf{R})} + \bar{\mathcal{V}}(\boldsymbol{x},\boldsymbol{x}_\mathsf{R}) \quad (4.9)$$

$$\begin{aligned}\dot{\bar{\mathcal{W}}} &= \xi^i\big(\bar{M}_{ij}(\boldsymbol{x})\dot{\xi}^j + \bar{\varGamma}_{ijk}(\boldsymbol{x})\xi^j\xi^k - \bar{M}'_{ij}(\boldsymbol{x},\boldsymbol{x}_\mathsf{R})\dot{\xi}^j_\mathsf{R} - \bar{\varGamma}'_{ijk}(\boldsymbol{x},\boldsymbol{x}_\mathsf{R})\xi^j_\mathsf{R}\xi^k_\mathsf{R} + \partial_i\bar{\mathcal{V}}(\boldsymbol{x},\boldsymbol{x}_\mathsf{R})\big)\\ &\quad + \xi^i_\mathsf{R}\big(\bar{M}_{ij}(\boldsymbol{x}_\mathsf{R})\dot{\xi}^j_\mathsf{R} + \bar{\varGamma}_{ijk}(\boldsymbol{x}_\mathsf{R})\xi^j_\mathsf{R}\xi^k_\mathsf{R} - \bar{M}'_{ij}(\boldsymbol{x}_\mathsf{R},\boldsymbol{x})\dot{\xi}^j - \bar{\varGamma}'_{ijk}(\boldsymbol{x}_\mathsf{R},\boldsymbol{x})\xi^j\xi^k + \partial_i\bar{\mathcal{V}}(\boldsymbol{x}_\mathsf{R},\boldsymbol{x})\big)\\ &\overset{(4.8)}{=} -(\xi^i - \varPsi^i_s(\boldsymbol{x},\boldsymbol{x}_\mathsf{R})\xi^s_\mathsf{R})\big(\bar{D}_{ij}(\boldsymbol{x})\xi^j - \bar{D}'_{ij}(\boldsymbol{x},\boldsymbol{x}_\mathsf{R})\xi^j_\mathsf{R}\big)\\ &\quad + \xi^i_\mathsf{R}\big(\partial_i\bar{\mathcal{V}}(\boldsymbol{x}_\mathsf{R},\boldsymbol{x}) + \varPsi^s_i(\boldsymbol{x},\boldsymbol{x}_\mathsf{R})\partial_s\bar{\mathcal{V}}(\boldsymbol{x},\boldsymbol{x}_\mathsf{R}) + \big(\bar{M}_{ij}(\boldsymbol{x}_\mathsf{R}) - \varPsi^s_i(\boldsymbol{x},\boldsymbol{x}_\mathsf{R})\bar{M}'_{sj}(\boldsymbol{x},\boldsymbol{x}_\mathsf{R})\big)\dot{\xi}^j_\mathsf{R}\\ &\quad + \big(\bar{\varGamma}_{ijk}(\boldsymbol{x}_\mathsf{R}) - \varPsi^s_i(\boldsymbol{x},\boldsymbol{x}_\mathsf{R})\bar{\varGamma}'_{sjk}(\boldsymbol{x},\boldsymbol{x}_\mathsf{R})\big)\xi^j_\mathsf{R}\xi^k_\mathsf{R} - \big(\bar{\varGamma}'_{ijk}(\boldsymbol{x}_\mathsf{R},\boldsymbol{x}) - \varPsi^s_i(\boldsymbol{x},\boldsymbol{x}_\mathsf{R})\bar{\varGamma}_{sjk}(\boldsymbol{x})\big)\xi^j\xi^k\big)\end{aligned} \quad (4.10)$$

Obviously the total energy $\bar{\mathcal{W}}$ is not a Lyapunov function for a general reference trajectory. It is, however, for the very special case of $\boldsymbol{\xi}_\mathsf{R} = \boldsymbol{0}$, i.e. proves stability for a constant reference configuration $\boldsymbol{x}_\mathsf{R} = const.$.

4.1.2 Free rigid body

Consider the free rigid body discussed in section 3.3 as a special case of a particle system. As motivated there we use the position $\boldsymbol{r}(t) \in \mathbb{R}^3$ and orientation matrix $\boldsymbol{R}(t) \in \mathbb{SO}(3)$ merged into the configuration matrix $\mathbf{G}(t) = \left[\begin{smallmatrix}\boldsymbol{R}(t) & \boldsymbol{r}(t)\\ \mathbf{0} & 1\end{smallmatrix}\right] \in \mathbb{SE}(3)$ as configuration coordinates. Expressing the particle positions as $\mathfrak{r}_p = \boldsymbol{r} + \boldsymbol{R}\mathfrak{h}_p$ and applying the same calculations as in (3.88) we can write the energies from (4.5) as

$$\bar{\mathcal{V}} = \sum\nolimits_p \tfrac{1}{2}\bar{\mathfrak{k}}_p\|\mathfrak{r}_p - \mathfrak{r}_{p\mathsf{R}}\|^2 = \tfrac{1}{2}\|\big(\mathbf{G} - \mathbf{G}_\mathsf{R}\big)^\top\|^2_{\bar{\mathbf{K}}'} \quad (4.11a)$$

$$\bar{\mathcal{R}} = \sum\nolimits_p \tfrac{1}{2}\bar{\mathfrak{d}}_p\|\dot{\mathfrak{r}}_p - \dot{\mathfrak{r}}_{p\mathsf{R}}\|^2 = \tfrac{1}{2}\|\big(\dot{\mathbf{G}} - \dot{\mathbf{G}}_\mathsf{R}\big)^\top\|^2_{\bar{\mathbf{D}}'} \quad (4.11b)$$

$$\bar{\mathcal{S}} = \sum\nolimits_p \tfrac{1}{2}\bar{\mathfrak{m}}_p\|\ddot{\mathfrak{r}}_p - \ddot{\mathfrak{r}}_{p\mathsf{R}}\|^2 = \tfrac{1}{2}\|\big(\ddot{\mathbf{G}} - \ddot{\mathbf{G}}_\mathsf{R}\big)^\top\|^2_{\bar{\mathbf{M}}'} \quad (4.11c)$$

$$\bar{\mathcal{T}} = \sum\nolimits_p \tfrac{1}{2}\bar{\mathfrak{m}}_p\|\dot{\mathfrak{r}}_p - \dot{\mathfrak{r}}_{p\mathsf{R}}\|^2 = \tfrac{1}{2}\|\big(\dot{\mathbf{G}} - \dot{\mathbf{G}}_\mathsf{R}\big)^\top\|^2_{\bar{\mathbf{M}}'} \quad (4.11d)$$

where

$$\bar{\mathbf{K}}' = \sum_p \bar{\mathfrak{k}}_p \begin{bmatrix} \mathfrak{h}_p\mathfrak{h}_p^\top & \mathfrak{h}_p^\top \\ \mathfrak{h}_p & 1 \end{bmatrix} = \begin{bmatrix} \bar{\boldsymbol{\Pi}}' & \bar{k}\bar{\boldsymbol{h}} \\ \bar{k}\bar{\boldsymbol{h}}^\top & \bar{k} \end{bmatrix}, \tag{4.12a}$$

$$\bar{\mathbf{D}}' = \sum_p \bar{\mathfrak{d}}_p \begin{bmatrix} \mathfrak{h}_p\mathfrak{h}_p^\top & \mathfrak{h}_p^\top \\ \mathfrak{h}_p & 1 \end{bmatrix} = \begin{bmatrix} \bar{\boldsymbol{\Upsilon}}' & \bar{d}\bar{\boldsymbol{l}} \\ \bar{d}\bar{\boldsymbol{l}}^\top & \bar{d} \end{bmatrix}, \tag{4.12b}$$

$$\bar{\mathbf{M}}' = \sum_p \bar{\mathfrak{m}}_p \begin{bmatrix} \mathfrak{h}_p\mathfrak{h}_p^\top & \mathfrak{h}_p^\top \\ \mathfrak{h}_p & 1 \end{bmatrix} = \begin{bmatrix} \bar{\boldsymbol{\Theta}}' & \bar{m}\bar{\boldsymbol{s}} \\ \bar{m}\bar{\boldsymbol{s}}^\top & \bar{m} \end{bmatrix}. \tag{4.12c}$$

As before we can interpret the entries of the *desired inertia matrix* $\bar{\mathbf{M}} = \mathrm{Vee}(\bar{\mathbf{M}}')$ as the *desired total mass* $\bar{m}$, *desired center of mass* $\bar{\boldsymbol{s}}$ and the *desired moment of inertia* $\bar{\boldsymbol{\Theta}} = \mathrm{Vee}(\bar{\boldsymbol{\Theta}}')$. The analog holds for the entries of the *desired damping matrix* $\bar{\mathbf{D}} = \mathrm{Vee}(\bar{\mathbf{D}}')$ and the *desired stiffness matrix* $\bar{\mathbf{K}} = \mathrm{Vee}(\bar{\mathbf{K}}')$.

Introduce the translational $\boldsymbol{v}(t) \in \mathbb{R}^3$ and angular velocity $\boldsymbol{\omega}(t) \in \mathbb{R}^3$ merged into $\boldsymbol{\xi} = [\boldsymbol{v}^\top, \boldsymbol{\omega}^\top]^\top = \mathrm{vee}(\mathbf{G}^{-1}\dot{\mathbf{G}})$ as velocity coordinates. Furthermore, we introduce the *configuration error* $\mathbf{G}_\mathrm{E} = \mathbf{G}_\mathsf{R}^{-1}\mathbf{G}$ and exploit the invariance of the norm to left translation of the argument to express the desired energies (4.11) as

$$\bar{\mathcal{V}} = \tfrac{1}{2}\|\big(\mathbf{I}_4 - \mathbf{G}_\mathrm{E}^{-1}\big)^\top\|^2_{\bar{\mathbf{K}}'} \tag{4.13a}$$

$$\bar{\mathcal{R}} = \tfrac{1}{2}\|\big(\mathrm{wed}(\boldsymbol{\xi}) - \mathbf{G}_\mathrm{E}^{-1}\,\mathrm{wed}(\boldsymbol{\xi}_\mathsf{R})\big)^\top\|^2_{\bar{\mathbf{D}}'} \tag{4.13b}$$

$$\bar{\mathcal{S}} = \tfrac{1}{2}\|\big(\mathrm{wed}(\dot{\boldsymbol{\xi}}) + \mathrm{wed}(\boldsymbol{\xi})^2 - \mathbf{G}_\mathrm{E}^{-1}\big(\mathrm{wed}(\dot{\boldsymbol{\xi}}_\mathsf{R}) + \mathrm{wed}(\boldsymbol{\xi}_\mathsf{R})^2\big)\big)^\top\|^2_{\bar{\mathbf{M}}'} \tag{4.13c}$$

$$\bar{\mathcal{T}} = \tfrac{1}{2}\|\big(\mathrm{wed}(\boldsymbol{\xi}) - \mathbf{G}_\mathrm{E}^{-1}\,\mathrm{wed}(\boldsymbol{\xi}_\mathsf{R})\big)^\top\|^2_{\bar{\mathbf{M}}'}. \tag{4.13d}$$

The resulting forces can be expressed as

$$\bar{\boldsymbol{f}}^\mathsf{K} = \boldsymbol{\nabla}\bar{\mathcal{V}} = \mathrm{vee2}\,\big((\mathbf{I}_4 - \mathbf{G}_\mathrm{E}^{-1})\bar{\mathbf{K}}'\big), \tag{4.14a}$$

$$\bar{\boldsymbol{f}}^\mathsf{D} = \frac{\partial\bar{\mathcal{R}}}{\partial\boldsymbol{\xi}} = \mathrm{vee2}\,\big((\mathrm{wed}(\boldsymbol{\xi}) - \mathbf{G}_\mathrm{E}^{-1}\,\mathrm{wed}(\boldsymbol{\xi}_\mathsf{R}))\bar{\mathbf{D}}'\big), \tag{4.14b}$$

$$\bar{\boldsymbol{f}}^\mathsf{M} = \frac{\partial\bar{\mathcal{S}}}{\partial\dot{\boldsymbol{\xi}}} = \mathrm{vee2}\,\big(\big(\mathrm{wed}(\dot{\boldsymbol{\xi}}) + \mathrm{wed}(\boldsymbol{\xi})^2 - \mathbf{G}_\mathrm{E}^{-1}\big(\mathrm{wed}(\dot{\boldsymbol{\xi}}_\mathsf{R}) + \mathrm{wed}(\boldsymbol{\xi}_\mathsf{R})^2\big)\big)\bar{\mathbf{M}}'\big) \tag{4.14c}$$

or more explicitly

$$\bar{\boldsymbol{f}}^\mathsf{K} = \begin{bmatrix} \bar{k}\boldsymbol{R}_\mathrm{E}^\top(\boldsymbol{r}_\mathrm{E} + (\boldsymbol{R}_\mathrm{E} - \mathbf{I}_3)\bar{\boldsymbol{h}}) \\ \bar{k}\,\mathrm{wed}(\bar{\boldsymbol{h}})\boldsymbol{R}_\mathrm{E}^\top\boldsymbol{r}_\mathrm{E} + 2\,\mathrm{vee}\,\big(\mathrm{Vee}(\bar{\boldsymbol{\Pi}})(\boldsymbol{R}_\mathrm{E} - \mathbf{I}_3)\big) \end{bmatrix} \tag{4.15a}$$

$$\bar{\boldsymbol{f}}^\mathsf{D} = \underbrace{\begin{bmatrix} \bar{d}\mathbf{I}_3 & \bar{d}\,\mathrm{wed}(\bar{\boldsymbol{l}})^\top \\ \bar{d}\,\mathrm{wed}(\bar{\boldsymbol{l}}) & \bar{\boldsymbol{\Upsilon}} \end{bmatrix}}_{\bar{\mathbf{D}}} \underbrace{\begin{bmatrix} \boldsymbol{v} \\ \boldsymbol{\omega} \end{bmatrix}}_{\boldsymbol{\xi}} - \begin{bmatrix} \bar{d}\boldsymbol{R}_\mathrm{E}^\top & \boldsymbol{R}_\mathrm{E}^\top\bar{d}\,\mathrm{wed}(\bar{\boldsymbol{l}})^\top \\ \bar{d}\,\mathrm{wed}(\bar{\boldsymbol{l}})\boldsymbol{R}_\mathrm{E}^\top & \mathrm{Wed}(\boldsymbol{R}_\mathrm{E}^\top\,\mathrm{Vee}(\bar{\boldsymbol{\Upsilon}}))\boldsymbol{R}_\mathrm{E}^\top \end{bmatrix} \underbrace{\begin{bmatrix} \boldsymbol{v}_\mathsf{R} \\ \boldsymbol{\omega}_\mathsf{R} \end{bmatrix}}_{\boldsymbol{\xi}_\mathsf{R}} \tag{4.15b}$$

$$\begin{aligned} \bar{\boldsymbol{f}}^\mathsf{M} = {} & \underbrace{\begin{bmatrix} \bar{m}\mathbf{I}_3 & \bar{m}\,\mathrm{wed}(\bar{\boldsymbol{s}})^\top \\ \bar{m}\,\mathrm{wed}(\bar{\boldsymbol{s}}) & \bar{\boldsymbol{\Theta}} \end{bmatrix}}_{\bar{\mathbf{M}}} \underbrace{\begin{bmatrix} \dot{\boldsymbol{v}} \\ \dot{\boldsymbol{\omega}} \end{bmatrix}}_{\dot{\boldsymbol{\xi}}} + \begin{bmatrix} \bar{m}\,\mathrm{wed}(\boldsymbol{\omega}) & -\bar{m}\,\mathrm{wed}(\boldsymbol{\omega})\,\mathrm{wed}(\bar{\boldsymbol{s}}) \\ \bar{m}\,\mathrm{wed}(\bar{\boldsymbol{s}})\,\mathrm{wed}(\boldsymbol{\omega}) & \mathrm{wed}(\mathrm{Vee}(\bar{\boldsymbol{\Theta}})\boldsymbol{\omega}) \end{bmatrix} \begin{bmatrix} \boldsymbol{v} \\ \boldsymbol{\omega} \end{bmatrix} \\ & - \begin{bmatrix} \bar{m}\boldsymbol{R}_\mathrm{E}^\top & \boldsymbol{R}_\mathrm{E}^\top\bar{m}\,\mathrm{wed}(\bar{\boldsymbol{s}})^\top \\ \bar{m}\,\mathrm{wed}(\bar{\boldsymbol{s}})\boldsymbol{R}_\mathrm{E}^\top & \mathrm{Wed}(\boldsymbol{R}_\mathrm{E}^\top\,\mathrm{Vee}(\bar{\boldsymbol{\Theta}}))\boldsymbol{R}_\mathrm{E}^\top \end{bmatrix} \begin{bmatrix} \dot{\boldsymbol{v}}_\mathsf{R} \\ \dot{\boldsymbol{\omega}}_\mathsf{R} \end{bmatrix} \\ & - \begin{bmatrix} \bar{m}\boldsymbol{R}_\mathrm{E}^\top\,\mathrm{wed}(\boldsymbol{\omega}_\mathsf{R}) & -\bar{m}\boldsymbol{R}_\mathrm{E}^\top\,\mathrm{wed}(\boldsymbol{\omega}_\mathsf{R})\,\mathrm{wed}(\bar{\boldsymbol{s}}) \\ \bar{m}\,\mathrm{wed}(\bar{\boldsymbol{s}})\boldsymbol{R}_\mathrm{E}^\top\,\mathrm{wed}(\boldsymbol{\omega}_\mathsf{R}) & \mathrm{Wed}(\boldsymbol{R}_\mathrm{E}^\top\,\mathrm{wed}(\boldsymbol{\omega}_\mathsf{R})\,\mathrm{Vee}(\bar{\boldsymbol{\Theta}}))\boldsymbol{R}_\mathrm{E}^\top \end{bmatrix} \begin{bmatrix} \boldsymbol{v}_\mathsf{R} \\ \boldsymbol{\omega}_\mathsf{R} \end{bmatrix} \end{aligned} \tag{4.15c}$$

The closed loop kinetic equation $\bar{\boldsymbol{f}}^{\mathsf{M}} + \bar{\boldsymbol{f}}^{\mathsf{D}} + \bar{\boldsymbol{f}}^{\mathsf{K}} = \mathbf{0}$ contains 30 tuning parameters within the matrices $\bar{\mathbf{M}}'$, $\bar{\mathbf{D}}'$, $\bar{\mathbf{K}}' \in \mathbb{SYM}^+(4)$. The characteristic polynomial of the first order approximation of the system about any constant configuration $\boldsymbol{x}_{\mathsf{R}} = const.$ is $\det(\bar{\mathbf{M}}\lambda^2 + \bar{\mathbf{D}}\lambda + \bar{\mathbf{K}})$ where $\bar{\mathbf{M}} = \mathrm{Vee}(\bar{\mathbf{M}}')$, etc..

blah

In contrast to this, the characteristic polynomial resulting from the computed torque method (see sec:ComputedTorque) for this system is $\det(\mathbf{I}_6\lambda^2 + \boldsymbol{K}_1\lambda + \boldsymbol{K}_2)$, which has $n(n+1) = 42$ tuning parameters within the matrixes $\boldsymbol{K}_1, \boldsymbol{K}_2 \in \mathbb{SYM}^+(6)$.

blah

A possible generalization of the rigid body potential $\bar{\mathcal{V}}$ which works with all $\frac{1}{2}n(n+1) = 21$ tuning parameters in a matrix $\bar{\mathbf{K}} \in \mathbb{SYM}^+(6)$ is given in sec:GenRigidBodyPotential.

4.1.3 Rigid body systems

Let the particles belong to a system of N rigid bodies with the body configurations ${}^a_b\mathbf{G}$ as discussed in section 3.4. The potential energy from (4.5) may be formulated as $\bar{\mathcal{V}} = \sum_{b=1}^N \frac{1}{2}\|\left({}^0_b\mathbf{G} - {}^0_b\mathbf{G}_{\mathsf{R}}\right)^\top\|^2_{{}^0_b\bar{\mathbf{K}}'}$ with a body stiffness matrix ${}^0_b\bar{\mathbf{K}}'$ resulting from (4.12) for each body. This potential only captures stiffness w.r.t. the absolute configurations ${}^0_b\mathbf{G}$. Depending on the control objective it may be equally reasonable to consider a stiffness associated with the relative configurations ${}^a_b\mathbf{G}$ as illustrated in Figure 4.1. Considering

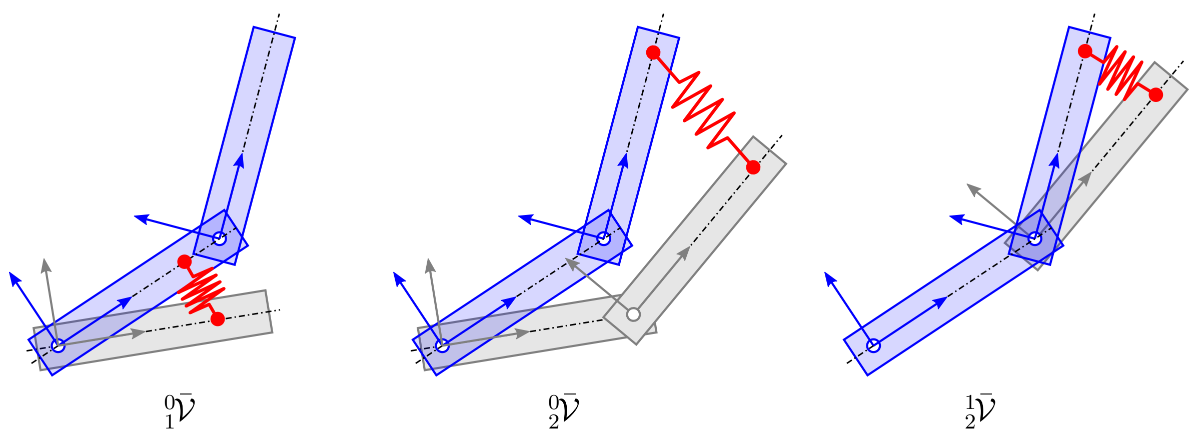

Figure 4.1: Different parts of the potential $\bar{\mathcal{V}}$ for a double pendulum

the same argument for damping and inertia, we propose the following energies for the control of a rigid body system:

$$\bar{\mathcal{V}} = \sum_{a,b=0}^{N} \overbrace{\tfrac{1}{2}\|\big({}^a_b\mathbf{G} - {}^a_b\mathbf{G}_\mathsf{R}\big)^\top\|^2_{{}^a_b\bar{\mathbf{K}}'}}^{{}^a_b\bar{\mathcal{V}}}, \qquad {}^a_b\bar{\mathbf{K}}' \in \mathbb{SYM}_0^+(4) \tag{4.16a}$$

$$\bar{\mathcal{R}} = \sum_{a,b=0}^{N} \tfrac{1}{2}\|\big({}^a_b\dot{\mathbf{G}} - {}^a_b\dot{\mathbf{G}}_\mathsf{R}\big)^\top\|^2_{{}^a_b\bar{\mathbf{D}}'}, \qquad {}^a_b\bar{\mathbf{D}}' \in \mathbb{SYM}_0^+(4) \tag{4.16b}$$

$$\bar{\mathcal{S}} = \sum_{a,b=0}^{N} \tfrac{1}{2}\|\big({}^a_b\ddot{\mathbf{G}} - {}^a_b\ddot{\mathbf{G}}_\mathsf{R}\big)^\top\|^2_{{}^a_b\bar{\mathbf{M}}'}, \qquad {}^a_b\bar{\mathbf{M}}' \in \mathbb{SYM}_0^+(4) \tag{4.16c}$$

$$\bar{\mathcal{T}} = \sum_{a,b=0}^{N} \tfrac{1}{2}\|\big({}^a_b\dot{\mathbf{G}} - {}^a_b\dot{\mathbf{G}}_\mathsf{R}\big)^\top\|^2_{{}^a_b\bar{\mathbf{M}}'}. \tag{4.16d}$$

Note that ${}^a_b\bar{\mathbf{K}}' = {}^b_a\bar{\mathbf{K}}'$ implies ${}^a_b\bar{\mathcal{V}} = {}^b_a\bar{\mathcal{V}}$ and ${}^a_a\bar{\mathcal{V}} = 0$ since ${}^a_a\mathbf{G} = {}^a_a\mathbf{G}_\mathsf{R} = \mathbf{I}_4$ and analog for damping and inertia.

Let the body configurations ${}^a_b\mathbf{G}(\boldsymbol{x})$ and the body velocities ${}^a_b\boldsymbol{\xi} = {}^a_b\boldsymbol{J}(\boldsymbol{x})\boldsymbol{\xi}$ be formulated in terms of suitable system coordinates $\boldsymbol{x}$ and $\boldsymbol{\xi}$, as discussed in section 3.4. With the shorthand notations ${}^a_b\mathbf{G}_\mathrm{E} = {}^a_b\mathbf{G}_\mathrm{E}(\boldsymbol{x}, \boldsymbol{x}_\mathsf{R}) = {}^a_b\mathbf{G}^{-1}(\boldsymbol{x}_\mathsf{R}){}^a_b\mathbf{G}(\boldsymbol{x})$ and ${}^a_b\boldsymbol{J} = {}^a_b\boldsymbol{J}(\boldsymbol{x})$, ${}^a_b\boldsymbol{J}_\mathsf{R} = {}^a_b\boldsymbol{J}(\boldsymbol{x}_\mathsf{R})$ we can express (4.16) as

$$\bar{\mathcal{V}} = \sum_{a,b} \tfrac{1}{2}\|\big(\mathbf{I}_4 - {}^a_b\mathbf{G}_\mathrm{E}^{-1}\big)^\top\|^2_{{}^a_b\bar{\mathbf{K}}'}, \tag{4.17a}$$

$$\bar{\mathcal{R}} = \sum_{a,b} \tfrac{1}{2}\|\big(\operatorname{wed}({}^a_b\boldsymbol{J}\boldsymbol{\xi}) - {}^a_b\mathbf{G}_\mathrm{E}^{-1}\operatorname{wed}({}^a_b\boldsymbol{J}_\mathsf{R}\boldsymbol{\xi}_\mathsf{R})\big)^\top\|^2_{{}^a_b\bar{\mathbf{D}}'}, \tag{4.17b}$$

$$\begin{aligned}\bar{\mathcal{S}} = \sum_{a,b} \tfrac{1}{2}\|\big(&\operatorname{wed}({}^a_b\boldsymbol{J}\dot{\boldsymbol{\xi}} + {}^a_b\dot{\boldsymbol{J}}\boldsymbol{\xi}) + \operatorname{wed}({}^a_b\boldsymbol{J}\boldsymbol{\xi})^2 \\ &- {}^a_b\mathbf{G}_\mathrm{E}^{-1}\big(\operatorname{wed}({}^a_b\boldsymbol{J}_\mathsf{R}\dot{\boldsymbol{\xi}}_\mathsf{R} + {}^a_b\dot{\boldsymbol{J}}_\mathsf{R}\boldsymbol{\xi}_\mathsf{R}) + \operatorname{wed}({}^a_b\boldsymbol{J}_\mathsf{R}\boldsymbol{\xi}_\mathsf{R})^2\big)\big)^\top\|^2_{{}^a_b\bar{\mathbf{M}}'}\end{aligned} \tag{4.17c}$$

$$\bar{\mathcal{T}} = \sum_{a,b} \tfrac{1}{2}\|\big(\operatorname{wed}({}^a_b\boldsymbol{J}\boldsymbol{\xi}) - {}^a_b\mathbf{G}_\mathrm{E}^{-1}\operatorname{wed}({}^a_b\boldsymbol{J}_\mathsf{R}\boldsymbol{\xi}_\mathsf{R})\big)^\top\|^2_{{}^a_b\bar{\mathbf{M}}'}. \tag{4.17d}$$

Plugging this into the original definition of the closed loop (4.7) we find:

The desired closed loop system for the particle based approach is given by

$$\bar{\boldsymbol{f}}^\mathsf{M} + \bar{\boldsymbol{f}}^\mathsf{D} + \bar{\boldsymbol{f}}^\mathsf{K} = \mathbf{0} \tag{4.18a}$$

where

$$\bar{\boldsymbol{f}}^\mathsf{K} = \boldsymbol{\nabla}\bar{\mathcal{V}} = \sum_{a,b} {}^a_b\boldsymbol{J}^\top \operatorname{vee2}\big((\mathbf{I}_4 - {}^a_b\mathbf{G}_\mathrm{E}^{-1}){}^a_b\bar{\mathbf{K}}'\big) \tag{4.18b}$$

$$\bar{\boldsymbol{f}}^\mathsf{D} = \frac{\partial\bar{\mathcal{R}}}{\partial\boldsymbol{\xi}} = \sum_{a,b} {}^a_b\boldsymbol{J}^\top \operatorname{vee2}\big((\operatorname{wed}({}^a_b\boldsymbol{J}\boldsymbol{\xi}) - {}^a_b\mathbf{G}_\mathrm{E}^{-1}\operatorname{wed}({}^a_b\boldsymbol{J}_\mathsf{R}\boldsymbol{\xi}_\mathsf{R})){}^a_b\bar{\mathbf{D}}'\big) \tag{4.18c}$$

$$\begin{aligned}\bar{\boldsymbol{f}}^\mathsf{M} = \frac{\partial\bar{\mathcal{S}}}{\partial\dot{\boldsymbol{\xi}}} = \sum_{a,b} {}^a_b\boldsymbol{J}^\top \operatorname{vee2}\big(\big(&\operatorname{wed}({}^a_b\boldsymbol{J}\dot{\boldsymbol{\xi}} + {}^a_b\dot{\boldsymbol{J}}\boldsymbol{\xi}) + \operatorname{wed}({}^a_b\boldsymbol{J}\boldsymbol{\xi})^2 \\ &- {}^a_b\mathbf{G}_\mathrm{E}^{-1}\big(\operatorname{wed}({}^a_b\boldsymbol{J}_\mathsf{R}\dot{\boldsymbol{\xi}}_\mathsf{R} + {}^a_b\dot{\boldsymbol{J}}_\mathsf{R}\boldsymbol{\xi}_\mathsf{R}) + \operatorname{wed}({}^a_b\boldsymbol{J}_\mathsf{R}\boldsymbol{\xi}_\mathsf{R})^2\big)\big){}^a_b\bar{\mathbf{M}}'\big)\end{aligned} \tag{4.18d}$$

The system inertia matrix $\bar{\boldsymbol{M}}$ can be recovered from the first term in (4.18d):

$$\sum\nolimits_{a,b} {}^a_b\boldsymbol{J}^\top \operatorname{vee2}\left(\operatorname{wed}({}^a_b\boldsymbol{J}\dot{\boldsymbol{\xi}})\,{}^a_b\bar{\mathbf{M}}'\right) = \underbrace{\sum\nolimits_{a,b} {}^a_b\boldsymbol{J}^\top \operatorname{Wed}({}^a_b\bar{\mathbf{M}}')\,{}^a_b\boldsymbol{J}}_{\bar{\boldsymbol{M}}}\,\dot{\boldsymbol{\xi}} = \frac{\partial^2\bar{\mathcal{S}}}{\partial\dot{\boldsymbol{\xi}}\partial\dot{\boldsymbol{\xi}}} = \frac{\partial^2\bar{\mathcal{T}}}{\partial\boldsymbol{\xi}\partial\boldsymbol{\xi}} \tag{4.19}$$

Though the body inertia matrices ${}^a_b\bar{\mathbf{M}}' \in \mathbb{SYM}^+_0(4)$ from (4.16c) are only required to be positive semi-definite, the resulting system inertia matrix $\bar{\boldsymbol{M}}(\boldsymbol{x}) \in \mathbb{SYM}^+(n)$ is required to be positive definite for the closed loop to be solvable.

4.2 Approach 2: Body based approach

The previous approach for the design of a closed loop has a vivid interpretation for the control energies and parameters. However, the total energy $\mathcal{W}$ does not, in general, serve as a Lyapunov function. In this section we attempt to modify the energies to account for this.

4.2.1 Free rigid body

Using the configuration error $\mathbf{G}_\mathrm{E} = \mathbf{G}_\mathsf{R}^{-1}\mathbf{G}$ and its velocity $\boldsymbol{\xi}_\mathrm{E} = \mathbf{G}_\mathrm{E}^{-1}\dot{\mathbf{G}}_\mathrm{E} = \boldsymbol{\xi} - \mathrm{Ad}^{-1}_{\mathbf{G}_\mathrm{E}}\boldsymbol{\xi}_\mathsf{R}$ we modify the energies from section 4.1 to

$$\bar{\mathcal{V}} = \tfrac{1}{2}\|(\mathbf{G}_\mathrm{E} - \mathbf{I}_4)^\top\|^2_{\bar{\mathbf{K}}'}, \qquad \bar{\mathbf{K}}' \in \mathbb{SYM}^+(4), \tag{4.20a}$$
$$\bar{\mathcal{R}} = \tfrac{1}{2}\|\dot{\mathbf{G}}_\mathrm{E}^\top\|^2_{\bar{\mathbf{D}}'} = \tfrac{1}{2}\|\operatorname{wed}(\boldsymbol{\xi}_\mathrm{E})^\top\|^2_{\bar{\mathbf{D}}'} = \tfrac{1}{2}\boldsymbol{\xi}_\mathrm{E}^\top\bar{\mathbf{D}}\boldsymbol{\xi}_\mathrm{E}, \qquad \bar{\mathbf{D}}' \in \mathbb{SYM}^+(4), \tag{4.20b}$$
$$\bar{\mathcal{S}} = \tfrac{1}{2}\|\ddot{\mathbf{G}}_\mathrm{E}^\top\|^2_{\bar{\mathbf{M}}'} = \tfrac{1}{2}\|(\operatorname{wed}(\dot{\boldsymbol{\xi}}_\mathrm{E}) + \operatorname{wed}(\boldsymbol{\xi}_\mathrm{E})^2)^\top\|^2_{\bar{\mathbf{M}}'}, \qquad \bar{\mathbf{M}}' \in \mathbb{SYM}^+(4), \tag{4.20c}$$
$$\bar{\mathcal{T}} = \tfrac{1}{2}\|\dot{\mathbf{G}}_\mathrm{E}^\top\|^2_{\bar{\mathbf{M}}'} = \tfrac{1}{2}\|\operatorname{wed}(\boldsymbol{\xi}_\mathrm{E})^\top\|^2_{\bar{\mathbf{M}}'} = \tfrac{1}{2}\boldsymbol{\xi}_\mathrm{E}^\top\bar{\mathbf{M}}\boldsymbol{\xi}_\mathrm{E} \tag{4.20d}$$

with usual substitution $\bar{\mathbf{M}} = \operatorname{Vee}(\bar{\mathbf{M}}')$. The closed loop forces are again defined as the derivatives of their corresponding energies. Using $\partial\boldsymbol{\xi}_\mathrm{E}/\partial\boldsymbol{\xi} = \mathbf{I}_6$ we have

$$\bar{\boldsymbol{f}}^\mathsf{K} = \boldsymbol{\nabla}\bar{\mathcal{V}} = \operatorname{vee2}\left((\mathbf{I}_4 - \mathbf{G}_\mathrm{E}^{-1})\bar{\mathbf{K}}'\right) \tag{4.21a}$$
$$\bar{\boldsymbol{f}}^\mathsf{D} = \frac{\partial\bar{\mathcal{R}}}{\partial\boldsymbol{\xi}} = \operatorname{vee2}\left(\operatorname{wed}(\boldsymbol{\xi}_\mathrm{E})\bar{\mathbf{D}}'\right) = \bar{\mathbf{D}}\boldsymbol{\xi}_\mathrm{E} \tag{4.21b}$$
$$\bar{\boldsymbol{f}}^\mathsf{M} = \frac{\partial\bar{\mathcal{S}}}{\partial\dot{\boldsymbol{\xi}}} = \operatorname{vee2}\left(\left(\operatorname{wed}(\dot{\boldsymbol{\xi}}_\mathrm{E}) + \operatorname{wed}(\boldsymbol{\xi}_\mathrm{E})^2\right)\bar{\mathbf{M}}'\right) = \bar{\mathbf{M}}\dot{\boldsymbol{\xi}}_\mathrm{E} - \mathrm{ad}^\top_{\boldsymbol{\xi}_\mathrm{E}}\bar{\mathbf{M}}\boldsymbol{\xi}_\mathrm{E} \tag{4.21c}$$

A crucial result of this approach is that the resulting closed loop equations can be written as *autonomous* equations for the configuration $\mathbf{G}_\mathrm{E}$ and velocity error $\boldsymbol{\xi}_\mathrm{E}$ as

$$\dot{\mathbf{G}}_\mathrm{E} = \mathbf{G}\operatorname{wed}(\boldsymbol{\xi}_\mathrm{E}), \qquad \bar{\mathbf{M}}\dot{\boldsymbol{\xi}}_\mathrm{E} - \mathrm{ad}^\top_{\boldsymbol{\xi}_\mathrm{E}}\bar{\mathbf{M}}\boldsymbol{\xi}_\mathrm{E} + \bar{\mathbf{D}}\boldsymbol{\xi}_\mathrm{E} + \operatorname{vee2}\left((\mathbf{I}_4 - \mathbf{G}_\mathrm{E}^{-1})\bar{\mathbf{K}}'\right) = \mathbf{0}. \tag{4.22}$$

A quite similar (though restricted to $\boldsymbol{s} = \boldsymbol{l} = \boldsymbol{h} = \mathbf{0}$) closed loop for the free rigid body is proposed in [Koditschek, 1989], though motivated from a Lie group point of view.

Total energy. The change of the total energy $\bar{\mathcal{W}} = \bar{\mathcal{T}} + \bar{\mathcal{V}}$ along the solutions of the closed loop (4.22) is

$$\dot{\bar{\mathcal{W}}} = \boldsymbol{\xi}_{\mathrm{E}}^{\top}\big(\bar{\mathbf{M}}\dot{\boldsymbol{\xi}}_{\mathrm{E}} + \mathrm{vee2}\left((\mathbf{I}_4 - \mathbf{G}_{\mathrm{E}}^{-1})\bar{\mathbf{K}}'\right)\big) = \underbrace{\boldsymbol{\xi}_{\mathrm{E}}^{\top}\mathrm{ad}_{\boldsymbol{\xi}_{\mathrm{E}}}^{\top}}_{=0}\bar{\mathbf{M}}\boldsymbol{\xi}_{\mathrm{E}} - \boldsymbol{\xi}_{\mathrm{E}}^{\top}\bar{\mathbf{D}}\boldsymbol{\xi}_{\mathrm{E}} = -2\bar{\mathcal{R}}. \tag{4.23}$$

Note that $\bar{\mathbf{K}}', \bar{\mathbf{D}}', \bar{\mathbf{M}}' \in \mathbb{SYM}^{+}(4)$ imply the positive definiteness of the total energy $\bar{\mathcal{W}}$ and the dissipation function $\bar{\mathcal{R}}$. Using this with the techniques from [Koditschek, 1989], one can show that "almost" all solutions of (4.22) converge to $\mathbf{G}_{\mathrm{E}} = \mathbf{I}_4$ and $\boldsymbol{\xi}_{\mathrm{E}} = \mathbf{0}$. The remaining solutions are the constant ($\boldsymbol{\xi}_{\mathrm{E}} = \mathbf{0}$) configurations $\mathbf{G}_{\mathrm{E}} \neq \mathbf{I}_4$ which are critical points of the potential $\bar{\mathcal{V}}$, see subsection 3.3.4. Roughly speaking, the configuration in which the body is 180° rotated to its reference.

4.2.2 Rigid body systems

For a rigid body system, let the body configurations ${}^a_b\mathbf{G} = {}^a_b\mathbf{G}(\boldsymbol{x})$ and the body velocities ${}^a_b\boldsymbol{\xi} = {}^a_b\boldsymbol{J}(\boldsymbol{x})\boldsymbol{\xi}$ be parameterized by the configuration $\boldsymbol{x}$ and velocity coordinates $\boldsymbol{\xi}$. So the body configuration errors ${}^a_b\mathbf{G}_{\mathrm{E}}$ and body velocity errors ${}^a_b\boldsymbol{\xi}_{\mathrm{E}}$ may be expressed as

$$\begin{aligned} {}^a_b\mathbf{G}_{\mathrm{E}}(\boldsymbol{x}, \boldsymbol{x}_{\mathsf{R}}) &= {}^a_b\mathbf{G}^{-1}(\boldsymbol{x}_{\mathsf{R}})\,{}^a_b\mathbf{G}(\boldsymbol{x}), && (4.24a)\\ {}^a_b\boldsymbol{\xi}_{\mathrm{E}}(\boldsymbol{x}, \boldsymbol{\xi}, \boldsymbol{x}_{\mathsf{R}}, \boldsymbol{\xi}_{\mathsf{R}}) &= {}^a_b\boldsymbol{J}(\boldsymbol{x})\boldsymbol{\xi} - \mathrm{Ad}^{-1}_{{}^a_b\mathbf{G}_{\mathrm{E}}(\boldsymbol{x},\boldsymbol{x}_{\mathsf{R}})}\,{}^a_b\boldsymbol{J}_{\mathsf{R}}(\boldsymbol{x}_{\mathsf{R}})\boldsymbol{\xi}_{\mathsf{R}}. && (4.24b) \end{aligned}$$

As done in subsection 4.1.3, the system energies are simply the sum over the energies associated with the absolute and relative body configurations:

$$\begin{aligned} \bar{\mathcal{V}} &= \sum\nolimits_{a,b} \tfrac{1}{2}\|({}^a_b\mathbf{G}_{\mathrm{E}} - \mathbf{I}_4)^{\top}\|^2_{{}^a_b\bar{\mathbf{K}}'}, && (4.25a)\\ \bar{\mathcal{R}} &= \sum\nolimits_{a,b} \tfrac{1}{2}\|\,\mathrm{wed}({}^a_b\boldsymbol{\xi}_{\mathrm{E}})^{\top}\|^2_{{}^a_b\bar{\mathbf{D}}'}, && (4.25b)\\ \bar{\mathcal{S}} &= \sum\nolimits_{a,b} \tfrac{1}{2}\|(\mathrm{wed}({}^a_b\dot{\boldsymbol{\xi}}_{\mathrm{E}}) + \mathrm{wed}({}^a_b\boldsymbol{\xi}_{\mathrm{E}})^2)^{\top}\|^2_{{}^a_b\bar{\mathbf{M}}'}, && (4.25c)\\ \bar{\mathcal{T}} &= \sum\nolimits_{a,b} \tfrac{1}{2}\|\,\mathrm{wed}({}^a_b\boldsymbol{\xi}_{\mathrm{E}})^{\top}\|^2_{{}^a_b\bar{\mathbf{M}}'}. && (4.25d) \end{aligned}$$

Overall, the desired controlled system for the body based approach takes the form

$$\bar{\boldsymbol{f}}^{\mathsf{M}} + \bar{\boldsymbol{f}}^{\mathsf{D}} + \bar{\boldsymbol{f}}^{\mathsf{K}} = \mathbf{0} \tag{4.26a}$$

where

$$\begin{aligned} \bar{\boldsymbol{f}}^{\mathsf{K}} &= \boldsymbol{\nabla}\bar{\mathcal{V}} = \sum\nolimits_{a,b} {}^a_b\boldsymbol{J}^{\top}\,\mathrm{vee2}\left((\mathbf{I}_4 - {}^a_b\mathbf{G}_{\mathrm{E}}^{-1})\,{}^a_b\bar{\mathbf{K}}'\right), && (4.26b)\\ \bar{\boldsymbol{f}}^{\mathsf{D}} &= \frac{\partial\bar{\mathcal{R}}}{\partial\boldsymbol{\xi}} = \sum\nolimits_{a,b} {}^a_b\boldsymbol{J}^{\top}\,{}^a_b\bar{\mathbf{D}}\,{}^a_b\boldsymbol{\xi}_{\mathrm{E}} && (4.26c)\\ \bar{\boldsymbol{f}}^{\mathsf{M}} &= \frac{\partial\bar{\mathcal{S}}}{\partial\dot{\boldsymbol{\xi}}} = \sum\nolimits_{a,b} {}^a_b\boldsymbol{J}^{\top}\left({}^a_b\bar{\mathbf{M}}\,{}^a_b\dot{\boldsymbol{\xi}}_{\mathrm{E}} - \mathrm{ad}^{\top}_{{}^a_b\boldsymbol{\xi}_{\mathrm{E}}}\,{}^a_b\bar{\mathbf{M}}\,{}^a_b\boldsymbol{\xi}_{\mathrm{E}}\right) && (4.26d) \end{aligned}$$

The change of the total energy $\bar{\mathcal{W}} = \bar{\mathcal{T}} + \bar{\mathcal{V}}$ along the solutions of (4.26) does *not* take a similar form to (4.23). Consequently there is no simple conclusion about stability.

4.3 Approach 3: Inspired by total energy

The previous approaches for the design of a closed loop also motived a total energy $\bar{\mathcal{W}}$. Unfortunately, it did, in general, not turn out to be useful for stability analysis. In this section we like to motivate yet another approach for the design of a closed loop dynamics for the tracking problem which is based on the total energy as Lyapunov function.

4.3.1 Overall structure

The general structure of this approach follows [Bullo and Murray, 1999].

Total energy. Initially we drop the rigid body structure of the system and only consider the coordinates $\boldsymbol{x}, \boldsymbol{\xi}$ and their kinematic relation $\dot{\boldsymbol{x}} = \boldsymbol{A}(\boldsymbol{x})\boldsymbol{\xi}$. Define the "total error energy" as

$$\bar{\mathcal{W}}(\boldsymbol{x}, \boldsymbol{\xi}, \boldsymbol{x}_\mathsf{R}, \boldsymbol{\xi}_\mathsf{R}) = \underbrace{\tfrac{1}{2}\| \overbrace{\boldsymbol{\xi} - \boldsymbol{Q}(\boldsymbol{x}, \boldsymbol{x}_\mathsf{R})\boldsymbol{\xi}_\mathsf{R}}^{\boldsymbol{\xi}_\mathrm{E}} \|^2_{\bar{\boldsymbol{M}}(\boldsymbol{x})}}_{\bar{\mathcal{T}}} + \bar{\mathcal{V}}(\boldsymbol{x}, \boldsymbol{x}_\mathsf{R}) \tag{4.27}$$

with the positive definite error potential $\bar{\mathcal{V}} : \mathbb{X} \times \mathbb{X} \to \mathbb{R}^+$, $\bar{\mathcal{V}}(\boldsymbol{x}, \boldsymbol{x}_\mathsf{R}) = 0 \;\Leftrightarrow\; \boldsymbol{x} = \boldsymbol{x}_\mathsf{R}$ and the positive definite inertia matrix $\bar{\boldsymbol{M}}(\boldsymbol{x}) \in \mathbb{SYM}^+(n)$. So far the transport map $\boldsymbol{Q} : \mathbb{X} \times \mathbb{X} \to \mathbb{R}^{n\times n}$ may be any regular matrix with $\boldsymbol{Q}(\boldsymbol{x}, \boldsymbol{x}) = \mathbf{I}_n$. Combination of these requirements yields the positive definiteness of the total energy, i.e.

$$\bar{\mathcal{W}}(\boldsymbol{x}, \boldsymbol{\xi}, \boldsymbol{x}_\mathsf{R}, \boldsymbol{\xi}_\mathsf{R}) \geq 0, \quad \bar{\mathcal{W}}(\boldsymbol{x}, \boldsymbol{\xi}, \boldsymbol{x}_\mathsf{R}, \boldsymbol{\xi}_\mathsf{R}) = 0 \;\Leftrightarrow\; \boldsymbol{x} = \boldsymbol{x}_\mathsf{R},\, \boldsymbol{\xi} = \boldsymbol{\xi}_\mathsf{R}. \tag{4.28}$$

Change of total energy. The time derivative of the total energy is

$$\begin{aligned} \dot{\bar{\mathcal{W}}} &= \boldsymbol{\xi}_\mathrm{E}^\top \big(\bar{\boldsymbol{M}}\dot{\boldsymbol{\xi}}_\mathrm{E} + \tfrac{1}{2}\dot{\bar{\boldsymbol{M}}}\boldsymbol{\xi}_\mathrm{E}\big) + \boldsymbol{\xi}^\top \boldsymbol{\nabla}\bar{\mathcal{V}} + \boldsymbol{\xi}_\mathsf{R}^\top \boldsymbol{\nabla}_\mathsf{R}\bar{\mathcal{V}}. \\ &= \boldsymbol{\xi}_\mathrm{E}^\top \big(\bar{\boldsymbol{M}}\dot{\boldsymbol{\xi}}_\mathrm{E} + \tfrac{1}{2}\dot{\bar{\boldsymbol{M}}}\boldsymbol{\xi}_\mathrm{E} + \boldsymbol{\nabla}\bar{\mathcal{V}}\big) + \boldsymbol{\xi}_\mathsf{R}^\top \big(\boldsymbol{\nabla}_\mathsf{R}\bar{\mathcal{V}} + \boldsymbol{Q}^\top \boldsymbol{\nabla}\bar{\mathcal{V}}\big). \end{aligned} \tag{4.29}$$

where $\boldsymbol{\nabla}_\mathsf{R} = \boldsymbol{A}^\top(\boldsymbol{x}_\mathsf{R})\frac{\partial}{\partial \boldsymbol{x}_\mathsf{R}}$. The second term vanishes if we require the transport map $\boldsymbol{Q}$ to fulfill

$$\boldsymbol{\nabla}_\mathsf{R}\bar{\mathcal{V}} = -\boldsymbol{Q}^\top \boldsymbol{\nabla}\bar{\mathcal{V}}. \tag{4.30}$$

With a positive definite damping matrix $\bar{\boldsymbol{D}} \in \mathbb{SYM}^+(n)$ and a yet to define skew symmetric matrix $\bar{\boldsymbol{S}} = -\bar{\boldsymbol{S}}^\top \in \mathbb{R}^{n\times n}$ we set the closed loop kinetics as

$$\bar{\boldsymbol{M}}\dot{\boldsymbol{\xi}}_\mathrm{E} + \tfrac{1}{2}\dot{\bar{\boldsymbol{M}}}\boldsymbol{\xi}_\mathrm{E} + \boldsymbol{\nabla}\bar{\mathcal{V}} = -(\bar{\boldsymbol{D}} + \bar{\boldsymbol{S}})\boldsymbol{\xi}_\mathrm{E}. \tag{4.31}$$

Plugging the closed loop kinetics (4.31) and the requirement on the transport map (4.30) into the change of energy (4.29) we obtain

$$\dot{\bar{\mathcal{W}}} = -\boldsymbol{\xi}_\mathrm{E}^\top \bar{\boldsymbol{D}}\boldsymbol{\xi}_\mathrm{E} = -\|\boldsymbol{\xi}_\mathrm{E}\|^2_{\bar{\boldsymbol{D}}}. \tag{4.32}$$

Since $\frac{\mathrm{d}}{\mathrm{d}t}\bar{\mathcal{W}}$ is only negative semidefinite, we can only conclude stability but not attractiveness. One can pursue the prove of attractiveness by adding a cross term as done in [Bullo and Murray, 1999, sec. 4.2].

Covariance of the closed loop. The skew symmetric matrix $\bar{\boldsymbol{S}}$ cancels out in the balance of energy, so is of no interest for tuning purposes. Instead it is used to ensure that the closed loop (4.31) is *covariant*, i.e. its definition is unchanged under a change of coordinates. While the stiffness force $\bar{f}_i^{\mathsf{K}} = \partial_i \bar{\mathcal{V}}$ and the dissipative force $\bar{f}_i^{\mathsf{D}} = \bar{D}_{ij}\xi_{\mathrm{E}}^j$ are tensors, the inertia force $\bar{f}_i^{\mathsf{M}} = \bar{M}_{ij}\dot{\xi}_{\mathrm{E}}^j + \frac{1}{2}\partial_k \bar{M}_{ij}\xi^k\xi_{\mathrm{E}}^j + \bar{S}_{ij}\xi_{\mathrm{E}}^j$ is not. A universal way is to derive a transformation law and put it as an additional requirement for the closed loop. This would still not lead to a unique definition for $\bar{\boldsymbol{S}}$.

However, regarding $\bar{M}_{ij}$ as the coefficients of a Riemannian metric, there are the coefficients of the unique Levi Civita connection already encountered in (3.31):

$$\bar{\Gamma}_{ijk} = \tfrac{1}{2}\big(\partial_k \bar{M}_{ij} + \partial_j \bar{M}_{ik} - \partial_i \bar{M}_{jk} + \gamma_{ij}^s \bar{M}_{sk} + \gamma_{ik}^s \bar{M}_{sj} - \gamma_{jk}^s \bar{M}_{si}\big), \quad i,j,k = 1,\dots,n. \tag{4.33}$$

This motivates the inertia force in the clearly covariant form

$$\bar{f}_i^{\mathsf{M}} = \bar{M}_{ij}\dot{\xi}_{\mathrm{E}}^j + \bar{\Gamma}_{ijk}\xi^k\xi_{\mathrm{E}}^j. \tag{4.34}$$

It may be realized by setting $\bar{S}_{ij} = \bar{\Gamma}_{ijk}\xi^k - \frac{1}{2}\dot{\bar{M}}_{ij} = \frac{1}{2}(\bar{\Gamma}_{ijk} - \bar{\Gamma}_{jik})\xi^k = -\bar{S}_{ji}$ in (4.31).

4.3.2 Special cases

Euclidean space. The existing literature on control of mechanical systems uses almost exclusively minimal generalized coordinates $\boldsymbol{q} \in \mathbb{R}^n$ and the velocity coordinates $\dot{\boldsymbol{q}}$. Then the model can we written as

$$\boldsymbol{M}(\boldsymbol{q})\ddot{\boldsymbol{q}} + \boldsymbol{C}(\boldsymbol{q},\dot{\boldsymbol{q}})\dot{\boldsymbol{q}} = \boldsymbol{f}^{\mathrm{A}} \tag{4.35}$$

where $C_{ij} = \Gamma_{ijk}\xi^k$ and $\boldsymbol{f}^{\mathrm{A}}$ collects the remaining forces. For a fully actuated system there exists an input transformation such that $\boldsymbol{f}^{\mathrm{A}}$ can be regarded as virtual inputs.

On the Euclidean space $\mathbb{R}^n$ it is reasonable to introduce error coordinates $\boldsymbol{q}_{\mathrm{E}} = \boldsymbol{q} - \boldsymbol{q}_{\mathsf{R}}$ and to use a quadratic error potential

$$\bar{\mathcal{V}} = \tfrac{1}{2}\boldsymbol{q}_{\mathrm{E}}^\top \bar{\boldsymbol{K}}\boldsymbol{q}_{\mathrm{E}}, \qquad \bar{\boldsymbol{K}} \in \mathbb{SYM}^+(n). \tag{4.36}$$

This error potential obviously has the transport map $\boldsymbol{Q} = \mathbf{I}_n$ and the resulting error velocity $\boldsymbol{\xi}_{\mathrm{E}} = \dot{\boldsymbol{q}}_{\mathrm{E}} = \dot{\boldsymbol{q}} - \dot{\boldsymbol{q}}_{\mathsf{R}}$. Furthermore it is reasonable to choose a constant dissipation matrix $\bar{\boldsymbol{D}} \in \mathbb{SYM}^+(n)$.

Joint PD-Control. Choosing the desired inertia identical to the model inertia $\bar{\boldsymbol{M}} = \boldsymbol{M}$, which also implies $\bar{\boldsymbol{C}} = \boldsymbol{C}$, yields the closed loop kinetics

$$\boldsymbol{M}(\boldsymbol{q})\ddot{\boldsymbol{q}}_{\mathrm{E}} + \boldsymbol{C}(\boldsymbol{q},\dot{\boldsymbol{q}})\dot{\boldsymbol{q}}_{\mathrm{E}} + \bar{\boldsymbol{D}}\dot{\boldsymbol{q}}_{\mathrm{E}} + \bar{\boldsymbol{K}}\boldsymbol{q}_{\mathrm{E}} = \mathbf{0}. \tag{4.37}$$

The resulting control law is

$$\boldsymbol{f}^{\mathrm{A}} = \boldsymbol{M}(\boldsymbol{q})\ddot{\boldsymbol{q}}_{\mathsf{R}} + \boldsymbol{C}(\boldsymbol{q},\dot{\boldsymbol{q}})\dot{\boldsymbol{q}}_{\mathsf{R}} - \bar{\boldsymbol{D}}\dot{\boldsymbol{q}}_{\mathrm{E}} - \bar{\boldsymbol{K}}\boldsymbol{q}_{\mathrm{E}}. \tag{4.38}$$

This approach is commonly called *joint proportional derivative controller* [Slotine and Li, 1991, sec. 9.1.1] or *augmented PD control law* [Murray et al., 1994, sec. 4.5.3], [Spong et al., 2006, sec. 8.2].

Computed torque. Choosing the desired inertia as $\bar{\boldsymbol{M}} = \mathbf{I}_n$, which implies $\bar{\boldsymbol{C}} = \mathbf{0}$ leads to the closed loop kinetics

$$\ddot{\boldsymbol{q}}_{\mathrm{E}} + \bar{\boldsymbol{D}}\dot{\boldsymbol{q}}_{\mathrm{E}} + \bar{\boldsymbol{K}}\boldsymbol{q}_{\mathrm{E}} = \mathbf{0}. \tag{4.39}$$

The resulting control law is

$$\boldsymbol{f}^{\mathrm{A}} = \boldsymbol{M}(\boldsymbol{q})\big(\ddot{\boldsymbol{q}}_{\mathsf{R}} - \bar{\boldsymbol{D}}\dot{\boldsymbol{q}}_{\mathrm{E}} - \bar{\boldsymbol{K}}\boldsymbol{q}_{\mathrm{E}}\big) + \boldsymbol{C}(\boldsymbol{q}, \dot{\boldsymbol{q}})\dot{\boldsymbol{q}}. \tag{4.40}$$

This approach is commonly called *computed torque* [Murray et al., 1994, sec. 4.5.2], [Slotine and Li, 1991, sec. 9.1.2] or *inverse dynamics control* [Spong et al., 2006, sec. 8.3].

These well established approaches are contained within the derived framework. However, as argued in the introduction of this chapter, the use of the Euclidean metric (4.36) only makes sense if the configuration space is indeed an Euclidean space. Application of this approach to e.g. the rigid body orientation would lead to quite awkward motion.

4.3.3 Free rigid body

Consider a single free rigid body as extensively discussed in section 3.3. We use the position $\boldsymbol{r}$ and orientation $\boldsymbol{R}$ combined in the matrix $\mathbf{G} \in \mathbb{SE}(3)$ as configuration coordinates and the linear velocity $\boldsymbol{v} = \boldsymbol{R}^\top\dot{\boldsymbol{r}}$ and angular velocity $\boldsymbol{\omega} = \mathrm{vee}(\boldsymbol{R}^\top\dot{\boldsymbol{R}})$ combined in $[\boldsymbol{v}^\top, \boldsymbol{\omega}^\top]^\top = \boldsymbol{\xi} = \mathrm{vee}(\mathbf{G}^{-1}\dot{\mathbf{G}})$ as velocity coordinates.

Potential and transport map. As for the previous approaches, a reasonable choice (motivated from linear springs in subsection 3.3.4) for the potential energy for a rigid body is

$$\bar{\mathcal{V}} = \tfrac{1}{2}\|(\mathbf{G} - \mathbf{G}_{\mathsf{R}})^\top\|^2_{\bar{\mathbf{K}}'}, \qquad \bar{\mathbf{K}}' \in \mathbb{SYM}^+(4). \tag{4.41}$$

The time derivative of the potential is

$$\begin{aligned}\dot{\bar{\mathcal{V}}} &= \mathrm{tr}\left((\mathbf{G} - \mathbf{G}_{\mathsf{R}})\bar{\mathbf{K}}'(\mathbf{G}\,\mathrm{wed}(\boldsymbol{\xi}) - \mathbf{G}_{\mathsf{R}}\,\mathrm{wed}(\boldsymbol{\xi}_{\mathsf{R}}))^\top\right)\\ &= \mathrm{tr}\left((\mathbf{I}_4 - \mathbf{G}^{-1}\mathbf{G}_{\mathsf{R}})\bar{\mathbf{K}}'\,\mathrm{wed}(\boldsymbol{\xi} - \mathrm{Ad}_{\mathbf{G}^{-1}\mathbf{G}_{\mathsf{R}}}\boldsymbol{\xi}_{\mathsf{R}})^\top\right)\\ &= \underbrace{(\boldsymbol{\xi} - \mathrm{Ad}_{\mathbf{G}^{-1}\mathbf{G}_{\mathsf{R}}}\boldsymbol{\xi}_{\mathsf{R}})}_{\boldsymbol{\xi}_{\mathrm{E}}}{}^\top\,\underbrace{\mathrm{vee2}\left((\mathbf{I}_4 - \mathbf{G}^{-1}\mathbf{G}_{\mathsf{R}})\bar{\mathbf{K}}'\right)}_{\boldsymbol{\nabla}\bar{\mathcal{V}}}.\end{aligned} \tag{4.42}$$

Recalling the identity $\boldsymbol{\nabla}\bar{\mathcal{V}} = \partial\dot{\bar{\mathcal{V}}}/\partial\boldsymbol{\xi}$, it is evident that $\boldsymbol{Q} = \mathrm{Ad}_{\mathbf{G}^{-1}\mathbf{G}_{\mathsf{R}}}$ is a transport map for this potential [1] . The potential $\bar{\mathcal{V}}$ and the resulting force $\bar{\boldsymbol{f}}^{\mathsf{K}} = \boldsymbol{\nabla}\bar{\mathcal{V}}$ coincides with the ones given for the previous approaches, already explicitly stated in (4.14a).

[1] It should be noted that the transport map given in (4.42) is not unique. One can check by direct calculation that the following matrix also fulfills the required relation (4.30):

$$\boldsymbol{Q} = \begin{bmatrix}\boldsymbol{R}^\top\boldsymbol{R}_{\mathsf{R}} & \mathrm{wed}\,\bar{\boldsymbol{h}}\,\boldsymbol{R}^\top\boldsymbol{R}_{\mathsf{R}} - \boldsymbol{R}^\top\boldsymbol{R}_{\mathsf{R}}\,\mathrm{wed}\,\bar{\boldsymbol{h}}\\ \mathbf{0} & \boldsymbol{R}^\top\boldsymbol{R}_{\mathsf{R}}\end{bmatrix}. \tag{4.43}$$

Damping. Using the same damping matrix $\bar{\boldsymbol{D}} = \operatorname{Vee} \bar{\mathbf{D}}'$ with $\bar{\mathbf{D}}' \in \mathbb{SYM}^+(4)$ as with the body based approach, we find the same damping force (4.21b).

Inertia. Using the same inertia matrix as for the body based approach $\bar{\boldsymbol{M}} = \operatorname{Vee} \bar{\mathbf{M}}'$ with $\bar{\mathbf{M}}' \in \mathbb{SYM}^+(4)$ we find the controlled inertial force $\bar{\boldsymbol{f}}^{\mathsf{M}}$ as

$$\bar{\boldsymbol{f}}^{\mathsf{M}} = \underbrace{\begin{bmatrix} \bar{m}\mathbf{I}_3 & \bar{m}(\operatorname{wed}\bar{\boldsymbol{s}})^\top \\ \bar{m}\operatorname{wed}\bar{\boldsymbol{s}} & \bar{\boldsymbol{\Theta}} \end{bmatrix}}_{\bar{\boldsymbol{M}}} \underbrace{\begin{bmatrix} \dot{\boldsymbol{v}}_{\mathrm{E}} \\ \dot{\boldsymbol{\omega}}_{\mathrm{E}} \end{bmatrix}}_{\dot{\boldsymbol{\xi}}_{\mathrm{E}}} + \underbrace{\begin{bmatrix} \bar{m}\operatorname{wed}\boldsymbol{\omega} & -\bar{m}\operatorname{wed}\boldsymbol{\omega}\operatorname{wed}\bar{\boldsymbol{s}} \\ \bar{m}\operatorname{wed}\bar{\boldsymbol{s}}\operatorname{wed}\boldsymbol{\omega} & \operatorname{wed}(\operatorname{Wed}\bar{\boldsymbol{\Theta}}\,\boldsymbol{\omega}) \end{bmatrix}}_{\bar{\boldsymbol{C}}(\boldsymbol{\xi}) = -\bar{\boldsymbol{C}}^\top(\boldsymbol{\xi})} \underbrace{\begin{bmatrix} \boldsymbol{v}_{\mathrm{E}} \\ \boldsymbol{\omega}_{\mathrm{E}} \end{bmatrix}}_{\boldsymbol{\xi}_{\mathrm{E}}}. \tag{4.44}$$

This result is similar to the previous body based approach (4.22), only differing by replacing $\bar{\boldsymbol{C}}(\boldsymbol{\xi})$ with $\bar{\boldsymbol{C}}(\boldsymbol{\xi}_{\mathrm{E}})$. Consequently with this approach the closed loop dynamics are not autonomous.

4.3.4 Rigid body systems

As for the previous approaches we use the rigid body structure, i.e. the configurations ${}^a_b\mathbf{G}(\boldsymbol{x})$ and velocities ${}^a_b\boldsymbol{\xi}(\boldsymbol{x}, \boldsymbol{\xi}) = {}^a_b\boldsymbol{J}(\boldsymbol{x})\boldsymbol{\xi}$, as inspiration for controlled kinetics. Assigning stiffness, damping and inertia ${}^a_b\bar{\mathbf{K}}', {}^a_b\bar{\mathbf{D}}', {}^a_b\bar{\mathbf{M}}' \in \mathbb{SYM}_0^+(4)$ to each absolute and relative configuration leads to the following potential energy $\bar{\mathcal{V}}$, damping $\bar{\boldsymbol{D}}$ and inertia matrix $\bar{\boldsymbol{M}}$:

$$\bar{\mathcal{V}}(\boldsymbol{x}, \boldsymbol{x}_{\mathsf{R}}) = \sum\nolimits_{a,b} \tfrac{1}{2}\|({}^a_b\mathbf{G}(\boldsymbol{x}) - {}^a_b\mathbf{G}(\boldsymbol{x}_{\mathsf{R}}))^\top\|^2_{{}^a_b\bar{\mathbf{K}}'}, \qquad {}^a_b\bar{\mathbf{K}}' \in \mathbb{SYM}_0^+(4) \tag{4.45a}$$

$$\bar{\boldsymbol{D}}(\boldsymbol{x}) = \sum\nolimits_{a,b} {}^a_b\boldsymbol{J}^\top(\boldsymbol{x})\ \operatorname{Vee}({}^a_b\bar{\mathbf{D}}')\,{}^a_b\boldsymbol{J}(\boldsymbol{x}), \qquad {}^a_b\bar{\mathbf{D}}' \in \mathbb{SYM}_0^+(4) \tag{4.45b}$$

$$\bar{\boldsymbol{M}}(\boldsymbol{x}) = \sum\nolimits_{a,b} {}^a_b\boldsymbol{J}^\top(\boldsymbol{x})\ \operatorname{Vee}({}^a_b\bar{\mathbf{M}}')\,{}^a_b\boldsymbol{J}(\boldsymbol{x}), \qquad {}^a_b\bar{\mathbf{M}}' \in \mathbb{SYM}_0^+(4) \tag{4.45c}$$

Note that the body matrices do not have to be positive definite, only the resulting system matrices and the potential have to be positive definite to ensure stability.

Transport map. The potential $\bar{\mathcal{V}}$ and the resulting force $\boldsymbol{\nabla}\bar{\mathcal{V}}$ are identical to the previous approaches, see e.g. (4.18b). For this energy based approach we require the existence of a transport map. The condition (4.30) for the transport map $\boldsymbol{Q}$ with the given potential (4.45a) may be expanded to

$$\sum\nolimits_{a,b} \left({}^a_b\boldsymbol{J}\boldsymbol{Q} - \operatorname{Ad}_{{}^a_b\mathbf{G}_{\mathrm{E}}^{-1}}\,{}^a_b\boldsymbol{J}_{\mathsf{R}}\right)^\top \operatorname{vee2}\left((\mathbf{I}_4 - {}^a_a\mathbf{G}_{\mathrm{E}}^{-1})\,{}^a_b\bar{\mathbf{K}}'\right) = \mathbf{0}. \tag{4.46}$$

with the shorthand notation ${}^a_b\mathbf{G}_{\mathrm{E}} = {}^a_b\mathbf{G}^{-1}(\boldsymbol{x}_{\mathsf{R}})\,{}^a_b\mathbf{G}_{\mathrm{E}}(\boldsymbol{x})$ and ${}^a_b\boldsymbol{J}_{\mathsf{R}} = {}^a_b\boldsymbol{J}(\boldsymbol{x}_{\mathsf{R}})$. There is no general solution for this, the transport map $\boldsymbol{Q}$ has to be computed for each example individually. A major caviat of this approach is that there is no general guaranty on the existence of a transport map.

4.4 Constant reference and linearization

Constant reference. For a constant reference configuration $\boldsymbol{x}_{\mathsf{R}} = const. \Rightarrow \boldsymbol{\xi}_{\mathsf{R}}, \dot{\boldsymbol{\xi}}_{\mathsf{R}} = \mathbf{0}$, the three proposed control templates lead to the same system

$$\dot{\boldsymbol{x}} = \boldsymbol{A}(\boldsymbol{x})\boldsymbol{\xi}, \qquad \bar{\boldsymbol{M}}(\boldsymbol{x})\dot{\boldsymbol{\xi}} + \bar{\boldsymbol{c}}(\boldsymbol{x},\boldsymbol{\xi}) + \bar{\boldsymbol{D}}(\boldsymbol{x})\boldsymbol{\xi} + \boldsymbol{\nabla}\bar{\mathcal{V}}(\boldsymbol{x},\boldsymbol{x}_{\mathsf{R}}) = \mathbf{0} \tag{4.47a}$$

where

$$\bar{\boldsymbol{M}}(\boldsymbol{x}) = \sum\nolimits_{a,b} \big({}^a_b\boldsymbol{J}(\boldsymbol{x})\big)^\top {}^a_b\bar{\mathbf{M}}\, {}^a_b\boldsymbol{J}(\boldsymbol{x}), \tag{4.47b}$$

$$\bar{\boldsymbol{c}}(\boldsymbol{x},\boldsymbol{\xi}) = \sum\nolimits_{a,b} \big({}^a_b\boldsymbol{J}(\boldsymbol{x})\big)^\top \big({}^a_b\bar{\mathbf{M}}\, {}^a_b\dot{\boldsymbol{J}}(\boldsymbol{x},\boldsymbol{\xi}) - \mathrm{ad}^\top_{{}^a_b\boldsymbol{J}(\boldsymbol{x})\boldsymbol{\xi}}\, {}^a_b\bar{\mathbf{M}}\, {}^a_b\boldsymbol{J}(\boldsymbol{x})\big)\boldsymbol{\xi} \tag{4.47c}$$

$$\bar{\boldsymbol{D}}(\boldsymbol{x}) = \sum\nolimits_{a,b} \big({}^a_b\boldsymbol{J}(\boldsymbol{x})\big)^\top {}^a_b\bar{\mathbf{D}}\, {}^a_b\boldsymbol{J}(\boldsymbol{x}), \tag{4.47d}$$

$$\boldsymbol{\nabla}\bar{\mathcal{V}}(\boldsymbol{x},\boldsymbol{x}_{\mathsf{R}}) = \sum\nolimits_{a,b} \big({}^a_b\boldsymbol{J}(\boldsymbol{x})\big)^\top \mathrm{vee2}\big((\mathbf{I}_4 - {}^a_b\mathbf{G}_{\mathrm{E}}^{-1}(\boldsymbol{x},\boldsymbol{x}_{\mathsf{R}}))\, {}^a_b\bar{\mathbf{K}}'\big) \tag{4.47e}$$

The total energy $\bar{\mathcal{W}} = \frac{1}{2}\boldsymbol{\xi}^\top \bar{\boldsymbol{M}}\boldsymbol{\xi} + \bar{\mathcal{V}}$ is a Lyapunov function for this system if the system inertia matrix $\bar{\boldsymbol{M}}$ and the potential energy $\bar{\mathcal{V}}$ are positive definite, and the system dissipation matrix $\bar{\boldsymbol{D}}$ is positive semi-definite.

Linearization. Assuming that the configuration of the system is close to its reference, i.e. $\boldsymbol{x} \approx \boldsymbol{x}_{\mathsf{R}}$. The first order approximation (see subsection 2.2.3) of (4.47) with $\boldsymbol{\varepsilon} = \boldsymbol{A}^+(\boldsymbol{x}_{\mathsf{R}})(\boldsymbol{x} - \boldsymbol{x}_{\mathsf{R}})$ is

$$\bar{\boldsymbol{M}}_0\ddot{\boldsymbol{\varepsilon}} + \bar{\boldsymbol{D}}_0\dot{\boldsymbol{\varepsilon}} + \bar{\boldsymbol{K}}_0\boldsymbol{\varepsilon} = \mathbf{0} \tag{4.48a}$$

where

$$\bar{\boldsymbol{M}}_0 = \bar{\boldsymbol{M}}(\boldsymbol{x}_{\mathsf{R}}) = \sum\nolimits_{a,b} \big({}^a_b\boldsymbol{J}(\boldsymbol{x}_{\mathsf{R}})\big)^\top {}^a_b\bar{\mathbf{M}}\, {}^a_b\boldsymbol{J}(\boldsymbol{x}_{\mathsf{R}}), \tag{4.48b}$$

$$\bar{\boldsymbol{D}}_0 = \bar{\boldsymbol{D}}(\boldsymbol{x}_{\mathsf{R}}) = \sum\nolimits_{a,b} \big({}^a_b\boldsymbol{J}(\boldsymbol{x}_{\mathsf{R}})\big)^\top {}^a_b\bar{\mathbf{D}}\, {}^a_b\boldsymbol{J}(\boldsymbol{x}_{\mathsf{R}}), \tag{4.48c}$$

$$\bar{\boldsymbol{K}}_0 = \boldsymbol{\nabla}^2\bar{\mathcal{V}}(\boldsymbol{x}_{\mathsf{R}},\boldsymbol{x}_{\mathsf{R}}) = \sum\nolimits_{a,b} \big({}^a_b\boldsymbol{J}(\boldsymbol{x}_{\mathsf{R}})\big)^\top {}^a_b\bar{\mathbf{K}}\, {}^a_b\boldsymbol{J}(\boldsymbol{x}_{\mathsf{R}}) \tag{4.48d}$$

4.5 Underactuated systems

The first three sections of this chapter motivated different desired closed loop dynamics which share the structure

$$\dot{\boldsymbol{x}} = \boldsymbol{A}(\boldsymbol{x})\boldsymbol{\xi}, \quad \bar{\boldsymbol{M}}(\boldsymbol{x})\dot{\boldsymbol{\xi}} + \bar{\boldsymbol{b}}(\boldsymbol{x},\boldsymbol{\xi},\boldsymbol{x}_{\mathsf{R}},\boldsymbol{\xi}_{\mathsf{R}},\dot{\boldsymbol{\xi}}_{\mathsf{R}}) = \mathbf{0}. \tag{4.49}$$

The system model with the available control input $\boldsymbol{u}$ has the form of (4.1):

$$\dot{\boldsymbol{x}} = \boldsymbol{A}(\boldsymbol{x})\boldsymbol{\xi}, \quad \boldsymbol{M}(\boldsymbol{x})\dot{\boldsymbol{\xi}} + \boldsymbol{b}(\boldsymbol{x},\boldsymbol{\xi}) = \boldsymbol{B}(\boldsymbol{x})\boldsymbol{u}. \tag{4.50}$$

For a fully actuated system, i.e. $\mathrm{rank}\,\boldsymbol{B} = n$, the combination of (4.49) and (4.50) can be solved for the system input $\boldsymbol{u}$ yielding the required control law:

$$\boldsymbol{u} = \boldsymbol{B}^{-1}\big(\boldsymbol{b} - \boldsymbol{M}\bar{\boldsymbol{M}}^{-1}\bar{\boldsymbol{b}}\big). \tag{4.51}$$

For an underactuated system, i.e. $\mathrm{rank}\,\boldsymbol{B} = p < n$, this is generally not possible.

4.5.1 Control law through static optimization

The idea. If the desired closed loop dynamics (4.49) cannot be achieved exactly, the next best thing is to get "as close as possible" while still obeying the model dynamics (4.50). In order to formalize the "as close as possible" we take again inspiration from mechanics, more precicely from Gauss' principle of least constraint, previously discussed in section 3.2: The free motion is the solution of the desired closed loop (4.49), the optimization metric is the desired closed loop inertia $\bar{\boldsymbol{M}}$ and the constraints are the model kinetics (4.50). Then the control law is the solution of the static optimization problem

$$\begin{array}{rl} \text{minimize} & \bar{\mathcal{G}} \;=\; \frac{1}{2}\|\dot{\boldsymbol{\xi}} + \bar{\boldsymbol{M}}^{-1}\bar{\boldsymbol{b}}\|^2_{\bar{\boldsymbol{M}}} \\ \text{subject to} & \boldsymbol{M}\dot{\boldsymbol{\xi}} + \boldsymbol{b} = \boldsymbol{B}\boldsymbol{u},\; \boldsymbol{u} \in \mathbb{R}^p \end{array} . \tag{4.52}$$

Explicit control law. Elimination of the acceleration $\dot{\boldsymbol{\xi}} = \boldsymbol{M}^{-1}(\boldsymbol{B}\boldsymbol{u} - \boldsymbol{b})$ from (4.52) leads to

$$\begin{aligned} \bar{\mathcal{G}} &= \tfrac{1}{2}\|\boldsymbol{M}^{-1}\boldsymbol{B}\boldsymbol{u} - \underbrace{(\boldsymbol{M}^{-1}\boldsymbol{b} - \bar{\boldsymbol{M}}^{-1}\bar{\boldsymbol{b}})}_{\tilde{\boldsymbol{a}}}\|^2_{\bar{\boldsymbol{M}}} \\ &= \tfrac{1}{2}\boldsymbol{u}^\top \underbrace{\boldsymbol{B}^\top\boldsymbol{M}^{-1}\bar{\boldsymbol{M}}\boldsymbol{M}^{-1}\boldsymbol{B}}_{\boldsymbol{H}}\boldsymbol{u} - \boldsymbol{u}^\top\boldsymbol{B}^\top\boldsymbol{M}^{-1}\bar{\boldsymbol{M}}\tilde{\boldsymbol{a}} + \tfrac{1}{2}\tilde{\boldsymbol{a}}^\top\bar{\boldsymbol{M}}\tilde{\boldsymbol{a}} \\ &= \tfrac{1}{2}\big(\boldsymbol{u} - \underbrace{\boldsymbol{H}^{-1}\boldsymbol{B}^\top\boldsymbol{M}^{-1}\bar{\boldsymbol{M}}\tilde{\boldsymbol{a}}}_{\boldsymbol{u}_0}\big)^\top\boldsymbol{H}\big(\boldsymbol{u} - \underbrace{\boldsymbol{H}^{-1}\boldsymbol{B}^\top\boldsymbol{M}^{-1}\bar{\boldsymbol{M}}\tilde{\boldsymbol{a}}}_{\boldsymbol{u}_0}\big) \\ &\qquad\qquad + \tfrac{1}{2}\tilde{\boldsymbol{a}}^\top\bar{\boldsymbol{M}}\underbrace{\big(\mathbf{I}_n - \boldsymbol{M}^{-1}\boldsymbol{B}\boldsymbol{H}^{-1}\boldsymbol{B}^\top\boldsymbol{M}^{-1}\bar{\boldsymbol{M}}\big)}_{\boldsymbol{P}^\perp}\tilde{\boldsymbol{a}} \\ &= \tfrac{1}{2}\|\boldsymbol{u} - \boldsymbol{u}_0\|^2_{\boldsymbol{H}} + \underbrace{\tfrac{1}{2}\|\boldsymbol{P}^\perp\tilde{\boldsymbol{a}}\|^2_{\bar{\boldsymbol{M}}}}_{\bar{\mathcal{G}}_0} . \end{aligned} \tag{4.53}$$

The control law, i.e. the solution of the minimization problem, is obviously $\boldsymbol{u} = \boldsymbol{u}_0$.

For the special case of a fully actuated system, i.e. $\boldsymbol{B}$ is invertible, the control law simplifies to $\boldsymbol{u}_0 = \boldsymbol{B}^{-1}(\boldsymbol{b} - \boldsymbol{M}\bar{\boldsymbol{M}}^{-1}\bar{\boldsymbol{b}})$ as already stated above. Furthermore, for this case, we have $\boldsymbol{P}^\perp = \boldsymbol{0}$ and consequently $\bar{\mathcal{G}}_0 = 0$.

Feasible closed loop kinetics. Plugging $\boldsymbol{u} = \boldsymbol{u}_0$ into the model (4.50) we obtain the actual closed loop kinetics:

$$\begin{aligned} \boldsymbol{M}\dot{\boldsymbol{\xi}} + \boldsymbol{b} &= \boldsymbol{B}\overbrace{\boldsymbol{H}^{-1}\boldsymbol{B}^\top\boldsymbol{M}^{-1}\bar{\boldsymbol{M}}(\boldsymbol{M}^{-1}\boldsymbol{b} - \bar{\boldsymbol{M}}^{-1}\bar{\boldsymbol{b}})}^{\boldsymbol{u}_0} \\ \Leftrightarrow \qquad \dot{\boldsymbol{\xi}} &= \boldsymbol{M}^{-1}\boldsymbol{B}\boldsymbol{H}^{-1}\boldsymbol{B}^\top\boldsymbol{M}^{-1}\bar{\boldsymbol{M}}(\boldsymbol{M}^{-1}\boldsymbol{b} - \bar{\boldsymbol{M}}^{-1}\bar{\boldsymbol{b}}) - \boldsymbol{M}^{-1}\boldsymbol{b} \\ \Leftrightarrow \qquad \bar{\boldsymbol{M}}\dot{\boldsymbol{\xi}} + \bar{\boldsymbol{b}} &= \underbrace{\bar{\boldsymbol{M}}\boldsymbol{P}^\perp\big(\bar{\boldsymbol{M}}^{-1}\bar{\boldsymbol{b}} - \boldsymbol{M}^{-1}\boldsymbol{b}\big)}_{\tilde{\boldsymbol{b}}} . \end{aligned} \tag{4.54}$$

We may interpret this additional vector[2] $\tilde{\boldsymbol{b}}(\boldsymbol{x}, \boldsymbol{\xi}, \boldsymbol{x}_\mathsf{R}, \boldsymbol{\xi}_\mathsf{R}, \dot{\boldsymbol{\xi}}_\mathsf{R}) \in \mathbb{R}^n$ as a force that makes the closed loop kinetics feasible, i.e. realizable with the available controls. The residual Gaussian constraint is $\bar{\mathcal{G}}_0 = \frac{1}{2}\|\tilde{\boldsymbol{b}}\|^2_{\bar{\boldsymbol{M}}^{-1}}$.

In general, the value $\bar{\mathcal{G}}_0$ is a measure of how much the resulting closed loop differs from the original desired system (4.49). One main goal when parameterizing the controller is to make $\bar{\mathcal{G}}_0$ as small as possible. Unfortunately the form of $\bar{\mathcal{G}}_0$ in (4.54) is not handy, mainly due to rank $\boldsymbol{P}^\perp = n - p$. In the following we like to find a more handy formulation.

4.5.2 Matching condition

Instead of elimiating the accelerations $\dot{\boldsymbol{\xi}}$ we may also eliminate the controls $\boldsymbol{u}$ from (4.52). Let $\boldsymbol{B}^\perp \in \mathbb{R}^{n\times(n-p)}$ be any orthogonal complement to $\boldsymbol{B}$, i.e. rank $\boldsymbol{B}^\perp = n - p$ and $\boldsymbol{B}^\top \boldsymbol{B}^\perp = \boldsymbol{0}$. With this (4.52) is equivalent to

$$\begin{aligned} \text{minimize} \quad & \bar{\mathcal{G}} = \tfrac{1}{2}\|\dot{\boldsymbol{\xi}} + \bar{\boldsymbol{M}}^{-1}\bar{\boldsymbol{b}}\|^2_{\bar{\boldsymbol{M}}} \\ \text{subject to} \quad & (\boldsymbol{B}^\perp)^\top\big(\boldsymbol{M}\dot{\boldsymbol{\xi}} + \boldsymbol{b}\big) = \boldsymbol{0} \end{aligned} . \tag{4.55}$$

Using the method of Lagrangian multipliers with $\mathcal{L} = \bar{\mathcal{G}} + \boldsymbol{\mu}^\top(\boldsymbol{B}^\perp)^\top\big(\boldsymbol{M}\dot{\boldsymbol{\xi}} + \boldsymbol{b}\big)$ leads to the neccessary condition

$$\begin{bmatrix} \frac{\partial \mathcal{L}}{\partial \dot{\boldsymbol{\xi}}} \\ \frac{\partial \mathcal{L}}{\partial \boldsymbol{\mu}} \end{bmatrix} = \begin{bmatrix} \bar{\boldsymbol{M}} & \boldsymbol{M}\boldsymbol{B}^\perp \\ (\boldsymbol{M}\boldsymbol{B}^\perp)^\top & \boldsymbol{0} \end{bmatrix} \begin{bmatrix} \dot{\boldsymbol{\xi}} \\ \boldsymbol{\mu} \end{bmatrix} + \begin{bmatrix} \bar{\boldsymbol{b}} \\ (\boldsymbol{B}^\perp)^\top \boldsymbol{b} \end{bmatrix} = \boldsymbol{0} \tag{4.56}$$

Using blockwise inversion we may solve

$$-\boldsymbol{\mu} = \underbrace{\big((\boldsymbol{M}\boldsymbol{B}^\perp)^\top \bar{\boldsymbol{M}}^{-1} \boldsymbol{M}\boldsymbol{B}^\perp\big)^{-1}}_{\boldsymbol{S}} \underbrace{(\boldsymbol{B}^\perp)^\top(\boldsymbol{M}\bar{\boldsymbol{M}}^{-1}\bar{\boldsymbol{b}} - \boldsymbol{b})}_{\boldsymbol{\lambda}}. \tag{4.57}$$

With this, the feasible closed loop kinetics and the residual Gaussian constraint may be expressed by

$$\bar{\boldsymbol{M}}\dot{\boldsymbol{\xi}} + \bar{\boldsymbol{b}} = \underbrace{\boldsymbol{M}\boldsymbol{B}^\perp \boldsymbol{S}\boldsymbol{\lambda}}_{\tilde{\boldsymbol{b}}}, \qquad \bar{\mathcal{G}}_0 = \tfrac{1}{2}\|\boldsymbol{\lambda}\|^2_{\boldsymbol{S}}. \tag{4.58}$$

It is much simpler to analyse $\boldsymbol{\lambda}$ which has only the dimension of the underactuation $n-p$ instead of $\tilde{\boldsymbol{b}}$ which has the full dimension n of the configuration space. Though it should be stressed that the values of $\bar{\mathcal{G}}_0$ and $\tilde{\boldsymbol{b}}$ are, as derived above, independent of the choice of $\boldsymbol{B}^\perp$.

The best case is, of course, if we achieve

$$\boldsymbol{\lambda} = (\boldsymbol{B}^\perp)^\top(\boldsymbol{M}\bar{\boldsymbol{M}}^{-1}\bar{\boldsymbol{b}} - \boldsymbol{b}) = \boldsymbol{0} \qquad \Rightarrow \qquad \tilde{\boldsymbol{b}} = \boldsymbol{0},\ \bar{\mathcal{G}}_0 = 0 \tag{4.59}$$

i.e. the desired closed loop is realized exactly. An approach based on this is discussed in [Bloch et al., 2000]. A condition similar to (4.59) is therein called the *the matching condition* and is required to be fulfilled exactly. However, the examples for which this approach is demonstrated restricts to stabilization tasks $\boldsymbol{\xi}_\mathsf{R} = \boldsymbol{0}$ for small academic systems.

[2]The coefficients $\tilde{\boldsymbol{b}}$ do indeed transform like a tensor, even though $\boldsymbol{b}$ and $\bar{\boldsymbol{b}}$ do not.

An advantage of the presented approach is that the control law $\boldsymbol{u} = \boldsymbol{u}_0$ is defined independently of whether the matching condition is fulfilled or not. Instead the quantity $\boldsymbol{\lambda}$, which we will call the *matching force* in the following, ensures that the control law is realizable.

4.5.3 Approximations

The matching force (4.59) may become very cumbersome for complex systems and might even be impossible to vanish with the given parameters. It might be instructive to analyse it for particular situations.

Zero error. Assume that the controller tracks the reference perfectly, i.e. $\boldsymbol{x} = \boldsymbol{x}_\mathsf{R}$ and $\boldsymbol{\xi} = \boldsymbol{\xi}_\mathsf{R}$. One may check that for this case the three approaches all yield $\bar{\boldsymbol{b}} = \bar{\boldsymbol{M}}\dot{\boldsymbol{\xi}}_\mathsf{R}$. The resulting matching force $\boldsymbol{\lambda}^{\text{ZeroError}}$ for this special case is

$$\boldsymbol{\lambda}^{\text{ZeroError}} = (\boldsymbol{B}^\perp(\boldsymbol{x}_\mathsf{R}))^\top (\boldsymbol{M}(\boldsymbol{x}_\mathsf{R})\dot{\boldsymbol{\xi}}_\mathsf{R} - \boldsymbol{b}(\boldsymbol{x}_\mathsf{R}, \boldsymbol{\xi}_\mathsf{R})) \tag{4.60}$$

Evidently, this is independent of the closed loop parameters, and should rather be regarded as a constraint on the *reference trajectory* $t \mapsto \boldsymbol{x}_\mathsf{R}(t)$. The condition $\boldsymbol{\lambda}^{\text{ZeroError}} = \boldsymbol{0}$ is essentially the model equation after elimination of the control inputs.

A very useful approach here is to formulate the reference trajectory in terms of a *flat output* [Fliess et al., 1995] of the model. The first step for a systematic construction of a flat output is commonly the elimination of the control inputs (see e.g. [Schlacher and Schöberl, 2007]) i.e. $\boldsymbol{\lambda}^{\text{ZeroError}} = \boldsymbol{0}$.

Small error. Assume that we a small error $\boldsymbol{\varepsilon} = \boldsymbol{A}^+(\boldsymbol{x}_\mathsf{R})(\boldsymbol{x} - \boldsymbol{x}_\mathsf{R})$ to a constant reference $\boldsymbol{\xi}_\mathsf{R} = \boldsymbol{0}$ as already considered in section 4.4. Then the model and the closed loop template may be approximated by

$$\boldsymbol{M}_0\ddot{\boldsymbol{\varepsilon}} + \boldsymbol{D}_0\dot{\boldsymbol{\varepsilon}} + \boldsymbol{K}_0\boldsymbol{\varepsilon} = \boldsymbol{B}(\boldsymbol{x}_\mathsf{R})\Delta\boldsymbol{u}, \tag{4.61a}$$

$$\bar{\boldsymbol{M}}_0\ddot{\boldsymbol{\varepsilon}} + \bar{\boldsymbol{D}}_0\dot{\boldsymbol{\varepsilon}} + \bar{\boldsymbol{K}}_0\boldsymbol{\varepsilon} = \boldsymbol{0} \tag{4.61b}$$

and the matching force $\boldsymbol{\lambda}^{\text{SmallError}}$ for this special case is

$$\begin{aligned}\boldsymbol{\lambda}^{\text{SmallError}} &= (\boldsymbol{B}^\perp(\boldsymbol{x}_\mathsf{R}))^\top \big(\boldsymbol{M}_0\bar{\boldsymbol{M}}_0^{-1}(\bar{\boldsymbol{D}}_0\dot{\boldsymbol{\varepsilon}} + \bar{\boldsymbol{K}}_0\boldsymbol{\varepsilon}) - (\boldsymbol{D}_0\dot{\boldsymbol{\varepsilon}} + \boldsymbol{K}_0\boldsymbol{\varepsilon})\big) \\ &= \underbrace{(\boldsymbol{B}^\perp(\boldsymbol{x}_\mathsf{R}))^\top \big(\boldsymbol{M}_0\bar{\boldsymbol{M}}_0^{-1}\bar{\boldsymbol{D}}_0 - \boldsymbol{D}_0\big)}_{\boldsymbol{\Lambda}_{\boldsymbol{D}}}\dot{\boldsymbol{\varepsilon}} + \underbrace{(\boldsymbol{B}^\perp(\boldsymbol{x}_\mathsf{R}))^\top \big(\boldsymbol{M}_0\bar{\boldsymbol{M}}_0^{-1}\bar{\boldsymbol{K}}_0 - \boldsymbol{K}_0\big)}_{\boldsymbol{\Lambda}_{\boldsymbol{K}}}\boldsymbol{\varepsilon}\end{aligned} \tag{4.62}$$

As $\boldsymbol{\varepsilon}$ and $\dot{\boldsymbol{\varepsilon}}$ can be arbitrary, the matrices $\boldsymbol{\Lambda}_{\boldsymbol{K}}$ and $\boldsymbol{\Lambda}_{\boldsymbol{D}}$ have to vanish, for $\boldsymbol{\lambda}^{\text{SmallError}}$ to vanish. For the following examples it will turn out that we can always find suitable parameters within $\bar{\boldsymbol{M}}_0$, $\bar{\boldsymbol{D}}_0$ and $\bar{\boldsymbol{K}}_0$ such that $\boldsymbol{\Lambda}_{\boldsymbol{K}} = \boldsymbol{\Lambda}_{\boldsymbol{D}} = \boldsymbol{0}$. Thus ensuring that at least the first order approximation of the actual matching force $\boldsymbol{\lambda}$ vanishes.

4.5.4 Systems with input constraints

In most control systems the control inputs $\boldsymbol{u}$ can not take arbitrary values, but due to practical limitations are required to be e.g. $u_a \in [-u_a^{\max}, u_a^{\max}], a = 1, \dots, p$. More generally we assume that the constraints can be written as $\boldsymbol{W}\boldsymbol{u} \leq \boldsymbol{l}$ where the inequality is understood componentwise. Adding this constraint to the original problem (4.52) is

$$\begin{aligned} \text{minimize} \quad & \bar{\mathcal{G}} \;=\; \tfrac{1}{2}\|\dot{\boldsymbol{\xi}} + \bar{\boldsymbol{M}}^{-1}\bar{\boldsymbol{b}}\|^2_{\bar{\boldsymbol{M}}} \\ \text{subject to} \quad & \boldsymbol{M}\dot{\boldsymbol{\xi}} + \boldsymbol{b} = \boldsymbol{B}\boldsymbol{u},\ \boldsymbol{W}\boldsymbol{u} \leq \boldsymbol{l},\ \boldsymbol{u} \in \mathbb{R}^p \end{aligned} \; . \tag{4.63}$$

With the elimination of $\dot{\boldsymbol{\xi}}$ as done in subsection 4.5.1 this is equivalent to

$$\begin{aligned} \text{minimize} \quad & \bar{\mathcal{G}} \;=\; \tfrac{1}{2}\|\boldsymbol{u} - \boldsymbol{u}_0\|^2_{\boldsymbol{H}} \\ \text{subject to} \quad & \boldsymbol{W}\boldsymbol{u} \leq \boldsymbol{l},\ \boldsymbol{u} \in \mathbb{R}^p \end{aligned} \tag{4.64}$$

with $\boldsymbol{H}$ and $\boldsymbol{u}_0$ defined in (4.53).

Given that $\boldsymbol{H} \in \mathbb{SYM}^+(p)$ by construction and the feasible set $\mathbb{U} = \{\boldsymbol{u} \in \mathbb{R}^p \,|\, \boldsymbol{W}\boldsymbol{u} \leq \boldsymbol{l}\}$ is convex, this problem has a unique solution, though it usually has to be computed numerically. For the following simulation results the MATLAB function `quadprog` was used and a C++ implementation of the Active-Set algorithm from [Nocedal and Wright, 2006, Algorithm 16.3] was used for the real-time implementation on the Multicopters.

If $\boldsymbol{u}_0 \in \mathbb{U}$ the solution is obviously $\boldsymbol{u} = \boldsymbol{u}_0$ and is independent of $\boldsymbol{H}$. If this is not the case the matrix $\boldsymbol{H}$ determines which components of $\boldsymbol{u}$ are prioritized. It is crucial to notice that $\boldsymbol{H}$ is not the tuning parameter here, but is computed from the desired system inertia $\bar{\boldsymbol{M}}$ and the model matrices, see (4.53). As evident from (4.63), the actual tuning parameter here is the desired closed loop inertia matrix $\bar{\boldsymbol{M}}$ which determines how the components of the system acceleration $\dot{\boldsymbol{\xi}}$ are prioritized when computing a feasible control force.

4.6 Summary and recipe

We have proposed three approaches for a control law for rigid body systems. Each of them formulated a sightly different template for the desired closed loop dynamics. The actual control law results from its combination with the model dynamics. For a fully actuated system the desired closed loop is achieved exactly. For an underactuated system or in the presence of input constraints one achieves closed loop dynamics that are “as close as possible“ to the desired dynamics in the sense that the resulting acceleration differs the least.

The implementation of the controller is determined by the rigid body parameterization ${}^a_b\mathbf{G}(\boldsymbol{x})$, the kinematics $\dot{\boldsymbol{x}} = \boldsymbol{A}(\boldsymbol{x})\boldsymbol{\xi}$ and the *desired* constitutive parameters ${}^a_b\bar{\mathbf{M}}$, ${}^a_b\bar{\mathbf{D}}$, ${}^a_b\bar{\mathbf{K}}$. It is crucial to note that the resulting controlled system is invariant to the chosen coordinates $\boldsymbol{x}, \boldsymbol{\xi}$ in the same way as the system model: Though the describing equations depend explicitly on the coordinates, the resulting motion of the closed loop system is the same for any choice of coordinates. This can be validated by checking the covariance of the closed loop equations.

What does affect the motion of the controlled system are the constitutive parameters, i.e. the values within ${}^a_b\bar{\mathsf{M}}$, ${}^a_b\bar{\mathsf{D}}$, ${}^a_b\bar{\mathsf{K}}$. These are associated with the rigid bodies and are completely independent of the system coordinates. For the energy based approach, the choice of a transport map might not be unique and consequently might also affect the motion.

THE recipe:

- Modeling: A recipe for the derivation of the equations of motion of a rigid body system was given in subsection 3.4.6:
  - Choose a set of (possibly redundant) configuration coordinates $\boldsymbol{x}(t) \in \mathbb{X} = \{\boldsymbol{x} \in \mathbb{R}^\nu \,|\, \boldsymbol{\phi}(\boldsymbol{x}) = \boldsymbol{0}\}$ and minimal velocity coordinates $\boldsymbol{\xi}(t) \in \mathbb{R}^n$, $n = \dim \mathbb{X}$ that are related by the kinematics matrix $\boldsymbol{A}(\boldsymbol{x}) \in \mathbb{R}^{\nu \times n}$:
  $$\dot{\boldsymbol{x}} = \boldsymbol{A}\boldsymbol{\xi} \tag{4.65a}$$
  - Formulate the rigid body configurations ${}^a_b\mathsf{G}(\boldsymbol{x}) \in \mathbb{SE}(3)$, $a, b = 0, \ldots, N$ in terms of the chosen coordinates. This determines the body Jacobians
  $${}^a_b\boldsymbol{J} = \tfrac{\partial}{\partial \dot{\boldsymbol{x}}} \operatorname{vee}\left({}^a_b\mathsf{G}^{-1} {}^a_b\dot{\mathsf{G}}\right)\boldsymbol{A} \tag{4.65b}$$
  - Compute the model inertia force $\boldsymbol{f}^{\mathrm{M}} = \boldsymbol{M}\dot{\boldsymbol{\xi}} + \boldsymbol{c}$ from the body inertias ${}^0_b\mathsf{M}'$ (see subsection 3.4.2)
  $$\boldsymbol{M} = \sum\nolimits_b {}^0_b\boldsymbol{J}^\top \operatorname{Vee}({}^0_b\mathsf{M}')\, {}^0_b\boldsymbol{J}, \;\; \boldsymbol{c} = \sum\nolimits_b {}^0_b\boldsymbol{J}^\top \big(\operatorname{Vee}({}^0_b\mathsf{M}')\, {}^0_b\dot{\boldsymbol{J}} - \operatorname{ad}^\top_{{}^0_b\boldsymbol{J}\boldsymbol{\xi}} \operatorname{Vee}({}^0_b\mathsf{M}')\, {}^0_b\boldsymbol{J}\big)\boldsymbol{\xi} \tag{4.65c}$$
  - The model kinetics are the balance of the inertia force $\boldsymbol{f}^{\mathrm{M}}$, the force of control inputs $\boldsymbol{B}\boldsymbol{u}$ and whatever other forces $\boldsymbol{f}^{\mathrm{A}}$ may act on the system
  $$\boldsymbol{M}\dot{\boldsymbol{\xi}} + \underbrace{\boldsymbol{c} + \boldsymbol{f}^{\mathrm{A}}}_{\boldsymbol{b}} = \boldsymbol{B}\boldsymbol{u} \tag{4.65d}$$
- Closed loop template
  - The template is computed from the body configurations ${}^a_b\mathsf{G}$, the body Jacobians ${}^a_b\boldsymbol{J}$ and the control parameters ${}^a_b\bar{\mathsf{K}}'$, ${}^a_b\bar{\mathsf{D}}'$, ${}^a_b\bar{\mathsf{M}}'$:
  $$\bar{\boldsymbol{M}} = \sum\nolimits_{a,b} {}^a_b\boldsymbol{J}^\top \operatorname{Vee}({}^a_b\bar{\mathsf{M}}')\, {}^a_b\boldsymbol{J} \tag{4.66a}$$
  $$\bar{\boldsymbol{f}}^{\mathsf{K}} = \sum\nolimits_{a,b} {}^a_b\boldsymbol{J}^\top \operatorname{vee2}\left((\mathbf{I}_4 - {}^a_b\mathsf{G}_{\mathrm{E}}^{-1})\, {}^a_b\bar{\mathsf{K}}'\right) \tag{4.66b}$$
  - particle-based approach (see subsection 4.1.3)
  $$\bar{\boldsymbol{f}}^{\mathsf{D}} = \sum\nolimits_{a,b} {}^a_b\boldsymbol{J}^\top \operatorname{vee2}\left(\left(\operatorname{wed}({}^a_b\boldsymbol{J}(\boldsymbol{x})\boldsymbol{\xi}) - {}^a_b\mathsf{G}_{\mathrm{E}}^{-1} \operatorname{wed}({}^a_b\boldsymbol{J}(\boldsymbol{x}_{\mathsf{R}})\boldsymbol{\xi}_{\mathsf{R}})\right){}^a_b\bar{\mathsf{D}}'\right) \tag{4.66c}$$
  $$\begin{aligned}\bar{\boldsymbol{c}} = \sum\nolimits_{a,b} {}^a_b\boldsymbol{J}^\top \operatorname{vee2}\Big(\big(&\operatorname{wed}({}^a_b\dot{\boldsymbol{J}}\boldsymbol{\xi}) + \operatorname{wed}({}^a_b\boldsymbol{J}\boldsymbol{\xi})^2 \\ &- {}^a_b\mathsf{G}_{\mathrm{E}}^{-1}\big(\operatorname{wed}({}^a_b\boldsymbol{J}_{\mathsf{R}}\dot{\boldsymbol{\xi}}_{\mathsf{R}} + {}^a_b\dot{\boldsymbol{J}}_{\mathsf{R}}\boldsymbol{\xi}_{\mathsf{R}}) + \operatorname{wed}({}^a_b\boldsymbol{J}_{\mathsf{R}}\boldsymbol{\xi}_{\mathsf{R}})^2\big)\big){}^a_b\bar{\mathsf{M}}'\Big)\end{aligned} \tag{4.66d}$$

– body-based approach (see subsection 4.2.2)

$$\bar{\boldsymbol{f}}^{\mathsf{D}} = \sum\nolimits_{a,b} {}^{a}_{b}\boldsymbol{J}^{\top}\operatorname{Vee}({}^{a}_{b}\bar{\mathbf{D}}'){}^{a}_{b}\boldsymbol{\xi}_{\mathrm{E}}, \qquad {}^{a}_{b}\boldsymbol{\xi}_{\mathrm{E}} = {}^{a}_{b}\boldsymbol{J}\boldsymbol{\xi} - \operatorname{Ad}_{{}^{a}_{b}\mathbf{G}_{\mathrm{E}}^{-1}}{}^{a}_{b}\boldsymbol{J}_{\mathsf{R}}\boldsymbol{\xi}_{\mathsf{R}}, \tag{4.66e}$$

$$\begin{aligned}\bar{\boldsymbol{c}} = \sum\nolimits_{a,b} {}^{a}_{b}\boldsymbol{J}^{\top}\big({}^{a}_{b}\bar{\mathbf{M}}({}^{a}_{b}\dot{\boldsymbol{J}}\boldsymbol{\xi} - \operatorname{Ad}_{{}^{a}_{b}\mathbf{G}_{\mathrm{E}}^{-1}}({}^{a}_{b}\boldsymbol{J}_{\mathsf{R}}\dot{\boldsymbol{\xi}}_{\mathsf{R}} + {}^{a}_{b}\dot{\boldsymbol{J}}_{\mathsf{R}}\boldsymbol{\xi}_{\mathsf{R}}) + \operatorname{ad}_{{}^{a}_{b}\boldsymbol{\xi}_{\mathrm{E}}}\operatorname{Ad}_{{}^{a}_{b}\mathbf{G}_{\mathrm{E}}^{-1}}{}^{a}_{b}\boldsymbol{J}_{\mathsf{R}}\boldsymbol{\xi}_{\mathsf{R}})\\ - \operatorname{ad}^{\top}_{{}^{a}_{b}\boldsymbol{\xi}_{\mathrm{E}}}{}^{a}_{b}\bar{\mathbf{M}}\,{}^{a}_{b}\boldsymbol{\xi}_{\mathrm{E}}\big),\end{aligned} \tag{4.66f}$$

– energy-based approach (see subsection 4.3.4, requires the choice of a transport map $\boldsymbol{Q}$)

$$\bar{\boldsymbol{f}}^{\mathsf{D}} = \bar{\boldsymbol{D}}\boldsymbol{\xi}_{\mathrm{E}}, \quad \bar{\boldsymbol{D}} = \sum\nolimits_{a,b} {}^{a}_{b}\boldsymbol{J}^{\top}\operatorname{Vee}({}^{a}_{b}\bar{\mathbf{D}}'){}^{a}_{b}\boldsymbol{J}, \quad \boldsymbol{\xi}_{\mathrm{E}} = \boldsymbol{\xi} - \boldsymbol{Q}\boldsymbol{\xi}_{\mathsf{R}} \tag{4.66g}$$

$$\bar{\boldsymbol{C}} = \sum\nolimits_{a,b} {}^{a}_{b}\boldsymbol{J}^{\top}\big(\operatorname{Vee}({}^{a}_{b}\bar{\mathbf{M}}'){}^{a}_{b}\dot{\boldsymbol{J}} + {}^{a}_{b}\bar{\mathbf{C}}\,{}^{a}_{b}\boldsymbol{J}\big), \quad {}^{a}_{b}\bar{\mathsf{C}}_{pq} = \Gamma_{pqr}({}^{a}_{b}\bar{\mathbf{M}}'){}^{a}_{b}J^{r}_{k}\xi^{k} \tag{4.66h}$$

$$\bar{\boldsymbol{c}} = \bar{\boldsymbol{C}}\boldsymbol{\xi}_{\mathrm{E}} - \bar{\boldsymbol{M}}(\boldsymbol{Q}\dot{\boldsymbol{\xi}}_{\mathsf{R}} + \dot{\boldsymbol{Q}}\boldsymbol{\xi}_{\mathsf{R}}), \tag{4.66i}$$

– The desired closed loop kinetics are

$$\bar{\boldsymbol{M}}\dot{\boldsymbol{\xi}} + \underbrace{\bar{\boldsymbol{c}} + \bar{\boldsymbol{f}}^{\mathsf{D}} + \bar{\boldsymbol{f}}^{\mathsf{K}}}_{\bar{\boldsymbol{b}}} = \boldsymbol{0} \tag{4.66j}$$

- Control law:
  – For the fully actuated case, the desired closed loop is realized by

$$\boldsymbol{u} = \boldsymbol{B}^{-1}(\boldsymbol{b} - \boldsymbol{M}\bar{\boldsymbol{M}}^{-1}\bar{\boldsymbol{b}}) \tag{4.67a}$$

  – In the underactuated case, the acceleration error measured by the Gaussian constraint, is minimized by (see subsection 4.5.1)

$$\boldsymbol{u} = (\boldsymbol{B}^{\top}\boldsymbol{M}^{-1}\bar{\boldsymbol{M}}\boldsymbol{M}^{-1}\boldsymbol{B})^{-1}\boldsymbol{B}^{\top}\boldsymbol{M}^{-1}(\bar{\boldsymbol{M}}\boldsymbol{M}^{-1}\boldsymbol{b} - \bar{\boldsymbol{b}}) \tag{4.67b}$$

Choosing an orthogonal complement $\boldsymbol{B}^{\perp}$ to the input matrix $\boldsymbol{B}$, i.e. $\operatorname{rank}\boldsymbol{B}^{\perp} = n - p$ and $\boldsymbol{B}^{\top}\boldsymbol{B}^{\perp} = \boldsymbol{0}$, the residual acceleration error can be written as $\bar{\mathcal{G}}_0 = \frac{1}{2}\|\boldsymbol{\lambda}\|^2_{\boldsymbol{S}}$ where (see subsection 4.5.2)

$$\boldsymbol{\lambda} = (\boldsymbol{B}^{\perp})^{\top}(\boldsymbol{M}\bar{\boldsymbol{M}}^{-1}\bar{\boldsymbol{b}} - \boldsymbol{b}) = \boldsymbol{0}, \qquad \boldsymbol{S} = \big((\boldsymbol{B}^{\perp})^{\top}\boldsymbol{M}\bar{\boldsymbol{M}}^{-1}\boldsymbol{M}\boldsymbol{B}^{\perp}\big)^{-1} \tag{4.67c}$$

By adjusting the control parameters within $\bar{\boldsymbol{M}}$ and $\bar{\boldsymbol{b}}$ one may try to minimize $\bar{\mathcal{G}}_0$.

4.7 Examples of fully actuated systems

4.7.1 Prismatic joint

Model. Probably the simplest example of a rigid body system is a single body moving in a prismatic joint, i.e. can only translate on one axis as illustrated on the left of Figure 4.2.

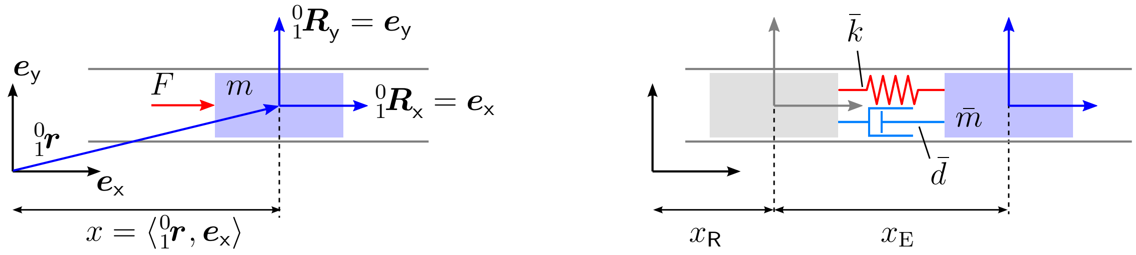

Figure 4.2: Model of a prismatic joint (left) and the closed loop (right)

The corresponding rigid body transformation is simply

$$
{}^0_1\mathbf{G} = \begin{bmatrix} 1 & 0 & 0 & x \\ 0 & 1 & 0 & 0 \\ 0 & 0 & 1 & 0 \\ 0 & 0 & 0 & 1 \end{bmatrix}. \tag{4.68}
$$

With the trivial choice of the velocity coordinate $\boldsymbol{\xi} = \dot{x}$, i.e. $\boldsymbol{A} = 1$, the equation of motion is

$$
m\ddot{x} = F. \tag{4.69}
$$

Closed loop. Due to the geometry of the model, only the controlled total mass ${}^0_1 m$ within the controlled body inertia matrix ${}^0_1\mathbf{M}$ contributes to the controlled kinetics and analog for the dissipation and stiffness. For the sake of readability we drop the body indices for the following examples of single bodies. So the only parameters contributing to the controlled kinetics are $\bar{m}, \bar{d}, \bar{k} \in \mathbb{R} > 0$.

For this example all three proposed control approaches are identical. With the displacement error $x_\mathrm{E} = x - x_\mathsf{R}$ the resulting energies are

$$
\bar{\mathcal{V}} = \tfrac{1}{2}\bar{k}x_\mathrm{E}^2, \qquad \bar{\mathcal{R}} = \tfrac{1}{2}\bar{d}\dot{x}_\mathrm{E}^2, \qquad \bar{\mathcal{T}} = \tfrac{1}{2}\bar{m}\dot{x}_\mathrm{E}^2, \qquad \bar{\mathcal{S}} = \tfrac{1}{2}\bar{m}\ddot{x}_\mathrm{E}^2. \tag{4.70}
$$

The potential has the obvious transport map $\boldsymbol{Q} = 1$ and the resulting closed loop kinetics are

$$
\bar{m}\ddot{x}_\mathrm{E} + \bar{d}\dot{x}_\mathrm{E} + \bar{k}x_\mathrm{E} = 0. \tag{4.71}
$$

The corresponding explicit control law is

$$
F = m\ddot{x}_\mathsf{R} - \tfrac{m\bar{d}}{\bar{m}}\dot{x}_\mathrm{E} - \tfrac{m\bar{k}}{\bar{m}}x_\mathrm{E}. \tag{4.72}
$$

An interpretation of the closed loop is given on the right side of Figure 4.2: The controlled body can be thought as being connected by a spring (stiffness $\bar{k}$) and a damper (viscosity $\bar{d}$) to its reference position x_R. The inertial force $\bar{m}\ddot{x}_\mathrm{E}$ reacts to the error acceleration, i.e. to the acceleration of the body relative to its reference acceleration $\ddot{z}_\mathsf{R}$. One could say the body has an inertia w.r.t. its reference.

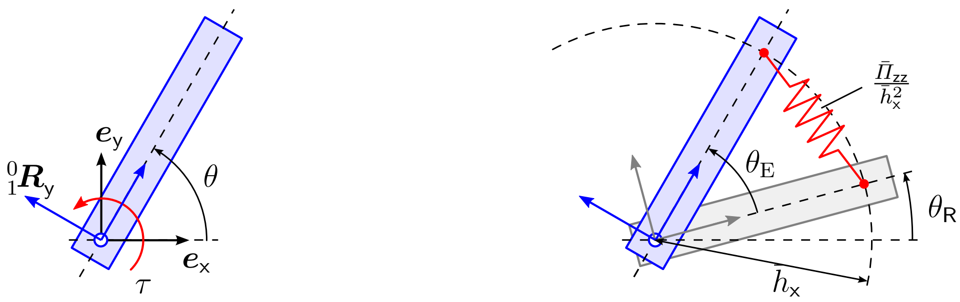

Figure 4.3: Revolute joint: rigid body constrained to rotate about an axis

4.7.2 Revolute joint

Model. Another elemental case is the revolute joint, i.e. a rigid body constrained to rotate about an axis as illustrated on the left side of Figure 4.3. With the joint angle θ the rigid body configuration may be written as

$$^0_1\mathbf{G} = \begin{bmatrix} \cos\theta & -\sin\theta & 0 & 0 \\ \sin\theta & \cos\theta & 0 & 0 \\ 0 & 0 & 1 & 0 \\ 0 & 0 & 0 & 1 \end{bmatrix}. \tag{4.73}$$

With the velocity coordinate $\boldsymbol{\xi} = \dot{\theta}$ the equation of motion is

$$\varTheta_{\mathsf{zz}}\ddot{\theta} = \tau. \tag{4.74}$$

Potential energy. Due to the geometry of the model, only the control parameters $\bar{\varTheta}_{\mathsf{zz}}, \bar{\varUpsilon}_{\mathsf{zz}}, \bar{\varPi}_{\mathsf{zz}} \in \mathbb{R} > 0$ contribute to the closed loop kinetics. With the angle error $\theta_\mathrm{E} = \theta - \theta_\mathsf{R}$ the potential may be written as

$$\bar{\mathcal{V}} = \bar{\varPi}_{\mathsf{zz}}(1 - \cos\theta_\mathrm{E}). \tag{4.75}$$

It has the obvious transport map $\boldsymbol{Q} = 1$. The potential could be realized by attaching a single linear spring with stiffness $\bar{\varPi}_{\mathsf{zz}}/\bar{h}_\mathsf{z}^2$ between desired configuration and actual configuration at a distance $\bar{h}_\mathsf{z}$ as illustrated on the right side of Figure 4.3. This also gives a vivid interpretation of the maximum on the potential at $\theta_\mathrm{E} = \pm\pi$.

Approach 1. The particle based approach leads to the following closed loop kinetics

$$\bar{\varTheta}_{\mathsf{zz}}(\ddot{\theta} - \ddot{\theta}_\mathsf{R}\cos\theta_\mathrm{E} - \dot{\theta}_\mathsf{R}^2\sin\theta_\mathrm{E}) + \bar{\varUpsilon}_{\mathsf{zz}}(\dot{\theta} - \dot{\theta}_\mathsf{R}\cos\theta_\mathrm{E}) + \bar{\varPi}_{\mathsf{zz}}\sin\theta_\mathrm{E} = 0. \tag{4.76}$$

The total energy $\bar{\mathcal{W}}$ and its time derivative are

$$\bar{\mathcal{W}} = \tfrac{1}{2}\bar{\varTheta}_\mathsf{z}(\dot{\theta}^2 - 2\dot{\theta}\dot{\theta}_\mathsf{R}\cos\theta_\mathrm{E} + \dot{\theta}_\mathsf{R}^2) + \bar{\varPi}_\mathsf{z}(1 - \cos\theta_\mathrm{E}), \tag{4.77a}$$

$$\begin{aligned} \tfrac{\mathrm{d}}{\mathrm{d}t}\bar{\mathcal{W}} &= -\bar{\varUpsilon}_\mathsf{z}(\dot{\theta} - \dot{\theta}_\mathsf{R}\cos\theta_\mathrm{E})^2 + \bar{\varPi}_\mathsf{z}\dot{\theta}_\mathsf{R}\sin\theta_\mathrm{E}(\cos\theta_\mathrm{E} - 1) \\ &\quad + \bar{\varTheta}_\mathsf{z}\dot{\theta}_\mathsf{R}\big(\ddot{\theta}_\mathsf{R}(1 - \cos^2\theta_\mathrm{E}) + (\dot{\theta}^2 - \dot{\theta}_\mathsf{R}^2\cos\theta_\mathrm{E})\sin\theta_\mathrm{E}\big) \end{aligned} \tag{4.77b}$$

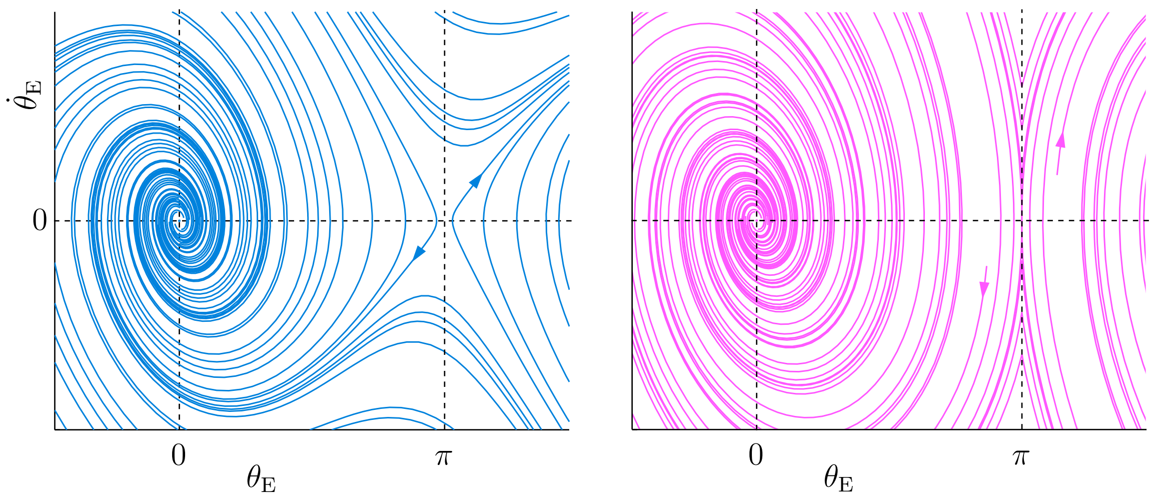

Figure 4.4: Phase plot for (4.79), left, and for (4.80), right

Without further assumptions on the reference trajectory $t \mapsto \theta_{\mathsf{R}}(t)$ the total energy is *not* a Lyapunov function for the closed loop. The linear approximation $\theta \approx \theta_{\mathsf{R}}$ of (4.76) has the characteristic polynomial

$$\lambda^2 + \tfrac{\bar{\Upsilon}_{\mathsf{z}}}{\bar{\Theta}_{\mathsf{z}}}\lambda + \left(\tfrac{\bar{\Pi}_{\mathsf{z}}}{\bar{\Theta}_{\mathsf{z}}} - \dot{\theta}_{\mathsf{R}}^2\right). \tag{4.78}$$

So even for the special case of constant reference velocity $\ddot{\theta}_{\mathsf{R}}(t) = 0$, we need $\frac{\bar{\Pi}_{\mathsf{z}}}{\bar{\Theta}_{\mathsf{z}}} > \dot{\theta}_{\mathsf{R}}^2$ to ensure local stability.

Approach 2 & 3. For this example the body-based and energy-based approaches lead to identical energies and closed loop kinetics:

$$\bar{\mathcal{R}} = \tfrac{1}{2}\bar{\Upsilon}_{\mathsf{zz}}\dot{\theta}_{\mathrm{E}}^2, \qquad \bar{\mathcal{T}} = \tfrac{1}{2}\bar{\Theta}_{\mathsf{zz}}\dot{\theta}_{\mathrm{E}}^2, \qquad \bar{\Theta}_{\mathsf{zz}}\ddot{\theta}_{\mathrm{E}} + \bar{\Upsilon}_{\mathsf{zz}}\dot{\theta}_{\mathrm{E}} + \bar{\Pi}_{\mathsf{zz}}\sin\theta_{\mathrm{E}} = 0. \tag{4.79}$$

The total energy $\bar{\mathcal{W}} = \bar{\mathcal{T}} + \bar{\mathcal{V}}$, $\dot{\bar{\mathcal{W}}} = -2\bar{\mathcal{R}}$ con be used to conclude that the system converges for *almost* all initial conditions $(\theta_{\mathrm{E}}(0), \dot{\theta}_{\mathrm{E}}(0))$. The remaining initial condition $\theta_{\mathrm{E}}(0) = \pm\pi$ and $\dot{\theta}_{\mathrm{E}}(0) = 0$ is instable, see Figure 4.4. As a physical interpretation: the controlled dynamics coincide with the dynamics of a damped physical pendulum.

Linear control. Since the model (4.74) is a linear differential equation, the following linear closed loop equation might also be reasonable

$$\bar{\Theta}_{\mathsf{zz}}\ddot{\theta}_{\mathrm{E}} + \bar{\Upsilon}_{\mathsf{zz}}\dot{\theta}_{\mathrm{E}} + \bar{\Pi}_{\mathsf{zz}}\theta_{\mathrm{E}} = 0. \tag{4.80}$$

The difference between the closed loop (4.79) and (4.80) may be visualized by the corresponding phase plots, see Figure 4.4: The linear control law leads to non-smooth phase curves at $\theta = \pm\pi$, which is the consequence of the linear design for a system whose configuration space is actually $\mathbb{S}^1 \ncong \mathbb{R}$. See [Konz and Rudolph, 2016, sec. 1.2] for a deeper discussion.

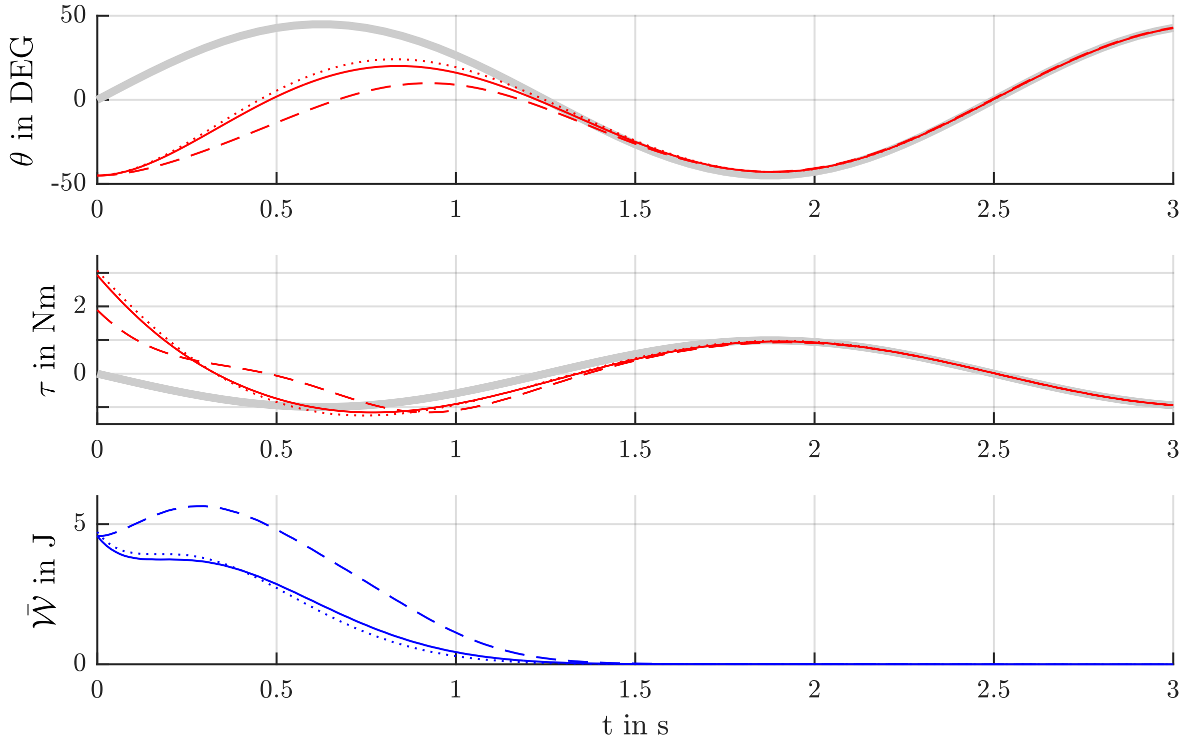

Figure 4.5: Simulation result for the revolute joint: gray line: reference, dashed line: particle-based approach, solid line: energy-based approach, dotted line: linear approach

Simulation results. Figure 4.5 shows simulation results comparing the three different approaches (4.76), (4.79) and (4.80) tracking a reference $\theta_{\mathsf{R}}(t) = \frac{\pi}{2}\sin(\frac{2\pi}{2.5}t)$. Evidently, all approaches fulfill the control objective, i.e. the joint angle θ converges to its reference θ_{R}.

4.7.3 Rigid body orientation

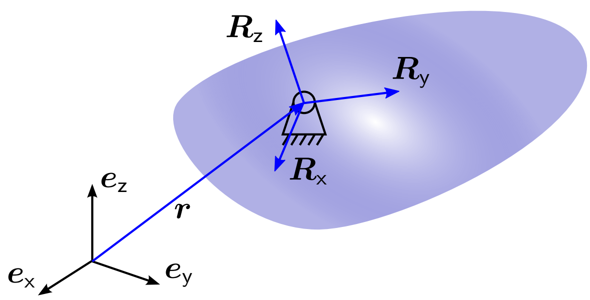

Figure 4.6: rigid body fixed at one point

Model. Consider a rigid body fixed at one point $\boldsymbol{r} = const.$ as illustrated in Figure 4.6. Its orientation may be parameterized by the coefficients of the rotation matrix $\boldsymbol{R} = [\boldsymbol{R}_{\mathsf{x}}, \boldsymbol{R}_{\mathsf{y}}, \boldsymbol{R}_{\mathsf{z}}] \in \mathbb{SO}(3)$. With the angular velocity $\boldsymbol{\omega} = \mathrm{Vee}(\boldsymbol{R}^\top \dot{\boldsymbol{R}})$ as velocity coordinates, the inertia matrix $\boldsymbol{\Theta}$ and the control torques $\boldsymbol{\tau}$ about the body fixed axes, the equations of motion may be written as

$$\dot{\boldsymbol{R}} = \boldsymbol{R}\,\mathrm{wed}(\boldsymbol{\omega}) \qquad \boldsymbol{\Theta}\dot{\boldsymbol{\omega}} + \mathrm{wed}(\boldsymbol{\omega})\boldsymbol{\Theta}\boldsymbol{\omega} = \boldsymbol{\tau}. \tag{4.81}$$

Potential energy. Only the parameters $\bar{\boldsymbol{\Theta}}$, $\bar{\boldsymbol{\Upsilon}}$ and $\bar{\boldsymbol{\Pi}}$ contribute to the closed loop kinetics. Using the attitude error $\boldsymbol{R}_{\mathrm{E}} = \boldsymbol{R}_{\mathsf{R}}^\top \boldsymbol{R}$ the error potential, its differential and Hessian are

$$\bar{\mathcal{V}} = \mathrm{tr}\left(\mathrm{Wed}(\bar{\boldsymbol{\Pi}})(\mathbf{I}_3 - \boldsymbol{R}_{\mathrm{E}})\right), \tag{4.82a}$$

$$\bar{\boldsymbol{f}}^{\mathsf{K}} = \boldsymbol{\nabla}\bar{\mathcal{V}} = \mathrm{vee2}(\mathrm{Wed}(\bar{\boldsymbol{\Pi}})\boldsymbol{R}_{\mathrm{E}}), \tag{4.82b}$$

$$(\boldsymbol{\nabla}^2\bar{\mathcal{V}})|_{\boldsymbol{R}=\boldsymbol{R}_{\mathsf{R}}} = \bar{\boldsymbol{\Pi}}. \tag{4.82c}$$

The potential has the transport map $\boldsymbol{Q} = \boldsymbol{R}_{\mathrm{E}}^\top$, so the velocity error for the energy based approach is $\boldsymbol{\omega}_{\mathrm{E}} = \boldsymbol{\omega} - \boldsymbol{R}_{\mathrm{E}}^\top \boldsymbol{\omega}_{\mathsf{R}}$ which coincides with the body velocity error.

Particle-based approach. The particle-based approach (4.18) leads to

$$\begin{aligned} \bar{\boldsymbol{f}}^{\mathsf{M}} &= \bar{\boldsymbol{\Theta}}\dot{\boldsymbol{\omega}} - \mathrm{Vee}(\boldsymbol{R}_{\mathrm{E}}^\top \mathrm{Wed}(\bar{\boldsymbol{\Theta}}))\boldsymbol{R}_{\mathrm{E}}^\top \dot{\boldsymbol{\omega}}_{\mathsf{R}} \\ &\qquad + \mathrm{wed}(\boldsymbol{\omega})\bar{\boldsymbol{\Theta}}\boldsymbol{\omega} + \mathrm{vee2}(\mathrm{Wed}(\bar{\boldsymbol{\Theta}})\,\mathrm{wed}(\boldsymbol{\omega}_{\mathsf{R}})^2\boldsymbol{R}_{\mathrm{E}}) && (4.83\text{a}) \\ \bar{\boldsymbol{f}}^{\mathsf{D}} &= \bar{\boldsymbol{\Upsilon}}\boldsymbol{\omega} - \mathrm{Vee}(\boldsymbol{R}_{\mathrm{E}}^\top \mathrm{Wed}(\bar{\boldsymbol{\Upsilon}}))\boldsymbol{R}_{\mathrm{E}}^\top \boldsymbol{\omega}_{\mathsf{R}} && (4.83\text{b}) \end{aligned}$$

Body-based approach. The body-based approach (4.26) leads to

$$\bar{\boldsymbol{f}}^{\mathsf{M}} = \bar{\boldsymbol{\Theta}}\dot{\boldsymbol{\omega}}_{\mathrm{E}} + \mathrm{wed}(\boldsymbol{\omega}_{\mathrm{E}})\bar{\boldsymbol{\Theta}}\boldsymbol{\omega}_{\mathrm{E}} \tag{4.84a}$$

$$\bar{\boldsymbol{f}}^{\mathsf{D}} = \bar{\boldsymbol{\Upsilon}}\boldsymbol{\omega}_{\mathrm{E}}. \tag{4.84b}$$

The corresponding control law coincides with the one proposed in [Koditschek, 1989]. The total energy $\bar{\mathcal{W}} = \frac{1}{2}\boldsymbol{\omega}_{\mathrm{E}}^\top \bar{\boldsymbol{\Theta}}\boldsymbol{\omega}_{\mathrm{E}} + \bar{\mathcal{V}}$ with $\dot{\bar{\mathcal{W}}} = -\boldsymbol{\omega}_{\mathrm{E}}^\top \bar{\boldsymbol{\Upsilon}}\boldsymbol{\omega}_{\mathrm{E}}$ serves as a Lyapunov function for the closed loop.

Energy-based approach. For the energy-based approach (4.31) leads to

$$\bar{\boldsymbol{f}}^{\mathsf{M}} = \bar{\boldsymbol{\Theta}}\dot{\boldsymbol{\omega}}_{\mathrm{E}} + \mathrm{wed}(\mathrm{Wed}(\bar{\boldsymbol{\Theta}})\boldsymbol{\omega})\boldsymbol{\omega}_{\mathrm{E}} \tag{4.85a}$$

$$\bar{\boldsymbol{f}}^{\mathsf{D}} = \bar{\boldsymbol{\Upsilon}}\boldsymbol{\omega}_{\mathrm{E}}. \tag{4.85b}$$

The corresponding control law coincides with one proposed in [Bullo and Murray, 1999]. The total energy is the same as the one for the body based approach. The two approaches only differ in the gyroscopic terms.

Linearization. For a small error to the reference we have

$$\boldsymbol{R} = \boldsymbol{R}_{\mathsf{R}} + \boldsymbol{R}_{\mathsf{R}}\,\mathrm{wed}(\boldsymbol{\varepsilon}), \qquad \boldsymbol{\omega} = \boldsymbol{\omega}_{\mathsf{R}} + \dot{\boldsymbol{\varepsilon}}, \qquad \bar{\boldsymbol{\Theta}}\ddot{\boldsymbol{\varepsilon}} + \bar{\boldsymbol{\Upsilon}}\dot{\boldsymbol{\varepsilon}} + \bar{\boldsymbol{\Pi}}\boldsymbol{\varepsilon} = 0. \tag{4.86}$$

4.7.4 Planar rigid body

A planar rigid body is a free rigid body in two dimensional space, i.e. it can translate in two dimensions and rotate about an perpendicular axis as illustrated in Figure 4.7. The model equations as well as the closed loop equations could be directly derived from the three dimensional rigid body by setting e.g. $v_{\mathsf{z}} = 0$, $\omega_{\mathsf{x}} = \omega_{\mathsf{y}} = 0$ and removing the trivial equations. However it might be still instructive to display the resulting equations.

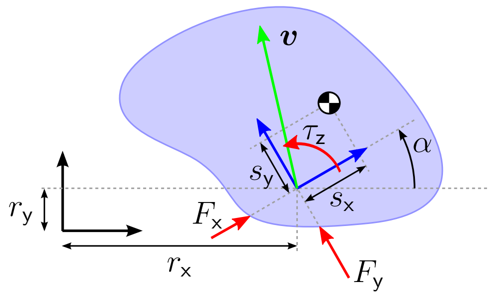

Figure 4.7: model of the planar rigid body

Coordinates and kinematics. As configuration coordinates $\boldsymbol{x}$ we use the position $r_{\mathsf{x}}, r_{\mathsf{y}}$ and the sine s_α and cosine c_α of the angle α. Consequently we have to impose the constraint $\mathrm{c}_\alpha^2 + \mathrm{s}_\alpha^2 - 1 = 0$ on the configuration coordinates. As velocity coordinates $\boldsymbol{\xi}$ we use the components $v_{\mathsf{x}}, v_{\mathsf{y}}$ of the translational velocity w.r.t. the body fixed frame as illustrated in Figure 4.7 and the angular velocity $\omega_{\mathsf{z}} = \dot{\alpha}$. This kinematic relation is

$$\frac{\mathrm{d}}{\mathrm{d}t}\underbrace{\begin{bmatrix} r_{\mathsf{x}} \\ r_{\mathsf{y}} \\ \mathrm{s}_\alpha \\ \mathrm{c}_\alpha \end{bmatrix}}_{\boldsymbol{x}} = \underbrace{\begin{bmatrix} \mathrm{c}_\alpha & -\mathrm{s}_\alpha & 0 \\ \mathrm{s}_\alpha & \mathrm{c}_\alpha & 0 \\ 0 & 0 & \mathrm{c}_\alpha \\ 0 & 0 & -\mathrm{s}_\alpha \end{bmatrix}}_{\boldsymbol{A}} \underbrace{\begin{bmatrix} v_{\mathsf{x}} \\ v_{\mathsf{y}} \\ \omega_{\mathsf{z}} \end{bmatrix}}_{\boldsymbol{\xi}} \tag{4.87}$$

The rigid body configuration ${}^0_1\mathbf{G}$ and the resulting body Jacobian ${}^0_1\boldsymbol{J}$ w.r.t. the chosen velocity coordinates are

$${}^0_1\mathbf{G} = \begin{bmatrix} \mathrm{c}_\alpha & -\mathrm{s}_\alpha & 0 & r_{\mathsf{x}} \\ \mathrm{s}_\alpha & \mathrm{c}_\alpha & 0 & r_{\mathsf{y}} \\ 0 & 0 & 1 & 0 \\ 0 & 0 & 0 & 1 \end{bmatrix}, \qquad {}^0_1\boldsymbol{J} = \begin{bmatrix} 1 & 0 & 0 \\ 0 & 1 & 0 \\ 0 & 0 & 0 \\ 0 & 0 & 0 \\ 0 & 0 & 0 \\ 0 & 0 & 1 \end{bmatrix} \tag{4.88}$$

Kinetic equation. Let the rigid body have the total mass m, the moment of inertia Θ_{z} and the coordinates $s_{\mathsf{x}}, s_{\mathsf{y}}$ of the center of mass w.r.t. the body fixed frame. As control input consider the forces $F_{\mathsf{x}}, F_{\mathsf{y}}$ and the torque τ_{z} as displayed in Figure 4.7. The resulting kinetic equation is

$$\underbrace{\begin{bmatrix} m & 0 & -ms_{\mathsf{y}} \\ 0 & m & ms_{\mathsf{x}} \\ -ms_{\mathsf{y}} & ms_{\mathsf{x}} & \Theta_{\mathsf{z}} \end{bmatrix}}_{\boldsymbol{M}} \underbrace{\begin{bmatrix} \dot{v}_{\mathsf{x}} \\ \dot{v}_{\mathsf{y}} \\ \dot{\omega}_{\mathsf{z}} \end{bmatrix}}_{\dot{\boldsymbol{\xi}}} + \begin{bmatrix} -m(v_{\mathsf{y}} + s_{\mathsf{x}}\omega_{\mathsf{z}})\omega_{\mathsf{z}} \\ m(v_{\mathsf{x}} - s_{\mathsf{y}}\omega_{\mathsf{z}})\omega_{\mathsf{z}} \\ m(s_{\mathsf{x}}v_{\mathsf{x}} + s_{\mathsf{y}}v_{\mathsf{y}})\omega_{\mathsf{z}} \end{bmatrix} = \underbrace{\begin{bmatrix} F_{\mathsf{x}} \\ F_{\mathsf{y}} \\ \tau_{\mathsf{z}} \end{bmatrix}}_{\boldsymbol{u}}. \tag{4.89}$$

Control parameters. For the controlled kinetics we chose the following non-zero parameters

$$ {}^0_1\bar{m},\, {}^0_1\bar{d},\, {}^0_1\bar{k} \in \mathbb{R}^+, \quad {}^0_1\bar{s}_{\mathsf{x}},\, {}^0_1\bar{s}_{\mathsf{y}},\, {}^0_1\bar{l}_{\mathsf{x}},\, {}^0_1\bar{l}_{\mathsf{y}},\, {}^0_1\bar{h}_{\mathsf{x}},\, {}^0_1\bar{h}_{\mathsf{y}} \in \mathbb{R}, \quad {}^0_1\bar{\Theta}_{\mathsf{z}},\, {}^0_1\bar{\Upsilon}_{\mathsf{z}},\, {}^0_1\bar{\Pi}_{\mathsf{z}} \in \mathbb{R}^+. \tag{4.90}$$

Since all parameters are associated with the configuration ${}^0_1\mathbf{G}$, we drop the indices in the following, i.e. $\bar{m} = {}^0_1\bar{m}$.

Potential. The potential, resulting from the chosen parameters (4.90), and its derivatives are

$$\begin{aligned}
\bar{\mathcal{V}} &= \tfrac{1}{2}\bar{k}(r_{\mathsf{x}}-r_{\mathsf{xR}})^2 + \tfrac{1}{2}\bar{k}(r_{\mathsf{y}}-r_{\mathsf{yR}})^2 + \bar{\Pi}_{\mathsf{z}}(1-\mathrm{c}_{\alpha_\mathrm{E}}) \\
&\quad + \bar{k}\bar{h}_{\mathsf{x}}(\mathrm{c}_\alpha-\mathrm{c}_{\alpha_\mathsf{R}})(r_{\mathsf{x}}-r_{\mathsf{xR}}) - \bar{k}\bar{h}_{\mathsf{y}}(\mathrm{s}_\alpha-\mathrm{s}_{\alpha_\mathsf{R}})(r_{\mathsf{x}}-r_{\mathsf{xR}}) \\
&\quad + \bar{k}\bar{h}_{\mathsf{y}}(\mathrm{c}_\alpha-\mathrm{c}_{\alpha_\mathsf{R}})(r_{\mathsf{y}}-r_{\mathsf{yR}}) - \bar{k}\bar{h}_{\mathsf{x}}(\mathrm{s}_\alpha-\mathrm{s}_{\alpha_\mathsf{R}})(r_{\mathsf{y}}-r_{\mathsf{yR}}) && (4.91\text{a}) \\
\boldsymbol{\nabla}\bar{\mathcal{V}} &= \begin{bmatrix} \bar{k}(\mathrm{c}_\alpha(r_{\mathsf{x}}-r_{\mathsf{xR}}) + \mathrm{s}_\alpha(r_{\mathsf{y}}-r_{\mathsf{yR}}) + \bar{h}_{\mathsf{x}}(1-\mathrm{c}_{\alpha_\mathrm{E}}) - \bar{h}_{\mathsf{y}}\mathrm{s}_{\alpha_\mathrm{E}}) \\ \bar{k}(-\mathrm{s}_\alpha(r_{\mathsf{x}}-r_{\mathsf{xR}}) + \mathrm{c}_\alpha(r_{\mathsf{y}}-r_{\mathsf{yR}}) + \bar{h}_{\mathsf{x}}\mathrm{s}_{\alpha_\mathrm{E}} + \bar{h}_{\mathsf{y}}(1-\mathrm{c}_{\alpha_\mathrm{E}})) \\ \bar{k}((\bar{h}_{\mathsf{x}}\mathrm{c}_\alpha + \bar{h}_{\mathsf{y}}\mathrm{s}_\alpha)(r_{\mathsf{y}}-r_{\mathsf{yR}}) - (\bar{h}_{\mathsf{y}}\mathrm{c}_\alpha + \bar{h}_{\mathsf{x}}\mathrm{s}_\alpha)(r_{\mathsf{x}}-r_{\mathsf{xR}})) + \bar{\Pi}_{\mathsf{z}}\mathrm{s}_{\alpha_\mathrm{E}} \end{bmatrix} && (4.91\text{b}) \\
\boldsymbol{\nabla}^2\bar{\mathcal{V}}|_{\mathsf{R}} &= \begin{bmatrix} \bar{k} & 0 & -\bar{k}\bar{h}_{\mathsf{y}} \\ 0 & \bar{k} & \bar{k}\bar{h}_{\mathsf{x}} \\ -\bar{k}\bar{h}_{\mathsf{y}} & \bar{k}\bar{h}_{\mathsf{x}} & \bar{\Pi}_{\mathsf{z}} \end{bmatrix} && (4.91\text{c})
\end{aligned}$$

The sine and cosine of the angle error $\alpha - \alpha_{\mathsf{R}}$ are introduced just for readability

$$\mathrm{c}_{\alpha_\mathrm{E}} = \mathrm{c}_\alpha\mathrm{c}_{\alpha_\mathsf{R}} + \mathrm{s}_\alpha\mathrm{s}_{\alpha_\mathsf{R}} = \cos(\alpha-\alpha_{\mathsf{R}}), \qquad \mathrm{s}_{\alpha_\mathrm{E}} = \mathrm{s}_\alpha\mathrm{c}_{\alpha_\mathsf{R}} - \mathrm{c}_\alpha\mathrm{s}_{\alpha_\mathsf{R}} = \sin(\alpha-\alpha_{\mathsf{R}}). \tag{4.92}$$

From the Hessian $\boldsymbol{\nabla}^2\bar{\mathcal{V}}|_{\mathsf{R}}$ at the critical point $\boldsymbol{x} = \boldsymbol{x}_{\mathsf{R}}$ one can see that (local) positive definiteness requires $\bar{\Pi}_{\mathsf{z}} > \bar{k}(\bar{h}_{\mathsf{x}}^2 + \bar{h}_{\mathsf{y}}^2)$. We will encounter the analog requirement for the controlled moment of inertia $\bar{\Theta}_{\mathsf{z}}$ and damping $\bar{\Upsilon}_{\mathsf{z}}$.

A transport map for (4.91a) is given by[3]

$$\underbrace{\begin{bmatrix} v_{\mathsf{xE}} \\ v_{\mathsf{yE}} \\ \omega_{\mathsf{zE}} \end{bmatrix}}_{\boldsymbol{\xi}_\mathrm{E}} = \underbrace{\begin{bmatrix} v_{\mathsf{x}} \\ v_{\mathsf{y}} \\ \omega_{\mathsf{z}} \end{bmatrix}}_{\boldsymbol{\xi}} - \underbrace{\begin{bmatrix} \mathrm{c}_{\alpha_\mathrm{E}} & \mathrm{s}_{\alpha_\mathrm{E}} & \mathrm{s}_\alpha(r_{\mathsf{x}}-r_{\mathsf{xR}}) - \mathrm{c}_\alpha(r_{\mathsf{y}}-r_{\mathsf{yR}}) \\ -\mathrm{s}_{\alpha_\mathrm{E}} & \mathrm{c}_{\alpha_\mathrm{E}} & \mathrm{c}_\alpha(r_{\mathsf{x}}-r_{\mathsf{xR}}) + \mathrm{s}_\alpha(r_{\mathsf{y}}-r_{\mathsf{yR}}) \\ 0 & 0 & 1 \end{bmatrix}}_{\boldsymbol{Q}} \underbrace{\begin{bmatrix} v_{\mathsf{xR}} \\ v_{\mathsf{yR}} \\ \omega_{\mathsf{zR}} \end{bmatrix}}_{\boldsymbol{\xi}_{\mathsf{R}}}. \tag{4.93}$$

[3] An alternative transport map corresponding to (4.43) is

$$\boldsymbol{Q} = \begin{bmatrix} \mathrm{c}_{\alpha_\mathrm{E}} & \mathrm{s}_{\alpha_\mathrm{E}} & \bar{h}_{\mathsf{x}}\mathrm{s}_{\alpha_\mathrm{E}} - \bar{h}_{\mathsf{y}}(\mathrm{c}_{\alpha_\mathrm{E}} - 1) \\ -\mathrm{s}_{\alpha_\mathrm{E}} & \mathrm{c}_{\alpha_\mathrm{E}} & \bar{h}_{\mathsf{x}}(\mathrm{c}_{\alpha_\mathrm{E}} - 1) + \bar{h}_{\mathsf{y}}\mathrm{s}_{\alpha_\mathrm{E}} \\ 0 & 0 & 1 \end{bmatrix}. \tag{4.94}$$

Particle-based approach. The damping and inertia force using the particle based approach are:

$$\bar{\boldsymbol{f}}^{\mathsf{D}} = \underbrace{\begin{bmatrix} \bar{d} & 0 & -\bar{d}\,\bar{l}_{\mathsf{y}} \\ 0 & \bar{d} & \bar{d}\,\bar{l}_{\mathsf{x}} \\ -\bar{d}\,\bar{l}_{\mathsf{y}} & \bar{d}\,\bar{l}_{\mathsf{x}} & \bar{\varUpsilon}_{\mathsf{z}} \end{bmatrix}}_{\boldsymbol{D}} \underbrace{\begin{bmatrix} v_{\mathsf{x}} \\ v_{\mathsf{y}} \\ \omega_{\mathsf{z}} \end{bmatrix}}_{\boldsymbol{\xi}} - \begin{bmatrix} \bar{d}\mathrm{c}_{\alpha_{\mathrm{E}}} & \bar{d}\mathrm{s}_{\alpha_{\mathrm{E}}} & \bar{d}(\bar{l}_{\mathsf{x}}\mathrm{s}_{\alpha_{\mathrm{E}}} - \bar{l}_{\mathsf{y}}\mathrm{c}_{\alpha_{\mathrm{E}}}) \\ -\bar{d}\mathrm{s}_{\alpha_{\mathrm{E}}} & \bar{d}\mathrm{c}_{\alpha_{\mathrm{E}}} & \bar{d}(\bar{l}_{\mathsf{x}}\mathrm{c}_{\alpha_{\mathrm{E}}} + \bar{l}_{\mathsf{y}}\mathrm{s}_{\alpha_{\mathrm{E}}}) \\ -\bar{d}(\bar{l}_{\mathsf{x}}\mathrm{s}_{\alpha_{\mathrm{E}}} + \bar{l}_{\mathsf{y}}\mathrm{c}_{\alpha_{\mathrm{E}}}) & \bar{d}(\bar{l}_{\mathsf{x}}\mathrm{c}_{\alpha_{\mathrm{E}}} - \bar{l}_{\mathsf{y}}\mathrm{s}_{\alpha_{\mathrm{E}}}) & \bar{\varUpsilon}_{\mathsf{z}}\mathrm{c}_{\alpha_{\mathrm{E}}} \end{bmatrix} \underbrace{\begin{bmatrix} v_{\mathsf{xR}} \\ v_{\mathsf{yR}} \\ \omega_{\mathsf{zR}} \end{bmatrix}}_{\boldsymbol{\xi}_{\mathsf{R}}}, \tag{4.95a}$$

$$\bar{\boldsymbol{f}}^{\mathsf{M}} = \underbrace{\begin{bmatrix} \bar{m} & 0 & -\bar{m}\,\bar{s}_{\mathsf{y}} \\ 0 & \bar{m} & \bar{m}\,\bar{s}_{\mathsf{x}} \\ -\bar{m}\,\bar{s}_{\mathsf{y}} & \bar{m}\,\bar{s}_{\mathsf{x}} & \bar{\varUpsilon}_{\mathsf{z}} \end{bmatrix}}_{\boldsymbol{D}} \underbrace{\begin{bmatrix} \dot{v}_{\mathsf{x}} \\ \dot{v}_{\mathsf{y}} \\ \dot{\omega}_{\mathsf{z}} \end{bmatrix}}_{\dot{\boldsymbol{\xi}}} + \begin{bmatrix} -\bar{m}(v_{\mathsf{y}} + \bar{s}_{\mathsf{x}}\omega_{\mathsf{z}})\omega_{\mathsf{z}} \\ \bar{m}(v_{\mathsf{x}} - \bar{s}_{\mathsf{y}}\omega_{\mathsf{z}})\omega_{\mathsf{z}} \\ \bar{m}(\bar{s}_{\mathsf{x}}v_{\mathsf{x}} + \bar{s}_{\mathsf{y}}v_{\mathsf{y}})\omega_{\mathsf{z}} \end{bmatrix}$$
$$- \begin{bmatrix} \bar{m}\mathrm{c}_{\alpha_{\mathrm{E}}} & \bar{m}\mathrm{s}_{\alpha_{\mathrm{E}}} & \bar{m}(\bar{s}_{\mathsf{x}}\mathrm{s}_{\alpha_{\mathrm{E}}} - \bar{s}_{\mathsf{y}}\mathrm{c}_{\alpha_{\mathrm{E}}}) \\ -\bar{m}\mathrm{s}_{\alpha_{\mathrm{E}}} & \bar{m}\mathrm{c}_{\alpha_{\mathrm{E}}} & \bar{m}(\bar{s}_{\mathsf{x}}\mathrm{c}_{\alpha_{\mathrm{E}}} + \bar{s}_{\mathsf{y}}\mathrm{s}_{\alpha_{\mathrm{E}}}) \\ -\bar{m}(\bar{s}_{\mathsf{x}}\mathrm{s}_{\alpha_{\mathrm{E}}} + \bar{s}_{\mathsf{y}}\mathrm{c}_{\alpha_{\mathrm{E}}}) & \bar{m}(\bar{s}_{\mathsf{x}}\mathrm{c}_{\alpha_{\mathrm{E}}} - \bar{s}_{\mathsf{y}}\mathrm{s}_{\alpha_{\mathrm{E}}}) & \bar{\varUpsilon}_{\mathsf{z}}\mathrm{c}_{\alpha_{\mathrm{E}}} \end{bmatrix} \underbrace{\begin{bmatrix} \dot{v}_{\mathsf{xR}} \\ \dot{v}_{\mathsf{yR}} \\ \dot{\omega}_{\mathsf{zR}} \end{bmatrix}}_{\dot{\boldsymbol{\xi}}_{\mathsf{R}}}$$
$$- \begin{bmatrix} -\bar{m}((v_{\mathsf{yR}} + \bar{s}_{\mathsf{x}}\omega_{\mathsf{zR}})\mathrm{c}_{\alpha_{\mathrm{E}}} - (v_{\mathsf{xR}} - \bar{s}_{\mathsf{y}}\omega_{\mathsf{zR}})\mathrm{s}_{\alpha_{\mathrm{E}}})\omega_{\mathsf{zR}} \\ \bar{m}((v_{\mathsf{yR}} + \bar{s}_{\mathsf{x}}\omega_{\mathsf{zR}})\mathrm{s}_{\alpha_{\mathrm{E}}} + (v_{\mathsf{xR}} - \bar{s}_{\mathsf{y}}\omega_{\mathsf{zR}})\mathrm{c}_{\alpha_{\mathrm{E}}})\omega_{\mathsf{zR}} \\ \bar{m}((\bar{s}_{\mathsf{x}}v_{\mathsf{xR}} + \bar{s}_{\mathsf{y}}v_{\mathsf{yR}})\mathrm{c}_{\alpha_{\mathrm{E}}} - (\bar{s}_{\mathsf{y}}v_{\mathsf{xR}} - \bar{s}_{\mathsf{x}}v_{\mathsf{yR}})\mathrm{s}_{\alpha_{\mathrm{E}}})\omega_{\mathsf{zR}} + \bar{\varTheta}_{\mathsf{z}}\mathrm{s}_{\alpha_{\mathrm{E}}}\omega_{\mathsf{zR}}^2 \end{bmatrix}. \tag{4.95b}$$

The corresponding total energy as defined in (4.5), is not a Lyapunov function for the closed loop.

Body-based approach. The damping and inertia force using the body-based approach are:

$$\bar{\boldsymbol{f}}^{\mathsf{D}} = \underbrace{\begin{bmatrix} \bar{d} & 0 & -\bar{d}\,\bar{l}_{\mathsf{y}} \\ 0 & \bar{d} & \bar{d}\,\bar{l}_{\mathsf{x}} \\ -\bar{d}\,\bar{l}_{\mathsf{y}} & \bar{d}\,\bar{l}_{\mathsf{x}} & \bar{\varUpsilon}_{\mathsf{z}} \end{bmatrix}}_{\boldsymbol{D}} \underbrace{\begin{bmatrix} v_{\mathsf{x}\mathrm{E}} \\ v_{\mathsf{y}\mathrm{E}} \\ \omega_{\mathsf{z}\mathrm{E}} \end{bmatrix}}_{\boldsymbol{\xi}_{\mathrm{E}}} \tag{4.96a}$$

$$\bar{\boldsymbol{f}}^{\mathsf{M}} = \underbrace{\begin{bmatrix} \bar{m} & 0 & -\bar{m}\bar{s}_{\mathsf{y}} \\ 0 & \bar{m} & \bar{m}\bar{s}_{\mathsf{x}} \\ -\bar{m}\bar{s}_{\mathsf{y}} & \bar{m}\bar{s}_{\mathsf{x}} & \bar{\varTheta}_{\mathsf{z}} \end{bmatrix}}_{\boldsymbol{M}} \underbrace{\begin{bmatrix} \dot{v}_{\mathsf{x}\mathrm{E}} \\ \dot{v}_{\mathsf{y}\mathrm{E}} \\ \dot{\omega}_{\mathsf{z}\mathrm{E}} \end{bmatrix}}_{\dot{\boldsymbol{\xi}}_{\mathrm{E}}} + \begin{bmatrix} 0 & -\bar{m}\omega_{\mathsf{z}\mathrm{E}} & -\bar{m}\bar{s}_{\mathsf{x}}\omega_{\mathsf{z}\mathrm{E}} \\ \bar{m}\omega_{\mathsf{z}\mathrm{E}} & 0 & -\bar{m}\bar{s}_{\mathsf{y}}\omega_{\mathsf{z}\mathrm{E}} \\ \bar{m}\bar{s}_{\mathsf{x}}\omega_{\mathsf{z}\mathrm{E}} & \bar{m}\bar{s}_{\mathsf{y}}\omega_{\mathsf{z}\mathrm{E}} & 0 \end{bmatrix} \begin{bmatrix} v_{\mathsf{x}\mathrm{E}} \\ v_{\mathsf{y}\mathrm{E}} \\ \omega_{\mathsf{z}\mathrm{E}} \end{bmatrix} \tag{4.96b}$$

where the velocity error $\boldsymbol{\xi}_{\mathrm{E}}$ was defined in (4.93). The total energy $\bar{\mathcal{W}} = \frac{1}{2}\boldsymbol{\xi}_{\mathrm{E}}^{\top}\boldsymbol{M}\boldsymbol{\xi}_{\mathrm{E}} + \bar{\mathcal{V}}$ is a Lyapunov function for the closed loop.

Energy-based approach. The damping and inertia forces using the energy-based approach are:

$$\bar{\boldsymbol{f}}^{\mathsf{D}} = \underbrace{\begin{bmatrix} \bar{d} & 0 & -\bar{d}\,\bar{l}_{\mathsf{y}} \\ 0 & \bar{d} & \bar{d}\,\bar{l}_{\mathsf{x}} \\ -\bar{d}\,\bar{l}_{\mathsf{y}} & \bar{d}\,\bar{l}_{\mathsf{x}} & \bar{\Upsilon}_{\mathsf{z}} \end{bmatrix}}_{\boldsymbol{D}} \underbrace{\begin{bmatrix} v_{\mathsf{x}\mathrm{E}} \\ v_{\mathsf{y}\mathrm{E}} \\ \omega_{\mathsf{z}\mathrm{E}} \end{bmatrix}}_{\boldsymbol{\xi}_{\mathrm{E}}}, \tag{4.97a}$$

$$\bar{\boldsymbol{f}}^{\mathsf{M}} = \underbrace{\begin{bmatrix} \bar{m} & 0 & -\bar{m}\bar{s}_{\mathsf{y}} \\ 0 & \bar{m} & \bar{m}\bar{s}_{\mathsf{x}} \\ -\bar{m}\bar{s}_{\mathsf{y}} & \bar{m}\bar{s}_{\mathsf{x}} & \bar{\Theta}_{\mathsf{z}} \end{bmatrix}}_{\boldsymbol{M}} \underbrace{\begin{bmatrix} \dot{v}_{\mathsf{x}\mathrm{E}} \\ \dot{v}_{\mathsf{y}\mathrm{E}} \\ \dot{\omega}_{\mathsf{z}\mathrm{E}} \end{bmatrix}}_{\dot{\boldsymbol{\xi}}_{\mathrm{E}}} + \begin{bmatrix} 0 & -\bar{m}\omega_{\mathsf{z}} & -\bar{m}\bar{s}_{\mathsf{x}}\omega_{\mathsf{z}} \\ \bar{m}\omega_{\mathsf{z}} & 0 & -\bar{m}\bar{s}_{\mathsf{y}}\omega_{\mathsf{z}} \\ \bar{m}\bar{s}_{\mathsf{x}}\omega_{\mathsf{z}} & \bar{m}\bar{s}_{\mathsf{y}}\omega_{\mathsf{z}} & 0 \end{bmatrix} \begin{bmatrix} v_{\mathsf{x}\mathrm{E}} \\ v_{\mathsf{y}\mathrm{E}} \\ \omega_{\mathsf{z}\mathrm{E}} \end{bmatrix}. \tag{4.97b}$$

The total energy $\bar{\mathcal{W}} = \frac{1}{2}\boldsymbol{\xi}_{\mathrm{E}}^{\top}\boldsymbol{M}\boldsymbol{\xi}_{\mathrm{E}} + \bar{\mathcal{V}}$ coincides with the total energy for the body-based approach and is a Lyapunov function for this closed loop as well. Note that the two approaches do differ in the gyroscopic terms, so do lead to different solutions of the closed loop dynamics.

Simulation result. In subsection 4.7.5 we will give and discuss a simulation result for the special parameter choice $\bar{s}_{\mathsf{x}} = \bar{l}_{\mathsf{x}} = \bar{h}_{\mathsf{x}} = 0$ and $\bar{s}_{\mathsf{y}} = \bar{l}_{\mathsf{y}} = \bar{h}_{\mathsf{y}} = 0$.

4.7.5 Free rigid body: decoupling of translational and rotational motion

The closed loop equations for a (free) three dimensional rigid body were given in subsection 4.1.2, subsection 4.2.1 and subsection 4.3.3. The reduced equations for the planar case were given in subsection 4.7.4. For most applications we like to *decouple* the translational and the rotational motion of the body.

Observing the closed loop equations one can see immediately that the coupling terms vanish if $\bar{\boldsymbol{s}} = \bar{\boldsymbol{l}} = \bar{\boldsymbol{h}} = \boldsymbol{0}$, i.e. the the chosen body fixed point $\boldsymbol{r}$ coincides with the center of mass, damping and stiffness. Then the rotational dynamics are identical to the closed loop given in subsection 4.7.3 (subsection 4.7.2 for the planar case), so are indeed decoupled/independent from the translational motion.

Translational dynamics. For the translational dynamics the situation is more difficult: Introduce $\boldsymbol{e} = \boldsymbol{r} - \boldsymbol{r}_{\mathsf{R}}$ as the components of the position error w.r.t. the inertial frame and $\boldsymbol{r}_{\mathrm{E}} = \boldsymbol{R}_{\mathsf{R}}^{\top}(\boldsymbol{r} - \boldsymbol{r}_{\mathsf{R}})$ as the components w.r.t. the reference frame. The translational dynamics for the different approaches and given transport map are equivalent to

particle-based:	$\bar{m}\ddot{\boldsymbol{e}} + \bar{d}\dot{\boldsymbol{e}} + \bar{k}\boldsymbol{e} = \boldsymbol{0}$	(4.98a)
body-based:	$\bar{m}\ddot{\boldsymbol{r}}_{\mathrm{E}} + \bar{d}\dot{\boldsymbol{r}}_{\mathrm{E}} + \bar{k}\boldsymbol{r}_{\mathrm{E}} = \boldsymbol{0}$	(4.98b)
energy-based:	$\bar{m}\big(\ddot{\boldsymbol{r}}_{\mathrm{E}} + \mathrm{wed}(\boldsymbol{\omega}_{\mathsf{R}})\dot{\boldsymbol{r}}_{\mathrm{E}}\big) + \bar{d}\dot{\boldsymbol{r}}_{\mathrm{E}} + \bar{k}\boldsymbol{r}_{\mathrm{E}} = \boldsymbol{0}$	(4.98c)

Translational energy. For the rigid body we can split the total energy $\bar{\mathcal{W}} = \bar{\mathcal{W}}_{\boldsymbol{r}} + \bar{\mathcal{W}}_{\boldsymbol{R}}$ into a part associated with the position $\bar{\mathcal{W}}_{\boldsymbol{r}}$ and one associated with the orientation $\bar{\mathcal{W}}_{\boldsymbol{R}}$. The rotational energies for the corresponding approaches coincide with the ones given in subsection 4.7.3 (subsection 4.7.2 for the planar case). The translational energies and their change along the solutions of (4.98) are

$$\begin{aligned} &\text{particle-based:} && \bar{\mathcal{W}}_{\boldsymbol{r}} = \tfrac{1}{2}\bar{k}\|\boldsymbol{e}\|^2 + \tfrac{1}{2}\bar{m}\|\dot{\boldsymbol{e}}\|^2, && \dot{\bar{\mathcal{W}}}_{\boldsymbol{r}} = -\bar{d}\|\dot{\boldsymbol{e}}\|^2 && \text{(4.99a)} \\ &\text{body-based:} && \bar{\mathcal{W}}_{\boldsymbol{r}} = \tfrac{1}{2}\bar{k}\|\boldsymbol{r}_{\mathrm{E}}\|^2 + \tfrac{1}{2}\bar{m}\|\dot{\boldsymbol{r}}_{\mathrm{E}}\|^2, && \dot{\bar{\mathcal{W}}}_{\boldsymbol{r}} = -\bar{d}\|\dot{\boldsymbol{r}}_{\mathrm{E}}\|^2 && \text{(4.99b)} \\ &\text{energy-based:} && \bar{\mathcal{W}}_{\boldsymbol{r}} = \tfrac{1}{2}\bar{k}\|\boldsymbol{r}_{\mathrm{E}}\|^2 + \tfrac{1}{2}\bar{m}\|\dot{\boldsymbol{r}}_{\mathrm{E}}\|^2, && \dot{\bar{\mathcal{W}}}_{\boldsymbol{r}} = -\bar{d}\|\dot{\boldsymbol{r}}_{\mathrm{E}}\|^2 && \text{(4.99c)} \end{aligned}$$

For their comparison note that

$$\|\boldsymbol{e}\| = \|\boldsymbol{r}_{\mathrm{E}}\|, \qquad \|\dot{\boldsymbol{e}}\| = \|\dot{\boldsymbol{r}}_{\mathrm{E}} + \mathrm{wed}(\boldsymbol{\omega}_{\mathsf{R}})\boldsymbol{r}_{\mathrm{E}}\|. \tag{4.100}$$

The crucial observation is that for all approaches the translational dynamics and energy are indeed independent of the actual orientation $\boldsymbol{R}$ and its velocity $\boldsymbol{\omega}$, but for some approaches they depend on their *reference* $\boldsymbol{R}_{\mathsf{R}}$ and $\boldsymbol{\omega}_{\mathsf{R}}$. For a constant reference orientation $\boldsymbol{R}_{\mathsf{R}} = \mathit{const.}$ and consequently $\boldsymbol{\omega}_{\mathsf{R}} = \mathbf{0}$ all four approaches are equivalent. Furthermore it is worth noting that the error dynamics as well as the energies are invariant to the reference trajectory $t \mapsto \boldsymbol{r}_{\mathsf{R}}(t)$ for the position.

Simulation. The difference between these cases will be discussed on simulation results for the simpler, yet as illustrative, example of a planar rigid body: The reference configuration is $r_{\mathsf{xR}}(t) = r_{\mathsf{yR}}(t) = 0$ and $\alpha_{\mathsf{R}}(t) = \pi t$ which yields the constant reference velocity $\boldsymbol{\xi}_{\mathsf{R}}(t) = [0, 0, \pi]$. The control parameters are set to $\bar{m} = 1$, $\bar{d} = 4$, $\bar{k} = 4$ (neglecting the units). The roots of the characteristic polynomial of (4.98c) are $\lambda \approx \{-0.5 \pm 0.6\mathrm{i}, -3.5 \pm 3.7\mathrm{i}\}$, resulting from the control parameters as well as the constant angular velocity $\omega_{\mathsf{zR}} = \pi$. The characteristic polynomial for the other approaches is independent of the reference trajectory and has a quadruple root at $\lambda = -2$.

Figure 4.8 shows the simulation result for the initial conditions $r_{\mathsf{x}}(0) = 0, r_{\mathsf{y}}(0) = 1$, $\alpha(0) = 0$ and $\boldsymbol{\xi}(0) = \mathbf{0}$. Observing from the inertial frame, top left of Figure 4.8, for approach 2 the body follows a straight line to its reference position, whereas for the other approaches spiral around it. Observing from the reference frame, top right of Figure 4.8, for approach 3 the body follows a direct path, given the initial velocity. The middle graph in Figure 4.8 shows the evolution of the translational energy $\bar{\mathcal{W}}_{\boldsymbol{r}}$. The difference in the initial values results from $\dot{\boldsymbol{e}}(0) = \mathbf{0}$, but $\dot{\boldsymbol{r}}_{\mathrm{E}}(0) \neq \mathbf{0}$. The bottom graph in Figure 4.8 shows the evolution of the euclidean distance $\|\boldsymbol{e}\| = \|\boldsymbol{r}_{\mathrm{E}}\|$. The rate of convergence for approach 2 and 3 are the same as could be expected from having the same characteristic polynomial.

Even though the energy based approach with the transport map from (4.42) might be mathematically the most elegant solution, its simulation result is not intuitive. Which approach is most desirable, depends given application. For indoor robots (like the multicopters discussed in the next chapter) it is probably most desirable if it corrects its position error following a straight line in the inertial frame.

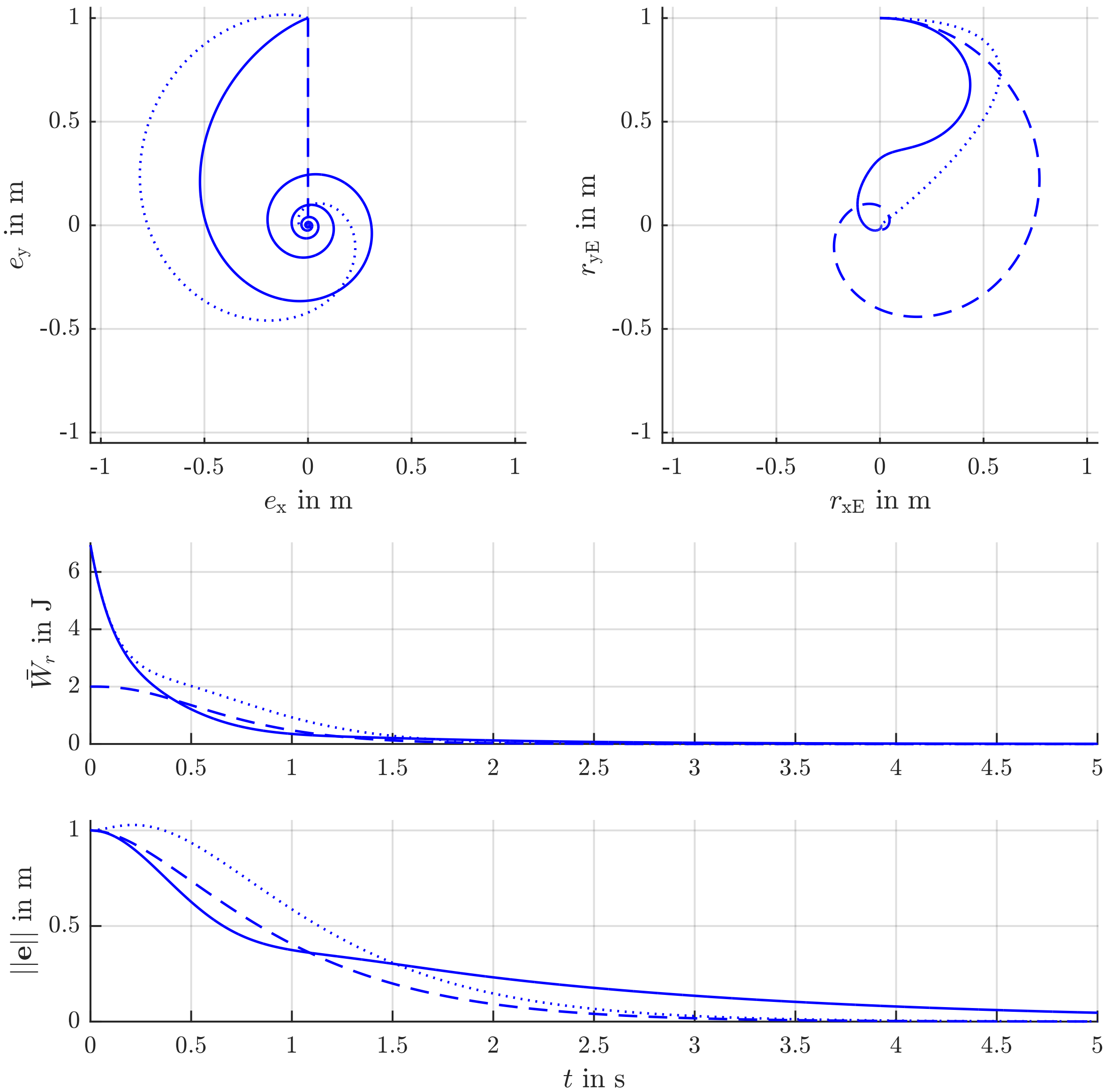

Figure 4.8: Simulation result for the planar rigid body. The solid line: energy-based approach with $\boldsymbol{Q} = \mathrm{Ad}_{\mathbf{G}^{-1}\mathbf{G}_\mathrm{R}}$, dashed line: particle-based approach, dotted line: body-based approach.

4.7.6 SCARA robot

As a simple example of a multi-body system we consider a SCARA robot as displayed in Figure 4.9. For the sake of demonstration we neglect the vertical axis and the tool orientation. The remaining two axis are sufficient to position a tool (red point in Figure 4.9) in the workspace (green shaded area).

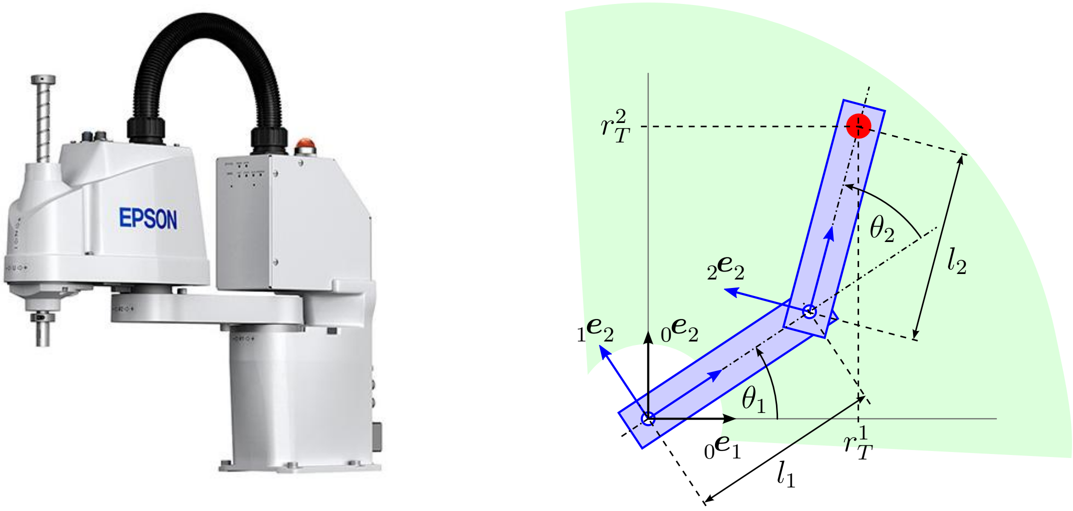

Figure 4.9: A Scara robot and its mechanical model (image www.epson.com)

Model. The model consists of two rigid bodies constraint by two revolute joints. A reasonable choice of coordinates are the relative joint angles $\boldsymbol{x} = [\theta_1, \theta_2]^\top$ and their derivatives $\boldsymbol{\xi} = [\dot\theta_1, \dot\theta_2]^\top$. The rigid body configurations are

$$ {}^0_1\mathbf{G} = \begin{bmatrix} \cos\theta_1 & -\sin\theta_1 & 0 & 0 \\ \sin\theta_1 & \cos\theta_1 & 0 & 0 \\ 0 & 0 & 1 & 0 \\ 0 & 0 & 0 & 1 \end{bmatrix}, \qquad {}^0_1\boldsymbol{J} = \begin{bmatrix} 0 & 0 \\ 0 & 0 \\ 0 & 0 \\ 0 & 0 \\ 0 & 0 \\ 1 & 0 \end{bmatrix} \tag{4.101a} $$

$$ {}^1_2\mathbf{G} = \begin{bmatrix} \cos\theta_2 & -\sin\theta_2 & 0 & l_1 \\ \sin\theta_2 & \cos\theta_2 & 0 & 0 \\ 0 & 0 & 1 & 0 \\ 0 & 0 & 0 & 1 \end{bmatrix}, \qquad {}^1_2\boldsymbol{J} = \begin{bmatrix} 0 & 0 \\ 0 & 0 \\ 0 & 0 \\ 0 & 0 \\ 0 & 0 \\ 0 & 1 \end{bmatrix}. \tag{4.101b} $$

Let ${}_1\Theta_\mathsf{z}$ be the moment of inertia of the first body about the first joint and l_1 be the distance between the two joints. The second body has the mass ${}_2m$, the center of mass $({}_2s_\mathsf{x}, {}_2s_\mathsf{y})$ and the moment of inertia ${}_2\Theta_\mathsf{z}$ about the second joint. The control forces are the joint torques $\boldsymbol{u} = [\tau_1, \tau_2]^\top$. Overall, the equations of motion for the SCARA robot are

$$ \begin{bmatrix} {}_1\Theta_\mathsf{z} + {}_2\Theta_\mathsf{z} + {}_2m l_1^2 + 2a(\theta_2) & {}_2\Theta_\mathsf{z} + a(\theta_2) \\ {}_2\Theta_\mathsf{z} + a(\theta_2) & {}_2\Theta_\mathsf{z} \end{bmatrix} \begin{bmatrix} \ddot\theta_1 \\ \ddot\theta_2 \end{bmatrix} + \begin{bmatrix} a'(\theta_2)(2\dot\theta_1\dot\theta_2 + \dot\theta_2^2) \\ -a'(\theta_2)\dot\theta_1^2 \end{bmatrix} = \begin{bmatrix} \tau_1 \\ \tau_2 \end{bmatrix} \tag{4.102} $$

where

$$a(\theta_2) = {}_2 m l_1 ({}_2 s_\mathsf{x} \cos\theta_2 - {}_2 s_\mathsf{y} \sin\theta_2), \qquad a'(\theta_2) = -{}_2 m l_1 ({}_2 s_\mathsf{x} \sin\theta_2 + {}_2 s_\mathsf{y} \cos\theta_2). \tag{4.103}$$

Controller parameterization 1. In the following we will discuss two different controller parameterizations for the SCARA. For the first parameterization the non-zero parameters are

$${}^0_1\bar{\Pi}_\mathsf{z}, {}^0_1\bar{\Upsilon}_\mathsf{z}, {}^0_1\bar{\Theta}_\mathsf{z}, \; {}^1_2\bar{\Pi}_\mathsf{z}, {}^1_2\bar{\Upsilon}_\mathsf{z}, {}^1_2\bar{\Theta}_\mathsf{z} \in \mathbb{R} > 0. \tag{4.104}$$

These parameters are directly associated with the errors $\theta_{i\mathrm{E}} = \theta_i - \theta_{i\mathsf{R}}, i = 1, 2$ of the joint angles. The resulting potential is

$$\bar{\mathcal{V}} = {}^0_1\bar{\Pi}_\mathsf{z}\big(1 - \cos\theta_{1\mathrm{E}}\big) + {}^1_2\bar{\Pi}_\mathsf{z}\big(1 - \cos\theta_{2\mathrm{E}}\big). \tag{4.105}$$

and obeys the transport map $\boldsymbol{Q} = \mathbf{I}_2$.

The resulting controlled kinetics for the body and energy-based approach are

$${}^{i-1}_{\;\;i}\bar{\Theta}_\mathsf{z}\ddot{\theta}_{i\mathrm{E}} + {}^{i-1}_{\;\;i}\bar{\Upsilon}_\mathsf{z}\dot{\theta}_{i\mathrm{E}} + {}^{i-1}_{\;\;i}\bar{\Pi}_\mathsf{z}\sin\theta_{i\mathrm{E}} = 0, \qquad i = 1, 2. \tag{4.106}$$

The controlled kinetics for the particle based approach yield

$${}^{i-1}_{\;\;i}\bar{\Theta}_\mathsf{z}\big(\ddot{\theta}_i - \ddot{\theta}_{i\mathsf{R}}\cos\theta_{i\mathrm{E}} - \dot{\theta}_{i\mathsf{R}}^2\sin\theta_{i\mathrm{E}}\big) + {}^{i-1}_{\;\;i}\bar{\Upsilon}_\mathsf{z}\big(\dot{\theta}_i - \dot{\theta}_{i\mathsf{R}}\cos\theta_{i\mathrm{E}}\big) + {}^{i-1}_{\;\;i}\bar{\Pi}_\mathsf{z}\sin\theta_{i\mathrm{E}} = 0, \qquad i = 1, 2. \tag{4.107}$$

With this parameterization the controlled kinetics coincide with two copies of the kinetics of the revolute joint discussed in subsection 4.7.2.

Controller parameterization 2. The non-zero parameters for another interesting parameterization of the controller are

$${}^0_2\bar{k}, {}^0_2\bar{d}, {}^0_2\bar{m} \in \mathbb{R} > 0, \quad {}^0_2\bar{h}_\mathsf{x} = {}^0_2\bar{l}_\mathsf{x} = {}^0_2\bar{s}_\mathsf{x} = l_2. \tag{4.108}$$

The resulting potential can be written as

$$\bar{\mathcal{V}}(\boldsymbol{x}, \boldsymbol{x}_\mathsf{R}) = \tfrac{1}{2}\,{}^0_2\bar{k}\,\|\boldsymbol{r}_\mathsf{T}(\boldsymbol{x}) - \boldsymbol{r}_\mathsf{T}(\boldsymbol{x}_\mathsf{R})\|^2 \qquad \boldsymbol{r}_\mathsf{T}(\boldsymbol{x}) = \begin{bmatrix} l_1\cos\theta_1 + l_2\cos(\theta_1+\theta_2) \\ l_1\sin\theta_1 + l_2\sin(\theta_1+\theta_2) \end{bmatrix}, \tag{4.109}$$

where $\boldsymbol{r}_\mathsf{T}$ is the position of the tool as illustrated in Figure 4.9. Using the *tool position error* $\boldsymbol{e}(\boldsymbol{x}, \boldsymbol{x}_\mathsf{R}) = \boldsymbol{r}_\mathsf{T}(\boldsymbol{x}) - \boldsymbol{r}_\mathsf{T}(\boldsymbol{x}_\mathsf{R})$ as error coordinates, we can apply the rule from (A.8) to compute the transport map as

$$\boldsymbol{Q}(\boldsymbol{x}, \boldsymbol{x}_\mathsf{R}) = \big(\boldsymbol{\nabla}\boldsymbol{r}_\mathsf{T}(\boldsymbol{x})\big)^{-1}\,\boldsymbol{\nabla}\boldsymbol{r}_\mathsf{T}(\boldsymbol{x}_\mathsf{R}). \tag{4.110}$$

The determinant of the differential $\det \boldsymbol{\nabla}\boldsymbol{r}_\mathsf{T}(\boldsymbol{x}) = \sin\theta_2$ reflects the well known singularity of the SCARA inverse kinematics, see e.g. [Murray et al., 1994, example 3.6].

The closed loop kinetics for the particle and energy-based approach in terms of the model coordinates $\boldsymbol{x}$ and the error velocity $\boldsymbol{\xi}_\mathrm{E} = \boldsymbol{\xi} - \boldsymbol{Q}\boldsymbol{\xi}_\mathrm{R}$ are

$$\begin{aligned}
&\underbrace{{}^0_2\bar{m}\begin{bmatrix} l_1^2 + 2l_1l_2\cos\theta_2 + l_2^2 & l_1l_2\cos\theta_2 + l_2^2 \\ l_1l_2\cos\theta_2 + l_2^2 & l_2^2 \end{bmatrix}}_{\bar{\boldsymbol{M}}}\dot{\boldsymbol{\xi}}_\mathrm{E} + {}^0_2\bar{m}l_1l_2\sin\theta_2\begin{bmatrix} -\dot\theta_2 & -\dot\theta_1 - \dot\theta_2 \\ \dot\theta_1 & 0 \end{bmatrix}\boldsymbol{\xi}_\mathrm{E} \\
&\qquad + \underbrace{{}^0_2\bar{d}\begin{bmatrix} l_1^2 + 2l_1l_2\cos\theta_2 + l_2^2 & l_1l_2\cos\theta_2 + l_2^2 \\ l_1l_2\cos\theta_2 + l_2^2 & l_2^2 \end{bmatrix}}_{\bar{\boldsymbol{D}}}\boldsymbol{\xi}_\mathrm{E} \\
&+ \underbrace{{}^0_2\bar{k}\begin{bmatrix} l_1^2\sin\theta_{1\mathrm{E}} + l_1l_2(\sin(\theta_{1\mathrm{E}} - \theta_{2\mathrm{R}}) + \sin(\theta_{1\mathrm{E}} + \theta_2)) + l_2^2\sin(\theta_{1\mathrm{E}} + \theta_{2\mathrm{E}}) \\ l_1l_2(\sin(\theta_{1\mathrm{E}} + \theta_2) - \sin(\theta_2)) + l_2^2\sin(\theta_{1\mathrm{E}} + \theta_{2\mathrm{E}}) \end{bmatrix}}_{\boldsymbol{\nabla}\bar{\mathcal{V}}} = \boldsymbol{0}.
\end{aligned} \tag{4.111a}$$

In terms of the tool position error $\boldsymbol{e}$ this is equivalent to the much simpler equation

$$ {}^0_2\bar{m}\ddot{\boldsymbol{e}} + {}^0_2\bar{d}\dot{\boldsymbol{e}} + {}^0_2\bar{k}\boldsymbol{e} = \boldsymbol{0}. \tag{4.111b}$$

With the body-based approach we get a similar closed loop that is not displayed or discussed here.

As mentioned above, the transport map $\boldsymbol{Q}$ contains terms with $1/\sin\theta_2$. Fortunately these terms cancel out in $\bar{\boldsymbol{M}}\boldsymbol{Q}$ and $\bar{\boldsymbol{D}}\boldsymbol{Q}$ in the closed loop equation (4.111a), so this singularity actually does not hurt in practice. This could also be expected since the particle based approach, which does not rely on the transport map, leads to the same closed loop.

A singularity that does hurt, is the inertia matrix with $\det\bar{\boldsymbol{M}} = ({}^0_2\bar{m}l_1l_2\sin\theta_2)^2$. This means that one can not compute the control law if $\sin\theta_2 = 0$. Recalling the mechanical model of the SCARA Figure 4.9, this singularity is evident from a geometric point of view: If $\sin\theta_2 = 0$ the tool can only move in a tangential direction to the boundary of the workspace but not radial. However, it should be stressed that this singularity is not a consequence of unsuitable configuration coordinates $\boldsymbol{x} = [\theta_1, \theta_2]^\top$. It is rather an intrinsic one resulting from forcing dynamics suitable for $\mathbb{R}^2$ on a system that has the configuration space $\mathbb{S}^2$.

Simulation result. Figure 4.10 and Figure 4.11 show a simulation results for the SCARA robot with the two proposed parameterizations. The robot starts in a rather random initial configuration. The reference configuration is constant till $t = 1\,\mathrm{s}$, then follows a straight line for the tool position till $t = 4\,\mathrm{s}$ and remains constant thereafter.

For both parameterizations the controlled total energy $\bar{\mathcal{W}}$ converges. The crucial difference between the two parameterizations is, though the tool position $\boldsymbol{r}_\mathrm{T}$ tracks its reference in both cases, the joint angles θ_1, θ_2 do not for the second parameterization. The reason for this is best understood when looking at the controlled potential energy $\bar{\mathcal{V}}$ illustrated in Figure 4.12: For parameterization 2 the potential has two minima $\bar{\mathcal{V}} = 0$ for which the tool is at its reference position, but with different joint angles. This is true for any tool position except the ones on the boundary of the workspace where $\theta_2 = 0$ or $\theta_2 = \pi$.

Which of the two parameterizations is "better" probably depends on the practical control task: If the actual joint configuration (θ_1, θ_2) matters then the control parameters associated with them, i.e. ${}^0_1\bar{\Pi}_\mathsf{z}, {}^0_1\bar{\Upsilon}_\mathsf{z}, \ldots$, are more suited for the control design. If one is only interested in the tool position $\boldsymbol{r}_\mathsf{T}$, then the parameters of the parameterization 2 are useful.

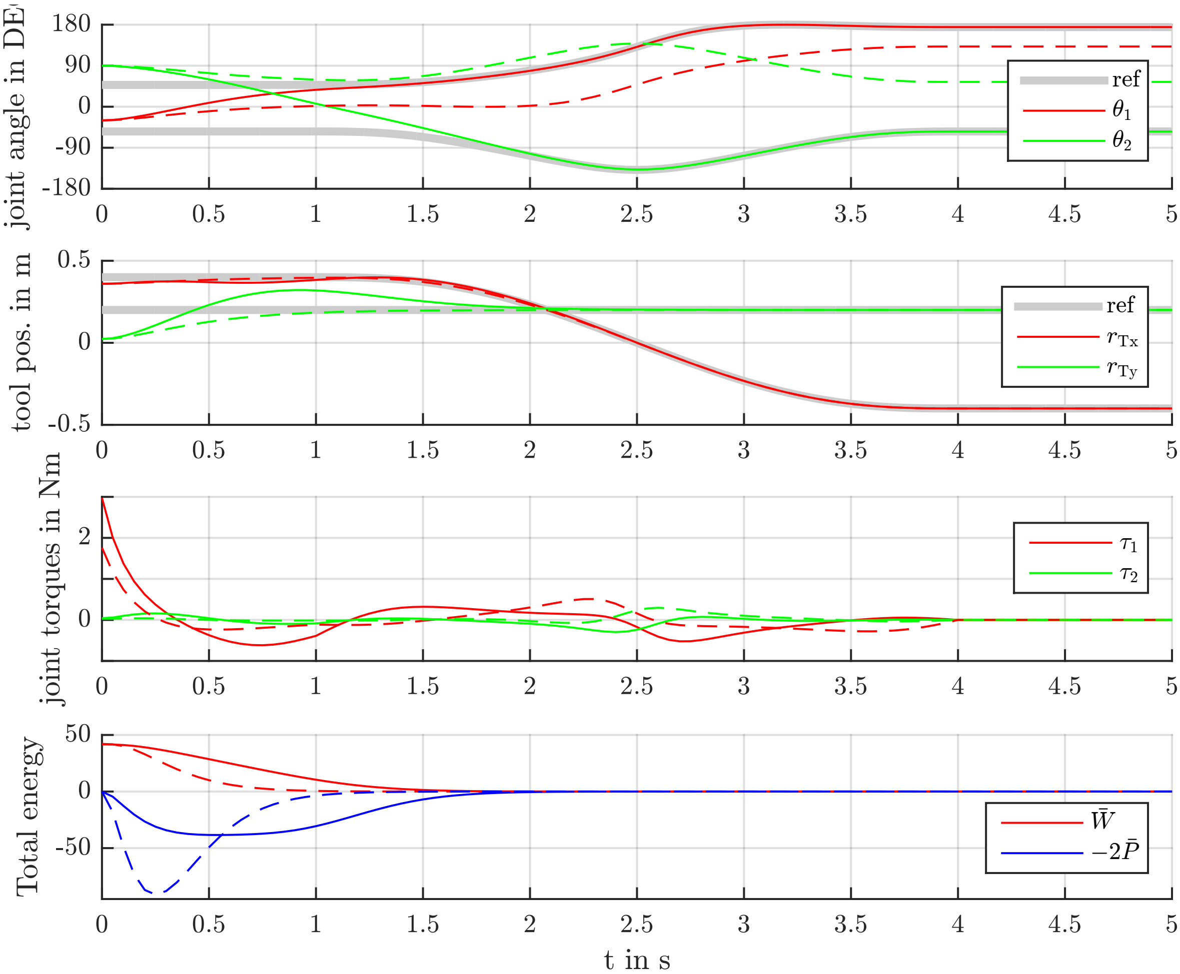

Figure 4.10: Simulation result for the SCARA with parameterization 1 (solid lines) and 2 (dashed lines)

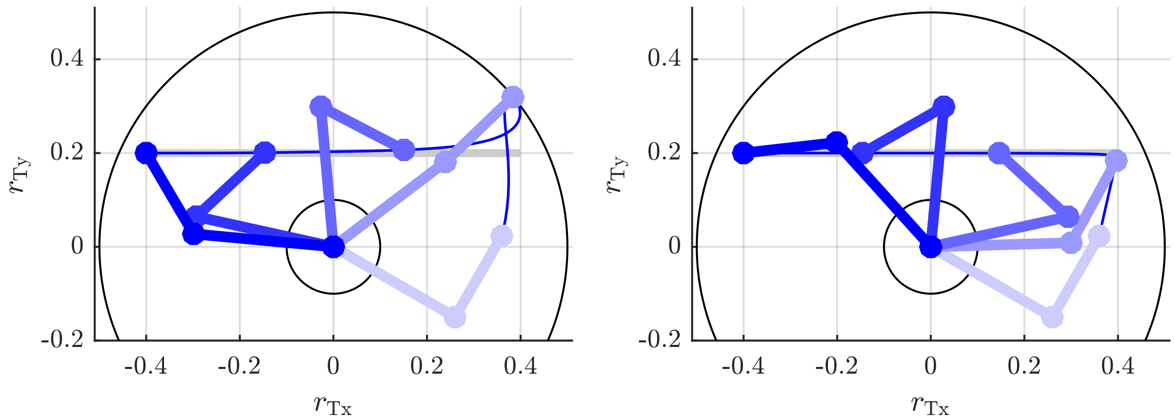

Figure 4.11: Snapshots for the simulation result for the SCARA with parameterization 1 (left) and 2 (right)

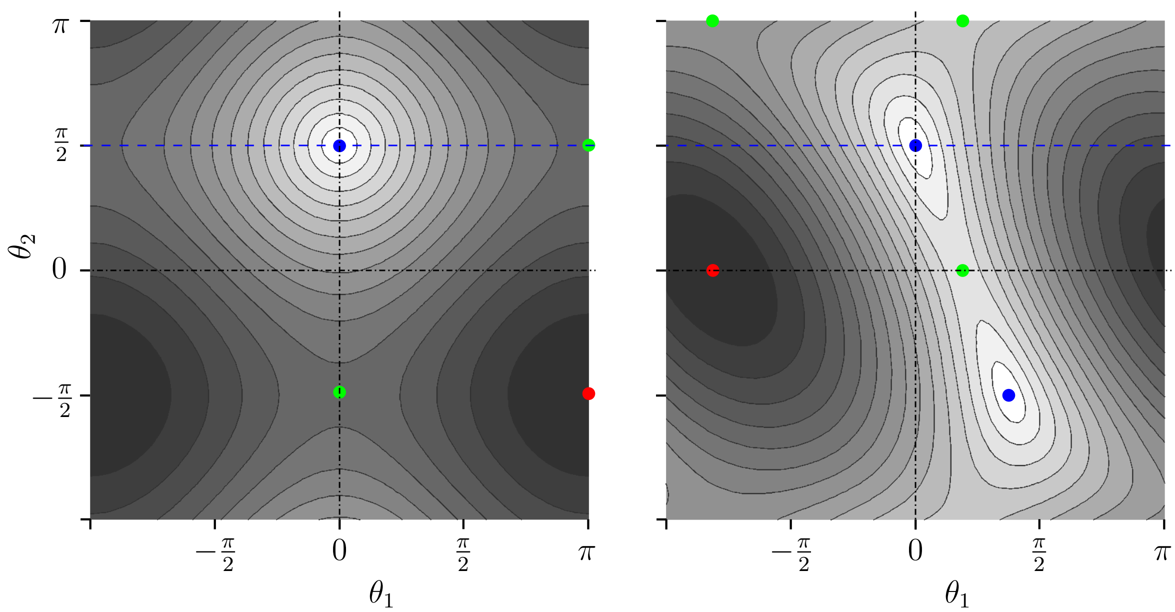

Figure 4.12: The controlled potential energy $\mathcal{V}$ for parameterization 1 (left) and 2 (right) for $\theta_{1\mathsf{R}} = 0$, $\theta_{2\mathsf{R}} = \frac{\pi}{2}$. Blue dots are minima, red are maxima and green are saddle points.

4.7.7 Robot arm

As a more complex multibody system we consider a robot arm as illustrated in Figure 4.13. For this example the model equations and the resulting closed loop equations become quite cumbersome and are not displayed explicitly. However this displays some benefits of the proposed control approach: One does not have to look at e.g. the actual system inertia matrix but only at the much less cumbersome body inertia matrices to conclude e.g. stability of the closed loop.

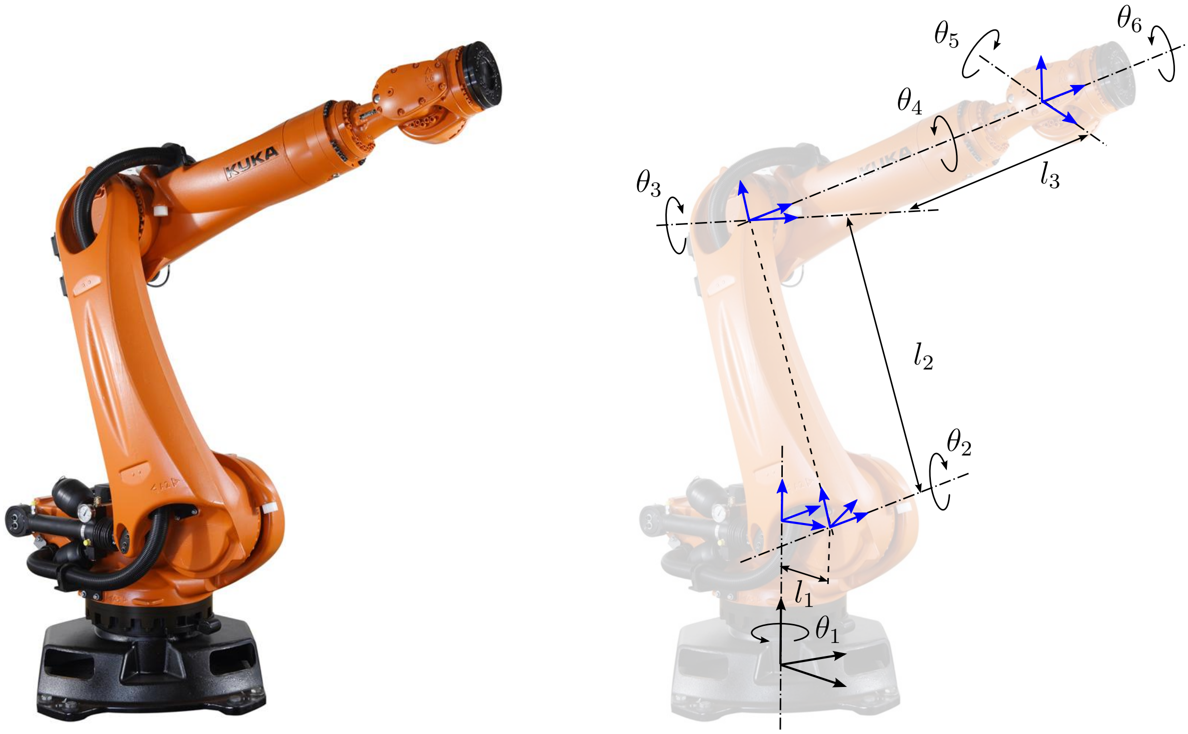

Figure 4.13: A model of a robot arm (background image from www.kuka.de)

Model. A reasonable choice of coordinates of the system are the joint angles $\boldsymbol{x} = [\theta_1, \ldots, \theta_6]^\top$ and trivial kinematics $\boldsymbol{\xi} = \dot{\boldsymbol{x}}$. The body configurations can be computed from the following relative transformations

$$
\begin{aligned}
{}^0_1\mathbf{G} &= \begin{bmatrix} \cos\theta_1 & -\sin\theta_1 & 0 & 0 \\ \sin\theta_1 & \cos\theta_1 & 0 & 0 \\ 0 & 0 & 1 & 0 \\ 0 & 0 & 0 & 1 \end{bmatrix}, &\qquad {}^1_2\mathbf{G} &= \begin{bmatrix} \cos\theta_2 & 0 & \sin\theta_2 & l_1 \\ 0 & 1 & 0 & 0 \\ -\sin\theta_2 & 0 & \cos\theta_2 & 0 \\ 0 & 0 & 0 & 1 \end{bmatrix}, \\
{}^2_3\mathbf{G} &= \begin{bmatrix} \cos\theta_3 & 0 & \sin\theta_3 & 0 \\ 0 & 1 & 0 & 0 \\ -\sin\theta_3 & 0 & \cos\theta_3 & l_2 \\ 0 & 0 & 0 & 1 \end{bmatrix}, &\qquad {}^3_4\mathbf{G} &= \begin{bmatrix} 1 & 0 & 0 & l_3 \\ 0 & \cos\theta_4 & -\sin\theta_4 & 0 \\ 0 & \sin\theta_4 & \cos\theta_4 & 0 \\ 0 & 0 & 0 & 1 \end{bmatrix}, \\
{}^4_5\mathbf{G} &= \begin{bmatrix} \cos\theta_5 & 0 & \sin\theta_5 & 0 \\ 0 & 1 & 0 & 0 \\ -\sin\theta_5 & 0 & \cos\theta_5 & 0 \\ 0 & 0 & 0 & 1 \end{bmatrix}, &\qquad {}^5_6\mathbf{G} &= \begin{bmatrix} 1 & 0 & 0 & 0 \\ 0 & \cos\theta_6 & -\sin\theta_6 & 0 \\ 0 & \sin\theta_6 & \cos\theta_6 & 0 \\ 0 & 0 & 0 & 1 \end{bmatrix}.
\end{aligned}
\tag{4.112}
$$

This together with the body inertia matrices and the gravity coefficients $\boldsymbol{a}_{\mathsf{G}}$ and the control forces, $\boldsymbol{u} = [\tau_1, \dots, \tau_6]^\top$ determines the equations of motion.

Controller parameterization 1: Joint space control. Like above we consider two different sets of controller parameterizations: For the first case, the nonzero control parameters are

$$\begin{aligned} {}^0_1\bar{\varPi}_{\mathsf{zz}}, {}^1_2\bar{\varPi}_{\mathsf{yy}}, {}^2_3\bar{\varPi}_{\mathsf{yy}}, {}^3_4\bar{\varPi}_{\mathsf{xx}}, {}^4_5\bar{\varPi}_{\mathsf{yy}}, {}^5_6\bar{\varPi}_{\mathsf{xx}} \in \mathbb{R} > 0 \\ {}^0_1\bar{\varUpsilon}_{\mathsf{zz}}, {}^1_2\bar{\varUpsilon}_{\mathsf{yy}}, {}^2_3\bar{\varUpsilon}_{\mathsf{yy}}, {}^3_4\bar{\varUpsilon}_{\mathsf{xx}}, {}^4_5\bar{\varUpsilon}_{\mathsf{yy}}, {}^5_6\bar{\varUpsilon}_{\mathsf{xx}} \in \mathbb{R} > 0 \\ {}^0_1\bar{\varTheta}_{\mathsf{zz}}, {}^1_2\bar{\varTheta}_{\mathsf{yy}}, {}^2_3\bar{\varTheta}_{\mathsf{yy}}, {}^3_4\bar{\varTheta}_{\mathsf{xx}}, {}^4_5\bar{\varTheta}_{\mathsf{yy}}, {}^5_6\bar{\varTheta}_{\mathsf{xx}} \in \mathbb{R} > 0 \end{aligned} \tag{4.113}$$

A transport map for the resulting potential energy is $\boldsymbol{Q} = \mathbf{I}_6$. The resulting closed loop kinetics are 6 decoupled equations identical to the ones for the SCARA (4.106) resp. (4.107).

Controller parameterization 2: Work space control. As a second case consider: For many applications the task of the robot arm is to control the position and orientation of a tool mounted at the end of its kinematic chain. This tool might have a particularly meaningful center point (TCP) and and principle axes. Let the configuration ${}^6_7\mathbf{G} = \mathit{const}.$ capture these tool specific parameters, for example the tip position and direction of a welding electrode as shown in Figure 4.14.

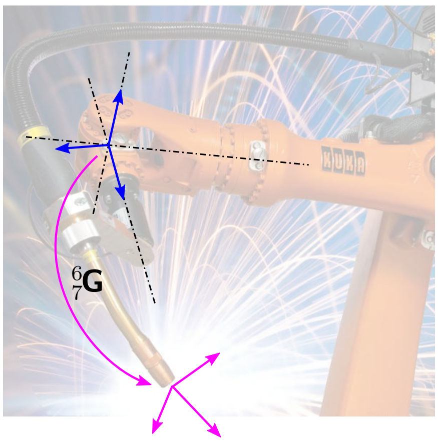

Figure 4.14: Welding tool attached to the robot arm (background image from www.kuka.de)

For this example it could be useful to control the tool as if it is a free rigid body (with its center of mass, damping and stiffness at the TCP) and not care about the particular mechanism that is used to give it this degree of freedom. This is achieved by the following nonzero control parameters

$${}^0_7\bar{k}, {}^0_7\bar{d}, {}^0_7\bar{m} \in \mathbb{R}^+, \qquad {}^0_7\bar{\boldsymbol{\varPi}}, {}^0_7\bar{\boldsymbol{\varUpsilon}}, {}^0_7\bar{\boldsymbol{\varTheta}} \in \mathbb{SYM}^+(3). \tag{4.114}$$

The resulting potential and corresponding transport map are

$$\bar{\mathcal{V}}(\boldsymbol{x}, \boldsymbol{x}_{\mathsf{R}}) = \tfrac{1}{2}\|(({}^0_7\mathbf{G}(\boldsymbol{x}_{\mathsf{R}}))^{-1}\, {}^0_7\mathbf{G}(\boldsymbol{x}) - \mathbf{I}_4)^\top\|^2_{{}^0_7\bar{\mathbf{K}}'}, \quad \boldsymbol{Q}(\boldsymbol{x}, \boldsymbol{x}_{\mathsf{R}}) = \left({}^7_0\boldsymbol{J}(\boldsymbol{x})\right)^{-1} {}^7_0\boldsymbol{J}(\boldsymbol{x}_{\mathsf{R}}). \tag{4.115}$$

The resulting closed loop dynamics of the robot arm may be written by plugging the absolute tool configuration ${}^0_7\mathbf{G}(\boldsymbol{x})$ and its reference ${}^0_7\mathbf{G}(\boldsymbol{x}_\mathsf{R})$ into the dynamics of a single rigid body for either of the three proposed approaches (4.14), (4.21) or (4.44).

The determinant of the transport map is

$$\det \boldsymbol{Q}(\boldsymbol{x}, \boldsymbol{x}_\mathsf{R}) = \frac{\det {}^0_7\boldsymbol{J}(\boldsymbol{x}_\mathsf{R})}{\det {}^0_7\boldsymbol{J}(\boldsymbol{x})}, \quad \det {}^0_7\boldsymbol{J}(\boldsymbol{x}) = -l_2 l_3(l_1 + l_2 \sin\theta_2 + l_3\cos(\theta_2+\theta_3))\cos\theta_3 \sin\theta_5 \tag{4.116}$$

If the term in the brackets vanishes means that the wrist lies on the axis of θ_1 and $\cos\theta_3 = 0$ is the case if the arm is completely straight which is the singularity we already encountered with the SCARA robot. The last three axis with angles θ_4, θ_5, θ_6 can be regarded as Euler angles in the sequence XYX and $\sin\theta_5 = 0$ is their singularity. Comparing this to the motivation example in section 1.2 we have the same problem but the other way around: The Euler angles are an absolutely appropriate choice of coordinates since the mechanism is realized like this. Consequently the configuration manifold of this part is $\mathbb{S}^1 \times \mathbb{S}^1 \times \mathbb{S}^1$ and we are assigning a control that was designed for $\mathbb{SO}(3)$.

Conclusion. The behavior of the two different parameterizations are quite analog to the two parameterizations of the SCARA robot. Which one is more suitable depends on the actual control task. Furthermore, the two presented parameterizations are just two special cases of which dynamics can be achieved with the more general approach of control of this work.

4.8 Examples of underactuated systems

4.8.1 Two masses connected by a spring

In order to illustrate the control approach for underactuated systems we consider the minimal example: Two bodies in prismatic joints connected by a linear spring but where only one is directly actuated by the force F as illustrated in Figure 4.15.

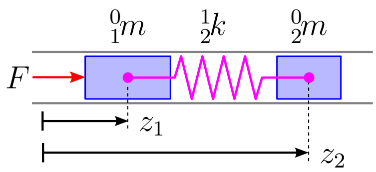

Figure 4.15: Model of two bodies connected by a spring

Model. We choose the absolute positions of the bodies as configuration coordinates $\boldsymbol{x} = [z_1, z_2]^\top$ and their derivative as velocity coordinates $\boldsymbol{\xi} = \dot{\boldsymbol{x}}$. With this the body configurations are

$$ {}^0_1\mathbf{G} = \begin{bmatrix} 1 & 0 & 0 & z_1 \\ 0 & 1 & 0 & 0 \\ 0 & 0 & 1 & 0 \\ 0 & 0 & 0 & 1 \end{bmatrix}, \qquad {}^0_2\mathbf{G} = \begin{bmatrix} 1 & 0 & 0 & z_2 \\ 0 & 1 & 0 & 0 \\ 0 & 0 & 1 & 0 \\ 0 & 0 & 0 & 1 \end{bmatrix}. \tag{4.117} $$

With the total mass ${}^0_1m$, ${}^0_2m$ of the individual bodies and the spring stiffness ${}^1_2k$ the resulting equations of motion may be written as

$$ \underbrace{\begin{bmatrix} {}^0_1m & 0 \\ 0 & {}^0_2m \end{bmatrix}}_{\boldsymbol{M}} \begin{bmatrix} \ddot{z}_1 \\ \ddot{z}_2 \end{bmatrix} + \underbrace{\begin{bmatrix} {}^1_2k & -{}^1_2k \\ -{}^1_2k & {}^1_2k \end{bmatrix}}_{\boldsymbol{K}} \begin{bmatrix} z_1 \\ z_2 \end{bmatrix} = \underbrace{\begin{bmatrix} 1 \\ 0 \end{bmatrix}}_{\boldsymbol{B}} F. \tag{4.118} $$

Desired closed loop. We assume general body inertia ${}^0_1\mathbf{M}, \ldots$, damping and stiffness. The three proposed control approaches lead to identical desired closed loop dynamics:

$$ \bar{\boldsymbol{M}}\ddot{\boldsymbol{e}} + \bar{\boldsymbol{D}}\dot{\boldsymbol{e}} + \bar{\boldsymbol{K}}\boldsymbol{e} = \mathbf{0}, \qquad \boldsymbol{e} = \boldsymbol{x} - \boldsymbol{x}_\mathsf{R} \tag{4.119} $$

where

$$ \bar{\boldsymbol{M}} = \begin{bmatrix} {}^0_1\bar{m} + {}^1_2\bar{m} & -{}^1_2\bar{m} \\ -{}^1_2\bar{m} & {}^0_2\bar{m} + {}^1_2\bar{m} \end{bmatrix}, \quad \bar{\boldsymbol{D}} = \begin{bmatrix} {}^0_1\bar{d} + {}^1_2\bar{d} & -{}^1_2\bar{d} \\ -{}^1_2\bar{d} & {}^0_2\bar{d} + {}^1_2\bar{d} \end{bmatrix}, \quad \bar{\boldsymbol{K}} = \begin{bmatrix} {}^0_1\bar{k} + {}^1_2\bar{k} & -{}^1_2\bar{k} \\ -{}^1_2\bar{k} & {}^0_2\bar{k} + {}^1_2\bar{k} \end{bmatrix}. \tag{4.120} $$

The corresponding potential $\bar{\mathcal{V}} = \frac{1}{2}\boldsymbol{e}^\top\bar{\boldsymbol{K}}\boldsymbol{e}$ has the obvious transport map $\boldsymbol{Q} = \mathbf{I}_2$.

Matching. The matching condition (4.59) for this example may be written as

$$ \boldsymbol{\lambda} = (\boldsymbol{B}^\perp)^\top(\boldsymbol{M}\bar{\boldsymbol{M}}^{-1}(-\bar{\boldsymbol{M}}\ddot{\boldsymbol{x}}_\mathsf{R} + \bar{\boldsymbol{D}}(\dot{\boldsymbol{x}} - \dot{\boldsymbol{x}}_\mathsf{R}) + \bar{\boldsymbol{K}}(\boldsymbol{x} - \boldsymbol{x}_\mathsf{R})) - \boldsymbol{K}\boldsymbol{x}) = \mathbf{0}. \tag{4.121} $$

Since this equation is linear in the system coordinates we can separate the into

$$ (\boldsymbol{B}^\perp)^\top(\boldsymbol{M}\ddot{\boldsymbol{x}}_\mathsf{R} + \boldsymbol{K}\boldsymbol{x}_\mathsf{R}) = \mathbf{0}. \tag{4.122a} $$
$$ (\boldsymbol{B}^\perp)^\top\boldsymbol{M}\bar{\boldsymbol{M}}^{-1}\bar{\boldsymbol{D}} = \mathbf{0}, \tag{4.122b} $$
$$ (\boldsymbol{B}^\perp)^\top\boldsymbol{M}\bar{\boldsymbol{M}}^{-1}(\bar{\boldsymbol{K}} - \boldsymbol{K}) = \mathbf{0}, \tag{4.122c} $$

Choosing $\boldsymbol{B}^\perp = [0, 1]^\top$ this is explicitly

$$ \ddot{z}_{2\mathsf{R}} + \varpi(z_{2\mathsf{R}} - z_{1\mathsf{R}}) = 0 \tag{4.123a} $$
$$ \begin{cases} {}^0_1\bar{m}\,{}^1_2\bar{d} - {}^1_2\bar{m}\,{}^0_1\bar{d} = 0 \\ {}^0_1\bar{m}\,{}^1_2\bar{d} + ({}^0_1\bar{m} + {}^1_2\bar{m})\,{}^0_2\bar{d} = 0 \end{cases} \tag{4.123b} $$
$$ \begin{cases} {}^0_1\bar{m}\,{}^1_2\bar{k} - {}^1_2\bar{m}\,{}^0_1\bar{k} = ({}^0_1\bar{m}\,{}^0_2\bar{m} + {}^0_1\bar{m}\,{}^1_2\bar{m} + {}^0_2\bar{m}\,{}^1_2\bar{m})\varpi \\ {}^0_1\bar{m}\,{}^1_2\bar{k} + ({}^0_1\bar{m} + {}^1_2\bar{m})\,{}^0_2\bar{k} = ({}^0_1\bar{m}\,{}^0_2\bar{m} + {}^0_1\bar{m}\,{}^1_2\bar{m} + {}^0_2\bar{m}\,{}^1_2\bar{m})\varpi \end{cases} \tag{4.123c} $$

where $\varpi = {}^1_2k/{}^0_2m$ is the sole model parameter relevant for the matching condition. The first part (4.123a) is a constraint on the reference trajectory as it is independent of tunable parameters. It can be resolved by acknowledging that z_2 is a *flat output* of the system and planing the reference trajectory accordingly, i.e.

$$z_{1\mathsf{R}} = z_{2\mathsf{R}} - \ddot{z}_{2\mathsf{R}}/\varpi. \tag{4.124}$$

The other conditions can be resolved by setting

$$ {}^{1}_{2}\bar{k} = \tfrac{{}^{1}_{2}\bar{m}}{{}^{0}_{1}\bar{m}}\,{}^{0}_{1}\bar{k} + \tfrac{{}^{0}_{1}\bar{m}\,{}^{0}_{2}\bar{m} + {}^{0}_{1}\bar{m}\,{}^{1}_{2}\bar{m} + {}^{0}_{2}\bar{m}\,{}^{1}_{2}\bar{m}}{{}^{0}_{1}\bar{m}}\varpi, \quad {}^{0}_{2}\bar{k} = -\tfrac{{}^{1}_{2}\bar{m}}{{}^{0}_{1}\bar{m}+{}^{1}_{2}\bar{m}}\,{}^{0}_{1}\bar{k}, \quad {}^{1}_{2}\bar{d} = \tfrac{{}^{1}_{2}\bar{m}}{{}^{0}_{1}\bar{m}}\,{}^{0}_{1}\bar{d}, \quad {}^{0}_{2}\bar{d} = -\tfrac{{}^{1}_{2}\bar{m}}{{}^{0}_{1}\bar{m}+{}^{1}_{2}\bar{m}}\,{}^{0}_{1}\bar{d}, \tag{4.125}$$

which leaves the 5 tuning parameters ${}^{0}_{1}\bar{k}$, ${}^{0}_{1}\bar{d}$, ${}^{0}_{1}\bar{m}$, ${}^{0}_{2}\bar{m}$ and ${}^{1}_{2}\bar{m}$.

The resulting control law is

$$\begin{aligned} F = {}^{0}_{1}m\,\ddot{z}_{1\mathsf{R}} + {}^{1}_{2}k(z_{1\mathsf{R}} - z_{2\mathsf{R}}) + \Big({}^{1}_{2}k + \tfrac{{}^{0}_{1}m({}^{1}_{2}\bar{m}\,{}^{1}_{2}k + {}^{0}_{2}m({}^{0}_{1}\bar{k} - {}^{1}_{2}\bar{k}))}{{}^{0}_{2}m({}^{0}_{1}\bar{m}+{}^{1}_{2}\bar{m})}\Big)e_1 \\ - \Big({}^{1}_{2}k - \tfrac{{}^{0}_{1}m({}^{1}_{2}\bar{m}\,{}^{1}_{2}k - {}^{0}_{2}m\,{}^{1}_{2}\bar{k})}{{}^{0}_{2}m({}^{0}_{1}\bar{m}+{}^{1}_{2}\bar{m})}\Big)e_2 - \tfrac{{}^{0}_{1}m({}^{0}_{1}\bar{d}+{}^{1}_{2}\bar{d})}{{}^{0}_{1}\bar{m}+{}^{1}_{2}\bar{m}}\dot{e}_1 + \tfrac{{}^{0}_{1}m\,{}^{1}_{2}\bar{d}}{{}^{0}_{1}\bar{m}+{}^{1}_{2}\bar{m}}\dot{e}_2. \end{aligned} \tag{4.126}$$

Pole placement. Tuning the design parameters under the given matching conditions might not be intuitive for this example. To resolve this we can fall back to the classical approach of placing the eigenvalues of the closed loop system (4.119). Taking into account the matching condition (4.125), the characteristic polynomial of (4.119) is

$$\tfrac{\det(\bar{\boldsymbol{M}}\lambda^2 + \bar{\boldsymbol{D}}\lambda + \bar{\boldsymbol{K}})}{\det \bar{\boldsymbol{M}}} = \lambda^4 + \underbrace{\tfrac{{}^{0}_{1}\bar{d}}{{}^{0}_{1}\bar{m}}}_{p_3}\lambda^3 + \underbrace{\tfrac{{}^{0}_{1}\bar{k} + ({}^{0}_{1}\bar{m} + {}^{0}_{2}\bar{m})\varpi}{{}^{0}_{1}\bar{m}}}_{p_2}\lambda^2 + \underbrace{\tfrac{\varpi\,{}^{0}_{1}\bar{d}}{{}^{0}_{1}\bar{m}+{}^{1}_{2}\bar{m}}}_{p_1}\lambda + \underbrace{\tfrac{\varpi\,{}^{0}_{1}\bar{k}}{{}^{0}_{1}\bar{m}+{}^{1}_{2}\bar{m}}}_{p_0}. \tag{4.127}$$

This can be solved for

$${}^{0}_{1}\bar{k} = \tfrac{{}^{1}_{2}\bar{m}p_0p_3}{\varpi p_3 - p_1}, \qquad {}^{0}_{1}\bar{d} = \tfrac{{}^{1}_{2}\bar{m}p_1p_3}{\varpi p_3 - p_1}, \qquad {}^{0}_{1}\bar{m} = \tfrac{{}^{1}_{2}\bar{m}p_1}{\varpi p_3 - p_1}, \qquad {}^{0}_{2}\bar{m} = \tfrac{{}^{1}_{2}\bar{m}(p_1p_2 - p_0p_3 - \varpi p_1)}{\varpi(\varpi p_3 - p_1)}. \tag{4.128a}$$

and ${}^{1}_{2}\bar{m} \in \mathbb{R} \neq 0$. Choosing any Hurwitz polynomial for the coefficients p_i guarantees the asymptotic stability of the closed loop. In order to conclude $\bar{\boldsymbol{M}} > 0$, $\bar{\boldsymbol{D}} \geq 0$ and $\bar{\boldsymbol{K}} > 0$ from the Hurwitz criterion $(p_0, p_1, p_2, p_3, p_1p_2 - p_0p_3, p_1p_2p_3 - p_1^2 - p_0p_3^2 > 0)$ we need $\operatorname{sign} {}^{1}_{2}\bar{m} = \operatorname{sign}(\varpi p_3 - p_1)$.

Conclusions. The resulting controller is equivalent to one that could be designed by standard linear state-feedback methods. However, this approach here might give some *physical* insight to the resulting closed loop system. For example that the closed loop system must have an inertial coupling (${}^{1}_{2}\bar{m} \neq 0$) of the two bodies, if one wants to tune all 4 poles.

4.8.2 PVTOL

The planar vertical take off landing aircraft (PVTOL) as depicted in Figure 4.16, is a common benchmark problem discussed in e.g. [Hauser et al., 1992] or [Fliess et al., 1999].

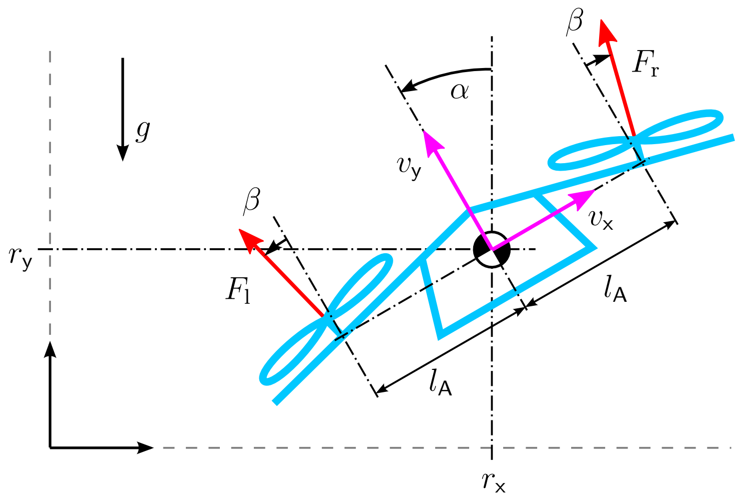

Figure 4.16: Model of the PVTOL

Model. The model of the PVTOL is a planar rigid body alredy discussed in subsection 4.7.4 supplemented with gravity and the specific actuation F_r, F_l depicted in Figure 4.16. Here, we chose the body fixed frame to be positioned at the center of mass, i.e. $s_\mathsf{x} = s_\mathsf{y} = 0$. The kinetic equation takes the form

$$\underbrace{\begin{bmatrix} m & 0 & 0 \\ 0 & m & 0 \\ 0 & 0 & \Theta_\mathsf{z} \end{bmatrix}}_{\boldsymbol{M}} \underbrace{\begin{bmatrix} \dot{v}_\mathsf{x} \\ \dot{v}_\mathsf{y} \\ \dot{\omega}_\mathsf{z} \end{bmatrix}}_{\dot{\boldsymbol{\xi}}} + \underbrace{\begin{bmatrix} m(g\sin\alpha - v_\mathsf{y}\omega_\mathsf{z}) \\ m(g\cos\alpha + v_\mathsf{x}\omega_\mathsf{z}) \\ 0 \end{bmatrix}}_{\boldsymbol{b}} = \underbrace{\begin{bmatrix} \sin\beta & -\sin\beta \\ \cos\beta & \cos\beta \\ l_\mathsf{A}\cos\beta & -l_\mathsf{A}\cos\beta \end{bmatrix}}_{\boldsymbol{B}} \underbrace{\begin{bmatrix} F_\mathrm{r} \\ F_\mathrm{l} \end{bmatrix}}_{\boldsymbol{u}}. \tag{4.129}$$

Reference trajectory. For the following we chose $\boldsymbol{B}^\perp = [1, 0, -\frac{\sin\beta}{l\cos\beta}]$ as a left complement to $\boldsymbol{B}$. With this, the matiching condition for the reference from (4.60) reads

$$\lambda^{\text{ZeroError}} = m\big(\dot{v}_\mathsf{xR} - \underbrace{\tfrac{\Theta_\mathsf{z}\sin\beta}{ml_\mathsf{A}\cos\beta}}_{\varepsilon}\dot{\omega}_\mathsf{zR} - \omega_\mathsf{zR}v_\mathsf{yR} + g\sin\alpha_\mathsf{R}\big) = 0 \tag{4.130}$$

This can be fulfilled by parameterizing the configuration through the flat output $y_\mathsf{1R} = r_\mathsf{xR} - \varepsilon\sin\alpha_\mathsf{R}$, $y_\mathsf{2R} = r_\mathsf{yR} + \varepsilon\cos\alpha_\mathsf{R}$ (see e.g. [Fliess et al., 1999]), i.e.

$$r_\mathsf{xR} = y_\mathsf{1R} - \varepsilon\frac{\ddot{y}_\mathsf{1R}}{\sqrt{\ddot{y}_\mathsf{1R}^2 + (\ddot{y}_\mathsf{2R} + g)^2}}, \tag{4.131}$$

$$r_\mathsf{yR} = y_\mathsf{2R} - \varepsilon\frac{\ddot{y}_\mathsf{2R} - g}{\sqrt{\ddot{y}_\mathsf{1R}^2 + (\ddot{y}_\mathsf{2R} + g)^2}}, \tag{4.132}$$

$$\alpha_\mathsf{R} = \operatorname{atan2}(\ddot{y}_\mathsf{1R}, \ddot{y}_\mathsf{2R} + g). \tag{4.133}$$

Note that this parameterization fails if $\ddot{y}_\mathsf{1R} = \ddot{y}_\mathsf{2R} + g = 0$, i.e. the body is in free fall.

Closed loop. As for the model, the closed loop templates are the ones the planar rigid body from subsection 4.7.4. Due to symmetry reasons we set the parameters $\bar{h}_\mathsf{x} = \bar{l}_\mathsf{x} = \bar{s}_\mathsf{x} = 0$.

Matching. The matching force $\boldsymbol{\lambda}$ from (4.57) with the orthogonal complement from above takes a rather cumbersome form and is not given explicitly here. Instead we will investigate its linear approximation about any reference trajectory with $\alpha_{\mathsf{R}} = 0$: The matrices of the linearized model and desired closed loop are

$$\boldsymbol{M}_0 = \begin{bmatrix} m & 0 & 0 \\ 0 & m & 0 \\ 0 & 0 & J \end{bmatrix}, \qquad \bar{\boldsymbol{M}}_0 = \begin{bmatrix} \bar{m} & 0 & -\bar{m}\bar{s}_{\mathsf{y}} \\ 0 & \bar{m} & 0 \\ -\bar{m}\bar{s}_{\mathsf{y}} & 0 & \bar{\Theta}_{\mathsf{z}} + \bar{m}\bar{s}_{\mathsf{y}}^2 \end{bmatrix}, \tag{4.134a}$$

$$\boldsymbol{D}_0 = \begin{bmatrix} 0 & 0 & 0 \\ 0 & 0 & 0 \\ 0 & 0 & 0 \end{bmatrix}, \qquad \bar{\boldsymbol{D}}_0 = \begin{bmatrix} \bar{d} & 0 & -\bar{d}\bar{l}_{\mathsf{y}} \\ 0 & \bar{d} & 0 \\ -\bar{d}\bar{l}_{\mathsf{y}} & 0 & \bar{\Upsilon}_{\mathsf{z}} + \bar{d}\bar{l}_{\mathsf{y}}^2 \end{bmatrix}, \tag{4.134b}$$

$$\boldsymbol{K}_0 = \begin{bmatrix} 0 & 0 & mg \\ 0 & 0 & 0 \\ 0 & 0 & 0 \end{bmatrix}, \qquad \bar{\boldsymbol{K}}_0 = \begin{bmatrix} \bar{k} & 0 & -\bar{k}\bar{h}_{\mathsf{y}} \\ 0 & \bar{k} & 0 \\ -\bar{k}\bar{h}_{\mathsf{y}} & 0 & \bar{\Pi}_{\mathsf{z}} + \bar{k}\bar{h}_{\mathsf{y}}^2 \end{bmatrix}. \tag{4.134c}$$

The conditions for $(\boldsymbol{B}^{\perp})^{\top}\big(\boldsymbol{M}_0\bar{\boldsymbol{M}}_0^{-1}\bar{\boldsymbol{D}}_0 - \boldsymbol{D}_0\big) = \boldsymbol{0}$ and $(\boldsymbol{B}^{\perp})^{\top}\big(\boldsymbol{M}_0\bar{\boldsymbol{M}}_0^{-1}\bar{\boldsymbol{K}}_0 - \boldsymbol{K}_0\big) = \boldsymbol{0}$ for the linearized matching force from (4.62) to vanish are equivalent to

$$\bar{k}\big(\bar{\Theta}_{\mathsf{z}} - \bar{m}(\bar{h}_{\mathsf{y}} - \bar{s}_{\mathsf{y}})(\bar{s}_{\mathsf{y}} - \varepsilon)\big) = 0, \tag{4.135a}$$

$$\bar{m}\bar{\Pi}_{\mathsf{z}}(\bar{s}_{\mathsf{y}} - \varepsilon) - \bar{k}\bar{h}_{\mathsf{y}}\big(\bar{\Theta}_{\mathsf{z}} - \bar{m}(\bar{h}_{\mathsf{y}} - \bar{s}_{\mathsf{y}})(\bar{s}_{\mathsf{y}} - \varepsilon)\big) = \bar{\Theta}_{\mathsf{z}}\bar{m}g, \tag{4.135b}$$

$$\bar{d}\big(\bar{\Theta}_{\mathsf{z}} - \bar{m}(\bar{l}_{\mathsf{y}} - \bar{s}_{\mathsf{y}})(\bar{s}_{\mathsf{y}} - \varepsilon)\big) = 0, \tag{4.135c}$$

$$\bar{m}\bar{\Upsilon}_{\mathsf{z}}(\bar{s}_{\mathsf{y}} - \varepsilon) - \bar{d}\,\bar{l}_{\mathsf{y}}\big(\bar{\Theta}_{\mathsf{z}} - \bar{m}(\bar{l}_{\mathsf{y}} - \bar{s}_{\mathsf{y}})(\bar{s}_{\mathsf{y}} - \varepsilon)\big) = 0. \tag{4.135d}$$

One solution for this is

$$\bar{\Theta}_{\mathsf{z}} = \bar{m}(\bar{h}_{\mathsf{y}} - \bar{s}_{\mathsf{y}})(\bar{s}_{\mathsf{y}} - \varepsilon), \qquad \bar{l}_{\mathsf{y}} = \bar{h}_{\mathsf{y}}, \qquad \bar{\Upsilon}_{\mathsf{z}} = 0, \qquad \bar{\Pi}_{\mathsf{z}} = \bar{m}g(\bar{h}_{\mathsf{y}} - \bar{s}_{\mathsf{y}}) \tag{4.136}$$

which leaves the parameters $\bar{k}, \bar{d}, \bar{m}, \bar{h}_{\mathsf{y}}, \bar{s}_{\mathsf{y}}$ for tuning. For the energies to be positive (semi) definite, i.e. $\bar{\boldsymbol{M}} > 0$, $\bar{\boldsymbol{D}} \geq 0$ and $\bar{\mathcal{V}} > 0$ we need

$$\bar{k}, \bar{d}, \bar{m} > 0, \qquad \bar{h}_{\mathsf{y}} > \bar{s}_{\mathsf{y}} > \varepsilon. \tag{4.137}$$

The remaining matching force is

$$\tilde{\boldsymbol{b}} = \frac{\bar{m}(\bar{h}_{\mathsf{y}} - \bar{s}_{\mathsf{y}})}{m(\bar{h}_{\mathsf{y}} - \varepsilon)} \begin{bmatrix} 1 \\ 0 \\ -\varepsilon \end{bmatrix} \lambda \tag{4.138}$$

where λ for the corresponding approach is

$$\lambda^{\text{ParticleBased}} = m(a_{\mathsf{yR}} - \varepsilon\omega_{\mathsf{zR}}^2)\sin\alpha_{\mathrm{E}} \tag{4.139a}$$

$$\lambda^{\text{BodyBased}} = m(a_{\mathsf{yR}}\sin\alpha_{\mathrm{E}} - r_{\mathsf{x}\mathrm{E}}\omega_{\mathsf{zR}}^2 + 2v_{\mathsf{y}\mathrm{E}}\omega_{\mathsf{zR}} + (\varepsilon(1 - \cos\alpha_{\mathrm{E}}) - r_{\mathsf{y}\mathrm{E}})\dot{\omega}_{\mathsf{zR}}) \tag{4.139b}$$

$$\lambda^{\text{EnergyBased}} = m(a_{\mathsf{yR}}\sin\alpha_{\mathrm{E}} - r_{\mathsf{x}\mathrm{E}}\omega_{\mathsf{zR}}^2 + v_{\mathsf{y}\mathrm{E}}\omega_{\mathsf{zR}} + (\varepsilon(1 - \cos\alpha_{\mathrm{E}}) - r_{\mathsf{y}\mathrm{E}})\dot{\omega}_{\mathsf{zR}}) \tag{4.139c}$$

where $a_{\mathsf{yR}} = \dot{v}_{\mathsf{yR}} + v_{\mathsf{xR}}\omega_{\mathsf{zR}} + g(\cos\alpha_{\mathsf{R}} - 1)$. Note that for a constant reference motion $\dot{\boldsymbol{v}}_{\mathsf{R}} = 0$ (which implies $\alpha_{\mathsf{R}} = 0$) the matching force vanishes $\lambda = 0$ for all approaches.

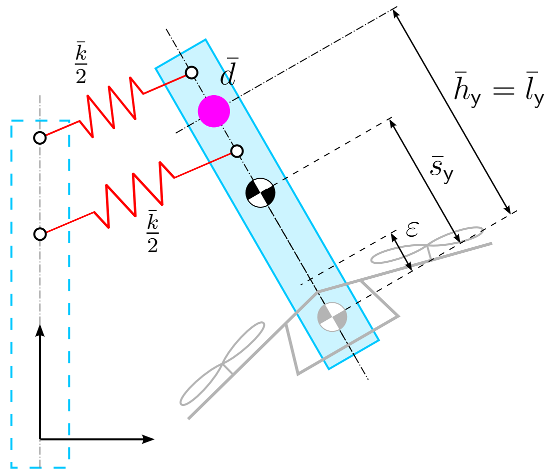

Figure 4.17: Interpretation of the controlled PVTOL as a mechanical system

Mechanical interpretation. The closed loop template is a planar rigid body with attached springs and dampers as motivated in section 3.3 but without gravity. Taking into account the parameter constraints (4.136), the controlled PVTOL corresponds to the mechanical system illustrated in Figure 4.17. The condition $\bar{h}_y > \bar{s}_y$ implies that the center of mass must be below the center of stiffness. As dicussed in subsection 4.7.5, $\bar{h}_y \neq \bar{s}_y$ results in a coupling between translational and rotational motion. From a stability/attractiveness point of view this is necessary: As there is no inherent rotational dissipation $\bar{\varUpsilon}_z = 0$, the correponding energy is dissipated through its coupling to the translational motion. The coupling also reflects the characteristic behaviour of the PVTOL that tilting is required for sideways motion.

Pole placement. Even if the tuning parameters might be mechanically intuitive, a classic pole placement approach can be instructive: The characteristic polynomial of the linearized system is

$$\begin{aligned}&\det(\bar{\boldsymbol{M}}\lambda^2 + \bar{\boldsymbol{D}}\lambda + \bar{\boldsymbol{K}})/\det \bar{\boldsymbol{M}} \\ &\qquad = (\lambda^2 + \tfrac{\bar{d}}{\bar{m}}\lambda + \tfrac{\bar{k}}{\bar{m}})\big(\lambda^4 + \tfrac{\bar{d}(\bar{h}_y-\varepsilon)}{\bar{m}(\bar{s}_y-\varepsilon)}\lambda^3 + \tfrac{\bar{k}(\bar{h}_y-\varepsilon)+\bar{m}g}{\bar{m}(\bar{s}_y-\varepsilon)}\lambda^2 + \tfrac{\bar{d}g}{\bar{m}(\bar{s}_y-\varepsilon)}\lambda + \tfrac{\bar{k}g}{\bar{m}(\bar{s}_y-\varepsilon)}\big) \end{aligned} \tag{4.140}$$

From a desired polynomial of forth degree $\lambda^4 + p_3\lambda^3 + p_2\lambda^2 + p_1\lambda + p_0$ we get the parameters

$$\bar{k} = \frac{\bar{m}\,p_0 p_1}{p_1p_2 - p_0p_3}, \quad \bar{h}_y = \varepsilon + \frac{g\,p_3}{p_1}, \quad \bar{\varTheta}_z = \frac{\bar{m}g^2(p_1p_2p_3 - p_1^2 - p_0p_3^2)}{(p_1p_2 - p_0p_3)^2}, \tag{4.141}$$

$$\bar{d} = \frac{\bar{m}\,p_1^2}{p_1p_2 - p_0p_3}, \quad \bar{s}_y = \varepsilon + \frac{g\,p_1}{p_1p_2 - p_0p_3}, \quad \bar{\varPi}_z = \frac{\bar{m}g^2(p_1p_2p_3 - p_1^2 - p_0p_3)}{p_1(p_1p_2 - p_0p_3)}, \tag{4.142}$$

and leaves an arbitrary choice for $\bar{m} > 0$. Note that the Hurwitz criterion $(p_0, p_1, p_2, p_3, p_1p_2 - p_0p_3, p_1p_2p_3 - p_1^2 - p_0p_3^2 > 0)$ implies that $\bar{k}, \bar{d}, \bar{\varTheta}_z, \bar{\varPi}_z > 0$ which ultimatly implies positive definiteness of the total energy and non-negativity of its derivative.

Simulation. A very similar control design approch for the PVTOL was presented in [Konz and Rudolph, 2016]. Therein on finds two examplary simulation results for stabilization and tracking or a looping trajectory.

The PVTOL is a simpler version of the 3d bicopter which will be discussed in the following and the simulation results there also apply to the PVTOL.

4.8.3 Quadcopter

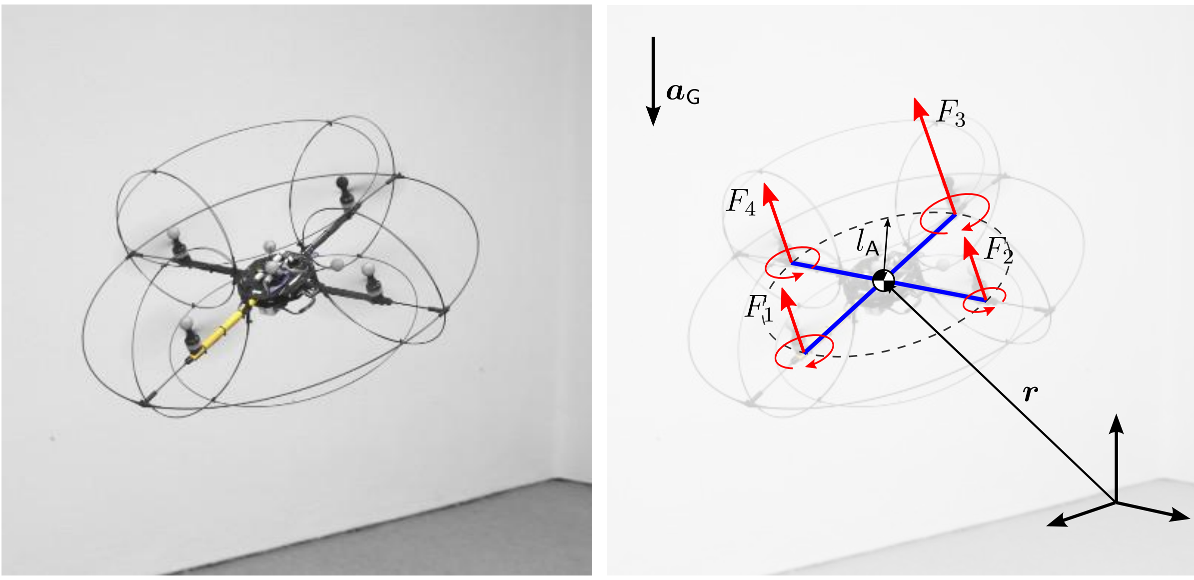

Figure 4.18: Model of the Quadcopter

Model. Mechanically, a quadcopter is a free 3d rigid body subject to gravity and the specific actuation as illustrated in Figure 4.18. It is reasonable to chose the center of mass as the reference point and assume that the body frame coincides with the priciple axes of inertia. Then the kinetic equation takes the form

$$\underbrace{\begin{bmatrix} m & 0 & 0 & 0 & 0 & 0 \\ 0 & m & 0 & 0 & 0 & 0 \\ 0 & 0 & m & 0 & 0 & 0 \\ 0 & 0 & 0 & \Theta_{\mathsf{y}} & 0 & 0 \\ 0 & 0 & 0 & 0 & \Theta_{\mathsf{x}} & 0 \\ 0 & 0 & 0 & 0 & 0 & \Theta_{\mathsf{z}} \end{bmatrix}}_{\boldsymbol{M}} \underbrace{\begin{bmatrix} \dot{v}_{\mathsf{x}} \\ \dot{v}_{\mathsf{y}} \\ \dot{v}_{\mathsf{z}} \\ \dot{\omega}_{\mathsf{x}} \\ \dot{\omega}_{\mathsf{y}} \\ \dot{\omega}_{\mathsf{z}} \end{bmatrix}}_{\dot{\boldsymbol{\xi}}} + \underbrace{\begin{bmatrix} m(v_{\mathsf{y}}\omega_{\mathsf{z}} - v_{\mathsf{z}}\omega_{\mathsf{y}} + R^{\mathsf{z}}_{\mathsf{x}} g) \\ m(v_{\mathsf{x}}\omega_{\mathsf{z}} - v_{\mathsf{z}}\omega_{\mathsf{x}} + R^{\mathsf{z}}_{\mathsf{y}} g) \\ m(v_{\mathsf{y}}\omega_{\mathsf{x}} - v_{\mathsf{x}}\omega_{\mathsf{y}} + R^{\mathsf{z}}_{\mathsf{z}} g) \\ (\Theta_{\mathsf{z}} - \Theta_{\mathsf{y}})\omega_{\mathsf{y}}\omega_{\mathsf{z}} \\ (\Theta_{\mathsf{x}} - \Theta_{\mathsf{z}})\omega_{\mathsf{x}}\omega_{\mathsf{z}} \\ (\Theta_{\mathsf{y}} - \Theta_{\mathsf{x}})\omega_{\mathsf{x}}\omega_{\mathsf{y}} \end{bmatrix}}_{\boldsymbol{b}} = \underbrace{\begin{bmatrix} 0 & 0 & 0 & 0 \\ 0 & 0 & 0 & 0 \\ 1 & 1 & 1 & 1 \\ 0 & l_{\mathsf{A}} & 0 & -l_{\mathsf{A}} \\ -l_{\mathsf{A}} & 0 & l_{\mathsf{A}} & 0 \\ -b_{\mathsf{F}} & b_{\mathsf{F}} & -b_{\mathsf{F}} & b_{\mathsf{F}} \end{bmatrix}}_{\boldsymbol{B}} \underbrace{\begin{bmatrix} F_1 \\ F_2 \\ F_3 \\ F_4 \end{bmatrix}}_{\boldsymbol{u}} \tag{4.143}$$

Reference trajectory. An obvious left complement for $\boldsymbol{B}$ is

$$(\boldsymbol{B}^{\perp})^{\top} = \begin{bmatrix} 1 & 0 & 0 & 0 & 0 & 0 \\ 0 & 1 & 0 & 0 & 0 & 0 \end{bmatrix}. \tag{4.144}$$

With this, the matiching condition for the reference from (4.60) are just the two first equations of (4.143):

$$\boldsymbol{\lambda}^{\text{ZeroError}} = m \begin{bmatrix} \dot{v}_{\mathsf{xR}} + v_{\mathsf{zR}}\omega_{\mathsf{yR}} - v_{\mathsf{yR}}\omega_{\mathsf{zR}} + R^{\mathsf{z}}_{\mathsf{xR}} g \\ \dot{v}_{\mathsf{yR}} + v_{\mathsf{xR}}\omega_{\mathsf{zR}} - v_{\mathsf{zR}}\omega_{\mathsf{xR}} + R^{\mathsf{z}}_{\mathsf{yR}} g \end{bmatrix} = \boldsymbol{0}. \tag{4.145}$$

This may be easily resolved by formulating the reference trajectory in terms of the systems flat output $\boldsymbol{r}$ and some parameterization of the orientation about the body fixed z-axis as done in [Konz and Rudolph, 2013].

Closed loop template. As the quadcopter is just a free rigid body with a particular actuation, the closed loop templates coincide with the ones given in subsection 4.1.2, subsection 4.2.1 and subsection 4.3.3. Due to symmetry considerations we set $\bar{s}_\mathsf{x} = \bar{s}_\mathsf{y} = 0$, $\bar{\Theta}_\mathsf{xx} = \bar{\Theta}_\mathsf{yy}$, $\bar{\Theta}_\mathsf{xy} = \bar{\Theta}_\mathsf{xz} = \bar{\Theta}_\mathsf{yz} = 0$ and analog for the stiffness and damping parameters.

Matching. The explicit matching conditions are too cumbersome to be displayed here. Instead we start again with the linearized version: The linearized system matrices for model and closed loop template are

$$\boldsymbol{M}_0 = \begin{bmatrix} m & 0 & 0 & 0 & 0 & 0 \\ 0 & m & 0 & 0 & 0 & 0 \\ 0 & 0 & m & 0 & 0 & 0 \\ 0 & 0 & 0 & \Theta_\mathsf{y} & 0 & 0 \\ 0 & 0 & 0 & 0 & \Theta_\mathsf{x} & 0 \\ 0 & 0 & 0 & 0 & 0 & \Theta_\mathsf{z} \end{bmatrix}, \quad \bar{\boldsymbol{M}}_0 = \begin{bmatrix} \bar{m} & 0 & 0 & 0 & \bar{m}\bar{s}_\mathsf{z} & 0 \\ 0 & \bar{m} & 0 & -\bar{m}\bar{s}_\mathsf{z} & 0 & 0 \\ 0 & 0 & \bar{m} & 0 & 0 & 0 \\ 0 & -\bar{m}\bar{s}_\mathsf{z} & 0 & \bar{\Theta}_\mathsf{x} + \bar{m}\bar{s}_\mathsf{z}^2 & 0 & 0 \\ \bar{m}\bar{s}_\mathsf{z} & 0 & 0 & 0 & \bar{\Theta}_\mathsf{x} + \bar{m}\bar{s}_\mathsf{z}^2 & 0 \\ 0 & 0 & 0 & 0 & 0 & \bar{\Theta}_\mathsf{z} \end{bmatrix},$$

$$\boldsymbol{D}_0 = \begin{bmatrix} 0 & 0 & 0 & 0 & 0 & 0 \\ 0 & 0 & 0 & 0 & 0 & 0 \\ 0 & 0 & 0 & 0 & 0 & 0 \\ 0 & 0 & 0 & 0 & 0 & 0 \\ 0 & 0 & 0 & 0 & 0 & 0 \\ 0 & 0 & 0 & 0 & 0 & 0 \end{bmatrix}, \quad \bar{\boldsymbol{D}}_0 = \begin{bmatrix} \bar{d} & 0 & 0 & 0 & \overline{dl}_\mathsf{z} & 0 \\ 0 & \bar{d} & 0 & -\overline{dl}_\mathsf{z} & 0 & 0 \\ 0 & 0 & \bar{d} & 0 & 0 & 0 \\ 0 & -\overline{dl}_\mathsf{z} & 0 & \bar{\Upsilon}_\mathsf{x} + \overline{dl}_\mathsf{z}^2 & 0 & 0 \\ \overline{dl}_\mathsf{z} & 0 & 0 & 0 & \bar{\Upsilon}_\mathsf{x} + \overline{dl}_\mathsf{z}^2 & 0 \\ 0 & 0 & 0 & 0 & 0 & \bar{\Upsilon}_\mathsf{z} \end{bmatrix},$$

$$\boldsymbol{K}_0 = \begin{bmatrix} 0 & 0 & 0 & 0 & -mg & 0 \\ 0 & 0 & 0 & mg & 0 & 0 \\ 0 & 0 & 0 & 0 & 0 & 0 \\ 0 & 0 & 0 & 0 & 0 & 0 \\ 0 & 0 & 0 & 0 & 0 & 0 \\ 0 & 0 & 0 & 0 & 0 & 0 \end{bmatrix}, \quad \bar{\boldsymbol{K}}_0 = \begin{bmatrix} \bar{k} & 0 & 0 & 0 & \bar{k}\bar{h}_\mathsf{z} & 0 \\ 0 & \bar{k} & 0 & -\bar{k}\bar{h}_\mathsf{z} & 0 & 0 \\ 0 & 0 & \bar{k} & 0 & 0 & 0 \\ 0 & -\bar{k}\bar{h}_\mathsf{z} & 0 & \bar{\Pi}_\mathsf{x} + \bar{k}\bar{h}_\mathsf{z}^2 & 0 & 0 \\ \bar{k}\bar{h}_\mathsf{z} & 0 & 0 & 0 & \bar{\Pi}_\mathsf{x} + \bar{k}\bar{h}_\mathsf{z}^2 & 0 \\ 0 & 0 & 0 & 0 & 0 & \bar{\Pi}_\mathsf{z} \end{bmatrix}.$$

Taking into account the symmetries between x and y directions, the remaining linearized matching conditions are

$$\bar{k}(\bar{\Theta}_\mathsf{x} - \bar{m}\bar{s}_\mathsf{z}(\bar{h}_\mathsf{z} - \bar{s}_\mathsf{z})) = 0 \tag{4.146a}$$
$$\bar{m}(\bar{\Theta}_\mathsf{x} g - \bar{\Pi}_\mathsf{x}\bar{s}_\mathsf{z}) + \bar{k}\bar{h}_\mathsf{z}(\bar{\Theta}_\mathsf{x} - \bar{m}\bar{s}_\mathsf{z}(\bar{h}_\mathsf{z} - \bar{s}_\mathsf{z})) = 0 \tag{4.146b}$$
$$\bar{d}(\bar{\Theta}_\mathsf{x} - \bar{m}\bar{s}_\mathsf{z}(\bar{h}_\mathsf{z} - \bar{s}_\mathsf{z})) = 0 \tag{4.146c}$$
$$-\bar{m}\bar{s}_\mathsf{z}\bar{\Upsilon}_\mathsf{x} + \overline{dl}_\mathsf{z}(\bar{\Theta}_\mathsf{x} - \bar{m}\bar{s}_\mathsf{z}(\bar{l}_\mathsf{z} - \bar{s}_\mathsf{z})) = 0 \tag{4.146d}$$

It is not surprising that these are identical to the previously encountered conditions (4.135) for the PVTOL for $\varepsilon = 0$. Consequently we use the same solution

$$\bar{l}_\mathsf{z} = \bar{h}_\mathsf{z}, \quad \bar{\Theta}_\mathsf{x} = \bar{\Theta}_\mathsf{y} = \bar{m}\bar{s}_\mathsf{z}(\bar{h}_\mathsf{z} - \bar{s}_\mathsf{z}), \quad \bar{\Upsilon}_\mathsf{x} = \bar{\Upsilon}_\mathsf{y} = 0, \quad \bar{\Pi}_\mathsf{x} = \bar{\Pi}_\mathsf{y} = \bar{m}g(\bar{h}_\mathsf{z} - \bar{s}_\mathsf{z}). \tag{4.147}$$

which leaves the tuning parameters $\bar{m}, \bar{d}, \bar{k}, \bar{s}_\mathsf{z}, \bar{h}_\mathsf{z}$ and $\bar{\Theta}_\mathsf{z}, \bar{\Upsilon}_\mathsf{z}, \bar{\Pi}_\mathsf{z}$.

Even with the linearized matching condtions fulfilled, the nonlinear matching condition is still to cumbersome to be displayed here. For the case of a constant reference velocity $\dot{\boldsymbol{v}}_{\mathsf{R}} = \mathbf{0}$ and its implications on the reference attitude, $\omega_{\mathsf{xR}} = \omega_{\mathsf{yR}} = 0$, we have the residual matching force

$$\tilde{\boldsymbol{b}} = \frac{\bar{m}}{m\bar{h}_{\mathsf{z}}} \begin{bmatrix} \bar{\Theta}_{\mathsf{z}}\omega_{\mathsf{x}}\omega_{\mathsf{z}} - \frac{1}{2}\bar{\Pi}_{\mathsf{z}}(R^{\mathsf{x}}_{\mathsf{z}\mathrm{E}} + R^{\mathsf{z}}_{\mathsf{x}\mathrm{E}}) \\ \bar{\Theta}_{\mathsf{z}}\omega_{\mathsf{y}}\omega_{\mathsf{z}} - \frac{1}{2}\bar{\Pi}_{\mathsf{z}}(R^{\mathsf{y}}_{\mathsf{z}\mathrm{E}} + R^{\mathsf{z}}_{\mathsf{y}\mathrm{E}}) \\ 0 \\ 0 \\ 0 \\ 0 \end{bmatrix}. \tag{4.148}$$

Tuning. The first set of parameters $\bar{m}, \bar{d}, \bar{k}, \bar{s}_{\mathsf{z}}, \bar{h}_{\mathsf{z}}$ may be tuned just as presented for the PVTOL, see Figure 4.17. The parameters accociated with the heading control may be set to $\bar{\Upsilon}_{\mathsf{z}} = 2\bar{\Theta}_{\mathsf{z}}\zeta\omega_0$ and $\bar{\Pi}_{\mathsf{z}} = \bar{\Theta}_{\mathsf{z}}\omega_0^2$ to obtain a desired bandwidth ω_0 and damping ratio ζ. The corresponding moment of inertia $\bar{\Theta}_{\mathsf{z}} > 0$ may be adjusted in relation to $\bar{\Theta}_{\mathsf{x}}$ as a priority factor between heading control and tilt control. This is most crucial if the quatcopter propellers are at their constraints and the control has to find a trade-off between maintaining its tilt (and consequently its position), or the heading. For most applications heading is less important than tilt so one may set $\bar{\Theta}_{\mathsf{z}} = 0.1\,\bar{\Theta}_{\mathsf{x}}$ as was done for the experiments with the LSR quadcopter presented in the next section.

Simulation results. The body based approach proposed here was also discussed in [Konz and Rudolph, 2021] which also showed simulation results for a looping trajectory. Furthermore, this approch was implemented for the experimental setup in the LSR quadcopter. The results are discussed in detail in the next chapter.

4.8.4 Bicopter

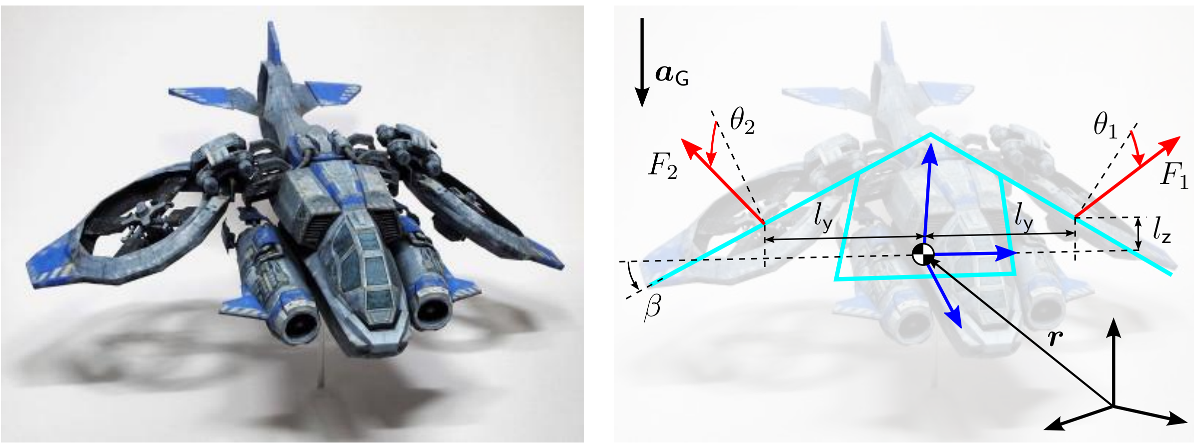

Figure 4.19: Model of a bicopter (background image: www.poppaper.net/80155164809)

Equations of motion. The bicopter considered here is a single rigid body with two tiltable propellers as illustrated in Figure 4.18. With the same coordinates as for the previous examples, the equations of motion are identical as well up to the generalized force from the propellers

$$\boldsymbol{f}^{\mathrm{U}} = \underbrace{\begin{bmatrix} 1 & 0 & 1 & 0 \\ 0 & \sin\beta_{\mathsf{F}} & 0 & -\sin\beta_{\mathsf{F}} \\ 0 & \cos\beta_{\mathsf{F}} & 0 & \cos\beta_{\mathsf{F}} \\ 0 & l'_{\mathsf{y}} & 0 & -l'_{\mathsf{y}} \\ l_{\mathsf{z}} & 0 & l_{\mathsf{z}} & 0 \\ -l_{\mathsf{y}} & 0 & l_{\mathsf{y}} & 0 \end{bmatrix}}_{\boldsymbol{B}} \underbrace{\begin{bmatrix} F_1 \sin\theta_1 \\ F_1\cos\theta_1 \\ F_2\sin\theta_2 \\ F_2\cos\theta_2 \end{bmatrix}}_{\boldsymbol{u}}. \tag{4.149}$$

with $l'_{\mathsf{y}} = l_{\mathsf{y}}\cos\beta_{\mathsf{F}} - l_{\mathsf{z}}\sin\beta_{\mathsf{F}}$. The transformation of the actual control inputs F_1, F_2 and θ_1, θ_2 to a auxiliary input $\boldsymbol{u}$ is used to achieve the linear form $\boldsymbol{f}^{\mathrm{U}} = \boldsymbol{B}\boldsymbol{u}$. Within the input constraints $2\,\mathrm{N} \leq F_i \leq 14\,\mathrm{N}$, $-30° \leq \theta_i \leq 30°$, $i = 1, 2$ this transformation is bijective. To account for the original constraints in the transformed input $\boldsymbol{u} \in \mathbb{R}^4$, a convex approximation illustrated in Figure 4.20 is used. These constraints can be written in the required form $\boldsymbol{W}\boldsymbol{u} \leq \boldsymbol{l}$.

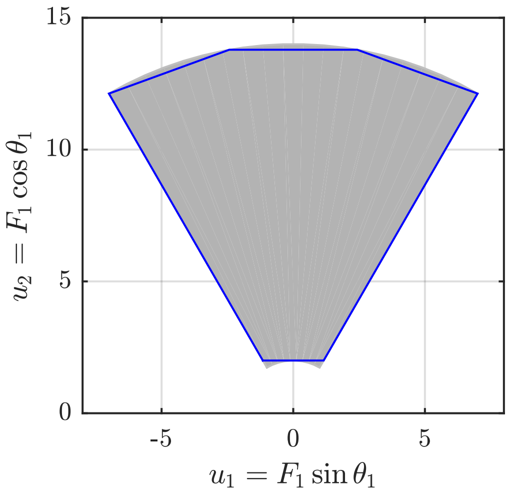

Figure 4.20: Approximation of the Bicopter input constraints

Reference trajectory. A possible left complement for $\boldsymbol{B}$ is

$$(\boldsymbol{B}^{\perp})^{\top} = \begin{bmatrix} l_{\mathsf{z}} & 0 & 0 & 0 & -1 & 0 \\ 0 & l'_{\mathsf{y}} & 0 & -\sin\beta_{\mathsf{F}} & 0 & 0 \end{bmatrix} \tag{4.150}$$

With this, the matching condition for the reference from (4.60) is

$$\boldsymbol{\lambda}^{\text{ZeroError}} = \begin{bmatrix} ml_{\mathsf{z}}\big(\dot{v}_{\mathsf{x}} + v_{\mathsf{y}}\omega_{\mathsf{z}} - v_{\mathsf{z}}\omega_{\mathsf{y}} - \varepsilon_{\mathsf{x}}(\dot{\omega}_{\mathsf{y}} + \frac{\Theta_{\mathsf{x}}-\Theta_{\mathsf{z}}}{\Theta_{\mathsf{y}}}\omega_{\mathsf{x}}\omega_{\mathsf{z}}) + R^{\mathsf{z}}_{\mathsf{x}}g\big) \\ ml'_{\mathsf{y}}\big(\dot{v}_{\mathsf{y}} + v_{\mathsf{x}}\omega_{\mathsf{z}} - v_{\mathsf{z}}\omega_{\mathsf{x}} + \varepsilon_{\mathsf{y}}(\dot{\omega}_{\mathsf{x}} + \frac{\Theta_{\mathsf{z}}-\Theta_{\mathsf{y}}}{\Theta_{\mathsf{x}}}\omega_{\mathsf{y}}\omega_{\mathsf{z}}) + R^{\mathsf{z}}_{\mathsf{y}}g\big) \end{bmatrix} = \boldsymbol{0}. \tag{4.151}$$

where

$$\varepsilon_{\mathsf{x}} = -\frac{\Theta_{\mathsf{y}}}{m l_{\mathsf{z}}}, \qquad \varepsilon_{\mathsf{y}} = \frac{\Theta_{\mathsf{x}} \sin\beta_{\mathsf{F}}}{m(l_{\mathsf{y}}\cos\beta_{\mathsf{F}} - l_{\mathsf{z}}\sin\beta_{\mathsf{F}})}. \tag{4.152}$$

For the general case[4] $\varepsilon_{\mathsf{x}} \neq \varepsilon_{\mathsf{y}}$ this system is probably not flat, so parameterization of a feasible reference trajectory is not trivial.

Closed loop template. As for the quadcopter, the closed loop templates are that of a free rigid body i.e. subsection 4.1.2, subsection 4.2.1 and subsection 4.3.3. However, in contrast to the quadcopter there are no assumtions on symmetries in the constitutive parameters.

Matching. As before we first consider the linearized matching condtions: It turns out that asymmetries in the constitutive parameters are not useful for resolving matching constraints. So we set $\bar{\Theta}_{\mathsf{xy}} = \bar{\Theta}_{\mathsf{xz}} = \bar{\Theta}_{\mathsf{yz}} = 0$, $\bar{s}_{\mathsf{x}} = \bar{s}_{\mathsf{y}} = 0$ and the same for damping and stiffness. The remaining linearized matching conditions may be fulfilled by constraining the parameters as

$$\bar{l}_{\mathsf{z}} = \bar{h}_{\mathsf{z}}, \qquad \bar{\Upsilon}_{\mathsf{x}} = \bar{\Upsilon}_{\mathsf{y}} = 0, \qquad \bar{\Pi}_{\mathsf{x}} = \bar{\Pi}_{\mathsf{y}} = \bar{m}g(\bar{h}_{\mathsf{z}} - \bar{s}_{\mathsf{z}}), \tag{4.153a}$$

$$\bar{\Theta}_{\mathsf{x}} = \bar{m}(\bar{h}_{\mathsf{z}} - \bar{s}_{\mathsf{z}})(\bar{s}_{\mathsf{z}} - \varepsilon_{\mathsf{y}}), \qquad \bar{\Theta}_{\mathsf{y}} = \bar{m}(\bar{h}_{\mathsf{z}} - \bar{s}_{\mathsf{z}})(\bar{s}_{\mathsf{z}} - \varepsilon_{\mathsf{x}}), \tag{4.153b}$$

which leaves the tuning parameters $\bar{m}, \bar{d}, \bar{k}, \bar{s}_{\mathsf{z}}, \bar{h}_{\mathsf{z}}$ and $\bar{\Theta}_{\mathsf{z}}, \bar{\Upsilon}_{\mathsf{z}}, \bar{\Pi}_{\mathsf{z}}$. Note, in contrast to the quadcopter, that $\varepsilon_{\mathsf{x}} \neq \varepsilon_{\mathsf{y}}$ implies $\bar{\Theta}_{\mathsf{x}} \neq \bar{\Theta}_{\mathsf{y}}$ and since the remaining relevant parameters are identical, the closed loop dynamics for x and y are different from another.

The remaining matching force in the stabilization case $\boldsymbol{\xi}_{\mathsf{R}} = \mathbf{0}$ is

$$\tilde{\boldsymbol{b}} = \frac{\bar{m}}{m}\begin{bmatrix} \frac{1}{\bar{h}_{\mathsf{z}} - \varepsilon_{\mathsf{x}}} & 0 \\ 0 & \frac{1}{\bar{h}_{\mathsf{z}} - \varepsilon_{\mathsf{y}}} \\ 0 & 0 \\ 0 & -\frac{\varepsilon_{\mathsf{y}}}{\bar{h}_{\mathsf{z}} - \varepsilon_{\mathsf{y}}} \\ \frac{\varepsilon_{\mathsf{x}}}{\bar{h}_{\mathsf{z}} - \varepsilon_{\mathsf{x}}} & 0 \\ 0 & 0 \end{bmatrix} \begin{bmatrix} \big(\bar{\Theta}_{\mathsf{z}} - \bar{m}(\bar{h}_{\mathsf{z}} - \bar{s}_{\mathsf{z}})(\frac{\Theta_{\mathsf{x}} - \Theta_{\mathsf{z}}}{\Theta_{\mathsf{y}}}\varepsilon_{\mathsf{x}} - \varepsilon_{\mathsf{y}})\big)\omega_{\mathsf{y}}\omega_{\mathsf{z}} - \frac{1}{2}\bar{\Pi}_{\mathsf{z}}(R^{\mathsf{x}}_{\mathrm{zE}} + R^{\mathsf{z}}_{\mathrm{xE}}) \\ \big(\bar{\Theta}_{\mathsf{z}} - \bar{m}(\bar{h}_{\mathsf{z}} - \bar{s}_{\mathsf{z}})(\frac{\Theta_{\mathsf{y}} - \Theta_{\mathsf{z}}}{\Theta_{\mathsf{x}}}\varepsilon_{\mathsf{y}} - \varepsilon_{\mathsf{x}})\big)\omega_{\mathsf{x}}\omega_{\mathsf{z}} - \frac{1}{2}\bar{\Pi}_{\mathsf{z}}(R^{\mathsf{y}}_{\mathrm{zE}} + R^{\mathsf{z}}_{\mathrm{yE}}) \end{bmatrix} \tag{4.154}$$

Simulation result. Since the bicopter model is probably not flat, generation of a feasible reference trajectory is not trivial. For the simulation example here we exploited that, if we set $r_{\mathsf{xR}} = 0$ and $R^{\mathsf{x}}_{\mathsf{x}} = 1$, the motion is constrained to the yz plane and the remaining model is essentially a PVTOL.

As a challanging reference trajectory a vertical circle was chosen.

[4]Even in the case $\varepsilon_{\mathsf{x}} = \varepsilon_{\mathsf{y}} \neq 0$ we would need $\Theta_{\mathsf{x}} = \Theta_{\mathsf{y}} = \Theta_{\mathsf{z}}$ for $\boldsymbol{r} + \boldsymbol{R\varepsilon}$ to be a flat output. The case $\varepsilon_{\mathsf{x}} = 0$ implies $\Theta_{\mathsf{y}} = 0$, which does not make physical sense.

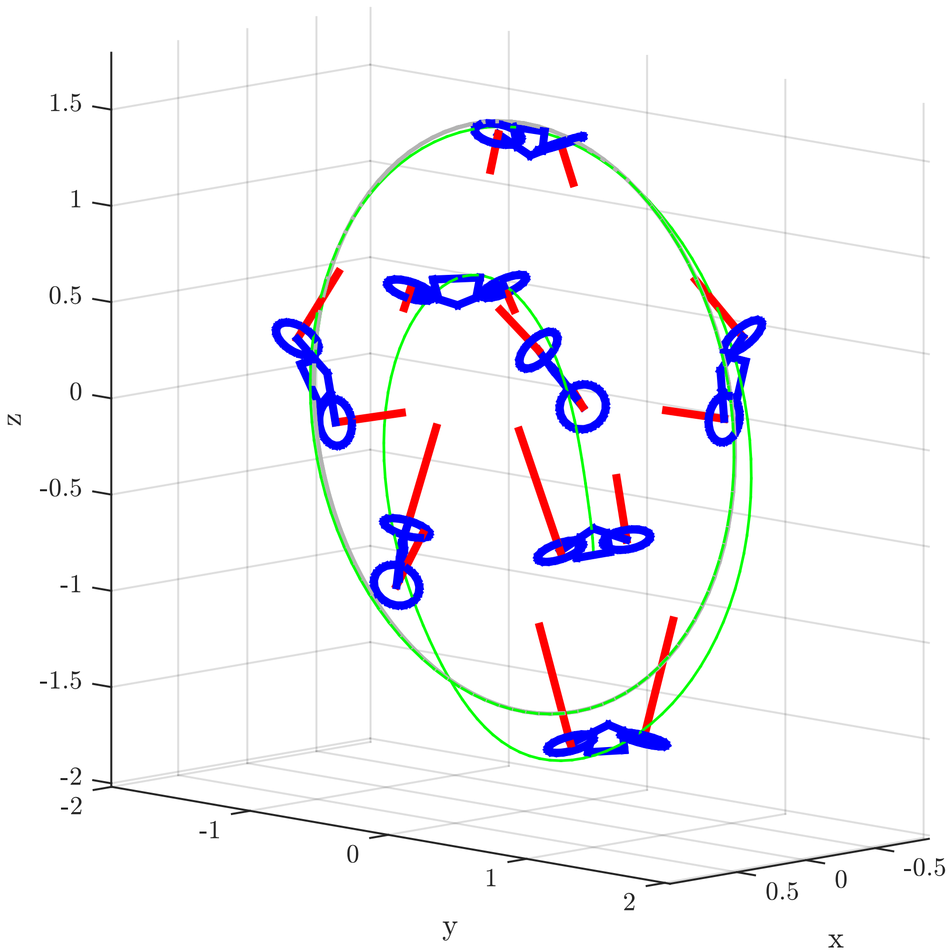

Figure 4.21: Snapshots for the simulation of the bicopter

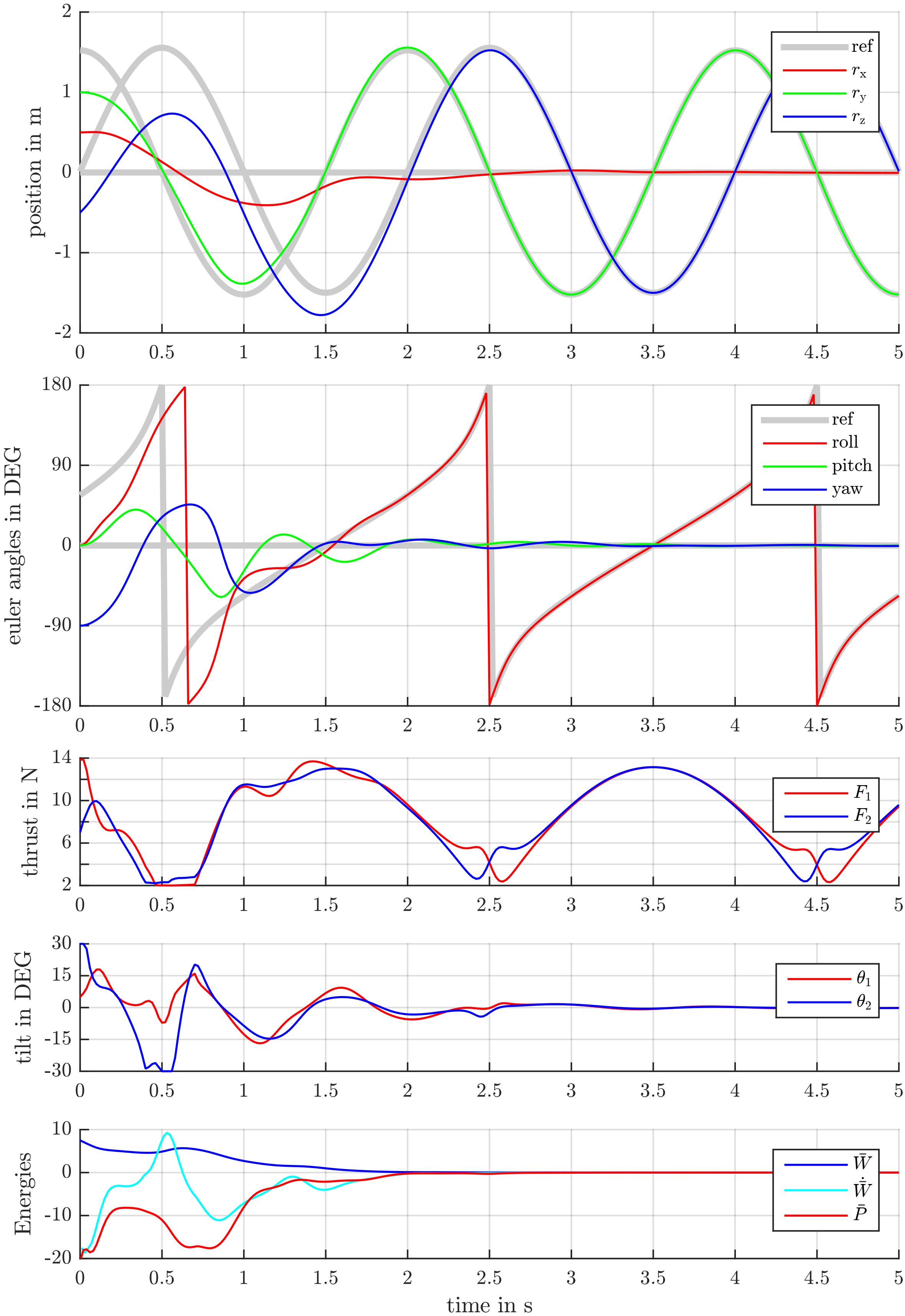

Figure 4.22: Simulation result for the bicopter

Chapter 5

Multicopter control realization

This chapter describes the realization and discusses the experimental results with the LSR-Multicopters. On the highest abstraction layer they can be regarded as a single rigid body with body fixed forces (the propellers forces and torques). The tracking control of these models has been extensively discussed in the previous chapter.

- Hardware realization
  - mechanical construction,
  - actuators/Propellers, power electronics
  - sensorics
  - communication
  - framework for controller implementation
- mathematical model of the multicopters (Quadcopter, Tricopter)
  - full model: multibody, servo dynamics, propeller model, propeller motor model
  - simplified model for control design
  - model validation
- control of the actuators to generate the required generalized force on the rigid body
  - propeller control
  - servo control
  - Quadcopter force vector control
- state estimation
  - misalignment correction
  - Sensor model: IMU & Vicon
  - velocity and bias observer
  - configuration observer

- reference generation
  - for pilot supporting control
  - for position control
- rigid body controller
  - pilot supporting control
  - full configuration control
  - comparison to other controllers
- control integral action
- experiments
  - Maneuver42
  - maneuver53 (flip)
  - loop (the real loop)

Chapter 6

Conclusion

Many machines, vehicles and robots may be modeled as rigid body systems, i.e. a number of interconnected, undeformable bodies subject to inertia, gravity, and other forces. Energy-based methods for derivation of their equations of motion, like the Lagrange formalism, are standard in engineering education and well established in the dedicated literature. These algorithms commonly rely on the use of a minimal set of generalized coordinates. This is appropriate for many applications, e.g. machines containing only one-dimensional joints. For systems whose configuration space is nonlinear, e.g. mobile robots whose configiguration space contains the rigid body attitude, the use of minimal coordinates necessarily leads to singularities. From the point of view of differential geometry, this is a well known fact.

[Konz and Rudolph, 2015] [Konz and Rudolph, 2018] [Irscheid et al., 2019], [Konz and Rudolph, 2021], [Kastelan et al., 2015] [Konz et al., 2018] [Konz et al., 2020]

Appendix A

TBD

A.1 On error coordinates

Error coordinates. Introduce (possibly redundant) error coordinates $\boldsymbol{e} \in \mathbb{R}^{\nu_e}$ as

$$\boldsymbol{e} = \boldsymbol{\chi}_{\mathrm{E}}(\boldsymbol{x}, \boldsymbol{x}_{\mathsf{R}}), \qquad \boldsymbol{\phi}_{\mathrm{E}}(\boldsymbol{e}) = 0. \tag{A.1}$$

and require that this relation is invertible with $\boldsymbol{x} = \boldsymbol{\chi}(\boldsymbol{e}, \boldsymbol{x}_{\mathsf{R}})$, i.e. $\boldsymbol{\chi}(\boldsymbol{\chi}_{\mathrm{E}}(\boldsymbol{x}, \boldsymbol{x}_{\mathsf{R}}), \boldsymbol{x}_{\mathsf{R}}) = \boldsymbol{x} \,\forall\, \boldsymbol{x} \in \mathbb{X}$. The inverse function theorem now implies that the differential $\boldsymbol{\nabla}\boldsymbol{\chi}_{\mathrm{E}} = \frac{\partial \boldsymbol{\chi}_{\mathrm{E}}}{\partial \boldsymbol{x}} \boldsymbol{A}$ has full rank: $\operatorname{rank}(\boldsymbol{\nabla}\boldsymbol{\chi}_{\mathrm{E}}) = \dim \mathbb{X} = n$.

Let $\boldsymbol{\Phi}_{\mathrm{E}}$ be the linear independent rows of $\partial \boldsymbol{\phi}_{\mathrm{E}} / \partial \boldsymbol{e}$. Then the derivative of the geometric constraint $\dot{\boldsymbol{\phi}}_{\mathrm{E}} = 0$ implies

$$\boldsymbol{\Phi}_{\mathrm{E}} \boldsymbol{\nabla}\boldsymbol{\chi}_{\mathrm{E}} = 0, \qquad \boldsymbol{\Phi}_{\mathrm{E}} \boldsymbol{\nabla}_{\mathsf{R}}\boldsymbol{\chi}_{\mathrm{E}} = 0, \tag{A.2}$$

Since the matrices $\boldsymbol{\nabla}\boldsymbol{\chi}_{\mathrm{E}}$ and $\boldsymbol{\Phi}_{\mathrm{E}}$ have full rank, their pseudo-inverses are

$$(\boldsymbol{\nabla}\boldsymbol{\chi}_{\mathrm{E}})^{+} = \big((\boldsymbol{\nabla}\boldsymbol{\chi}_{\mathrm{E}})^{\top} (\boldsymbol{\nabla}\boldsymbol{\chi}_{\mathrm{E}})\big)^{-1} (\boldsymbol{\nabla}\boldsymbol{\chi}_{\mathrm{E}})^{\top}, \qquad (\boldsymbol{\nabla}\boldsymbol{\chi}_{\mathrm{E}})^{+} (\boldsymbol{\nabla}\boldsymbol{\chi}_{\mathrm{E}}) = \mathbf{I}_n \tag{A.3}$$

$$\boldsymbol{\Phi}_{\mathrm{E}}^{+} = \boldsymbol{\Phi}_{\mathrm{E}}^{\top} \big(\boldsymbol{\Phi}_{\mathrm{E}} \boldsymbol{\Phi}_{\mathrm{E}}^{\top}\big)^{-1}, \qquad \boldsymbol{\Phi}_{\mathrm{E}} \boldsymbol{\Phi}_{\mathrm{E}}^{+} = \mathbf{I}_{\nu_e - n}. \tag{A.4}$$

Furthermore, due to the orthogonality $\boldsymbol{\Phi}_{\mathrm{E}} \boldsymbol{\nabla}\boldsymbol{\chi}_{\mathrm{E}} = 0$ we have

$$(\boldsymbol{\nabla}\boldsymbol{\chi}_{\mathrm{E}})(\boldsymbol{\nabla}\boldsymbol{\chi}_{\mathrm{E}})^{+} + \boldsymbol{\Phi}_{\mathrm{E}}^{+} \boldsymbol{\Phi}_{\mathrm{E}} = \mathbf{I}_{\nu_e}. \tag{A.5}$$

Error potential. We require that the potential $\bar{\mathcal{V}}$ can be expressed as a function $\bar{\mathcal{V}}_{\mathrm{E}}$ of the error coordinates $\boldsymbol{e}$ alone, i.e.

$$\bar{\mathcal{V}}(\boldsymbol{x}, \boldsymbol{x}_{\mathsf{R}}) = \bar{\mathcal{V}}_{\mathrm{E}}(\boldsymbol{\chi}_{\mathrm{E}}(\boldsymbol{x}, \boldsymbol{x}_{\mathsf{R}})). \tag{A.6}$$

Now the requirement (4.30) for the transport map $\boldsymbol{Q}$ can be written as

$$\begin{aligned}
\boldsymbol{\nabla}_{\mathsf{R}}\bar{\mathcal{V}} + \boldsymbol{Q}^{\top}\boldsymbol{\nabla}\bar{\mathcal{V}} &= \big(\boldsymbol{\nabla}_{\mathsf{R}}\boldsymbol{\chi}_{\mathrm{E}} + \boldsymbol{\nabla}\boldsymbol{\chi}_{\mathrm{E}}\boldsymbol{Q}\big)^{\top}\frac{\partial\bar{\mathcal{V}}_{\mathrm{E}}}{\partial\boldsymbol{e}} \\
&= \Big(\underbrace{\big((\boldsymbol{\nabla}\boldsymbol{\chi}_{\mathrm{E}})(\boldsymbol{\nabla}\boldsymbol{\chi}_{\mathrm{E}})^{+} + \boldsymbol{\Phi}_{\mathrm{E}}^{+}\boldsymbol{\Phi}_{\mathrm{E}}\big)}_{\mathbf{I}_{\nu_e}}\boldsymbol{\nabla}_{\mathsf{R}}\boldsymbol{\chi}_{\mathrm{E}} + \boldsymbol{\nabla}\boldsymbol{\chi}_{\mathrm{E}}\boldsymbol{Q}\Big)^{\top}\frac{\partial\bar{\mathcal{V}}_{\mathrm{E}}}{\partial\boldsymbol{e}} \\
&= \big((\boldsymbol{\nabla}\boldsymbol{\chi}_{\mathrm{E}})^{+}(\boldsymbol{\nabla}_{\mathsf{R}}\boldsymbol{\chi}_{\mathrm{E}}) + \boldsymbol{Q}\big)^{\top}(\boldsymbol{\nabla}\boldsymbol{\chi}_{\mathrm{E}})^{\top}\frac{\partial\bar{\mathcal{V}}_{\mathrm{E}}}{\partial\boldsymbol{e}} + \boldsymbol{\Phi}_{\mathrm{E}}^{+}\underbrace{\boldsymbol{\Phi}_{\mathrm{E}}\boldsymbol{\nabla}_{\mathsf{R}}\boldsymbol{\chi}_{\mathrm{E}}}_{0}\frac{\partial\bar{\mathcal{V}}_{\mathrm{E}}}{\partial\boldsymbol{e}} = 0 \qquad \text{(A.7)}
\end{aligned}$$

which has the simple solution

$$\boldsymbol{Q} = -(\boldsymbol{\nabla}\boldsymbol{\chi}_{\mathrm{E}})^{+}(\boldsymbol{\nabla}_{\mathsf{R}}\boldsymbol{\chi}_{\mathrm{E}}). \qquad \text{(A.8)}$$

Error kinematics. With the same approach as above we can derive a kinematic relation between the error coordinates $\boldsymbol{e}$ and the error velocity $\boldsymbol{\xi}_{\mathrm{E}} = \boldsymbol{\xi} - \boldsymbol{Q}\boldsymbol{\xi}_{\mathsf{R}}$ as

$$\begin{aligned}
\dot{\boldsymbol{e}} &= (\boldsymbol{\nabla}\boldsymbol{\chi}_{\mathrm{E}})\boldsymbol{\xi} + (\boldsymbol{\nabla}_{\mathsf{R}}\boldsymbol{\chi}_{\mathrm{E}})\boldsymbol{\xi}_{\mathsf{R}} \\
&= (\boldsymbol{\nabla}\boldsymbol{\chi}_{\mathrm{E}})\boldsymbol{\xi} + \underbrace{\big((\boldsymbol{\nabla}\boldsymbol{\chi}_{\mathrm{E}})(\boldsymbol{\nabla}\boldsymbol{\chi}_{\mathrm{E}})^{+} + \boldsymbol{\Phi}_{\mathrm{E}}^{+}\boldsymbol{\Phi}_{\mathrm{E}}\big)}_{\mathbf{I}_{\nu_e}}\boldsymbol{\nabla}_{\mathsf{R}}\boldsymbol{\chi}_{\mathrm{E}}\boldsymbol{\xi}_{\mathsf{R}} \\
&= (\boldsymbol{\nabla}\boldsymbol{\chi}_{\mathrm{E}})\underbrace{\big(\boldsymbol{\xi} + (\boldsymbol{\nabla}\boldsymbol{\chi}_{\mathrm{E}})^{+}(\boldsymbol{\nabla}_{\mathsf{R}}\boldsymbol{\chi}_{\mathrm{E}})\boldsymbol{\xi}_{\mathsf{R}}\big)}_{\boldsymbol{\xi}_{\mathrm{E}}} + \boldsymbol{\Phi}_{\mathrm{E}}^{+}\underbrace{\boldsymbol{\Phi}_{\mathrm{E}}(\boldsymbol{\nabla}_{\mathsf{R}}\boldsymbol{\chi}_{\mathrm{E}})}_{0}\boldsymbol{\xi}_{\mathsf{R}} \qquad \text{(A.9)}
\end{aligned}$$

Bibliography

[Abraham and Marsden, 1978] Abraham, R. and Marsden, J. E. (1978). *Foundations of Mechanics*. Westview Press.

[Appell, 1900] Appell, P. E. (1900). Sur une forme générale des équations de la dynamique. *J. Reine Angew. Math.*, 121:310–319.

[Arnold, 1989] Arnold, V. I. (1989). *Mathematical Methods of Classical Mechanics*, volume 60 of *Graduate Texts in Mathematics*. Springer, New York.

[Bloch et al., 2000] Bloch, A. M., Leonard, N. E., and Marsden, J. E. (2000). Controlled Lagrangians and the stabilization of mechanical systems. I. The first matching theorem. *IEEE Trans. on Automatic Control*, 45(12):2253–2270.

[Boltzmann, 1897] Boltzmann, L. (1897). *Vorlesungen ueber die Pincipe der Mechanik*. Johan Ambrosius Barth.

[Boltzmann, 1902] Boltzmann, L. (1902). Über die Form der Lagrangeschen Gleichungen für nichtholonome, generalisierte Koordinaten. In *Wissenschaftliche Abhandlungen*, volume 3, pages 682–692. Johann Ambrosius Barth.

[Bremer, 2008] Bremer, H. (2008). *Elastic Multibody Dynamics: A Direct Ritz Approach*. Springer.

[Bryson, 1975] Bryson, A. E. (1975). *Applied optimal control: optimization, estimation and control*. CRC Press.

[Bullo and Murray, 1999] Bullo, F. and Murray, R. M. (1999). Tracking for fully actuated mechanical systems: A geometric framework. *Automatica*, 35(1):17–34.

[Courant and Hilbert, 1924] Courant, R. and Hilbert, D. (1924). *Methoden der Mathematischen Physik*. Julius Springer.

[Davenport, 1968] Davenport, P. B. (1968). A vector approach to the algebra of rotations with applications. *NASA Technical Note D-4696*.

[Denavit and Hartenberg, 1955] Denavit, J. and Hartenberg, R. (1955). A kinematic notation for lower-pair mechanisms based on matrices. *Journal of Applied Mechanics*, 22(2):215–221.

[Desloge, 1987] Desloge, E. A. (1987). Relationship between Kane's equations and the Gibbs-Appell equations. *Journal of Guidance, Control, and Dynamics*, 10(1):120–122.

[Einstein, 1916] Einstein, A. (1916). Hamiltonsches Prinzip und allgemeine Relativitätstheorie. *Sitzungsberichte der Preussischen Akademie der Wissenschaften zu Berlin.*

[Fliess et al., 1999] Fliess, M., Levine, J., Martin, P., and Rouchon, P. (1999). A Lie-Bäcklund approach to equivalence and flatness of nonlinear systems. *IEEE Trans. Automat. Contr.*, 44(5):922–937.

[Fliess et al., 1995] Fliess, M., Lévine, J., Martin, P., and Rouchon, P. (1995). Flatness and defect of non-linear systems: introductory theory and examples. *International Journal of Control*, 61(6):1327–1361.

[Frankel, 1997] Frankel, T. (1997). *The Geometry of Physics.* Cambridge University Press.

[Galilei, 1638] Galilei, G. (1638). *Discorsi e dimostrazioni matematiche intorno a due nuove scienze.* Appresso gli Elsevirii.

[Gauß, 1829] Gauß, C. F. (1829). Über ein neues allgemeines Grundgesetz der Mechanik. *Journal für die reine und angewandte Mathematik.*

[Gibbs, 1879] Gibbs, J. W. (1879). On the fundamental formulae of dynamics. *Am. J. Math.*, 2(1):49–64.

[Goldstein, 1951] Goldstein, H. (1951). *Classical Mechanics.* Addison-Wesley.

[Golub and Loan, 1996] Golub, G. H. and Loan, C. F. V. (1996). *Matrix Computations.* Johns Hopkins.

[Grafarend and Kühnel, 2011] Grafarend, E. W. and Kühnel, W. (2011). A minimal atlas for the rotation group SO(3). *GEM-International Journal on Geomathematics*, 2(1):113–122.

[Hall, 2015] Hall, B. (2015). *Lie Groups, Lie Algebras, and Representations*, volume 222 of *Graduate Texts in Mathematics.* Springer, 2nd edition.

[Hamel, 1904a] Hamel, G. (1904a). Die Lagrange-Eulerschen Gleichungen der Mechanik. *Z. für Mathematik u. Physik*, 50:1–57.

[Hamel, 1904b] Hamel, G. (1904b). Über die virtuellen Verschiebungen in der Mechanik. *Mathematische Annalen*, 59:416–434.

[Hamel, 1949] Hamel, G. (1949). *Theoretische Mechanik.* Springer.

[Hauser et al., 1992] Hauser, J., Sastry, S., and Meyer, G. (1992). Nonlinear control design for slightly non-minimum phase systems: Application to V/STOL aircraft. *Automatica*, 28(4):664–679.

[Hooke, 1678] Hooke, R. (1678). *Lectures De Potentia Restitutiva, or of Spring. Explaining the Power of Springing Bodies.* Printed for John Martyn Printer to the Royal Society.

[Horn and Johnson, 1985] Horn, R. A. and Johnson, C. R. (1985). *Matrix Analysis.* Cambridge University Press.

[Irscheid et al., 2019] Irscheid, A., Konz, M., and Rudolph, J. (2019). A flatness-based approach to the control of distributed parameter systems applied to load transportation with heavy ropes. In Kondratenko, Y. P., Chikrii, A. A., Gubarev, V. F., and Kacprzyk, J., editors, *Advanced Control Techniques in Complex Engineering Systems: Theory and Applications*, pages 279–294. Springer.

[Kabsch, 1976] Kabsch, W. (1976). A solution for the best rotation to relate two sets of vectors. *Acta Crystallographica*, A32(5):922.

[Kane and Levinson, 1985] Kane, T. R. and Levinson, D. A. (1985). *Dynamics*. McGraw Hill.

[Kastelan et al., 2015] Kastelan, D., Konz, M., and Rudolph, J. (2015). Fully actuated tricopter with pilot-supporting control. In *Proc. 1st IFAC Workshop on Advanced Control and Navigation for Autonomous Aerospace Vehicles ACNAAV 15*, pages 79–84.

[Klein, 1926] Klein, F. (1926). *Vorlesungen über die Entwicklung der Mathematik im 19. Jahrhundert*. Julius Springer.

[Koditschek, 1989] Koditschek, D. E. (1989). The Application of Total Energy as a Lyapunov Function for Mechanical Control Systems. In Marsden, J. E., Krishnaprasad, P. S., and Simo, J. C., editors, *Dynamics and Control of Multibody Systems*, volume 97 of *Contemporary Mathematics*, pages 131–157. American Mathematical Society.

[Konz et al., 2018] Konz, M., Kastelan, D., Gerbet, D., and Rudolph, J. (2018). Practical challenges of fully-actuated tricopter control. In *Proc. of MECHATRONICS 2018*, pages 128–135.

[Konz et al., 2020] Konz, M., Kastelan, D., and Rudolph, J. (2020). Tracking Control for a Fully-Actuated UAV. In Yan, X., Bradley, D., Russell, D., and Moore, P., editors, *Reinventing Mechatronics*, pages 127–144. Springer.

[Konz and Rudolph, 2013] Konz, M. and Rudolph, J. (2013). Quadrotor tracking control based on a moving frame. In *Proc. 9th IFAC Symposium on Nonlinear Control Systems*, pages 80–85.

[Konz and Rudolph, 2015] Konz, M. and Rudolph, J. (2015). Equations of motion with redundant coordinates for mechanical systems on manifolds. In *Proc. 8th Vienna Int. Conf. on Mathematical Modelling*, pages 681–682.

[Konz and Rudolph, 2016] Konz, M. and Rudolph, J. (2016). Beispiele für einen direkten Zugang zu einer globalen, energiebasierten Modellbildung und Regelung von Starrkörpersystemen. *at - Automatisierungstechnik*, 64(2):96–109.

[Konz and Rudolph, 2018] Konz, M. and Rudolph, J. (2018). Redundant configuration coordinates and nonholonomic velocity coordinates in analytical mechanics. In *Proc. 9th Vienna Int. Conf. on Mathematical Modelling*, page 409–414.

[Konz and Rudolph, 2021] Konz, M. and Rudolph, J. (2021). Gauss's principle and tracking control of underactuated mechanical systems. In *Proc. 7th IFAC Workshop on Lagrangian and Hamiltonian Methods for Nonlinear Control LHMNC*, pages 365–370.

[Lanczos, 1986] Lanczos, C. (1986). *The Variational Principles of Mechanics*. Dover Publications, 4 edition.

[Landau and Lifshitz, 1960] Landau, L. D. and Lifshitz, E. M. (1960). *Mechanics*, volume 1 of *Course of Theoretical Physics*. Pergamon Press.

[Landau and Lifshitz, 1971] Landau, L. D. and Lifshitz, E. M. (1971). *The Classical Theory of Fields*, volume 2 of *Course of Theoretical Physics*. Pergamon Press.

[Lee, 2003] Lee, J. M. (2003). *Introduction to Smooth Manifolds*. Springer.

[Lesser, 1992] Lesser, M. (1992). A Geometric Interpretation of Kane's Equations. *Proceedings of the Royal Society of London*, 436(1896):69–87.

[Lewis, 1996] Lewis, A. D. (1996). The geometry of the Gibbs-Appell equations and Gauss's Principle of Least Constraint. *Reports on Mathematical Physics*, 38(1):11–28.

[Lurie, 2002] Lurie, A. I. (2002). *Analytical Mechanics*. Springer.

[Martin et al., 1997] Martin, P., Murray, R. M., and Rouchon, P. (1997). Flat systems, equivalence and trajectory generation. In *Mini-course ECC'97*.

[Misner et al., 1973] Misner, C. W., Thorne, K. S., and Wheeler, J. A. (1973). *Gravitation*. W. H. Freeman and Company.

[Murray et al., 1994] Murray, R. M., Li, Z., and Sastry, S. S. (1994). *A Mathematical Introduction to Robotic Manipulation*. CRC Press.

[Murray et al., 1995] Murray, R. M., Rathinam, M., and Sluis, W. (1995). Differential flatness of mechanical control systems: A catalog of prototype systems. In *Proceedings of the ASME International Congressand Exposition*.

[Newton, 1687] Newton, I. (1687). *Philosophiae naturalis principia mathematica*. Jussu Societatis Regiae ac Typis Josephi Streater.

[Newton, 1846] Newton, I. (1846). *The Mathematical Principles of Natural Philosophy, Translated into English by A. Motte and N. W. Chittenden*. Daniel Adee.

[Nocedal and Wright, 2006] Nocedal, J. and Wright, S. J. (2006). *Numerical Optimization*. Springer, 2nd edition.

[Olfati-Saber, 2001] Olfati-Saber, R. (2001). *Nonlinear Control of Underactuated Mechanical Systems with Applications to Robotics and Aerospace Vehicles*. PhD thesis, Massachusetts Institute of Technology, Cambridge, MA.

[Papastavridis, 2002] Papastavridis, J. G. (2002). *Analytical Mechanics*. World Scientific.

[Penrose, 1955] Penrose, R. (1955). A generalized inverse for matrices. *Mathematical proceedings of the Cambridge philosophical society*, 51(3):406–413.

[Päsler, 1968] Päsler, M. (1968). *Prinzipe der Mechanik*. Walter de Gruyter & Co.

[Rathinam and Murray, 1998] Rathinam, M. and Murray, R. M. (1998). Configuration flatness of lagrangian systems underactuated by one control. *SIAM Journal of Control and Optimization*, 36(1):164–179.

[Rayleigh, 1877] Rayleigh, J. W. S. B. (1877). *The Theory of Sound*. Macmillan and Co.

[Roberson and Schwertassek, 1988] Roberson, R. E. and Schwertassek, R. (1988). *Dynamics of Multibody Systems*. Springer.

[Schlacher and Schöberl, 2007] Schlacher, K. and Schöberl, M. (2007). Construction of flat outputs by reduction and elimination. *CD Proceedings IFAC Symposium on Nonlinear Control Systems*, pages 666–671.

[Shabana, 2005] Shabana, A. A. (2005). *Dynamics of Multibody Systems*. Cambridge University Press, 3 edition.

[Slotine and Li, 1991] Slotine, J.-J. and Li, W. (1991). *Applied Nonlinear Control*. Springer.

[Spivak, 1999] Spivak, M. (1999). *A Comprehensive Introduction to Differential Geometry*. Publish or Perish.

[Spong et al., 2006] Spong, M. W., Hutchinson, S., and Vidyasagar, M. (2006). *Robot Modeling and Control*. Wiley.

[Szabó, 1956] Szabó, I. (1956). *Höhere Technische Mechanik*. Springer.

[Wahba, 1965] Wahba, G. (1965). A least squares estimate of satellite attitude. *SIAM Review*, 7(3):409.

[Wittenburg, 2008] Wittenburg, J. (2008). *Dynamics of Multibody Systems*. Springer, 2 edition.

Appendix B

Templates

B.1 Math fonts

Latin alphabet in math mode

default	$A\ B\ C\ D\ E\ F\ G\ H\ I\ J\ K\ L\ M\ N\ O\ P\ Q\ R\ S\ T\ U\ V\ W\ X\ Y\ Z$ $a\ b\ c\ d\ e\ f\ g\ h\ i\ j\ k\ l\ m\ n\ o\ p\ q\ r\ s\ t\ u\ v\ w\ x\ y\ z$
mathrm	$\mathrm{A\ B\ C\ D\ E\ F\ G\ H\ I\ J\ K\ L\ M\ N\ O\ P\ Q\ R\ S\ T\ U\ V\ W\ X\ Y\ Z}$ $\mathrm{a\ b\ c\ d\ e\ f\ g\ h\ i\ j\ k\ l\ m\ n\ o\ p\ q\ r\ s\ t\ u\ v\ w\ x\ y\ z}$
mathsf	$\mathsf{A\ B\ C\ D\ E\ F\ G\ H\ I\ J\ K\ L\ M\ N\ O\ P\ Q\ R\ S\ T\ U\ V\ W\ X\ Y\ Z}$ $\mathsf{a\ b\ c\ d\ e\ f\ g\ h\ i\ j\ k\ l\ m\ n\ o\ p\ q\ r\ s\ t\ u\ v\ w\ x\ y\ z}$
mathtt	$\mathtt{A\ B\ C\ D\ E\ F\ G\ H\ I\ J\ K\ L\ M\ N\ O\ P\ Q\ R\ S\ T\ U\ V\ W\ X\ Y\ Z}$ $\mathtt{a\ b\ c\ d\ e\ f\ g\ h\ i\ j\ k\ l\ m\ n\ o\ p\ q\ r\ s\ t\ u\ v\ w\ x\ y\ z}$
boldsymbol	$\boldsymbol{A\ B\ C\ D\ E\ F\ G\ H\ I\ J\ K\ L\ M\ N\ O\ P\ Q\ R\ S\ T\ U\ V\ W\ X\ Y\ Z}$ $\boldsymbol{a\ b\ c\ d\ e\ f\ g\ h\ i\ j\ k\ l\ m\ n\ o\ p\ q\ r\ s\ t\ u\ v\ w\ x\ y\ z}$
mathbf	$\mathbf{A\ B\ C\ D\ E\ F\ G\ H\ I\ J\ K\ L\ M\ N\ O\ P\ Q\ R\ S\ T\ U\ V\ W\ X\ Y\ Z}$ $\mathbf{a\ b\ c\ d\ e\ f\ g\ h\ i\ j\ k\ l\ m\ n\ o\ p\ q\ r\ s\ t\ u\ v\ w\ x\ y\ z}$
mathfrak	$\mathfrak{A\ B\ C\ D\ E\ F\ G\ H\ I\ J\ K\ L\ M\ N\ O\ P\ Q\ R\ S\ T\ U\ V\ W\ X\ Y\ Z}$ $\mathfrak{a\ b\ c\ d\ e\ f\ g\ h\ i\ j\ k\ l\ m\ n\ o\ p\ q\ r\ s\ t\ u\ v\ w\ x\ y\ z}$
mathcal	$\mathcal{A\ B\ C\ D\ E\ F\ G\ H\ I\ J\ K\ L\ M\ N\ O\ P\ Q\ R\ S\ T\ U\ V\ W\ X\ Y\ Z}$
mathbb	$\mathbb{A\ B\ C\ D\ E\ F\ G\ H\ I\ J\ K\ L\ M\ N\ O\ P\ Q\ R\ S\ T\ U\ V\ W\ X\ Y\ Z}$

Greek alphabet in math mode

default			Γ	Δ				Θ			Λ			Ξ		Π		Σ		Υ	Φ		Ψ	Ω
	α	β	γ	δ	ϵ	ζ	η	θ	ι	κ	λ	μ	ν	ξ	o	π	ρ	σ	τ	υ	ϕ	χ	ψ	ω
var	A	B	$\varGamma$	$\varDelta$	E	Z	H	$\varTheta$	I	K	$\varLambda$	M	N	$\varXi$	O	$\varPi$	P	$\varSigma$	T	$\varUpsilon$	$\varPhi$	X	$\varPsi$	$\varOmega$
					ε			ϑ								ϖ	ϱ	ς			φ			
boldsymbol			$\boldsymbol{\Gamma}$	$\boldsymbol{\Delta}$				$\boldsymbol{\Theta}$			$\boldsymbol{\Lambda}$			$\boldsymbol{\Xi}$		$\boldsymbol{\Pi}$		$\boldsymbol{\Sigma}$		$\boldsymbol{\Upsilon}$	$\boldsymbol{\Phi}$		$\boldsymbol{\Psi}$	$\boldsymbol{\Omega}$
	$\boldsymbol{\alpha}$	$\boldsymbol{\beta}$	$\boldsymbol{\gamma}$	$\boldsymbol{\delta}$	$\boldsymbol{\epsilon}$	$\boldsymbol{\zeta}$	$\boldsymbol{\eta}$	$\boldsymbol{\theta}$	$\boldsymbol{\iota}$	$\boldsymbol{\kappa}$	$\boldsymbol{\lambda}$	$\boldsymbol{\mu}$	$\boldsymbol{\nu}$	$\boldsymbol{\xi}$	$\boldsymbol{o}$	$\boldsymbol{\pi}$	$\boldsymbol{\rho}$	$\boldsymbol{\sigma}$	$\boldsymbol{\tau}$	$\boldsymbol{\upsilon}$	$\boldsymbol{\phi}$	$\boldsymbol{\chi}$	$\boldsymbol{\psi}$	$\boldsymbol{\omega}$
var	$\boldsymbol{A}$	$\boldsymbol{B}$	$\boldsymbol{\varGamma}$	$\boldsymbol{\varDelta}$	$\boldsymbol{E}$	$\boldsymbol{Z}$	$\boldsymbol{H}$	$\boldsymbol{\varTheta}$	$\boldsymbol{I}$	$\boldsymbol{K}$	$\boldsymbol{\varLambda}$	$\boldsymbol{M}$	$\boldsymbol{N}$	$\boldsymbol{\varXi}$	$\boldsymbol{O}$	$\boldsymbol{\varPi}$	$\boldsymbol{P}$	$\boldsymbol{\varSigma}$	$\boldsymbol{T}$	$\boldsymbol{\varUpsilon}$	$\boldsymbol{\varPhi}$	$\boldsymbol{X}$	$\boldsymbol{\varPsi}$	$\boldsymbol{\varOmega}$
					$\boldsymbol{\varepsilon}$			$\boldsymbol{\vartheta}$								$\boldsymbol{\varpi}$	$\boldsymbol{\varrho}$	$\boldsymbol{\varsigma}$			$\boldsymbol{\varphi}$			
mathsf	Α	Β	Γ	Δ	Ε	Ζ	Η	Θ	Ι	Κ	Λ	Μ	Ν	Ξ	Ο	Π	Ρ	Σ	Τ	ϒ	Φ	Χ	Ψ	Ω
	α	β	γ	δ	ε	ζ	η	θ	ι	κ	λ	μ	ν	ξ	ο	π	ρ	σ	τ	υ	φ	χ	ψ	ω
mathbf	$\mathbf{A}$	$\mathbf{B}$	$\mathbf{\Gamma}$	$\mathbf{\Delta}$	$\mathbf{E}$	$\mathbf{Z}$	$\mathbf{H}$	$\mathbf{\Theta}$	$\mathbf{I}$	$\mathbf{K}$	$\mathbf{\Lambda}$	$\mathbf{M}$	$\mathbf{N}$	$\mathbf{\Xi}$	$\mathbf{O}$	$\mathbf{\Pi}$	$\mathbf{P}$	$\mathbf{\Sigma}$	$\mathbf{T}$	$\mathbf{\Upsilon}$	$\mathbf{\Phi}$	$\mathbf{X}$	$\mathbf{\Psi}$	$\mathbf{\Omega}$

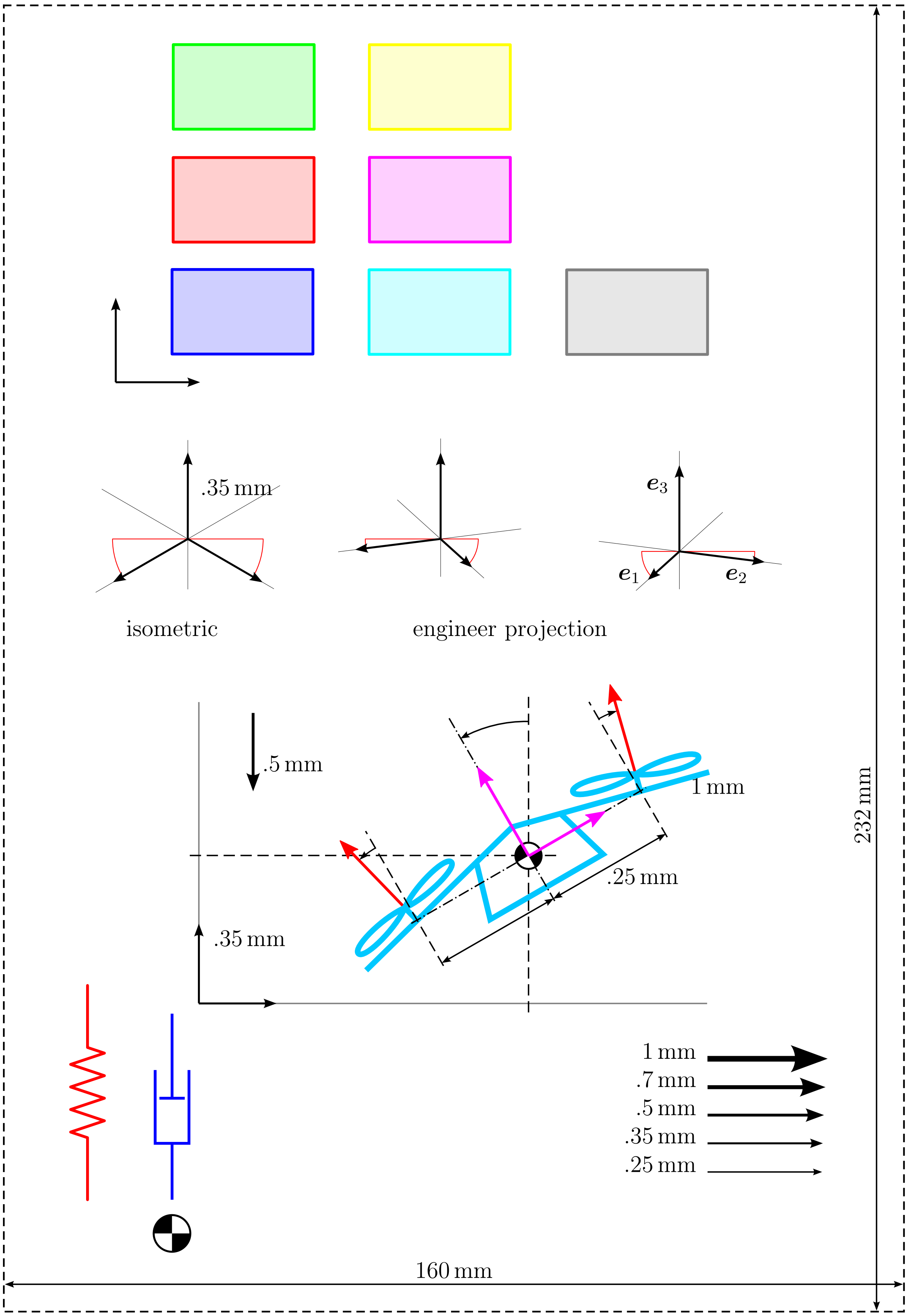

Figure B.1: Inkscape figure template